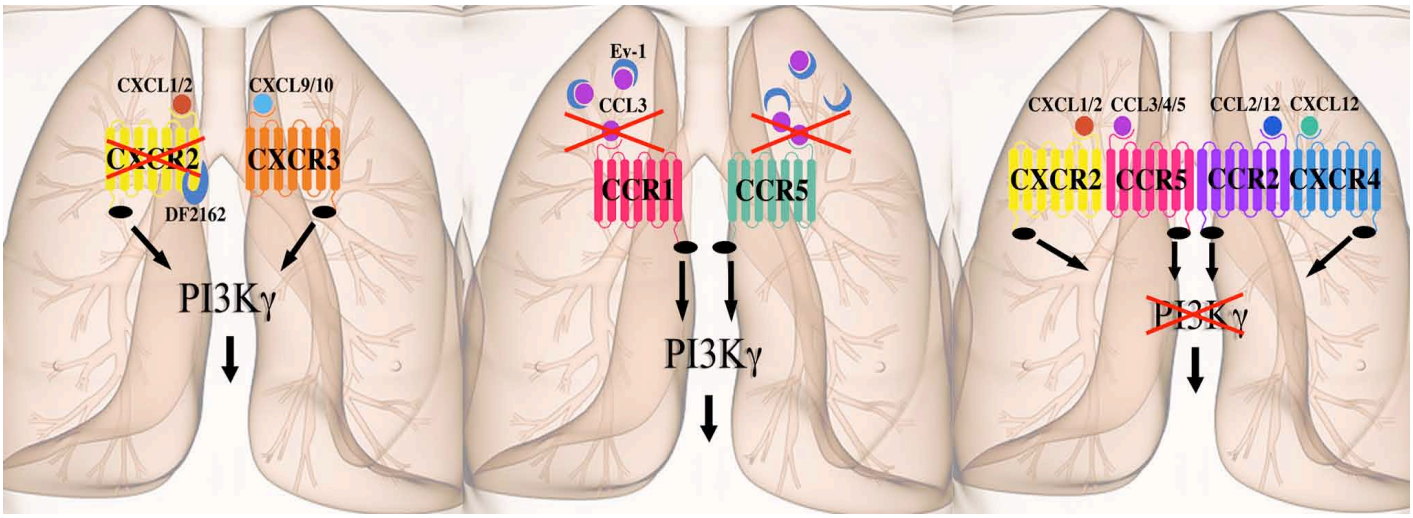
Universidade Federal de Minas Gerais

Instituto de Ciências Biológicas

INTERVENÇÃO FARMACOLÓGICA NO SISTEMA QUIMIOCINAS:

POSSÍVEIS ALVOS PARA O TRATAMENTO DA FIBROSE PULMONAR.



REMO DE CASTRO RUSSO

Belo Horizonte

Minas Gerais

2009

REMO DE CASTRO RUSSO

INTERVENÇÃO FARMACOLÓGICA NO SISTEMA QUIMIOCINAS:

POSSÍVEIS ALVOS PARA O TRATAMENTO DA FIBROSE PULMONAR.

Tese apresentada ao Departamento de Bioquímica e Imunologia do Instituto de Ciências Biológicas da Universidade Federal de Minas Gerais, como requisito parcial à obtenção do titulo de Doutor em Ciências: Imunologia.

Orientador: Prof. Dr. Mauro Martins Teixeira
(Departamento de Bioquímica e Imunologia)

Belo Horizonte

Instituto de Ciências Biológicas da Universidade Federal de Minas Gerais

Dezembro de 2009

Universidade Federal de Minas Gerais -
Curso de Pós-Graduação em Bioquímica e Imunologia ICB/UFMG
Av. Antônio Carlos, 6627 – Pampulha
31270-901 – Belo Horizonte – MG
e-mail: pg-biq@icb.ufmg.br (31)3499-2615

ATA DA DEFESA DA TESE DE DOUTORADO DE REMO DE CASTRO RUSSO. Aos vinte e um dias do mês de dezembro de 2009 às 10:00 horas, reuniu-se no Instituto de Ciências Biológicas da Universidade Federal de Minas Gerais a Comissão Examinadora da tese de doutorado, indicada *ad referendum* do Colegiado do Curso, para julgar, em exame final, o trabalho intitulado "Intervenção farmacológica no sistema quimiocinas: possíveis alvos para o tratamento da fibrose pulmonar", requisito final para a obtenção do grau de Doutor em Ciências: Imunologia. Abrindo a sessão o Presidente da Comissão, Dr. Mauro Martins Teixeira da Universidade Federal de Minas Gerais, após dar a conhecer aos presentes o teor das Normas Regulamentares do Trabalho Final, passou a palavra ao candidato para apresentação de seu trabalho. Seguiu-se a argüição pelos examinadores, com a respectiva defesa do candidato. Logo após a Comissão se reuniu, sem a presença do candidato e do público, para julgamento e expedição do resultado final. Foram atribuídas as seguintes indicações: Dra. Patrícia Machado Rodrigues e Silva Martins da Fundação Oswaldo Cruz-RJ, aprovado; Dra. Patricia Rieken Macedo Rocco da Universidade Federal do Rio de Janeiro, aprovado; Dra. Fabiana Simão Machado da Universidade Federal de Minas Gerais, aprovado; Dra. Denise Carmona Cara Machado da Universidade Federal de Minas Gerais, aprovado; Dr. Mauro Martins Teixeira, orientador, da Universidade Federal de Minas Gerais, aprovado. Pelas indicações o candidato foi considerado APROVADO. O resultado final foi comunicado publicamente ao candidato pelo Presidente da Comissão. Nada mais havendo a tratar o Presidente da Comissão encerrou a reunião e lavrou a presente Ata que será assinada por todos os membros participantes da Comissão Examinadora. Belo Horizonte, 21 de dezembro de 2009.

Dra. Patricia Machado Rodrigues e Silva Martins – FIOCRUZ-RJ

Dra. Patricia Rieken Macedo Rocco – UFRJ

Dra. Denise Carmona Cara Machado – UFMG

Dra. Fabiana Simão Machado – UFMG

Dr. Mauro Martins Teixeira – orientador – UFMG

Profa. Andréa Mara Macedo
Coordenadora do Curso de Pós - Graduação em
Bioquímica e Imunologia
Instituto de Ciências Biológicas - UFMG

"O homem argumenta, a natureza age."

Voltaire

AGRADECIMENTOS

Ao meu orientador, Prof. Mauro Martins Teixeira, por ser não só um exemplo de dedicação, mas por ser um grande cientista e prover o que foi necessário à minha formação durante estes oito anos no seu laboratório. Agradeço pela acolhida, paciência e ensinamentos.

Aos meus grandes amigos, parceiros, comparsas, cúmplices e co-autores, de hoje e outrora, Rodrigo, Lucíola, Letícia, Adriano, Ester, e especialmente a Cris, por serem meu bom senso, pelo respeito, carinho, ajuda nos experimentos com "n=147" até altas horas da madrugada, discussões científicas e idéias mirabolantes, pelo convívio e sorrisos nos rostos.

A todos os colegas e freqüentadores do Laboratório de Imunofarmacologia, Flopes, Katita, Caio, Flavão, Elisão, Daniel Cisalpino, Maria, Cristiano, Márcia, David, Norinne, Milene, Lívia, Fernanda, Luciana, Landa, Vivian, Dani Sachs, Mila, Angélica, Antônio Lúcio, Adaliene, Tracília, Gustavo, Fred, Marina, Maria Clara, Carol, Larissa, Fernandão, Roberta, Silvana, Vanessa Mendonça, por toda aleatoriedade dinâmica diária. Às minhas colegas de longa data, Valdinéria, Dani (e todo grupo) e Vanessa (e todo grupo), por esses oito anos de convívio no laboratório.

À Bárbara, minha aluninha, por toda disponibilidade e boa vontade nos ajudando em todos os experimentos.

Aos professores membros da banca de doutorado, Dra. Patrícia Machado Rodrigues e Silva Martins, Dra. Patrícia Rieken Macedo Rocco, Dra. Denise Carmona Cara e Dra. Fabiana Simão Machado, e também aos professores suplentes Dr. Marco Aurélio Martins e Dr. André Talvani, pela disponibilidade, atenção e por aceitarem o convite.

A Ilma e Dora, por todo apoio técnico dado.

Ao Prof. Dr. Alberto Mantovani e Prof. Dr. Massimo Locati, pela grande oportunidade de poder desenvolver parte deste doutorado na Itália, onde tive oportunidade de crescer e *per la pastasciutta.* Sem dúvida, esta foi uma grande experiência.

Aos colegas do Istituto Clinico Humanitas e Laboratorio de Biologia dei Leucociti, por este um ano e meio de convívio espetacular, regado a cafés científicos e carinho milanês.

A todos co-autores dos estudos em que estive envolvido, pela oportunidade de trabalhar lado a lado e pela grande ajuda nas emergências experimentais.

Ao Prof. Geovanni Dantas Cassali, pela colaboração e imensa ajuda com as análises histopatológicas.

Ao Dr. Francesco Colotta e Riccardo Bertini (Dompè, Itália), pelo fornecimento dos fármacos antagonistas de receptores CXCR1/2.

À Dr. Amanda E. I. Proudfoot (Merck Serono, Suíça), pelo fornecimento da Evasina.

Ao Jamil, do Laboratório de Enzimologia e Físico-Química de Proteínas.

À CAPES, CNPq, FAPEMIG e INNOCHEM pelo financiamento do trabalho e bolsas.

À Celise do Departamento de Bioquímica e Imunologia, por todo auxílio e atenção.

Aos colegas do curso de Bases I e II, e Claudiney, pelos momentos juntos.

Aos colegas do ICB, Chico, Quelé, Gabriel, Daniel, Raonas pela diversão nos momentos mais oportunos e pelas discussões sobre quimiocinas e interleucinas de número primo nos momentos mais inoportunos no buteco.

Aos meus pais, Jones e Antônia, irmãs Rafaela e Raissa, e família, pelo carinho e incentivo em todos os momentos da minha vida.

Aos meus sogros pelo apoio e incentivos constantes.

À minha Ana Luiza, pela participação na minha vida em todos momentos, me apoiando e fazendo seguir em frente. Agradeço muito por caminharmos juntos, por todo carinho e por tudo aquilo que você é.

Enfim, agradeço a todos que colaboraram direta ou indiretamente para a execução deste trabalho.

LISTA DE ABREVIATURAS E SIGLAS

6Ckine – Chemokine with 6 cisteines

AIDS – Acquired Immunodeficiency Syndrome

AKT- V-akt murine thymoma viral oncogene homolog 1

ALI – Acute Lung Injury

AMP – Adenosine Monophosphate

AP-2 – Adaptin 2

BAL – Bronchoalveolar Lavage

CD18 – leukocyte β_2-integrin

CKBP – Chemokine-binding Protein

CLF – Chemokine-Like Functions

COPD – Chronic Obstructive Pulmonary Disease

CTGF – Connective Tissue Growth Factor

D6 – Chemokine Decoy Receptor D6

DARC – Duffy Antigen Receptor for Chemokines

EGF – Epidermal Growth Factor

EMT – Epithelial-to-Mesenchymal Transition

FGF – Fibroblast Growth Factor

FITC – Fluorescein Isothiocyanate

GAGs – Glycosaminoglycans

GPCRs – G-protein Coupled Receptors

HGF – Hepatocyte Growth Factor

HIV –Human Immunodeficiency Virus

ICAM-1 – Inter-Cellular Adhesion Molecule-1

IFN – Interferon

IL – Interleucina

IP-10 – Interferon-Inducible Protein-10

IP_3 – Inositol 1,4,5-trisphosphate

IPF – Idiopathic Pulmonary Fibrosis

MAP kinase – Mitogen-Activated Protein Kinases

MCP-1 – Monocyte Chemoattractant Protein-1

MHC – Major Histocompatibility Complex

MIF – Macrophage Migration Inhibitory Factor

MIP-1α – Macrophage Inflammatory Protein-1-alpha

MIP-1β – Macrophage Inflammatory Protein-1-beta

MMPs – Matrix Metalloproteinases

mTOR – Mammalian Target of Rapamycin

NF-κB – Nuclear Factor kappa B

PAF – Platelet-Activating Factor

PDGF – Platelet-Derived Growth Factor

PGP –Pro-Gly-Pro Tripeptide

PI3K – Phosphoinositide 3-Kinases

RANTES – Regulated upon Activation, Normal T-cell Expressed, and Secreted

SDF-1 – Stromal cell-Derived Factor-1

TARC – Thymus and Activation Regulated Chemokine

TGF-β – Transforming Growth Factor beta

Th – T-helper type response

TIMPs – Tissue Inhibitor of Metalloproteinases

TNFα – Tumor Necrosis Factor-alpha

VEGF – Vascular Endothelial Growth Factor

VILI – Ventilator-Induced Lung Injury

RESUMO

A fibrose pulmonar é uma doença crônica respiratória letal cujos sinais clínicos incluem uma piora da dispnéia, perda progressiva do volume pulmonar e troca gasosa anormal. A fibrose pode ser desencadeada por fenômenos inflamatórios pulmonares que geralmente precedem a deposição de colágeno no parênquima pulmonar. Inicialmente, o uso de corticosteróides foi utilizado como estratégia para seu tratamento, com finalidade de reduzir a inflamação pulmonar e também a fibroplasia. Porém, o aparecimento de efeitos adversos durante o período de tratamento limitaram sua aplicação terapêutica. Dados clínicos têm revelado uma estreita correlação entre a fibrose pulmonar, os níveis de quimiocinas circulantes ou no lavado bronco-alveolar, e o perfil leucocitário encontrado. Diante deste cenário, as quimiocinas se tornam importantes alvos para o tratamento da fibrose pulmonar, uma vez que são responsáveis por guiarem as respostas inflamatória e fibrogênica.

Esta tese de doutorado reúne dados sobre o estudo de novos fármacos capazes de inibir a fibrose pulmonar induzida de maneira experimental em camundongos e revela diferentes formas de intervir no sistema quimiocina durante processos inflamatórios e fibrogênicos pulmonares. Os alvos utilizados para estudo foram: (i) o receptor de quimiocina CXCR2, (ii) a quimiocina CCL3 e (iii) o elemento de sinalização comum dos receptores de quimiocinas, a PI3Kγ. A administração oral do *antagonista alostérico não-competitivo de receptores CXCR2 (DF2162)* no modelo de fibrose pulmonar induzida por bleomicina foi responsável pelo efeito protetor observado nos animais quando tratados de maneira preventiva (do dia 0 ao 16) ou terapêutica (do dia 8 ao 16). A redução da fibrose pulmonar nos animais tratados com *DF2162* pareceu ser causada pelos efeitos inibitórios sobre a angiogênese, podendo até ser de natureza dual, por inibição da transmigração neutrofílica para as vias aéreas. Através do uso da *proteína ligadora de quimiocinas-CCL3 (Evasin-1),* isolada e clonada de glândulas salivares do carrapato *Rhipicephalus sanguineus*, estudamos os efeitos inibitórios de CCL3 durante a inflamação pulmonar e fibrose induzida por bleomicina. O tratamento preventivo (do dia 0 ao 25) e terapêutico (do dia 8 ao 25) com *Evasin-1* causou a redução da fibrose pulmonar em camundongos, associada a um menor infiltrado leucocitário e redução da produção de citocinas pro-fibrogênicas. Por último, para avaliar a participação de um elemento comum da via de sinalização intracelular utilizada pelos receptores de quimiocinas, a PI3Kγ, no desenvolvimento da fibrose pulmonar, animais deficientes para a isoforma γ da PI3K foram desafiados com bleomicina. A deficiência para PI3Kγ causou atenuação da fibrose e aumento na sobrevida dos animais, além de apresentarem redução no influxo leucocitário nas vias aéreas. A inibição da PI3Kγ também gerou modificações funcionais em células endoteliais e fibroblastos *in vitro*, sugerindo que PI3Kγ participa do processo de angiogênese e na secreção de colágeno por fibroblastos. Em conjunto, estes dados demonstram uma possível modulação do sistema quimiocinas no contexto de patologias inflamatórias pulmonares e oferecem novos fármacos como candidatos para o tratamento da fibrose pulmonar. Futuros ensaios clínicos poderão validar seu uso terapêutico.

ABSTRACT

Pulmonary fibrosis is a chronic respiratory lethal disease whose clinical signs include a worsening of dyspnea, progressive loss of lung volume and abnormal gas exchange. Fibrosis may be triggered by a series of inflammatory lung condition that usually precedes the deposition of collagen in the lung parenchyma. Initially, the use of corticosteroids was used as a strategy for the treatment of pulmonary fibrosis in order to reduce the pulmonary inflammation as well fibroplasia. However, the appearance of adverse effects during the treatment period limited their therapeutic application. Clinical data have shown a close correlation between pulmonary fibrosis, levels of circulating chemokines or boncho-alveolar lavage, and white blood cell counts. In this scenario, the chemokines become important targets for the treatment of pulmonary fibrosis, since they are responsible for guiding the inflammatory and fibrogenic responses.

This thesis presents a compilation study of new drugs that may inhibit lung fibrosis induced experimentally in mice and reveals different ways of intervening in the chemokine system during pulmonary inflammatory and fibrogenic process. The targets used for the study were: (i) the chemokine receptor CXCR2, (ii) the chemokine CCL3 and (iii) the common element of signaling pathway of chemokine receptors, the PI3Kγ. The oral administration of the *allosteric antagonist non-competitive of CXCR2 receptor (DF2162)* in bleomycin-induced pulmonary fibrosis mice model, was responsible for the protective effect observed in animals when treated in a preventively (from day 0 to 16) or therapeutic (from day 8 to 16) schedule. The reduction of pulmonary fibrosis in those animals treated with *DF2162* appeared to be caused by inhibitory effects on angiogenesis, and may even be of dual nature, via inhibition of neutrophil transmigration into the airways. Through the use of the *chemokine binding proteins-CCL3 (Evasin-1)*, first isolated and cloned from salivary glands of *Rhipicephalus sanguineus*, we studied the inhibitory effects of CCL3 during bleomycin-induced pulmonary inflammation and fibrosis. Preventive (from day 0 to 25) and therapeutic (from day 8 to 25) treatments with *Evasin-1* caused a reduction of pulmonary fibrosis in mice, associated with a lower leukocyte infiltration and reduced production of pro-fibrogenic cytokines. Finally, to evaluate the importance of a common element of intracellular signaling pathway used by chemokine receptors, the PI3Kγ, in the development of pulmonary fibrosis, deficient animals for the γ isoform of PI3K were challenged with bleomycin. PI3Kγ deficiency led to attenuation of fibrosis and increased animal survival, besides a reduction in leukocyte influx into the airways. The inhibition of PI3Kγ also caused functional changes in endothelial cells and fibroblasts *in vitro*, suggesting that PI3Kγ participates in the process of angiogenesis and the secretion of collagen by fibroblasts. Together, these data demonstrate a potential modulation of the chemokine system in inflammatory lung disease's context and provide new drug candidates for the pulmonary fibrosis treatment. Future clinical trials may validate their therapeutic use.

SUMÁRIO

1. INTRODUÇÃO.....10

1.1. Inflamação..... 11

1.2. O sistema quimiocina.....16

1.3. Inflamação pulmonar.....23

1.4. Fibrose pulmonar.....27

1.5. Quimiocinas e fibrose pulmonar.....31

1.6. Quimiocinas como alvo farmacológico.....35

2. JUSTIFICATIVA E OBJETIVO GERAL.....38

3. TRABALHOS CIENTÍFICOS.....40

3.1. *Role of the chemokine receptor CXCR2 in bleomycin-induced pulmonary inflammation and fibrosis*.....41

3.2. *Ticks produce highly selective chemokine binding proteins with antiinflammatory activity*.....54

3.3. *Therapeutic effects of Evasin-1, a CCL3-Binding Protein, in bleomycin-induced lung fibrosis in mice.*.....68

3.4. *PI3K-γ plays a critical role enhancing pulmonary injury and fibrosis induced by bleomycin in mice.*.....98

4. DISCUSSÃO E CONCLUSÕES GLOBAIS.....143

5. REFERÊNCIAS BIBLIOGRÁFICAS.....150

6. ANEXOS.....159

6.1. *Tissue- and stimulus-dependent role of phosphatidylinositol 3-kinase isoforms for neutrophil recruitment induced by chemoattractants in vivo.*.....161

6.2. *Role of the chemokine scavenger receptor D6 in balancing inflammation and immune activation.*.....170

6.3. *IL-33 induces antigen-specific IL-5+ T cells and promotes allergic-induced airway inflammation independent of IL-4.*.....184

1. INTRODUÇÃO

1.1. Inflamação

A inflamação é definida como uma reação secundária a lesões traumáticas, danos químicos ou físicos, de natureza auto-imune ou em resposta a agentes infecciosos, visando a restauração da homeostase (1). Atua de forma importante como mecanismo de regulação fisiológico-imune, conservado ao longo da história evolutiva, contribuindo para o bem estar do indivíduo (2). Este tipo de resposta do sistema imune é guiado inicialmente por componentes inatos, tais como proteínas sinalizadoras, seus receptores e alguns grupos celulares, e posteriormente com participação de elementos da imunidade adquirida. Modificações na micro-circulação, migração leucocitária através do leito vascular e liberação de moléculas solúveis nos tecidos danificados são as principais características da inflamação (2).

A reação inflamatória local caracteriza-se, inicialmente, por vaso-constrição arteriolar transitória causada pela contração do músculo liso vascular. Em seguida, ocorre vaso-dilatação e aumento da permeabilidade vascular devido a alterações no endotélio vascular, resultando no aumento do fluxo sanguíneo local, hiperemia, e na exsudação de líquido rico em proteínas plasmáticas, ou edema. Seguem-se, então, nas vênulas pós-capilares, alterações na capacidade adesiva do endotélio, com conseqüente aumento do rolamento de leucócitos e posterior migração direcional e seletiva destes da circulação para o sítio lesionado (3, 4). No início do processo, os neutrófilos são particularmente prevalentes. Esses leucócitos são responsáveis pela resposta fagocítica imediata e pela ação destrutiva dos seus conteúdos granulares. Estes produtos tóxicos são secretados por grânulos citoplasmáticos, que se fundem à membrana para a liberação de peróxido de hidrogênio, ácido hipocloroso, proteinases, gelatinases, colagenases, elastase, defensinas, mieloperoxidase e espécies reativas de oxigênio. São também os neutrófilos uma das principais fontes de mediadores inflamatórios, contribuindo para a amplificação da lesão nos tecidos (5-7). Em seguida, fagócitos

mononucleares e linhagens linfocitárias se acumulam no sítio lesionado e, uma vez ativados, produzem moléculas inflamatórias responsáveis pela cronicidade do processo inflamatório. Além disso, macrófagos exercem importante atividade fagocítica, envolvida na destruição celular e remoção de restos teciduais. Estes fagócitos posteriormente desaparecem por apoptose ou deslocamento para os vasos linfáticos (8-10).

Alterações microvasculares de caráter proliferativo são denominadas neo-formações vasculares ou angiogênese. Ocorrem durante o processo inflamatório e possuem importante participação na regulação da resposta imune, pois contribuem diretamente para ativação, função, distribuição e retenção de leucócitos nos mais variados tecidos, além de direcioná-los ao encontro de estímulos inflamatórios e demais tipos celulares (11). Além de participar em funções homeostáticas, tais como o desenvolvimento embrionário e processos reparatórios do tipo cicatricial, a angiogênese contribui para o suprimento de oxigênio e nutrientes, bem como para a remoção de metabólitos da excreção, e até mesmo no desenvolvimento de tumores (11, 12).

Ao final de uma resposta inflamatória, geralmente após a eliminação do agente lesivo, ocorre a resolução do processo inflamatório, que consiste no término do recrutamento celular com reversão das alterações vasculares. É seguida por redução do número de leucócitos causada por apoptose, remoção dos restos teciduais e regeneração, visando a restauração da função fisiológica natural tecidual (13). Porém, quando falhas ocorrem nesta fase de decaimento inflamatório, a inflamação pode se tornar persistente e causar maior destruição do tecido. Neste contexto, ocorre o reparo funcional no qual o tecido não regenerado é substituído por tecido conjuntivo, levando à cicatrização (2, 13). Tal como na angiogênese e inflamação, o reparo tecidual é regulado por mediadores solúveis e elementos da matriz extracelular. Envolve uma coordenada ativação, migração, proliferação e diferenciação de

diversos tipos celulares, dentre estes, leucócitos, células endoteliais e fibroblastos (14) (Figura-1).

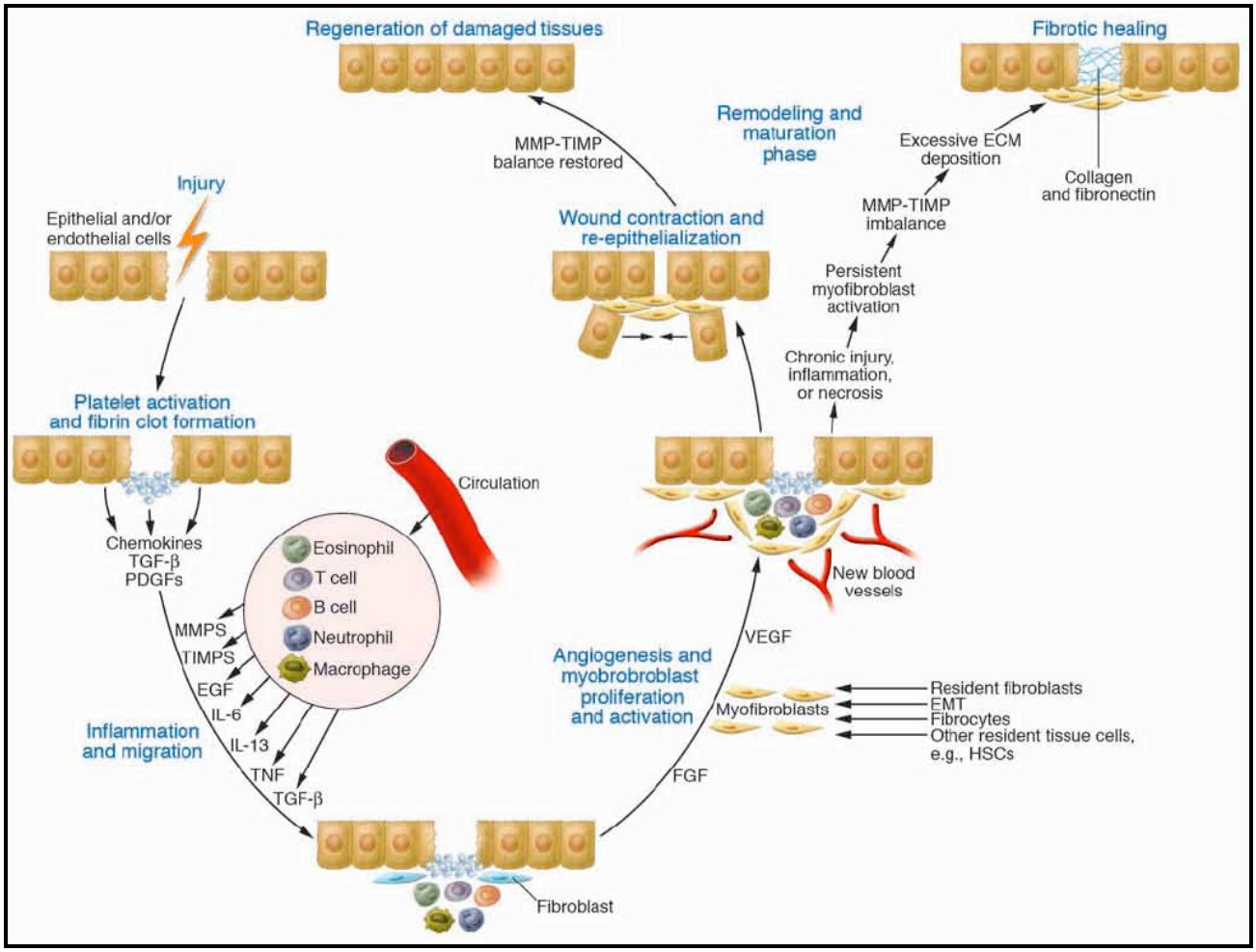


Figura-1: Resultado da cicatrização de feridas: regeneração ou fibrose tecidual. *Subseqüentemente à lesão tecidual, células epiteliais e endoteliais produzem mediadores do processo inflamatório, disparam a cascata de coagulação que leva à formação do coágulo. Isso é seguido por uma fase inflamatória e proliferativa, em que leucócitos são recrutados, ativados e induzidos à proliferação, pelas quimiocinas e fatores de crescimento. Os leucócitos ativados produzem citocinas pró-fibrogênicas, IL-13 e TGF-β_1. Células epiteliais, endoteliais e miofibroblastos ativados produzem metaloproteinases (MMPs), que perturbam a estrutura da membrana basal, além da produção adicional de citocinas e quimiocinas que recrutam neutrófilos, macrófagos, linfócitos e eosinófilos, que participam como componentes do mecanismo de reparo tecidual. Macrófagos e neutrófilos ativados eliminam os restos celulares, células mortas e organismos invasores. Logo após a fase inicial inflamatória, miofibroblastos produzem componentes da matriz extra-celular e as células endoteliais formam novas vasos sanguíneos. Na fase subseqüente de remodelamento e maturação, miofibroblastos estimulam a contração da ferida. Fibras colágenas são produzidas e organizadas pelos fibroblastos, os vasos sanguíneos retornam ao normal e a cicatriz é eliminada. As células epiteliais se dividem e migram sobre a membrana basal restaurando os tecidos danificados por regeneração. Entretanto, no caso de lesões crônicas, o processo natural de cicatrização é perturbado. A inflamação, necrose tecidual e infecções persistentes, levam à ativação crônica de leucócitos e miofibroblastos, que contribuem para o acúmulo excessivo de elementos da matriz extra-celular, promovendo a formação permanente da cicatriz fibrótica.* ***Retirado de:*** *Wynn, T. A., J Clin Invest. 2007 Mar;117(3):524-9.*

Os mediadores inflamatórios são moléculas solúveis que atuam localmente na lesão ou de forma sistêmica. São originários do plasma, de células inflamatórias ou dos tecidos lesados, e apresentam redundância funcional. Sistemas derivados do plasma, tais como complemento, cininas e fibrinogênio, são ativados e seus produtos serão responsáveis pelos efeitos inflamatórios, assim como os produtos de células que produzem mediadores lipídicos, espécies reativas de oxigênio, citocinas e quimiocinas (2, 15, 16). Por exemplo, o Fator de Ativação Plaquétaria (PAF) é um fosfolipídio derivado de membrana envolvido na ativação de endotélio e leucócitos, induzindo a produção de citocinas e quimiocinas por estas células, além de ser um importante mediador de condições inflamatórias pulmonares (17). Óxido nítrico e peróxido de hidrogênio são liberados por leucócitos inflamatórios e fagócitos na presença de patógenos, ativando o endotélio vascular e induzindo proliferação e produção de mediadores solúveis (18).

As citocinas são proteínas secretadas com função na regulação da resposta imune, podendo regular também o tráfego e organização celulares em órgãos linfóides. As citocinas, em geral, agem como fatores de crescimento na diferenciação e proliferação celular, e na maturação de células de medula óssea. Algumas são quimiotáticas e possuem propriedades ativadoras e supressoras, incluindo indução da morte celular programada nos mais diversos grupos celulares que determinam a natureza da resposta imune (19). Dentre elas, destacamos a tríade pró-inflamatória clássica, a IL-1β (Interleucina-1β), IL-6 e TNF-α, que causam modificações locais, tais como edema e exsudação, ou podem agir de forma sistêmica quando sinalizam de forma parácrina, maturando e recrutando leucócitos da medula e até desencadear febre (2, 19, 20). Outras citocinas, como IL-4, IL-5 e IL-13, participam de respostas alérgicas e induzem a diferenciação de eosinófilos, produção de muco por células caliciformes e mudança de isotipo de anticorpos (19). O Fator de Crescimento Transformante (TGF-β_1) é uma citocina de função pleiotrópica, produzido por células como macrófagos, fibroblastos e linfócitos. Esta molécula é capaz de induzir repostas proliferativas envolvidas na angiogênese

e fibrose. Juntamente com a IL-10, o TGF-β_1 possui um importante papel como modulador negativo de respostas imunes, suprimindo proliferação celular e induzindo apoptose, além de participar do processo de tolerância a alérgenos (19, 20). O Interferon-γ (IFN-γ) é um mediador relacionado a respostas virais, inibindo sua replicação, e é produzido por linfócitos e células *Natural Killer*, atuando também na apresentação de antígeno, expressão de moléculas de MHC (Complexo de Histocompatibilidade Principal) do tipo I e II, e estimulação da secreção de citocinas nos demais leucócitos (19). Pertencentes à família das citocinas, as quimiocinas, denominadas citocinas quimioatrativas (21), desempenham um importante papel em processos inflamatórios, primeiramente por guiarem o recrutamento e ativação de leucócitos para o sítio inflamatório e também por participarem dos processos de resolução e reparo (22). A seguir, será discutido um pouco mais sobre a biologia do sistema quimiocina.

1.2. O sistema quimiocina

Quimiocinas são grupos de moléculas relativamente pequenas (8 a 12 kDa) pertencentes a classe das citocinas, as quais exercem importante papel na biologia dos leucócitos, uma vez que controlam atividades de recrutamento e de ativação nos estados basal e inflamatório, guiando e direcionando os movimentos dos leucócitos (23). Além disso, outros tipos celulares, incluindo células epiteliais, endoteliais, do músculo liso e parenquimais, sofrem ação das quimiocinas (24, 25). São atribuídas às quimiocinas e seus receptores as propriedades de haptotaxia de leucócitos, controle da proliferação e embriogênese. Durante um processo patofisiológico, as quimiocinas contribuem para angiogênese, recrutamento e transmigração de leucócitos, remodelamento vascular e tecidual, eliminação de patógenos, apresentação de antígenos, cronificação da inflamação e reparo/cicatrização de tecidos, fibrose, tumorogênese e também são co-receptores para HIV (21, 23-26). Portanto, as quimiocinas são consideradas importantes tanto na homeostase quanto na patologia (12, 21, 24, 26, 27).

O sistema quimiocina em mamíferos é complexo, compreendendo cerca de 50 ligantes, constitutivos ou induzidos (Figura-2), e 20 receptores de sete domínios transmenbrânicos pertencentes à classe A dos receptores acoplados a proteína G (GPCR) do tipo *rhodopisin-like* (28). As quimiocinas são consideravelmente promíscuas quanto à ativação de receptores. Neste sistema, encontramos uma redundância funcional: a maioria dos receptores interage com vários ligantes e a maioria das quimiocinas interage com mais de um receptor (25) (*ver* Figura-5a). Atualmente são conhecidas 28 quimiocinas CC (CCL1-28), 16 quimiocinas CXC (CXCL1-16), duas quimiocinas C (XCL1-2), uma CX_3C (CX_3CL1) e uma C_6C (CCL21) que interagem com 10 receptores CC (CCR1-10), seis receptores CXC (CXCR1-6), um receptor XC (XCR1) e um receptor CX3C (CX3CR1), respectivamente (24); alguns receptores não possuem ligantes conhecidos e são classificados como sendo do tipo

órfão. Os receptores de quimiocinas são estruturalmente relacionados e sub-classificados de acordo com a posição relativa dos resíduos de cisteína conservados. Os membros do grupo de quimiocinas mais numeroso, CC ou a subfamília de quimiocinas–β, tem as primeiras duas cisteínas adjacentes. No grupo CXC, ou quimiocinas-α, as duas primeiras cisteínas estão separadas por um único aminoácido; alguns membros desta sub-família contêm um motivo, imediatamente antes da primeira cisteína amino-terminal, denominado ELR (Glutamato-Leucina-Arginina), o qual é responsável pela segmentação em dois sub-grupos: quimiocinas CXC-ELR^{+} e CXC-ELR^{-}. As subfamílias CX_3C e C são caracterizadas por terem as duas primeiras cisteínas separadas por três aminoácidos, e ausência da primeira e terceira cisteína, respectivamente (21, 27, 29). Este sistema complexo de receptores é amplamente distribuído sobre sub-tipos celulares, leucocitários e não-leucocitários. A expressão de uma combinação característica de receptores confere propriedades especificas sobre estas células, que pode variar durante os diversos estágios de maturação e ativação (24, 28) (Figura-2).

As quimiocinas são peptídeos que têm afinidade de ligação a heparanas sulfatadas, heparina e glicosaminoglicanas na matriz extracelular, que servem de sítio de ancoragem destes mediadores e possuem propriedades em criar um gradiente de quimiocinas essencial para o processo de haptotaxia (30, 31). Durante um processo inflamatório, várias proteases, tais como serino-proteases, metaloproteinases e dipeptidil peptidases, regulam a atividade biológicas das quimiocinas. Através da clivagem, estas são liberadas de seus sítios de fixação na matriz, de forma a criar um gradiente de concentração causado pela sua solubilização, podendo também se tornar ativas ou inativas, ou mudar funcionalmente de agonistas para antagonistas de seus receptores (29). A maior parte das quimiocinas é produzida e em seguida secretada, sendo as exceções CX_3CL1 e CXCL16, que são moléculas trensmembranares que necessitam ser clivadas proteoliticamente para que formem um gradiente solúvel quimiotático (32).

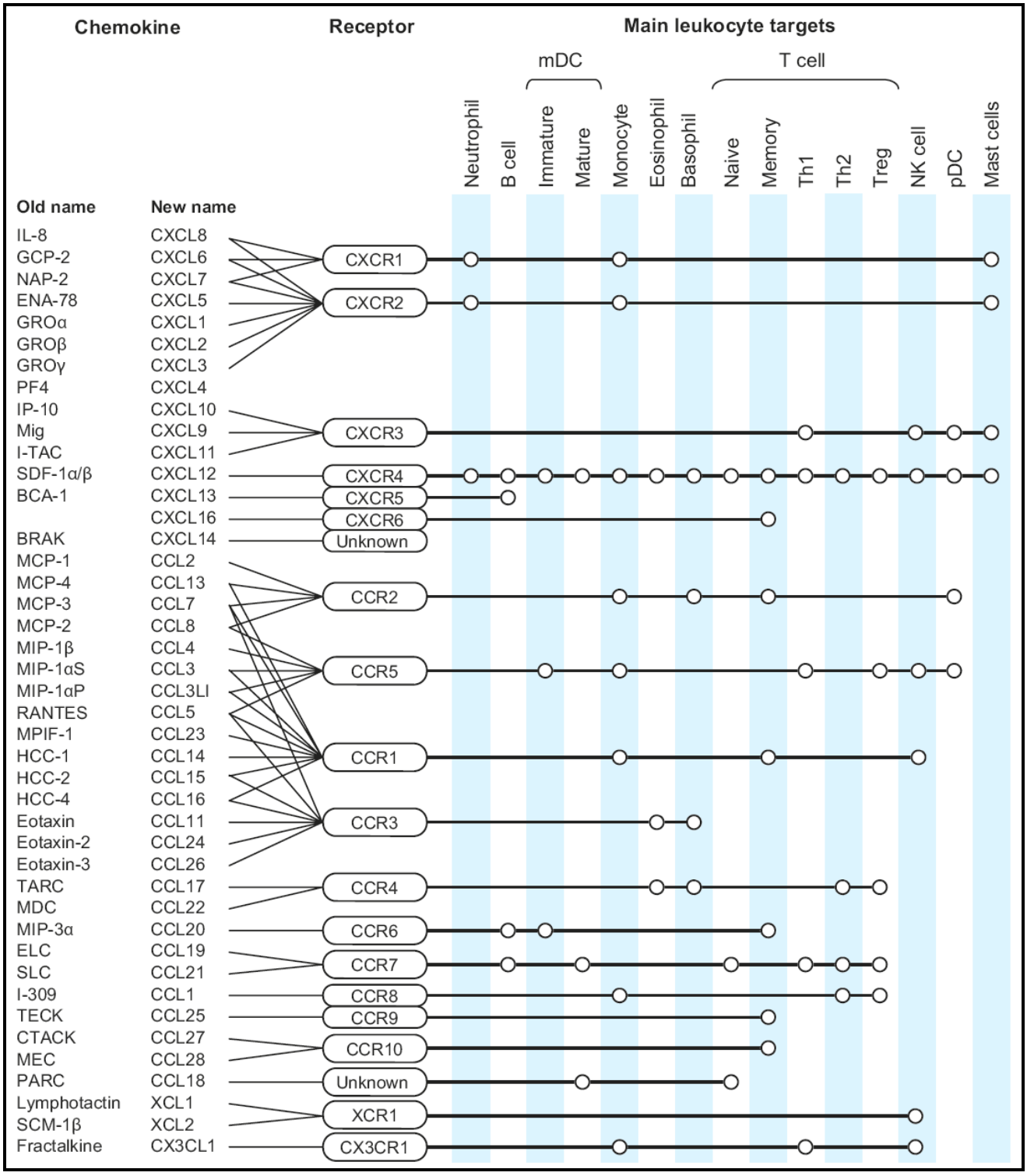


Figura-2: Quimiocinas humanas e seus receptores. *A velha e nova nomenclatura das quimiocinas, os seus receptores específicos e a distribuição destes receptores nos leucócitos.* ***Retirado de:*** *Viola, A., Annu Rev Pharmacol Toxicol. 2008;48:171-97.*

Um interessante detalhe é a atividade dual apresentada pelas quimiocinas, que naturalmente agem como antagonistas de receptores de sua mesma classe, independente de clivagem. Como exemplo, podemos citar alguns agonistas de receptores do tipo CXCR, que exercem funções como antagonistas de receptores CCR. Desta forma, uma quimiocina é agonista de seu respectivo receptor, mas exibe capacidade inibitória de outros receptores de quimiocinas, impedindo ou competindo pela ligação (33-36).

O domínio de interação dos receptores de quimiocinas consiste em três voltas extracelulares e uma porção amino-terminal, que se unem para ligar ao núcleo da quimiocina ligante (29). A sinalização mediada pela formação do complexo quimiocina:receptor causa uma mudança conformacional na estrutura terciária deste receptor e subseqüente endocitose, que dispara sinais de ativação intracelulares. A dissociação das sub-unidades G_{α} e $G_{\beta\gamma}$ causada pela sinalização do receptor de quimiocinas disparam a ativação de adenilato ciclase, fosfolipase-Cβ, PI3K, GTPases pequenas e canais iônicos, que levam ao aumento dos níveis de AMP (adenosina monofosfato) cíclico, inositol trifosfato (IP_3) e cálcio intracelular, alterando o estado de ativação celular (21, 37). Dentre estas alterações, encontramos a polimerização de filamentos de actina e polarização celular, aumento da capacidade fagocítica e aumento da sobrevida celular, translocação de NF-κB e transcrição de genes pró-inflamatórios, com aumento de produção de quimiocinas e expressão de seus receptores via *de novo* (27-29).

A interação da quimiocina com seu receptor, além de ativar as vias de sinalização intracelular leva à modificação de vacúolos e organelas citoplasmáticas, necessária para duas funções básicas: (i) reciclagem de receptores, e (ii) degradação de quimiocinas e receptores. Essas duas funções são de extrema importância para a regulação dos níveis de receptores na membrana, proferindo capacidade regulatória sobre a atividade celular e, também, como mecanismo de controle pós-transcricional dos níveis de quimiocinas pela sua atividade como

scavenger natural, tanto em condições patológicas como homeostáticas, respectivamente (27, 38, 39). Após a ligação da molécula com seu receptor, este é internalizado rapidamente via endocitose mediada por clatrina, associada principalmente a duas moléculas adaptadoras, adaptina 2 (AP-2) e β-arrestina, em um processo dependente de GTPases pequenas. Então, os complexos quimiocina:receptor são dissociados pela acidificação dos endossomos, que se fundem aos lisossomos imaturos (*early*) onde as quimicinas são degradadas pela ação do baixo pH destas vesículas. Posteriormente, os receptores são ubiquitinados e degradados nos lisossomos maduros (*late*). Alternativamente, os endossomos ácidos contendo receptores se fundem ao retículo endoplasmático com posterior fusão com a membrana celular, completando a reciclagem do receptor. Várias modificações nos receptores, tais como nas quimiocinas, também alteram a citrulinação, palmitolação, sulfatação e glicosilação interferindo na sua sinalização, tráfego e reciclagem (40, 41).

Os receptores de quimiocinas estão distribuídos na superfície celular e funcionam como sensores do meio externo, atuando de forma dinâmica, ao transmitirem sinais químicos extracelulares até o seu núcleo. Precisamente, estão localizados em *lipid rafts*, que são micelas flutuantes de colesterol presentes na membrana celular, importantes para o processo de oligodimerização de receptores, tanto na forma homodímera como heterodímeros, contribuindo para uma alteração da estrutura quaternária destes. A mudança estrutural atribui novas propriedades funcionais como co-internalização e até dessensibilização cruzada do receptor. Da mesma forma, quimiocinas se homo- ou hetero-oligomerizam de forma natural nos organismos quando presentes em altas concentrações, potencializando suas atividades sobre seus receptores (28, 42).

O sistema quimiocina também apresenta um grupo de receptores atípicos, classificados funcionalmente por apresentarem uma promiscuidade de ligações com seus agonistas e uma aparente incapacidade de disparar um sinal de ativação após sua interação.

Os receptores funcionais do tipo *decoy* são estruturalmente idênticos aos acoplados à proteína G, mas em suas condições naturais, estão desacoplados da maquinaria de sinalização, e por isso não transduzem um sinal positivo de ativação. Esta inabilidade de sinalização é conseqüência das modificações na seqüência canônica do motivo DRYLAIV, responsável por acoplar os receptores à proteína G. Ao contrário dos demais receptores de quimiocinas, os receptores *decoy* se ligam e seqüestram seus ligantes específicos, desenvolvendo uma importante função de *scavenger*, ou seja, diminuição dos níveis de quimiocinas. Assim, estes receptores atípicos competem com os receptores que normalmente sinalizam via proteína G, seqüestrando o ligante e degradando-o, desempenhando um estratégia primária de regulação negativa sobre quimiocinas inflamatórias, e também um mecanismo de controle pós-transcricional destas (43-45). Três receptores do tipo *scavengers* foram descritos com propriedades de se ligar a quimiocinas com alta afinidade. O primeiro foi chamado inicialmente de DARC (*Duffy antigen receptor for chemokines*), descrito com uma alta promiscuidade de ligação a quimiocinas CC e CXC, e encontrado sobre eritrócitos. DARC também está envolvido na apresentação de quimiocinas, desempenhando função em seu transporte e movimento da face sub-luminal para a face luminal do endotélio vascular, contribuindo, assim, para a migração trans-endotelial de leucócitos (43, 46).

D6 foi o segundo receptor descrito, com propriedades restritas apenas sobre as quimiocinas CC inflamatórias, sem sinalização ou atividade quimiotática detectada. Os receptores D6 são distribuídos sobre as células endoteliais linfáticas, principal portal de passagem de leucócitos para o linfonodo, na placenta, onde são responsáveis pela inibição da resposta inflamatória durante o desenvolvimento fetal. Também são expressos nos tecidos considerados “barreiras”, tais como pele, intestino e pulmão. Sua expressão é detectada no fígado, baço e tireóide, e também são expressos em leucócitos presentes no sítio de inflamação, em lesões da pele e inflamação pulmonar (27, 43, 44, 47-51). Atualmente, CCXCKR, ao contrário de DARC e D6 que fazem o *clearence* de quimiocinas inflamatórias,

é o único receptor *scavenger* de quimiocinas do tipo CC com propriedades homeostáticas (52).

Como o sistema de quimiocinas segue padrões molecular e funcional conservados ao longo da história evolutiva, implicando funções moduladoras imunes no processo de inflamação e infecção, patógenos co-evoluíram burlando ou evadindo o sistema imune do hospedeiro, através de mimetismo molecular. Atualmente são descritas várias quimiocinas e *decoys* codificados por patógenos, tais como receptores solúveis, antagonistas e proteínas-ligantes de quimiocinas (CKBPs) e antagonistas de glicosaminoglicanas. Estes mecanismos de evasão são produzidos por vírus (herpesvírus, poxvírus, citomegalovírus e vaccinia vírus), protozoários (*Plasmodium sp.* e *Toxoplasma gondii*), helmintos (*Schistosoma mansoni*) e ectoparasitas sanguíneos como o carrapato (*Rhipicephalus sanguineus*) (27, 53, 54).

Além das proteínas quimiocina-miméticas codificadas por patógenos que ativam seus receptores, recentemente foi apresentado um novo subtipo de moléculas não estruturalmente relacionadas às quimiocinas, denominadas "função quimiocina-*like"* (CLF), mas com capacidade de ativar e disparar sinais através de seus receptores (55). Dentre estas, estão as β-defensinas, que se ligam ao CCR6; a citocina chamada fator inibitório de migração de macrófagos (MIF), que é reconhecido por CXCR2 e CXCR4; e o tripeptídio Pro-Gly-Pro (PGP), liberados pela degradação do colágeno através da atividade das metaloproteinases (MMPs), que apresenta seqüência similar às quimiocinas ligantes do receptor CXCR2. Estas moléculas são ligantes endógenos não cognatos dos receptores de quimiocinas, que ampliam complexidade regulatória deste sistema (56-58).

1.3. Inflamação pulmonar

O pulmão pode ser dividido estruturalmente em duas partes principais: as vias aéreas centrais que compreendem traquéia, brônquios e bronquíolos terminais e o parênquima periférico composto por bronquíolos respiratórios, ductos alveolares e alvéolos. A parede alveolar é composta aproximadamente por 8% de pneumócitos do tipo I, 16% de pneumócitos do tipo II, 30% de células do endotélio capilar, 36% de células intersticiais e 10% de macrófagos alveolares. Dois tipos de células recobrem a superfície alveolar: os pneumócitos do tipo I são células epiteliais escamosas de revestimento enquanto os pneumócitos do tipo II são células cubóides, responsáveis pela produção de proteína surfactante. Macrófagos e fibroblastos compõem o grupo de células presentes no interstício, responsáveis pela manutenção e organização da membrana basal do alvéolo pulmonar (6).

Possuindo características estruturais únicas, o pulmão é considerado um importante órgão vascular, mas apresenta diferenças substanciais aos demais leitos vasculares sistêmicos. Geralmente, o extravasamento de leucócitos, tais como neutrófilos, ocorre no leito vascular diretamente das vênulas pós-capilares para o interstício. Entretanto, a migração no pulmão ocorre diretamente através dos capilares alveolares para dentro do alvéolo, e é influenciada pela anatomia e organização da parede alveolar. Este tipo de estrutura possibilita interações com células epiteliais, fibroblastos, células epiteliais alveolares do tipo I e II, que guiam a migração de leucócitos do leito capilar alveolar através do endotélio, espaço intersticial, e epitélio alveolar (6). O leito capilar alveolar possui uma arquitetura distinta que favorece a migração de células inflamatórias no pulmão.

O leito capilar alveolar é uma rede complexa interconectada de pequenos seguimentos capilares que passam de arteríolas para vênulas à medida que atravessam as paredes alveolares (aproximadamente oito paredes alveolares), que possuem aproximadamente 50 capilares. Comparado às demais grandes veias, o leito vascular pulmonar contém

aproximadamente 50 vezes mais neutrófilos, linfócitos e monócitos. O *tethering e rolamento*, mecanismos envolvidos na captura de leucócitos em grades vasos, aparentemente não são necessários no leito capilar alveolar. Vários seguimentos capilares possuem diâmetro de 2-15 μm, enquanto neutrófilos possuem um diâmetro esférico de 6-8 μm. Assim, em 50% dos seguimentos capilares estas células são obrigadas a se deformar, alongando-se para atravessar estes capilares, o que possibilita um maior contato com o endotélio e uma circulação pulmonar lenta (6).

Durante uma inflamação pulmonar, leucócitos seqüestrados nos capilares sofrem um processo de envolvimento físico e mudanças na adesão, não apenas em neutrófilos, mas também em células do endotélio. Citocinas e quimiocinas causam ativação e mudanças no citoesqueleto de leucócitos que são retidos e congestionam nos segmentos capilares, com liberação de protease e espécies reativas de oxigênio, amplificando o dano pulmonar. A migração através do endotélio capilar alveolar pode ocorrer de forma paracelular ou transcelular, mas apresentam preferência por migração em junções tri-celulares às margens de três células endoteliais (6) (Figura-3).

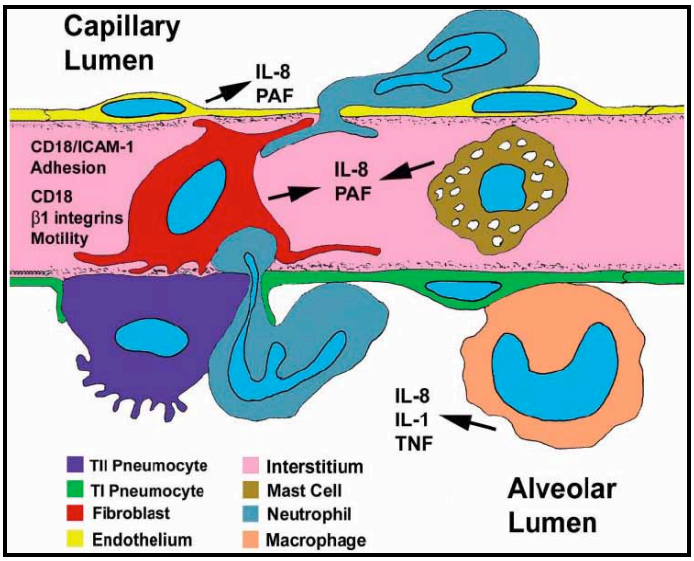


Figura-3: Diagrama ilustrativo da migração leucocitária no pulmão. *Neutrófilos migram diretamente do lúmen dos capilares da parede alveolar para o espaço alveolar, utilizam geralmente as junções tri-celulares endoteliais e são guiados até as vias aéreas por fibroblastos intersticiais, onde emergem na junção tri-celular entre dois pneumócitos do tipo I e um pneumócito do tipo II.* ***Retirado de:*** *Burns, A. R., Physiol Rev. 2003 Apr;83(2):309-36.*

Dentro do interstício, cada fibroblasto está posicionado bi-direcionalmente preenchendo os espaços nas membranas basal endotelial e basal epitelial, abaixo dos pneumócitos do tipo II. Os leucócitos que passaram por ali emergem dentro da compacta parede intersticial, onde fibroblastos e neutrófilos entram em contato principalmente por interações de adesão mediada por ICAM-1 e CD18, respectivamente. Em seguida, os fibroblastos guiam os neutrófilos até as junções tri-celulares da membrana basal, às margens de dois pneumócitos do tipo I e um pneumócito do tipo II. Através destes orifícios os leucócitos ganham o espaço sub-epitelial onde pneumócitos do tipo II direcionam o restante da migração através do epitélio, alcançando as vias aéreas (6) (Figura-3).

O acúmulo de leucócitos no trato respiratório baixo é característico dos estágios inflamatórios mais agudos. Após um dano tecidual causado por agentes lesivos, células epiteliais e endoteliais morrem por necrose ou apoptose, e funcionam como sentinelas disparando sinais que levam à produção de fatores envolvidos no reparo, tais como IL-10, IL-13 e TGF-β_1 (59). As demais células sobreviventes produzem mediadores do processo inflamatório em resposta ao estímulo estressante, tais como IFN-γ, TNF-α, IL-1β, VEGF, CXCL8, CXCL9, CCL2, CCL3, CCL5 que estimulam a proliferação, migração e ativação de leucócitos e células residentes (60). Esta inflamação pulmonar gerada pelo insulto inicial também contribui para o dano de células residentes e destruição dos tecidos. Localmente, há ativação da cascata de fibrinogênio e plaquetas são recrutadas, causando vaso-dilatação e aumento da permeabilidade vascular no pulmão, com migração de leucócitos para as áreas lesadas, contribuindo para o edema intersticial. Durante este processo de migração, metaloproteinases (MMP-1, -2, -7 e -9) clivam os constituintes da matriz extracelular permitindo o extravasamento de leucócitos, mas ao mesmo tempo alteram a estrutura do parênquima pulmonar separando o epitélio da membrana basal (59-63).

A natureza da resposta inflamatória pulmonar é influenciada dramaticamente pelo tipo de agente lesivo específico e pela produção de citocinas no micro-ambiente constituídos pelas células residentes danificadas e células inflamatórias. As respostas pró-inflamatórias pulmonares em resposta a patógenos e durante a auto-imunidade, podem ser associadas a respostas do tipo Th1 (T "*Helper*" 1) (64) ou Th17 (65-67), caracterizadas pela produção de TNF-α, IL-1β, IFN-γ e IL-17, IL-23, IL-22, respectivamente, e IL-21 e IL-25 em condições alérgicas (68-70). Respostas pulmonares de caráter alérgico podem ser desencadeadas pela produção de citocinas do tipo Th2 (59, 64, 71, 72), tais como IL-3, IL-4, IL-5, IL-9, IL-13. Estes tipos de respostas inflamatórias são controlados por respostas do tipo Th3, ou reguladora, na qual IL-10 e TGF-β_1 são os principais fatores implicados nos mecanismos de resolução e tolerância de respostas imunes, mas implicam também no reparo e fibrogênese (59, 71, 73). Juntamente com o sistema do complemento, cininas, fibrinogênio e produtos celulares, como mediadores lipídicos, espécies reativas de oxigênio e quimiocinas, as citocinas serão responsáveis pelos efeitos inflamatórios pulmonares.

Células endoteliais e fibroblastos ativados e em proliferação são encontrados nestes sítios inflamatórios, em resposta ao grande número de mediadores secretados. Fibroblastos, macrófagos e neutrófilos são capazes de manter esta resposta inflamatória crônica (74, 75). Quando o dano permanece crônico, e na presença de uma contínua produção de VEGF e quimiocinas CXC, células endoteliais entram em processo vasculogênico (formação de novos vasos) e brotamento de novas ramificações capilares surge a partir dos vasos sanguíneos existentes, processo este denominado angiogênese (59), que garante o suprimento de fatores e nutrientes para o acúmulo de leucócitos e proliferação de células mesenquimais nos tecidos inflamados cronicamente (76). Este mecanismo sustenta a formação do tecido de granulação e posteriormente contribui para o processo de cicatrização e fibrose do tecido, na ausência de re-epitelização pulmonar.

1.4. Fibrose pulmonar

A fibrose pulmonar é o estágio final comum entre um grupo diverso de distúrbios pulmonares conhecidos como Doenças Intersticiais Pulmonares. Estas são agrupadas por apresentarem manifestações clínicas semelhantes, classificadas por alterações patológicas, fisiológicas e radiográficas, com diversos graus de morbidade (77). Dentre estas, destacamos com grande importância a Fibrose Pulmonar Idiopática, doença crônica fibro-proliferativa letal, de origem desconhecida e sem terapêutica eficaz, caracterizada pela deposição excessiva de colágeno no interstício pulmonar. Seus sinais clínicos incluem uma piora da dispnéia, perda progressiva do volume pulmonar e troca gasosa anormal (78-80). A fibrose pulmonar idiopática tem uma prevalência média de 30 para cada 100.000 pessoas, com uma incidência média de 34.000 novos casos anualmente nos Estados Unidos (81). Geralmente, a morte associada a esta patologia é devida à perda progressiva da função pulmonar ao longo do tempo, o que leva ao colapso respiratório de seu portador, que apresenta uma sobrevida média de 3 a 5 anos após seu diagnóstico (78).

Sobre a origem da fibrose pulmonar idiopática, estudos têm investigado exaustivamente quais seriam os fenômenos precedentes responsáveis pelo desencadeamento desta patologia, embora sua ontogênese permaneça ainda controversa e pouco conhecida (82, 83). A grande busca, neste caso, tem sido direcionada a entender os eventos celulares e moleculares que expliquem os achados histopatológicos característicos desta doença. Atualmente são propostas algumas hipóteses acerca de sua origem, em que a fibrose ocorre por causa de uma eventual falha de comunicação entre células epiteliais e fibroblastos, independente de inflamação pulmonar prévia, ou pode se desenvolver através de uma rota inflamatória, na qual a fibrose é resultado de uma alveolite precedente (63, 82-86). Por exemplo, a Transição Epitelial–Mesenquimal (EMT) contribui como uma possível causa da fibrose (87). Neste caso, as células epiteliais sofrem metaplasia em presença de dano tecidual

em condições não-inflamatórias e, sem requerer divisão celular, se diferenciam em células mesenquimais, tais como fibroblastos e miofibroblastos (88). De fato, as células pulmonares apresentam uma característica natural peculiar, possuem certa plasticidade fenotípica, como as células alveolares do tipo II, que se trans-diferenciam em células alveolares do tipo I, que contribuem para re-epitelização e homeostase pulmonar (89). Porém, no caso da Transição Epitelial–Mesenquimal, esta mudança fenotípica contribui diretamente para a deposição de componentes da matriz extracelular, sendo causada pela presença de fatores de crescimento como Fator de Crescimento Epidermal (EGF), Fator de Crescimento de Hepatócitos (HGF), Fator de Crescimento de Fibroblastos (FGF) e TGF-β_1, uma vez que estes mesmos fatores possuem propriedades fibrogênicas (84-87, 90). Entretanto, a fibrose pulmonar é geralmente precedida por um dano pulmonar inflamatório crônico, e neste contexto, a excessiva fibrogênese é o resultado de um reparo inapropriado (59, 63, 91).

Os componentes da matriz extracelular são renovados constantemente e dependem diretamente de proteases específicas denominadas metaloproteinases. A matriz extracelular é constituída de uma rede complexa de macromoléculas que preenchem os espaços intercelulares. Entre suas malhas circula o líquido tecidual, originado na microcirculação, que banha as células e retorna aos vasos sanguíneos ou linfáticos. As macromoléculas da matriz extracelular podem estar estruturadas em forma de fibras ou sob a forma de substância amorfa. Os componentes da matriz são sintetizados e secretados por fibroblastos, células epiteliais e musculares lisas como constituintes das lâminas basais sob a forma de proteínas, como: (i) proteínas fibrosas (fibras colágenas, reticulares e elastina); (ii) proteínas de aderência (laminina e fibronectina) que fixam as células na matriz; (iii) glicosaminoglicanas e proteoglicanas, que formam um gel altamente hidratado que compõe a substância fundamental amorfa (92). A síntese e atividade da matriz são reguladas por citocinas, proteases, elastases e MMPs secretadas por fagócitos e seus inibidores naturais encontrados

nos tecidos (TIMPs), garantindo um balanço fisiológico entre a produção de matriz e sua degradação (61, 62).

A fibrogênese patológica tem sido referida como uma resposta de cicatrização de feridas fora do controle. O reparo de tecidos danificados é um processo biológico fundamental que permite a substituição ordenada de células mortas ou avariadas após uma lesão tecidual. Este tipo de lesão pode ser causado por diversos estímulos agudos ou crônicos, tais como infecções, reações auto-imunes e lesão química (73). O processo de reparo envolve duas fases distintas: uma fase regenerativa em que células danificadas são substituídas por células do mesmo tipo sem deixar traços de uma lesão, e uma fase de fibroplasia ou fibrose, em que o tecido conectivo substitui células do parênquima (73, 91). Ao contrário da resposta inflamatória aguda, caracterizada pela rápida resolução das alterações vasculares e leucocitárias, a fibrose pulmonar geralmente é o resultado de uma resposta inflamatória crônica, definida pelo caráter persistente (59, 91). Neste último caso, encontramos inflamação pulmonar crônica, lesão tecidual e reparo acontecendo simultaneamente (59). A contínua produção de fatores de crescimento, proteases, fatores angiogênicos, quimiocinas, e citocinas fibrogênicas são características do remodelamento progressivo, agindo como promotores da excessiva deposição de elementos da matriz extracelular no espaço parenquimático, que destroem a arquitetura normal pulmonar (59, 61, 77, 79, 91).

Dentre as possíveis causas da fibrose pulmonar, o desequilíbrio das funções de catabolismo e regeneração tecidual poderia ser responsável pela excessiva cicatrização decorrente de inflamações crônicas precedentes (59) (Figura-4). Neste caso, uma atividade desequilibrada entre as MMPs (metaloproteinases) e TIMPs (inibidores teciduais de metaloproteinases), levando ao aumento da atividade de MMPs, contribui para o dano tecidual, rompendo a membrana basal e permitindo maior influxo de leucócitos. Por outro lado, níveis elevados de TIMPs reduzem o *turnover* de matriz extracelular, que leva ao

aumento da deposição de colágeno (61, 62). O tempo de sobrevida e ativação dos fibroblastos também é responsável pela excessiva fibrose, já que essas células são os maiores produtores de colágeno nos sítios de inflamação crônica e o aumento na sua apoptose garante o sucesso da cicatrização reduzida (93). Diferentes proporções entre as taxas de apoptose das células epiteliais e re-epitelização alveolar contribuem para o desenvolvimento da fibrose pulmonar. Na ausência de uma re-epitelização ideal, mecanismos celulares de retirada dos detritos apoptóticos produzem citocinas relacionadas com o processo de resolução com atividade fibrogênica, como o TGF-β_1 (94, 95). A fibrose pulmonar também é considerada uma resposta a níveis elevados de quimiocinas, como por exemplo elevados níveis de CXC ELR$^+$ e baixos de CXC ELR$^-$, contribuindo para um ambiente pró-angiogênico (96) (Figura-4). Outras quimiocinas da família CC agem diretamente no recrutamento de fibrócitos, precursores mesenquimais derivados da medula que se diferenciam em miofibroblastos (96-98), e ativação de fibroblastos (99). A seguir estudaremos em detalhe o papel das quimiocinas na fibrose pulmonar.

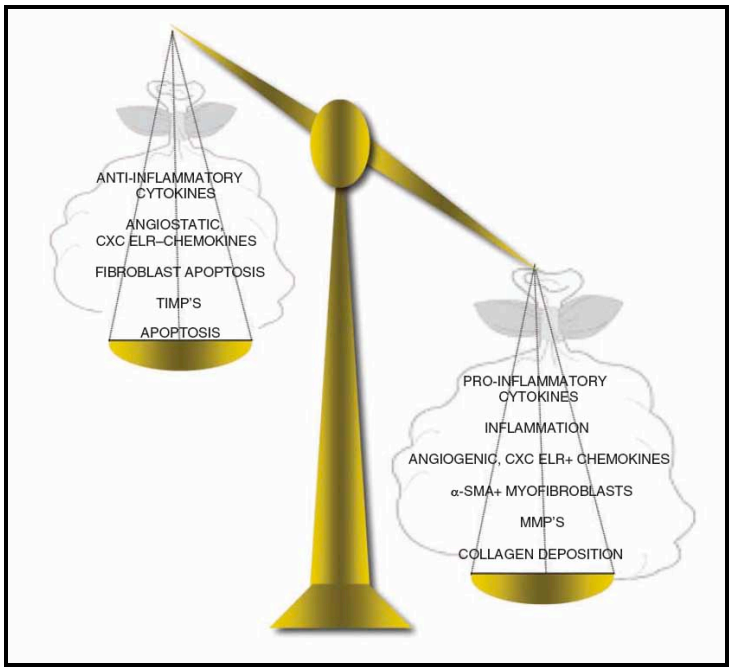


Figura-4: A fibrose como resultado de uma resposta cicatricial desbalanceada. *Para haver uma cicatrização não patológica, uma resposta cicatricial deve ser mantida balanceada através de ciclos de retroalimentação negativa, com um equilíbrio entre o catabolismo e o processo regenerativo.* ***Retirado de:*** *Wilson, M. S., Mucosal Immunol. 2009 Mar;2(2):103-21.*

1.5. Quimiocinas e fibrose pulmonar

A patogênese da fibrose pulmonar é causada por uma sinalização desregulada ou inflamação, em que as quimiocinas são responsáveis pela manutenção da homeostase dos tecidos e coordenam a resposta à lesão (64, 84). Dados clínicos têm revelado uma estreita correlação entre fibrose pulmonar idiopática, níveis de quimiocinas circulantes ou no lavado bronco-alveolar (BAL), e perfil leucocitário. Estudos iniciais investigaram o mecanismo de recrutamento e ativação de neutrófilos no pulmão de pacientes com IPF. Foi detectado um aumento dos transcritos de RNA para CXCL8 (IL-8) em macrófagos alveolares, associado a elevados níveis de IL-8 e número alto de neutrófilos no BAL (100). IL-8 também apresentou atividades pró-angiogênica, ao contrário de CXCL10 (IP-10), que é pró-angiostática e geralmente encontrada em BAL de indivíduos sadios (101). Posteriormente, a determinação dos níveis de IL-8 no soro de pacientes foi sugerida como um parâmetro clínico do monitoramento de pacientes com IPF, pois elevados níveis circulantes correlacionavam ao grau da alveolite neutrofílica observada (102). Fibrócitos presentes na circulação de pacientes com IPF apresentam receptores CXCR4 associados a elevados níveis de seu agonista CXCL12 (SDF-1), indicando que precursores de miofibroblastos são recrutados da circulação para o foco da fibrose (103). Estes dados sugerem que quimiocinas da família CXC exercem funções duais na patologia da IPF, controlando o influxo de neutrófilos, angiogênese e fibroplasia.

Membros da família CC das quimiocinas estiveram relacionados com a migração e ativação de macrófagos, linfócitos e fibroblastos. Sobre a natureza da migração de macrófagos associada à CCL2 (MCP-1) em pacientes com IPF, foi demonstrado que as células epiteliais e fibroblastos são os maiores produtores desta quimiocina e responsáveis pela migração macrofágica e produção de colágeno por fibroblastos (99, 104). Os níveis de CCL22 (TARC) também foram detectados elevados em BAL de pacientes com IPF, sendo

responsáveis pelo recrutamento e ativação de macrófagos alveolares CCR4+ (105). A linfocitose alveolar em pacientes com IPF esteve associada ao aumento dos níveis de CCL3 (MIP-1α), CCL4 (MIP-1β) e CCL5 (RANTES) no BAL, também com participação de eosinófilos e macrófagos alveolares (106-108). Análises das biópsias de indivíduos com IPF mostraram aumento da expressão do receptor CCR7 especificamente em fibroblastos, que apresentaram capacidade quimiotática na presença de CCL21 (6Ckine) e de ativação, sugerindo que esta interação pode modular o desenvolvimento da fibrose pulmonar (109).

Para entender melhor os aspectos relacionados com o papel das quimiocinas no desenvolvimento da fibrose pulmonar idiopática, modelos de fibrose pulmonar têm sido desenvolvidos usando cobaias através da administração de agentes lesivos de forma intra-traqueal, tais como FITC, sílica e bleomicina (110). A bleomicina pertence à família dos glicolipídios classificados como antibióticos citotóxicos, primeiramente isolada da cepa *Streptomyces verticillus* em 1966 por Umezawa e colaboradores (111). Na clínica, o uso desta molécula está relacionado com o tratamento de neoplasias, carcinomas e linfomas de boca, esôfago e pulmão, mas seu uso é restrito devido a manifestações tóxicas pulmonares. Dentre seus efeitos colaterais estão pneumonite intersticial, que em 46% dos casos evolui para fibrose (111). A fibrose pulmonar experimental induzida por bleomicina em animais é um modelo sistemático de investigação dos mecanismos celulares e bioquímicos envolvidos na patogênese da fibrose pulmonar, uma vez que durante este processo o tecido pulmonar sofre mudanças morfológicas e bioquímicas que se assemelham às observadas em pacientes (75, 110). A bleomicina é geralmente administrada de forma intra-traqueal em modelos experimentais, e causa dano tecidual por estresse oxidativo, com conseqüentes quebras duplas e simples de DNA e RNA. Após este dano inicial, uma inflamação pulmonar é disparada e se auto-sustenta, evoluindo para o reparo excessivo e fibrose. Após o dano tecidual causado pela ação da bleomicina, as células presentes no tecido pulmonar, destacando-se dentre estas as

células epiteliais, endoteliais e macrófagos residentes, liberam quimiocinas que orquestram toda a resposta inflamatória subseqüente (60).

Vários mecanismos acerca do papel das quimiocinas têm sido elucidados através do modelo de fibrose pulmonar induzida por bleomicina em camundongos, principalmente pela disponibilidade de anticorpos bloqueadores e pelo uso de animais geneticamente modificados, de forma a super-expressar ou suprimir genes destas moléculas e seus receptores (112). Diversos trabalhos vêm mostrando que interferências em algumas quimiocinas ou em seus receptores podem influenciar o desenvolvimento da fibrose pulmonar. Como por exemplo, CXCL9, CXCL10 e CXCL11, agonistas de receptores CXCR3 exibem atividade anti-fibrogênica secundária à redução da angiogênese pulmonar, quando administradas de forma exógena. A deleção do receptor CXCR3 ou de seus agonistas, e também o bloqueio através de anticorpos, aumentou a susceptibilidade ao desenvolvimento da fibrose induzida por bleomicina em camundongos (113-116). Em contrapartida, a neutralização de CXCL2 usando anticorpos ou através do uso de antagonistas bloqueadores de receptores CXCR2 reduziu a angiogênese e inflamação neutrofílica no modelo induzido por bleomicina (117, 118), demonstrando uma função pró-fibrogênica deste receptor e seus cognatos, corroborando o observado em pacientes (101).

CCR2 é o principal receptor de CCL2, responsável pelo tráfego de monócitos e macrófagos para sítios de inflamação, sendo alvo de investigação no contexto da fibrose pulmonar. Experimentos usando terapia gênica anti-CCL2 em camundongos demonstram a capacidade de atenuar a fibrose pulmonar induzida por bleomicina (119). De fato, esta atenuação pode ser causada pela redução do infiltrado e atividade macrofágica no tecido pulmonar, como demonstrado em camundongos CCR2 deficientes desafiados com bleomicina (120). Outros estudos também demonstraram que a deficiência de CCR2 e CCL2, ou a neutralização de CCL2 e CCL12 modificavam o recrutamento de fibrócitos e fibroblastos

para os pulmões, causando redução na proliferação, na produção de colágeno e no *homing* de fibrócitos, sugerindo ainda que CCR2 é um modulador da responsividade a TGF-β_1 em fibroblastos (98, 99, 121, 122). Atualmente, os mecanismos que controlam o recrutamento de fibrócitos para os sítios de fibro-proliferação têm sido alvo de profundas investigações. Estas células também expressam os receptores CXCR4 e CCR5, sendo que CXCL12 e CCL3 são responsáveis pelo acúmulo e produção de colágeno, respectivamente. A neutralização de CXCL12 ou o bloqueio de receptores CXCR4 foram capazes de reduzir a fibrose induzida por bleomicina pela redução do influxo pulmonar de fibrócitos circulantes (123-126), tão quanto em animais duplo-deficientes para CCL3-CCR5 (97), demonstrando uma atividade fibrogênica diretamente ligada às quimiocinas.

De modo geral, o papel das quimiocinas ligadas ao processo de fibrose pulmonar está bem relacionado com a inflamação causada pelo recrutamento de diferentes populações leucocitárias. A ausência de CCR5 e CCL3 causa uma redução no influxo pulmonar de macrófagos produtores de TGF-β_1 e polimorfonucleares, que estiveram associados a uma menor fibrose (97). Além do recrutamento macrofágico dependente de CCR2-CCL2, CCL17 participa da migração de macrófagos CCR4 positivos (127), e a deficiência de CCR4 modula negativamente a produção de espécies reativas de oxigênio responsável pela fibrose pulmonar (128). O número reduzido de eosinófilos e neutrófilos, além de menor quadro fibrótico, também foram encontrados em animais deficientes tanto pra CCL11 quanto para seu receptor CCR3 (129). Da mesma forma, a neutralização de CCR1 reduz linfócitos CD4, células dendríticas e deposição de colágeno (130). Portanto, estudos como estes são de grande valor, pois além de contribuir para o entendimento dos mecanismos envolvidos no desenvolvimento desta patologia, indica novos caminhos que sugerem o bloqueio das atividades das quimiocinas como novos alvos terapêuticos para a fibrose pulmonar idiopática.

1.6. Quimiocinas como alvo farmacológico

Aproximadamente 20 anos se passaram desde a identificação das quimiocinas, já descritas em várias patologias inflamatórias agudas, crônicas, auto-imunes, alérgicas e infecciosas, além do câncer e síndrome de imunodeficiência adquirida (AIDS). Resultados de diversos estudos farmacológicos, usando anticorpos neutralizantes ou animais deficientes para componentes dos sistema quimiocinas, têm destacado o potencial terapêutico que este sistema complexo possui durante o desenvolvimento de patologias inflamatórias. Porém, a interação das quimiocinas com seus receptores é caracterizada por uma promiscuidade considerável, em que existem vários ligantes para um receptor e vários receptores para um só ligante, o que vem a ser um fator que dificulta o desenvolvimento de fármacos seletivos (Figura-5a) (131, 132). Atualmente, uma variedade de compostos modificadores das atividades das quimiocinas tem sido apresentada, com o objetivo de impedir a interação destas com seus respectivos receptores.

Uma das formas de bloquear a interação quimiocina:receptor é através da neutralização dos ligantes. Anticorpos anti-quimiocinas se ligam a estas proteínas opsonizando-as, impedindo sua ligação ao receptor (Figura-5b) (132). Seguindo a mesma linha, proteínas ligantes de quimiocinas (*Chemokine-binding proteins* - CKBPs) causam alterações em sua estrutura quaternária, modificando sua atividade na ligação a seu receptor (Figura-5b e 6d) (132). A segunda forma de interferir na atividade das quimiocinas é através do bloqueio de receptores utilizando anticorpos anti-receptores (Figure-6a) ou inibidores antagonistas de baixo peso molecular (Figura-5c e 6b). Estes podem ser classificados em (i) antagonistas ortostéricos, que se ligam no mesmo sítio dos agonistas endógenos competindo pela ligação via bloqueio, e (ii) antagonistas alostéricos, que se ligam ao receptor numa região diferente daquela do agonista endógeno, causando uma mudança conformacional que impede o reconhecimento da quimiocina (131).

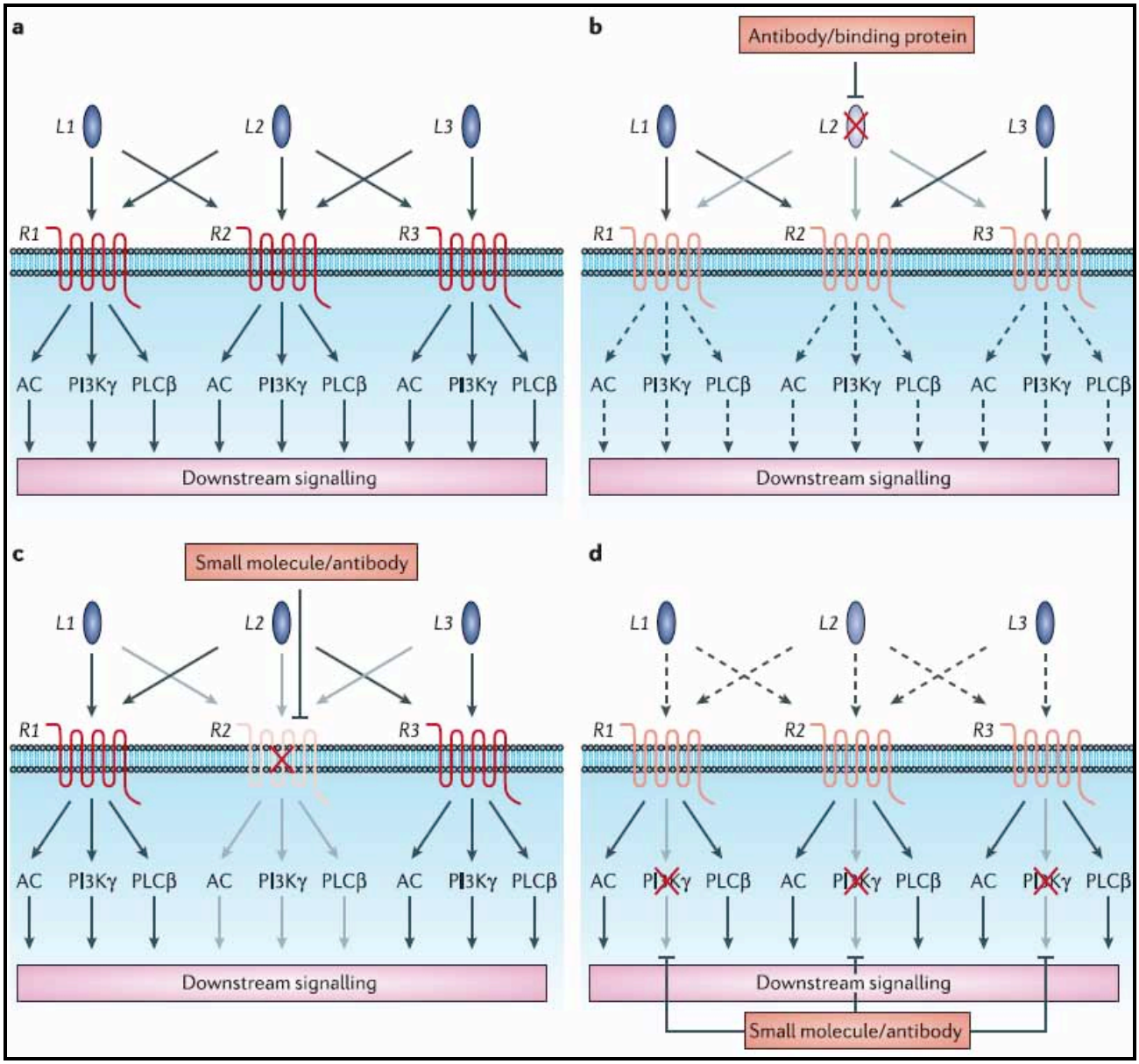


Figura-5: Estratégias para interferir em processos mediados por quimiocinas/receptores de quimiocina. a) *Redundância do sistema quimiocina: vários ligantes (L1-L3) para um receptor (R1-R3), vários receptores para um ligante.* ***b)*** *Intervenção farmacológica no nível de quimiocina (L1-L3), através do uso de anticorpos ou proteínas ligantes de quimiocinas (CKBPs).* ***c)*** *Intervenção farmacológica a nível de receptor (R1-R3), através de antagonistas de receptor ou anticorpos anti-receptor.* ***d)*** *Intervenção farmacológica no nível da sinalização de receptores, através do uso de moléculas de baixo peso molecular ou anticorpos contra componentes da cascata de sinalização intracelular compartilhada entre os receptores de quimiocina.* ***Retirado de:*** *Rückle, T., Nat Rev Drug Discov. 2006 Nov;5(11):903-18.*

Juntamente a estas, outras moléculas inibidoras têm sido descritas, como as quimiocinas modificadas que competem com as naturais pelo sítio de ancoragem presente nas glicosaminoglicanas de matriz (Figura-6c), impedindo a formação de um gradiente de concentração quimiotático (30, 132). Recentemente, a inibição das vias de sinalização

intracelular PI3K, mTOR e MAP kinases, disparadas pelos receptores em resposta às quimiocinas, tem ganhado grande destaque no desenvolvimento de novos fármacos. Através do bloqueio do sinal gerado pela formação do complexo quimiocina:receptor, é possível a regulação negativa da atividade biológica de células inflamatórias ou em proliferação (Figura-5d), além de agir de forma abrangente sobre a capacidade sinalizadora de inúmeros receptores que possuem vias de sinalização comuns (37).

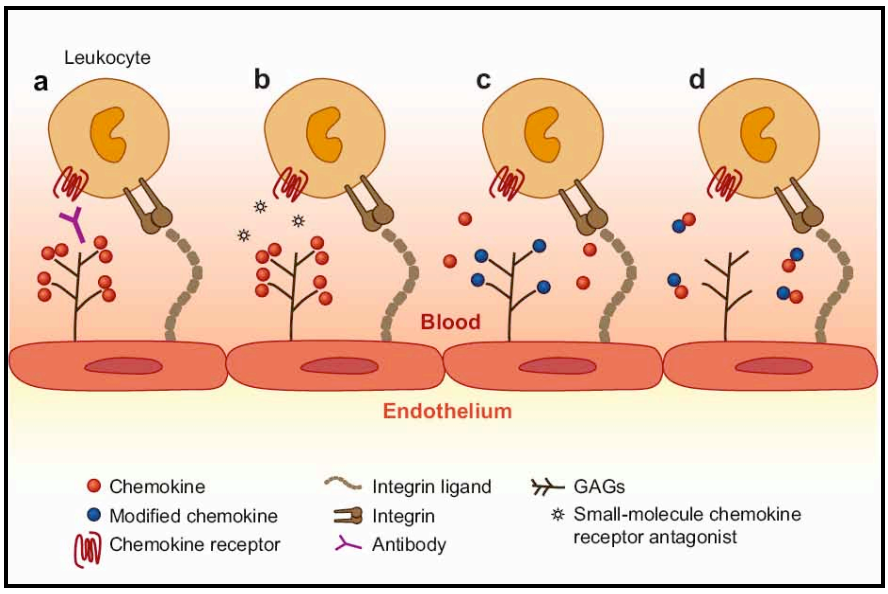


Figura-6: Estratégias para interferir em processos mediados por quimiocinas/receptores de quimiocina. *A migração de leucócitos para os sítios de inflamação podem ser bloqueados através de:* ***a)*** *anticorpos anti-receptor.* ***b)*** *antagonistas de receptores.* ***c)*** *quimiocinas não-funcionais que se ligam às glicosaminoglicanas (GAGs) e não ativam o receptor, competindo com o ligante pelo sítio de ancoragem na matriz.* ***d)*** *quimiocinas não-funcionais que se ligam a outras quimiocinas, impedindo que se liguem nos sítios de ancoragem nas glicosaminoglicanas (GAGs).* ***Retirado de:*** *Viola, A., Annu Rev Pharmacol Toxicol. 2008;48:171-97.*

Considerando que as quimiocinas possuem a característica distinta de direcionar o recrutamento e ativação de diversas populações celulares pela seletiva expressão dos seus receptores, o bloqueio da migração patológica poderia ser benéfico para indivíduos que sofrem de doenças inflamatórias e auto-imunes. Neste contexto, as quimiocinas e seus receptores se tornam importantes alvos de intervenção terapêutica.

2. JUSTIFICATIVA E OBJETIVO GERAL

O sistema quimiocina compreende uma complexa rede de sinais que orquestram várias funções nos mais diversos tipos leucocitários e demais populações celulares, que vão desde a manutenção da homeostase fisiológica até condições patológicas. Neste último caso, as quimiocinas têm sido apontadas como moléculas críticas reguladoras dos processos patofisiológicos pulmonares, responsáveis pela resposta contra patógenos, rejeição de transplantes e tumorogênese (133-137).

Apesar dos grandes avanços no entendimento acerca da biologia do sistema quimiocina e no desenvolvimento experimental de novos fármacos que possuem atividades moduladoras sobre a rede de eventos moleculares e celulares envolvidos no processo inflamatório, pouco ainda se sabe sobre o papel da modulação terapêutica deste sistema durante processos inflamatórios crônicos e fibro-proliferativos pulmonares (138-140).

Assim, o objetivo geral do presente estudo foi investigar a contribuição das quimiocinas e seus receptores para o processo de desenvolvimento da fibrose pulmonar em camundongos, de forma induzida pela administração de bleomicina. Dentre os objetivos específicos, nosso estudo visou estudar a participação dos receptores CXCR1/2, a participação da quimiocina CCL3, e a participação da PI3Kγ, uma via de sinalização comum entre diversos GPCRs, no desenvolvimento da fibrose pulmonar. Para isso, foram utilizadas três formas de intervenção: (i) bloqueio de receptores por antagonistas alostéricos não-competitivos, (ii) neutralização da quimiocina através de proteínas ligantes de quimiocinas (CKBP), e (iii) ausência da isoforma γ da PI3K pelo uso de animais geneticamente deficientes.

3. TRABALHOS CIENTÍFICOS

3.1. Trabalho cientifico – 1

RUSSO, R. C.; GUABIRABA, R.; GARCIA, C. C.; BARCELOS, L. S.; ROFFÊ, E.; SOUZAS, A. L. S.; AMARAL, F. A.; CISALPINO, D.; CASSALI, G. D.; DONI, A.; BERTINI, R.; TEIXEIRA, M. M. ***Role of the chemokine receptor CXCR2 in bleomycin-induced pulmonary inflammation and fibrosis.*** **Am J Respir Cell Mol Biol.** 2009 Apr;40(4):410-21.

Os objetivos específicos deste estudo foram:

1. Caracterizar os efeitos inibitórios do antagonista alostérico não-competitivo de receptores CXCR1/2, DF2162, sobre a inflamação e fibrose pulmonar induzida por bleomicina *in vivo*.

2. Estudar e comparar os efeitos nos regimes preventivo e terapêutico de tratamento com DF2162 durante a fibrose pulmonar induzida por bleomicina *in vivo.*

3. Avaliar os efeitos da administração antagonista alostérico não-competitivo de receptor CXCR1/2 sobre funções endoteliais humanas estimuladas com quimiocina *in vitro*.

Role of the Chemokine Receptor CXCR2 in Bleomycin-Induced Pulmonary Inflammation and Fibrosis

Remo C. Russo[1], Rodrigo Guabiraba[1], Cristiana C. Garcia[1], Lucíola S. Barcelos[1], Ester Roffê[1], Adriano L. S. Souza[1], Flávio A. Amaral[1], Daniel Cisalpino[1], Geovanni D. Cassali[2], Andrea Doni[3], Riccardo Bertini[4], and Mauro M. Teixeira[1]

[1]Laboratório de Imunofarmacologia, Departamento de Bioquímica e Imunologia, and [2]Departamento de Patologia Geral, Instituto de Ciências Biológicas, Universidade Federal de Minas Gerais, Belo Horizonte, MG, Brazil; [3]Istituto Clinico Humanitas (ICH), IRCCS, Department of Immunology and Inflammation, Rozzano, Milan, Italy; and [4]Department of Preclinical Pharmacology, Dompé pha.r.ma s.p.a., L'Aquila, Italy

Pulmonary fibrosis is characterized by chronic inflammation and excessive collagen deposition. Neutrophils are thought to be involved in the pathogenesis of lung fibrosis. We hypothesized that CXCR2-mediated neutrophil recruitment is essential for the cascade of events leading to bleomycin-induced pulmonary fibrosis. CXCL1/KC was detected as early as 6 hours after bleomycin instillation and returned to basal levels after Day 8. Neutrophils were detected in bronchoalveolar lavage and interstitium from 12 hours and peaked at Day 8 after instillation. Treatment with the CXCR2 receptor antagonist, DF2162, reduced airway neutrophil transmigration but led to an increase of neutrophils in lung parenchyma. There was a significant reduction in IL-13, IL-10, CCL5/RANTES, and active transforming growth factor (TGF)-β_1 levels, but not on IFN-γ and total TGF-β_1, and enhanced granulocyte macrophage–colony-stimulating factor production in DF2162-treated animals. Notably, treatment with the CXCR2 antagonist led to an improvement of the lung pathology and reduced collagen deposition. Using a therapeutic schedule, DF2162 administered from Days 8 to 16 after bleomycin reduced pulmonary fibrosis and levels of active TGF-β_1 and IL-13. DF2162 treatment reduced bleomycin-induced expression of von Willebrand Factor, a marker of angiogenesis, in the lung. *In vitro*, DF2162 reduced the angiogenic activity of IL-8 on human umbilical vein endothelial cells. In conclusion, we show that CXCR2 plays an important role in mediating fibrosis after bleomycin instillation. The compound blocks angiogenesis and the production of pro-angiogenic cytokines, and decreases IL-8–induced endothelial cell activation. An effect on neutrophils does not appear to account for the major effects of the blockade of CXCR2 in the system.

Keywords: CXCR2; neutrophil; angiogenesis; bleomycin; fibrosis

CLINICAL RELEVANCE

These findings may assist in the development of new therapies for lung fibrosis and broaden our understanding of the biology of neutrophils, CXCR2, and mechanisms of lung fibrosis.

Idiopathic pulmonary fibrosis (IPF) is a common end-stage of a group of heterogeneous disorders characterized by excessive and progressive lung interstitial collagen deposition. It is an untreatable disease with unknown etiology that affects approximately 100,000 people in the United States (1, 2). Pulmonary fibrosis has been proposed to result from abnormal lung healing in response to an injury to the alveolar epithelium (3).

Bleomycins are a family of glycopeptides antibiotics (4) with potent anti-tumor activity against a range of lymphomas, head and neck cancers, and germ-cell tumors (5). The therapeutic efficacy of bleomycin is limited by development of lung fibrosis (6, 7). Bleomycin instillation in the lung is the most frequently used experimental model to investigate cellular and biochemical mechanisms relevant for the pathogenesis of pulmonary injury and fibrosis. Bleomycin is usually administered in a high dose by single intratracheal instillation, and induces morphologic and biochemical changes in animal lungs that resemble those observed in human IPF (8). The pulmonary response to bleomycin injury is complex, requiring the coordinated expression of different cytokines and chemokines, as well as proliferation and migration of multiple cell types, including leukocytes, epithelial cells, endothelial cells, and fibroblasts (9).

Chemokines are small chemoattractant molecules that act on specific seven-transmembrane chemokine receptors and induce the activation and recruitment of leukocytes (10, 11). Chemokines may also modulate angiogenesis, wound healing, and tumorogenesis via interaction with leukocytes, endothelial cells, and fibroblasts (12), and are grouped into four categories—CXC, CC, C, and CX3C—based upon the presence of conserved cysteine residues within the mature peptides (10). It has been suggested that activation of the chemokine receptor CXCR2 by the chemokines CXCL1/KC (keratinocyte-derived chemokine) and CXCL2/MIP-2 (macrophage inflammatory protein-2) may play a relevant role in angiogenesis (13, 14), neutrophil recruitment into sites of inflammation (15–17), and hypernociception (18). Although neutrophils play an essential role in host defense against several pathogens (19), neutrophilic inflammation and angiogenesis process may also contribute to the pathogenesis of a range of chronic syndromes, including pulmonary fibrosis (20–22). The present study was performed to test the hypothesis that CXCR2-mediated neutrophil recruitment plays an important role in the development of pulmonary fibrosis. To this end, we evaluated the effect of a long-acting orally bioavailable antagonist of the receptor CXCR2, DF2162 (17, 18), in a model of pulmonary fibrosis induced by bleomycin in mice.

MATERIALS AND METHODS

Animals, Drugs, and Reagents

Eight- to 10-week-old male C57Bl/6J (WT) mice obtained from Centro de Bioterismo (CEBIO) of the Universidade Federal de Minas Gerais (UFMG, Brazil) and maintained in the animal facilities of Laboratório de Imunofarmacologia, Department of Biochemistry and Immunology (UFMG, Brazil), with filtered water, food *ad libitum*, and in a controlled

(*Received in original form October 4, 2007 and in final form July 16, 2008*)

This investigation received financial support from the Coordenação de Aperfeiçoamento de Pessoal de Nível Superior (CAPES/Brazil), Fundação de Amparo a Pesquisa do Estado de Minas Gerais (FAPEMIG/Brazil), Conselho Nacional de Desenvolvimento Científico e Tecnológico (CNPq/Brazil), and the European Union's Sixth Framework Programme (INNOCHEM project grant LSHB-CT-2005-518167).

Correspondence and requests for reprints should be addressed to Mauro M. Teixeira, M.D., Ph.D., Laboratório de Imunofarmacologia, Departamento de Bioquímica e Imunologia, Instituto de Ciências Biológicas, Universidade Federal de Minas Gerais, Avenida Antônio Carlos, 6627, CEP 30882-650–Pampulha, Belo Horizonte, MG, Brazil. E-mail: mmtex@icb.ufmg.br

Am J Respir Cell Mol Biol Vol 40. pp 410–421, 2009
Originally Published in Press as DOI: 10.1165/rcmb.2007-0364OC on October 3, 2008
Internet address: www.atsjournals.org

environment (temperature and humidity) were used in the present study. All experiments were conducted under conditions approved by the local animal ethics committee, CETEA/UFMG (Protocol number 146/06). Bleomycin sulfate (Blenoxane; Bristol-Myers Squibb, New York, NY); ketamine (Dopalen; Vetbrands, São Paulo, Brazil); xylazine (Calmiun; Agener União Saúde Animal S.A., São Paulo, Brazil); carboxymethylcellulose (Sigma Chemical Co., St. Louis, MO); PBS (phosphate buffered saline, pH 7.4); recombinant human CXCL-8/IL-8 (R&D Systems, Minneapolis, MN); endothelial cell basal medium-2 (EBM-2; Cambrex BioScience, Walkersville, MD); Growth factor-reduced Matrigel matrix (BD Bioscience, Bedford, MA). DF2162 was synthesized at Dompé Research and Development (Dompé S.p.A., L'Aquila, Italy).

Bleomycin-Induced Lung Injury and Fibrosis in Mice

Animals were anesthetized intraperitoneally with 80 μl of a ketamine and xylazine solution (3.2 mg/kg and 0.16 mg/kg, respectively) before tracheotomy. A single 25-μl injection containing 0.125 U of bleomycin (Blenoxane; Bristol-Meyers) diluted in PBS, or PBS only (control group), was instilled intratracheally using Hamilton syringes. In each time-point after bleomycin, or PBS administration, animals were killed by a lethal dose of ketamine and xylazine, to perform bronchoalveolar lavage and collect lung samples for biochemical and histologic analysis.

Experimental Protocol for Treatment with CXCR2 Receptor Blocker

Bleomycin-instilled mice received oral twice-daily treatment with vehicle or DF2162 (17, 18), a CXCR2-selective functional blocker derivative of reparexin (15, 16). DF2162 was given by oral gavage in 100 μl of 0.25% carboxymethylcellulose diluted in PBS. The vehicle group received 100 μl of 0.25% carboxymethylcellulose only. First of all, we performed a dose–response study with DF2162 (1.2, 6, and 30 mg/kg/dose) from Day 0 (the day of bleomycin instillation) to evaluate lung inflammation 2 days after. At a later moment, DF2162 was given at 6 mg/kg/dose from Days 0 to 16, and lung inflammation and fibrosis were evaluated at Days 2, 8, and 16 after bleomycin challenge. Finally, we evaluated the effects of late administration of 6 mg/kg/dose DF2162 from Days 8 to 16 on lung inflammation and fibrosis; evaluation was on Day 16 after bleomycin challenge.

Bronchoalveolar Lavage

Bronchoalveolar lavage (BAL) was performed to obtain leukocytes from alveolar spaces. The trachea was exposed and a 1.7-mm-outside-diameter polyethylene catheter was inserted. BAL was performed by washing the lungs three times with three different 1-ml aliquots of PBS. BAL samples (~ 2.7–3.0 ml each) were centrifuged at 600 × *g* for 10 minutes at 4°C. The supernatant was used for enzyme-linked immunosorbent assay (ELISA) and the cell pellet used to evaluate the number of infiltrating leukocytes. The total number of leukocytes was determined by counting leukocytes in a modified Neubauer chamber. Differential counts were obtained from cytospin (Shandon III) preparations by evaluating the percentage of each leukocyte on a slide stained with May-Grünwald-Giemsa.

Quantification of Neutrophil Accumulation in Lung Tissue by Myeloperoxidase Activity Measurement

The extent of neutrophil accumulation in lung tissue was measured by assaying myeloperoxidase activity, as previously described (23). Using the conditions described below, this methodology is selective for the determination of neutrophils over macrophages (data not shown). Before lung removal, the pulmonary vasculature was perfused with 3 ml of PBS through the right ventricle, and the organ was removed and frozen at −70°C. Upon thawing, the tissue (0.1 g of tissue per 1.9 ml of buffer) was homogenized in a pH 4.7 buffer (0.1 M NaCl, 0.02 M Na_2PO_4, 0.015 M Na_2EDTA), centrifuged at 3,000 × *g* for 10 minutes, and the pellet subjected to hypotonic lyses (1.5 ml of 0.2% NaCl solution followed by an addition 30 seconds later of an equal volume of a solution containing NaCl 1.6% and glucose 5%). After a further centrifugation, the pellet was resuspended in 0.05 M Na_2PO_4 buffer (pH 5.4) containing 0.5% hexadecyl-trimethylammonium bromide (HTAB) and re-homogenized. One-milliliter aliquots of the suspension were transferred into 1.5-ml microtubes followed by three freeze-thaw cycles using liquid nitrogen. The aliquots were then centrifuged for 15 minutes at 3,000 × *g* to perform the assay.

MPO Assay Reaction

The assay employed 25 μl of 3,3′-5,5′-tetramethylbenzidine (TMB; Sigma), dissolved in dimethyl sulfoxide (DMSO; Merck, Darmstadt, Germany) at a final concentration of 1.6 mM, 100 μl of H_2O_2, dissolved in phosphate buffer (pH 5.4) containing HTAB in a final concentration of 0.002% vol/vol and 25 μl of supernatant from tissue sample processed. The reaction was started at 37°C for 5 minutes in a 96-well microplate by adding the supernatant and the TMB solution. After that, H_2O_2 was added and followed by a new incubation at 37°C for 5 minutes. The reaction was stopped by adding 100 μl of 1 M H_2SO_4 and quantified at 450 nm in a spectrophotometer (Emax; Molecular Devices, Sunnyvale, CA). Neutrophil number in each sample was calculated from a standard curve of neutrophils obtained from the peritoneal cavity of 5% casein-treated animals and processed in the same way. The results were expressed as relative number of neutrophils per mg of wet tissue.

Hydroxyproline Determination

Fragments (100 mg) of lungs were removed for hydroxyproline determination, as an indirect measurement of collagen content (24). Briefly, tissues were homogenized in 0.2% saline, frozen, and lyophilized. The assay was performed with 20 mg of the lyophilized material subjected to alkaline hydrolysis in 300 μl of H_2O plus 75 μl of 10 M NaOH at 120°C for 20 minutes. An aliquot of 50 μl of the hydrolyzed tissue was added to 450 μl of Chloramine T oxidizing reagent (0.056 M Chloramine T and n-propanol 10% in acetate-citrate buffer [pH 6.5]) and allowed to react for 20 minutes. A hydroxyproline standard curve was prepared likewise. Color was developed by the addition of 500 μl of 1 M p-dimethylaminebenzaldehyde diluted in n-propanol–perchloric acid (2:1 [vol/vol]). The absorbance was quantified at 550 nm in a spectrophotometer (Emax; Molecular Devices).

ELISA for Assessment of Cytokine and Chemokine Concentrations in BAL and Lungs

The concentration of the cytokines IFN-γ, IL-10, IL-13, GM-CSF, and TGF-β_1 (active and total forms), and chemokines CXCL1/KC and CCL5/RANTES was measured in lungs; and CXCL1/KC, CXCL2/MIP-2, CXCL9/MIG, and CXCL10/IP-10 was measured in BAL by ELISA. The assays were performed using Kits from R&D Systems (DuoSet kits) and according to the manufacturer's instructions.

One hundred milligrams of lung tissue from both controls and treated animals were homogenized in 1 ml of PBS (0.4 M NaCl and 10 mM de $NaPO_4$) containing anti-proteases (0.1 mM phenylmethilsulfonyl fluoride, 0.1 mM benzethonium chloride, 10 mM EDTA, and 20 KI aprotinin A) and 0.05% Tween 20. The samples were then centrifuged for 10 minutes at 3,000 × *g* and the supernatant immediately used for ELISA. All samples were assayed in duplicate.

Histopathologic and Morphometric Analysis

The left lung was removed and fixed in 10% neutral phosphate-buffered formalin (pH 7.4). The tissues were dehydrated gradually in ethanol, embedded in paraffin, cut into 4-μm sections, stained with hematoxilin and eosin (H&E) or Gomori's Trichrome, and examined under light microscopy. Slides with lung sections stained with H&E were analyzed by a pathologist blinded to the experiment. For the quantitative analysis of Gomori's Trichrome area, images covering 326,000 μm^2 of lung sections were captured with a digital camera (Optronics DEI-470; Goleta, CA) connected to a microscope (Olympus IX70; Hamburg, Germany) with a magnification of ×200, and collagen (*green areas stained by Gomori's trichrome*) was measured with the software Image Pro-Plus (Media Cybernetics, Silver Spring, MD). At least 20 images were obtained for each animal, with $n = 6$ per group. Results were expressed as the mean green area per μm^2. This morphometrical index was used to describe lung collagen deposition.

Real-Time PCR

Lungs of vehicle-treated or DF2162-treated mice were removed at Day 16 after intratracheal bleomycin instillation for analysis of von Willebrand Factor (vWF) mRNA expression. Total RNA was isolated from lungs by using an Illustra RNAspin Mini RNA Isolation Kit (GE Healthcare). The RNA obtained was suspended in diethyl pyrocarbonate–

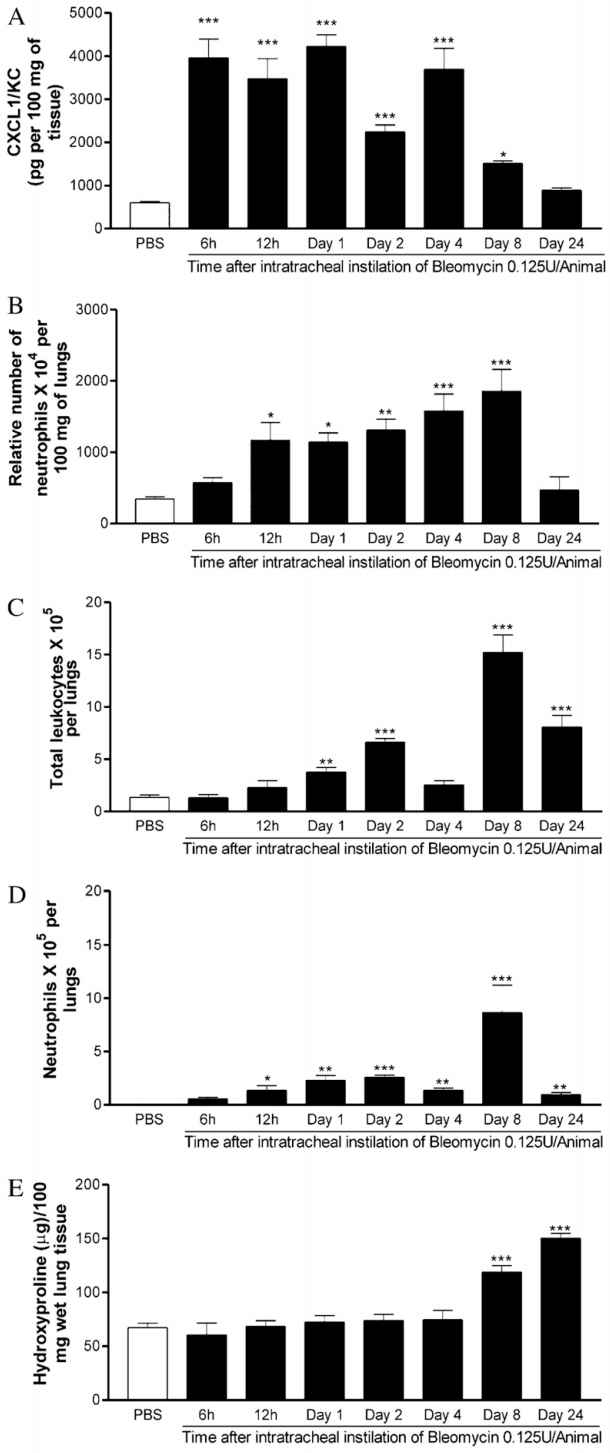


Figure 1. Time course of bleomycin-induced lung inflammation and fibrosis. The following parameters were evaluated: (*A*) CXCL1/KC production in lungs; (*B*) neutrophil influx into the lungs, as assessed by myeloperoxidase (MPO) assay; transmigration of (*C*) total leukocytes and (*D*) neutrophils into bronchoalveolar lavage (BAL) fluid; and (*E*) lung collagen deposition, as assessed by hydroxyproline measurement. Animals were given a single intratracheal challenge of bleomycin (0.125 U) (*solid bars*) or PBS (control, *open bars*) and evaluated at the given times after challenge. Results are representative of two experiments and are shown as the mean ± SEM of seven to eight animals in each group. $*P < 0.05$, $**P < 0.01$, and $***P < 0.001$, respectively, when compared with PBS.

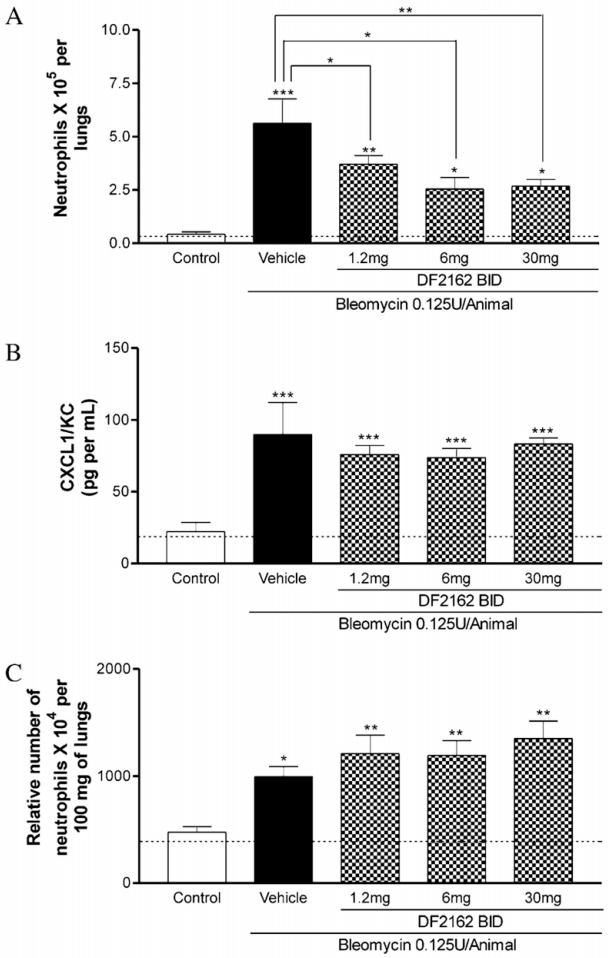


Figure 2. Dose-dependent effects of treatment with DF2162 in a model of bleomycin-induced lung injury. Animals were given a single intratracheal challenge of bleomycin (0.125 U) (*solid bars*) or PBS (control, *open bars*) and evaluated 2 days after challenge. DF2162 was given orally (twice daily) at the doses of 1.2, 6, or 30 mg/kg (*cross-hatched bars*). The following parameters were evaluated: (*A*) Number of neutrophils in BAL fluid; (*B*) CXCL1/KC levels in BAL; and (*C*) neutrophil influx into the lung, as assessed by MPO assay. The *dotted lines across the graphs* represent values in naïve animals. Results are representative of two experiments and are shown as the mean ± SEM of seven to eight animals in each group. $*P < 0.05$, $**P < 0.01$, and $***P < 0.001$, respectively, when compared with vehicle-given bleomycin-challenged mice.

treated water and stocked at −70°C until use. Real-time RT-PCR was performed on an ABI PRISM 7900 sequence-detection system (Applied Biosystems, Warrington, UK) by using SYBR Green PCR Master Mix (Applied Biosystems) after a reverse transcription reaction of 1 μg of RNA by using M-MLV reverse transcriptase (Promega, Madison, WI). The relative level of gene expression was determined by the comparative threshold cycle method as described by the manufacturer, whereby data for each sample were normalized to hypoxanthine phosphoribosyltransferase (HPRT) and expressed as a fold change compared with PBS-instilled control mice. The following primer pairs were used: HPRT, 5′-GTTGG TTACAGGCCAGACTTTGTTG-3′ (forward) and 5′-GAGGGTA GGCTGGCCTATAGGCT-3′ (reverse); and vWF, 5′-GCGCTATC ATGTATGAAGTCAGGTT-3′ (forward) and 5′-CACAGATTCCG CAAAGACCAT-3′ (reverse).

In Vitro Experiments

Cell culture. Primary endothelial cells were obtained from human umbilical veins (HUVEC) as described previously (25). HUVECs were

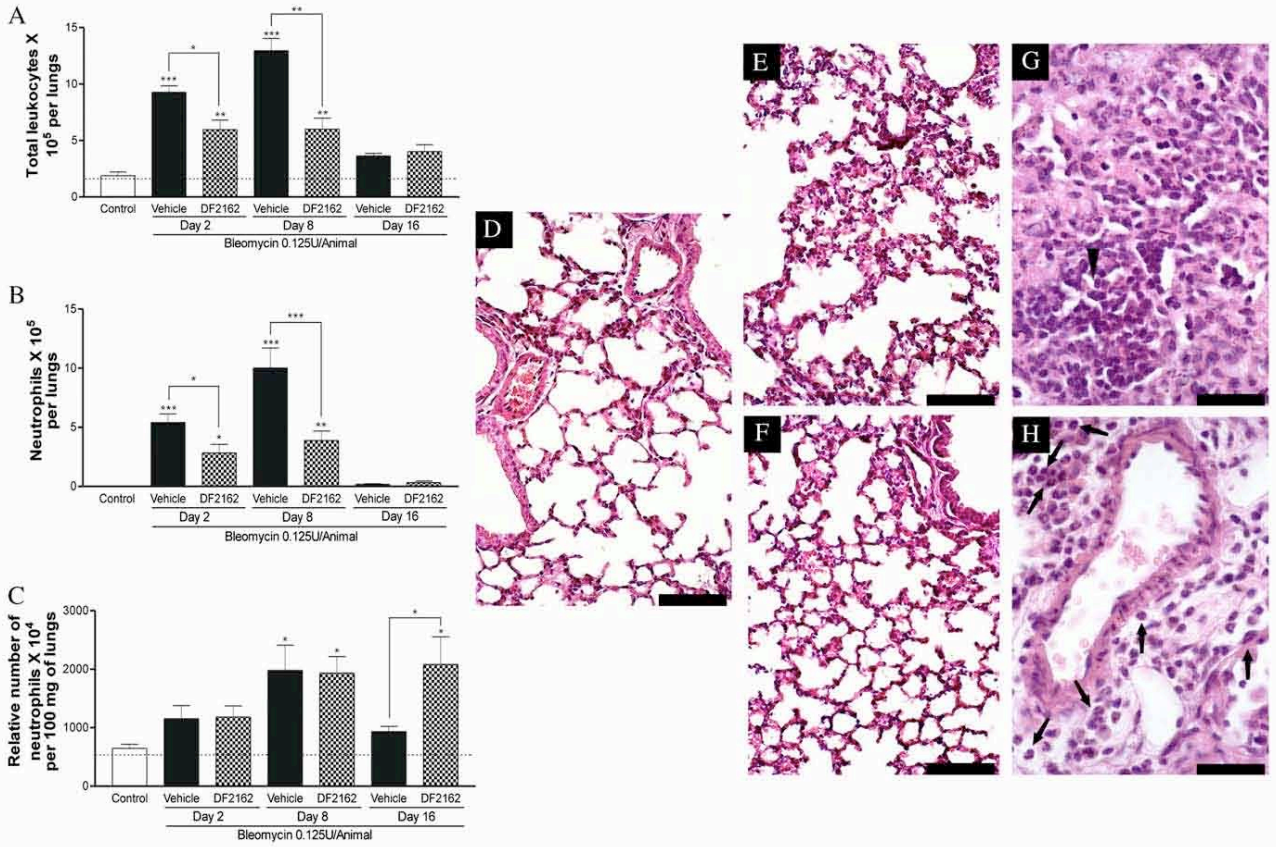


Figure 3. Effects of DF2162 treatment on lung inflammation induced by bleomycin. Animals were given a single intratracheal challenge of bleomycin (0.125 U) (*solid bars*) or PBS (Control, *open bars*) and evaluated 2, 8, and 16 days after challenge. DF2162 was given orally (twice daily) at the dose 6 mg/kg (*cross-hatched bars*) from Day 0 to Day 16. The following parameters were evaluated: (*A*) total number of leukocytes and (*B*) neutrophils in BAL fluid; (*C*) neutrophil influx into the lung, as assessed by MPO assay. The *dotted lines across the graphs* represent values in naïve animals. Results are representative of two experiments and are shown as the mean ± SEM of seven to eight animals in each group. $^{*}P < 0.05$, $^{**}P < 0.01$, and $^{***}P < 0.001$, respectively, when compared with vehicle-given bleomycin-challenged mice. Representative sections of hematoxylin and eosin–stained lungs of (*D*) control and (*E–H*) bleomycin-challenged animals are also shown. At Day 2 (*bars* = 50 μm) note the bleomycin-induced lung infiltrate (*E*) that was diminished in DF2162-treated animals (*F*). At Day 16 (*bars* = 25 μm), note the presence of mononuclear cell infiltrate (*G*, *arrowhead*) after bleomycin challenge. After treatment with DF2162 there was persistence of neutrophils in lung parenchyma (*H*, *arrows*).

seeded on 0.2% wt/vol gelatin-coated 25-cm^2 tissue culture flasks and cultured in endothelial cell basal medium-2 (EBM-2) containing 20% fetal calf serum (FCS), 50 mg/ml endothelial cell growth supplement (ECGS) (Collaborative Research, Inc, Bedford, MA), and 100 mg/ml heparin (Sigma) until they reached confluence. Cells were passaged up to two times before use and then placed in suspension by trypsinization.

Cell proliferation assay. The proliferation assay was performed as described previously (26). Briefly, 96-well culture plates were with 0.2% wt/vol gelatin. Approximately 5×10^3 HUVECs were plated in EBM-2 supplemented with 20% FCS, 50 μg/ml ECGS, and 100 μg/ml heparin in gelatin-precoated 96-well, and allowed to adhere for 6 hours. The medium was then removed and the cells were washed twice with serum-free medium. Serum-free EBM-2 containing 1% Nutridoma (Roche diagnostics GmbH, Mannheim, Germany), ECGS, heparin, and 0.037 MBq/ml (1 μCi/ml) methyl 3(^{3}H)-thymidine (GE Healthcare GmbH, Milan, Italy) in the presence or absence of human recombinant IL-8 (10 ng/ml) and/or DF2162 (as described bellow) was then added to the wells and left incubating for 24 h at 37°C in the presence of 5% CO_2. After incubation time, nonadherent cells were removed by washing twice with ice-cold PBS. Then, 50 μl 10% ice-cold trichloroacetic acid (TCA) was added to each well and the precipitates were collected on a filter using a filtration manifold. Filters were extensively washed with distilled water and then suspended in scintillation fluid. Counts per minute (CPM) were quantified using a scintillator counter. For the blockade approach, DF2162 was diluted in EBM-2 medium containing 0.01% of dimethyl sulfoxide (DMSO; Sigma) to three different final concentrations: 0.01, 0.1, and 1 μM. The cells were pretreated for 1 hour with either vehicle (EBM-2+DMSO) or DF2162 before the addition of human IL-8.

Scratch assay. For the scratch assay, 5×10^5 HUVECs were plated in gelatin-precoated 24-well culture plate and incubated in EBM-2 medium supplemented with 20% FCS, 50 μg/ml ECGS, and 100 μg/ml heparin for 24 hours at 37°C in presence of CO_2 5%. The confluent cells were starved for 1 hour in EBM-2 medium with 5% FCS before starting the experiments. Confluent cell monolayer was then scraped with a yellow pipette tip to generate scratch wounds and rinsed twice with serum-free EBM-2 to remove debris. EBM-2 medium with 5% FCS was added to the cells, which had been pretreated for 1 hour with vehicle (0.01% DMSO in EBM-2) or DF2162 (0.1 μM) before the addition of human IL-8 (10 ng/ml). The cells were then incubated at 37°C in presence of 5% CO_2. Scratches were photographed immediately and 12 hours after the scraping. Images were obtained using a Nikon digital camera coupled to a ×10 objective on a Zeiss Axiovert microscope (Zeiss, Thornwood, NY) and the wound area was measured using the software NIH ImageJ.

HUVEC capillary-like structure formation assay. An *in vitro* capillary-like structure formation assay was performed as described earlier (27). Briefly, forty-eight-well culture plates (Nunc, Nalge Europe; Neerijse, Belgium) were pre-coated at 4°C with 150 μl of Growth factor–reduced Matrigel matrix, which was then allowed to solidify at 37°C for 30 minutes. HUVECs, 5×10^4 per well, were

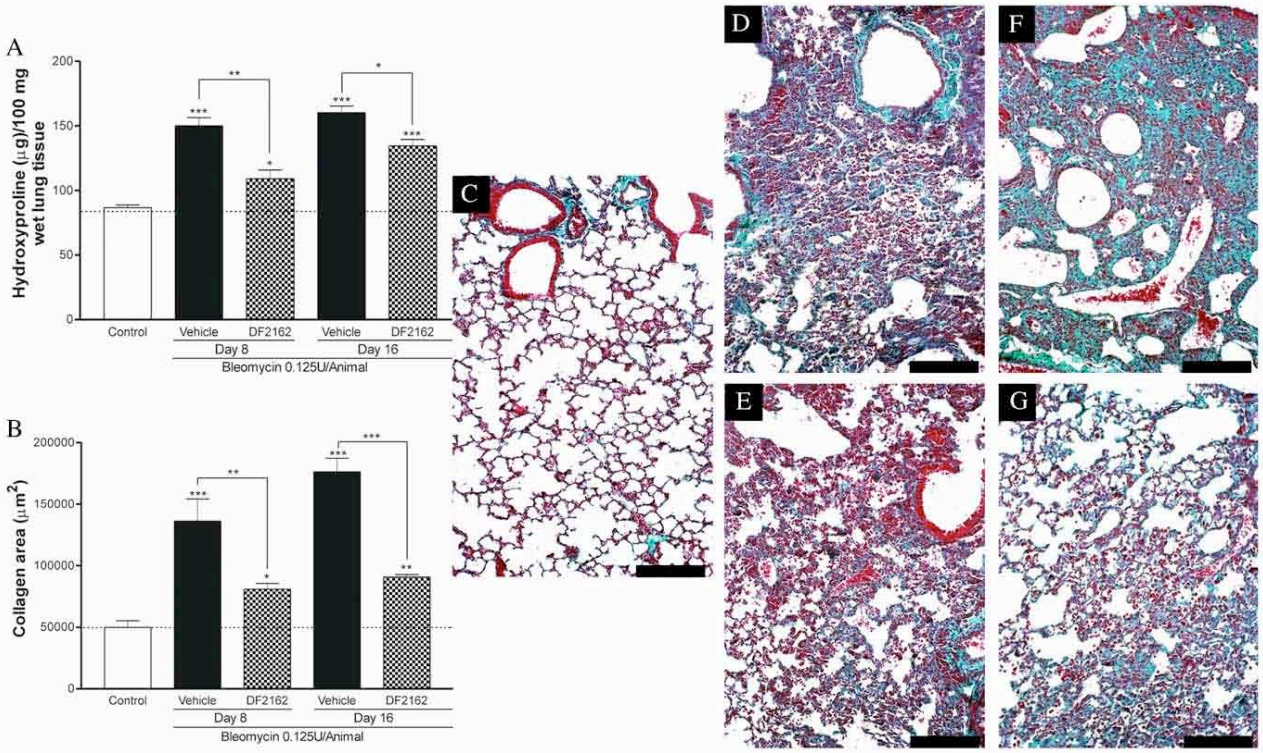


Figure 4. Effects of DF2162 treatment on lung fibrosis induced by bleomycin. Animals were given a single intratracheal challenge of bleomycin (0.125 U) (*solid bars*) or PBS (Control, *open bars*) and evaluated 8 and 16 days after challenge. DF2162 was given orally (twice daily) at the dose 6 mg/kg (*cross-hatched bars*) from Day 0 to Day 16. The following parameters were evaluated: lung collagen deposition, as assessed by (*A*) hydroxyproline measurement and (*B*) morphometric analysis of Gomori's trichrome–stained areas. The *dotted lines across the graphs* represent values in naïve animals. Results are representative of two experiments and are shown as the mean ± SEM of seven to eight animals in each group. $*P < 0.05$, $**P < 0.01$, and $***P < 0.001$, respectively, when compared with vehicle-given bleomycin-challenged mice. Representative sections of Gomori's trichrome–stained lungs of (*C*) control and (*D–G*) bleomycin-challenged animals are also shown. Note the large areas of collagen deposition (shown in *green*) at Days 8 (*D*) and 16 (*F*) after bleomycin challenge. DF2162 treatment decreased the amount and modified the pattern of collagen deposition at Days 8 (*E*) and 16 (*G*) after challenge (*bars* = 100 μm).

suspended in EBM-2 medium supplemented with 20% FCS, 50 μg/ml ECGS, and 100 μg/ml heparin and seeded on the Matrigel-coated plates. The cells had been pretreated for 1 hour with either vehicle (0.01% DMSO in EBM-2) or DF2162 (0.1 μM) before the addition of human IL-8 (10 ng/ml). The plates were incubated for 24 hours at 37°C in presence of 5% CO_2, and the wells were then photographed using a Nikon digital camera coupled to a ×10 objective on a Zeiss Axiovert microscope to determine qualitative influence of DF2162 on the ability of the HUVECs to form capillary-like structures.

Statistical Analysis

All results are presented as the mean ± SEM. Normalized data were analyzed by one-way ANOVA and differences between groups were assessed using the Student-Newman-Keuls *post hoc* test, using Software GraphPad Prism 3.0. Differences were considered significant at $P < 0.05$.

RESULTS

Kinetics of Chemokine Production, Neutrophil Influx, and Fibrosis Formation after Bleomycin Challenge

BAL and lung tissue were obtained at various time points after bleomycin or saline instillation. The chemokine CXCL1/KC peak was already detectable in lungs of bleomycin-instilled animals at 6 hours, remained elevated till 24 hours, and dropped slightly by 2 days after bleomycin challenge. There was a secondary peak of the chemokine at Day 4, which dropped again at Day 8 after challenge. Thereafter, the levels of CXCL1/KC returned to baseline (Figure 1A). At 12 hours, neutrophils started to accumulate progressively in the lungs, as quantified by MPO, with a peak at Day 8 (Figure 1B). An increase in lung macrophages number was observed at Day 24 (data not shown). In BAL, the total leukocytes count showed a biphasic fashion, with a first peak at Day 2 and a second one at Day 8 (Figure 1C). Neutrophils were detected in BAL 12 hours after bleomycin instillation. Neutrophil influx increased then peaked on Day 2, dropped slightly by Day 4, and reached a greater peak at Day 8, thus having biphasic recruitment similar to that observed with total cells (Figure 1D). The deposition of collagen in lung interstitium, as determined by hydroxyproline quantification, was first noticed at Day 8 after bleomycin instillation and increased steadily thereafter (Figure 1E). Therefore, the progressive collagen deposition in lungs is preceded by an increase in neutrophil influx associated with high levels of CXCL1/KC production. Our next question was whether blockade of CXCR2, the receptor for CXCL1/KC, could reduce lung neutrophil inflammation and subsequent fibrosis.

Dose-Dependent Effects of DF2162, a CXCR2 Antagonist, after Bleomycin Challenge

To obtain an optimal dose of DF2162 for the chronic experiments, mice were treated orally with vehicle or DF2162 (1.2, 6, and 30 mg/kg/dose, twice daily). Neutrophil accumulation and lung CXCL1/KC production were evaluated 2 days after bleomycin challenge. Neutrophil recruitment into airway space was inhibited in a dose-dependent manner, with maximal inhibition

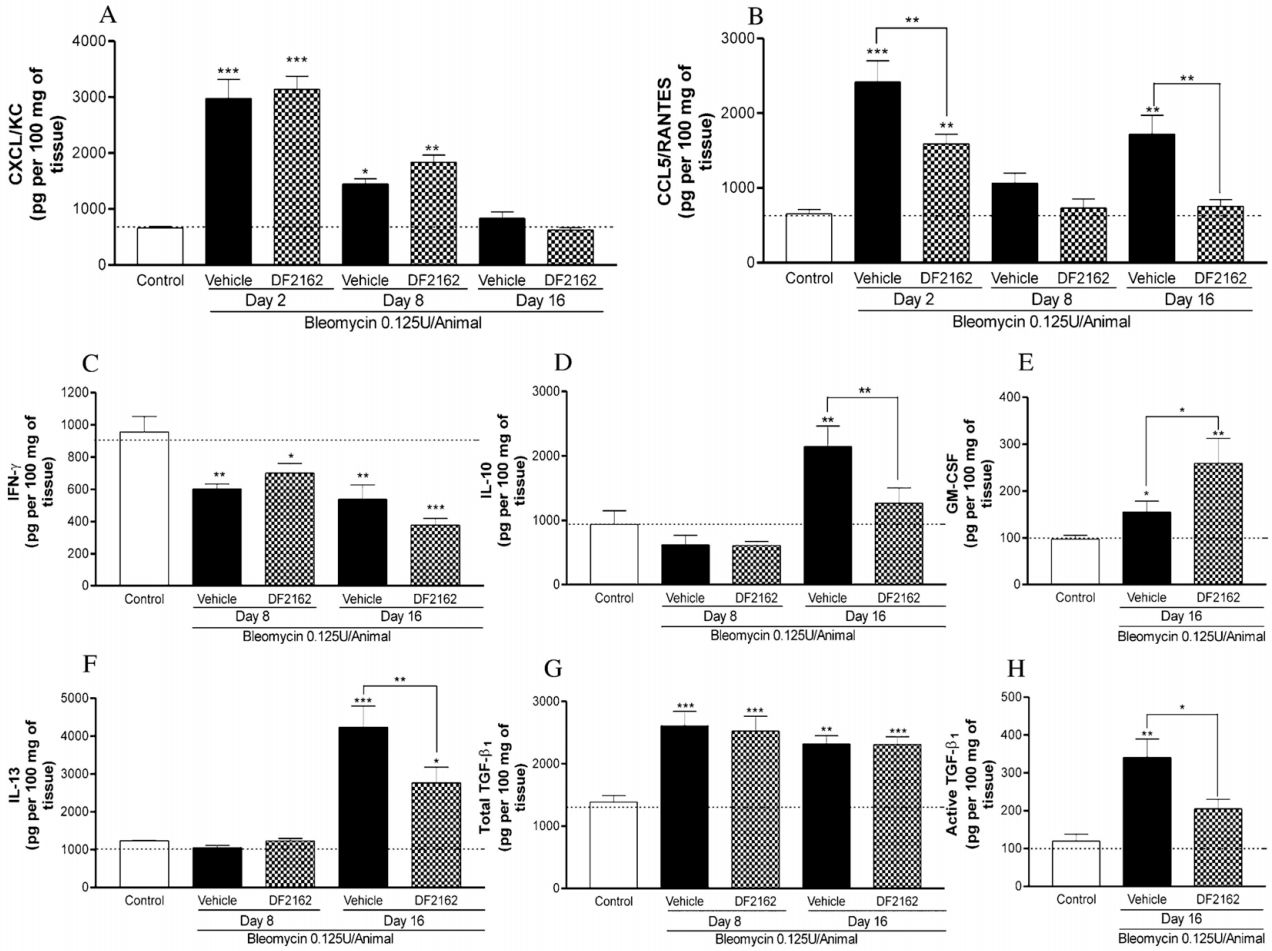


Figure 5. Effects of DF2162 treatment on the cytokines and chemokines production in lung induced by bleomycin. Animals were given a single intratracheal challenge of bleomycin (0.125 U) (*solid bars*) or PBS (Control, *open bars*) and evaluated at various times after challenge. DF2162 was given orally (twice daily) at the dose 6 mg/kg (*cross-hatched bars*) from Day 0 to Day 16. The following soluble mediators were evaluated by enzyme-linked immunosorbent assay in lung tissue: (*A*) CXCL1/KC, (*B*) CCL5/RANTES, (*C*) IFN-γ, (*D*) IL-10, (*E*) granulocyte macrophage–colony-stimulating factor (GM-CSF), (*F*) IL-13, (*G*) total transforming growth factor (TGF)-β_1, and (*H*) active TGF-β_1. The *dotted lines across the graphs* represent values in naïve animals. Results are representative of two experiments and are shown as the mean ± SEM of seven to eight animals in each group. *$P < 0.05$, **$P < 0.01$, and ***$P < 0.001$, respectively, when compared with vehicle-given bleomycin-challenged mice.

observed with 6 mg/kg/dose (Figure 2A). The compound did not affect the pulmonary levels of CXCL1/KC (Figure 2B). Despite its ability to prevent neutrophil influx into BAL, DF2162 had no effect on neutrophil accumulation in lung tissue, as assayed by MPO (Figure 2C). The dose of 6 mg/kg/dose, twice daily, was then used in all further studies.

Pulmonary Inflammation Is Reduced by the CXCR2 Antagonist

Treatment with DF2162 (6 mg/kg/dose, twice daily, from Day 0) led to a significant inhibition of the accumulation of total leukocytes in alveolar fluid at Days 2 and 8 after bleomycin instillation (Figure 3A). This appeared to be resultant of a significant reduction in the recruitment of neutrophils at Days 2 and 8 (Figure 3B). There were few neutrophils in BAL fluid at Day 16 after bleomycin instillation, and the compound failed to affect the total number of cells at that time point (Figures 3A and 3B). DF2162 was not able to prevent neutrophil accumulation in lung tissues at Days 2 and 8 after bleomycin instillation. Actually, neutrophil accumulation in lung tissue was greater in DF2162 than in vehicle-treated animals at Day 16 (Figure 3C).

Histopathologic analysis by H&E, 2 days after bleomycin challenge, showed that there was an increase in thickness of the alveolar wall that was associated with interstitial edema, hyperemia, and characteristic leukocyte exudation (Figure 3E). In DF2162-treated mice, there was a reduction of alveolar wall edema, hyperemia, and leukocyte influx into the alveolar spaces at Day 2 after bleomycin (Figure 3F). At Day 16, lungs of vehicle-treated mice showed intense interstitial infiltration of lymphocytes and mononuclear cells (Figure 3G, *arrowhead*). In DF2162-treated mice, there were fewer lymphocytes, mononuclear cells, and overall number of cells, but an increase in the number of neutrophils in lung parenchyma (Figure 3H, *arrows*), concurring with MPO data (Figure 3C).

Pulmonary Fibrosis Is Reduced by the CXCR2 Antagonist

Bleomycin administration caused a progressive increase in collagen deposition at Days 8 and 16 after challenge in the vehicle- but not in the DF2162-treated mice, as assessed by measurement of hydroxyproline content (Figure 4A). Likewise, DF2162 treatment significantly diminished collagen deposition as assessed by morphometric analysis in Gomori's Trichrome–stained sections

(Figure 4B). The pattern of collagen deposition between vehicle- and DF2162-treated mice was different; at Day 8, vehicle-treated mice exhibited diffuse interstitial pneumonitis, increased alveolar wall thickness, and mild fibrosis (Figure 4D), whereas DF2162-treated animals presented focal interstitial pneumonia and reduced septal thickness and fibrosis (Figure 4E). At Day 16, vehicle-treated mice presented diffuse and dense pulmonary fibrosis with intense remodeling and loss of normal pulmonary architecture (Figure 4F). These changes were much less intense in DF2162-treated mice, which developed focal lung fibrosis with preserved areas of parenchyma (Figure 4G).

Effect of the CXCR2 Antagonist on Chemokine and Cytokine Production during Bleomycin-Induced Lung Injury and Fibrosis

Next, the effects of DF2162 on the levels of chemokines and cytokines induced by bleomycin were determined in lung tissue and BAL. The CXCR2 antagonist had no effect on levels of the neutrophil-active chemokine CXCL1/KC in lungs (Figure 5A), or CXCL1/KC and CXCL2/MIP-2 in BAL (Table 1). Levels of CCL5/RANTES in lungs of DF2162-treated mice were significantly lower than those of vehicle-treated animals (Figure 5B). In contrast, the concentration of CXCL9/MIG in BAL fluid was greater in DF2162 than vehicle-treated mice at Day 2 after instillation of bleomycin (Table 1).

Levels of the proinflammatory cytokine IFN-γ were significantly different from background in vehicle- or DF2162-treated mice (Figure 5C). There was a significant increase in IL-10 production in lung tissue 16 days after bleomycin challenge, which was blocked by DF2162 treatment (Figure 5D). In contrast, DF2162 administration caused an increase in lung levels of GM-CSF at Day 16 after bleomycin challenge when compared with vehicle-treated mice (Figure 5E). No differences on VEGF levels were observed between DF2162-treated versus vehicle-treated mice (data not shown).

Lung levels of the profibrogenic cytokines IL-13 and total and active TGF-β_1 were also evaluated. DF2162 administration caused a reduction in lung levels of IL-13, when compared with vehicle-treated mice, at Day 16 after bleomycin challenge (Figure 5F). Levels of total and active TGF-β_1 were increased after bleomycin instillation. Although DF2162 treatment did not affect the total levels of TGF-β_1, the production of active form of TGF-β_1 was drastically reduced at Day 16 when compared with vehicle-treated mice (Figures 5G and 5H).

Effects of Late Administration of DF2162 on Inflammation and Fibrosis Induced by Bleomycin

To determine whether DF2162 treatment have any therapeutic benefit, we investigated the effects of delayed DF2162 administration (6 mg/kg/dose, twice daily, from Days 8 to 16 after bleomycin instillation). Experiments were started on Day 8 because this is after the initial acute inflammatory phase. No significant changes were observed either in total leukocytes in BAL or neutrophil migration into alveolar space (Figures 6A and 6B, respectively) as well as interstitium at Day 16 after bleomycin instillation (Figure 6C). Lung levels of the proinflammatory GM-CSF (Figure 6D) and profibrogenic cytokines, active TGF-β_1 (Figure 6F) and IL-13 (Figure 6G), were significantly reduced after late DF2162 administration when compared with vehicle-treated mice at Day 16 after bleomycin challenge. No differences on total TGF-β_1 levels were observed between DF2162-treated versus vehicle-treated mice (Figure 6E).

Lung fibrosis was assessed by hydroxyproline deposition and morphometry of Gomori's Trichrome–stained lung sections. The delayed treatment with DF2162 significantly diminished lung collagen deposition at Day 16 when compared with vehicle-treated mice (Figures 6H and 6I). In Gomori's Trichrome–stained section, diffuse and dense pulmonary fibrosis was observed in vehicle-treated mice (Figure 6J). In DF2162-treated animals, there was focal lung fibrosis with preserved areas of lung parenchyma and reduced septal thickness (Figure 6K).

Effects of DF2162 on Angiogenesis

BAL fluid obtained from DF2162- or vehicle-treated mice were used to measure the levels of pro-angiogenic and angiostatic chemokines in airway spaces. We found same levels of the pro-angiogenic chemokines CXCL1/KC and CXCL2/MIP-2 in vehicle-treated and DF2162-treated mice, whereas there was a significant increase in the levels of the angiostatic chemokines CXCL9/MIG and CXCL10/IP-10 in samples of DF2162-treated when compared with vehicle-treated mice (Table 2).

Next, to investigate a possible effect of DF2162 treatment in lung angiogenesis, we examine the expression of the endothelial-specific marker vWF (25). Bleomycin administration enhanced vWF gene expression at Day 16, as demonstrated by quantitative PCR. DF2162 administration significantly reduced the expression of vWF mRNA in lungs (Figure 7A).

To determine the effect of DF2162 on IL-8–induced HUVEC proliferation, cells were cultured in medium containing 10 ng/ml of human IL-8 in the absence or presence of DF2162 (0.01, 0.1, and 1 μM). Cell proliferation induced by IL-8 was significantly reduced in DF2162-treated cells, with the maximal inhibition of approximately 50% observed at 1 μM when compared with medium alone plus DMSO (Figure 7B).

Next, to investigate the effect of DF2162 on IL-8–induced HUVEC, we performed a scratch assay and compared the migration of HUVECs in presence of IL-8 (10 ng/ml) or IL-8 (10 ng/ml) plus DF2162 (0.1 μM). We found that HUVEC migration induced by IL-8 was significantly decreased in the DF2162-treated group (Figure 7C). We also examined the effect of DF2162 on endothelial cell organization into capillary-like structures. Endothelial cells were plated on Matrigel-coated 24-well plate with medium containing IL-8 (10 ng/ml) or IL-8

TABLE 1. EFFECTS OF DF2162 TREATMENT ON CHEMOKINES PRODUCTION IN BRONCHOALVEOLAR LAVAGE FLUID IN BLEOMYCIN-INDUCED LUNG INJURY

		Bronchoalveolar Lavage Fluid	
Groups	Chemokine	Day 2	Day 8
Control	CXCL1/KC	22.3 + 6.30	
Bleo+vehicle		89.8 + 22.29*	34.2 + 7.20
Bleo+DF2162		75.8 + 6.31*	25.4 + 3.36
Control	CXCL2/MIP-2	39.0 + 4.33	
Bleo+vehicle		83.3 + 4.18*	38.9 + 3.58
Bleo+DF2162		73.8 + 6.33*	38.6 + 3.24
Control	CXCL9/MIG	136.7 + 25.63	
Bleo+vehicle		355.9 + 57.19*	399.8 + 105.4
Bleo+DF2162		570.8 + 33.26*†	373.7 + 18.09

Animals were given a single intratracheal challenge of bleomycin (0.125 U) or PBS (Control) and evaluated at Days 2 and 8 after challenge. DF2162 was given orally twice a day at the dose 6 mg/kg (Bleo+DF2162). The following chemokines were evaluated by enzyme-linked immunosorbent assay in bronchoalveolar lavage fluid: CXCL1/KC, CXCL2/MIP-2, and CXCL9/MIG. Results are representative of two experiments and are shown as the mean + SEM of seven to eight animals in each group.

* $P < 0.05$ when comparing all groups with control group.

† $P < 0.05$ when comparing vehicle-given bleomycin-challenged and DF2162-treated bleomycin-challenged mice.

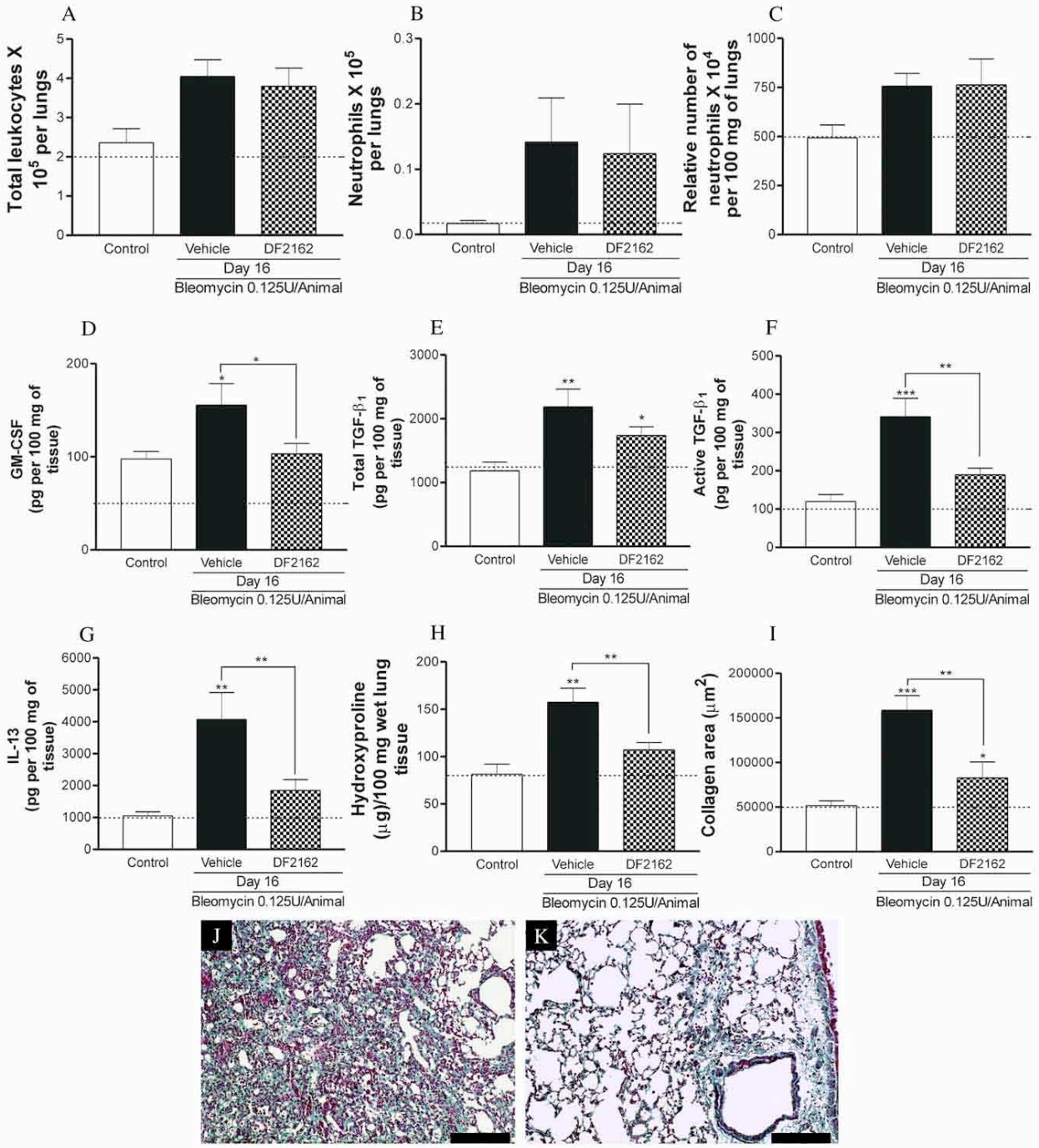


Figure 6. Effects of the delayed administration of DF2162 on inflammation and fibrosis induced by bleomycin. Animals were given a single intratracheal challenge of bleomycin (0.125 U) (*solid bars*) or PBS (Control, *open bars*) and evaluated at Day 16 after challenge. DF2162 was given orally (twice daily) at the dose 6 mg/kg (*cross-hatched bars*) from Day 8 to Day 16. The following parameters were evaluated: (*A*) number of total leukocytes and (*B*) neutrophils in BAL fluid; (C) neutrophil influx into the lung, as assessed by MPO assay; (*D*) GM-CSF, (*E*) total TGF-β_1, (*F*) active TGF-β_1, and (*G*) IL-13 levels in lungs; and lung collagen deposition, as assessed by (*H*) hydroxyproline measurement and (*I*) morphometric analysis of Gomori's trichrome–stained areas. The *dotted lines across the graphs* represent values in naïve animals. Results are representative of two experiments and are shown as the mean ± SEM of seven to eight animals in each group. $^*P < 0.05$, $^{**}P < 0.01$, and $^{***}P < 0.001$, respectively, when compared with vehicle-given bleomycin-challenged mice. Representative sections of Gomori's trichrome–stained lungs of bleomycin-challenged (*J* and *K*) animals are also shown. Note the large areas of collagen deposition (shown in *green*) at Day 16 (*J*) after bleomycin challenge. DF2162 treatment decreased the amount and modified the pattern of collagen deposition at Day 16 (*K*) after challenge (*bars* = 100 μm).

TABLE 2. EFFECTS OF DF2162 TREATMENT ON ANGIOGENIC/ANGIOSTATIC CHEMOKINES PRODUCTION IN BRONCHOALVEOLAR LAVAGE FLUID IN BLEOMYCIN-INDUCED LUNG INJURY

	Bronchoalveolar Lavage Fluid	
Groups	Chemokine	Day 16
Control	CXCL1/KC	35.35 + 2.23
Bleo+vehicle		80.51 + 24.27*
Bleo+DF2162 (0–16 d)		91.14 + 15.89*
Bleo+DF2162 (8–16 d)		95.57 + 23.28*
Control	CXCL2/MIP-2	39.00 + 2.72
Bleo+vehicle		71.49 + 16.22*
Bleo+DF2162 (0–16 d)		85.06 + 10.10*
Bleo+DF2162 (8–16 d)		84.29 + 18.04*
Control	CXCL9/MIG	121.60 + 11.01
Bleo+vehicle		110. 60 + 7.22
Bleo+DF2162 (0–16 d)		183.50 + 31.81*†
Bleo+DF2162 (8–16 d)		205.80 + 34.89*†
Control	CXCL10/IP-10	50.38 + 2.25
Bleo+vehicle		69.19 + 5.30*
Bleo+DF2162 (0–16 d)		107.90 + 10.95*
Bleo+DF2162 (8–16 d)		115.90 + 21.38*†

Animals were given a single intratracheal challenge of bleomycin (0.125 U) or PBS (Control) and evaluated at 16 d after challenge. DF2162 was given orally twice a day at the dose 6 mg/kg from Day 0 to Day 16 or from Day 8 to Day 16 (Bleo+DF2162 [0–16 d] or Bleo+DF2162 [8–16 d], respectively. The following chemokines were evaluated by enzyme-linked immunosorbent assay in bronchoalveolar lavage fluid: CXCL1/KC, CXCL2/MIP-2, CXCL9/MIG, and CXCL10/IP-10. Results are representative of two experiments and are shown as the mean + SEM of five to seven animals in each group.

* $P < 0.05$ when comparing all groups with control group.

† $P < 0.05$ when comparing vehicle-given bleomycin-challenged and DF2162-treated bleomycin-challenged mice.

(10 ng/ml) plus DF2162 (0.1 μM). After 24 hours of incubation, we observed in endothelial cells incubated with medium containing IL-8 an increased of long and thin capillary-like formation without cell agglomerates into the capillary junctions (Figure 7F). HUVECs treated with both IL-8 and DF2162 (0.1 μM) displayed cell agglomerates into the capillary junctions and thickness (Figure 7G), and demonstrated similar morphology observed in DMSO-treated cells (Figure 7E).

DISCUSSION

In this study, we showed the protective and therapeutic effects of DF2162, a long-acting antagonist of the chemokine receptor CXCR2 (17, 18), on the progression of lung fibrosis in bleomycin-instilled mice. Our main findings were that blockade of CXCR2 resulted in: (*1*) reduction of neutrophil migration into the airways, but not lung parenchyma; (*2*) reduction of the production of the fibrogenic cytokines IL-13 and active TGF-β_1; (*3*) amelioration of overall lung pathology and reduction of collagen accumulation; (*4*) decreases expression of vWF expression, a marker of angiogenesis, in the lung; and (*5*) decreased proliferation, migration and capillary-like organization induced by IL-8 on endothelial cells *in vitro*.

Initial studies designed to understand IPF pathogenesis have primarily focused on mechanisms related to fibroplasia and deposition of extracellular matrix (28, 29). However, multiple disorders associated with changes in extracellular matrix deposition are also associated to excessive inflammatory response and lung injury (30). Up to date, the real contribution of inflammation to trigger this pathology is controversial and still in constant discussion (31, 32). Pulmonary fibrosis can be either caused by chronic inflammation (33) or by a disrupted cross-talk between epithelial cells and fibroblast (28), which can occur in the absence of inflammation (34). Tissue damage after lung injury and inflammation seems to be a pivotal process, necessary to trigger the excessive and progressive scaring of lungs (33). Some studies have related an important role for neutrophils in the inflammatory process that precedes lung fibrosis induced by bleomycin (35, 36), but a recent study showed that neutrophil depletion with anti-PMN antibodies did not alter the susceptibility to bleomycin-induced pulmonary fibrosis (37). Therefore, the association between pulmonary fibrosis and inflammation is incompletely understood and remains unsolved.

In our study, we demonstrated a temporal relation between early lung CXCL1/KC production, neutrophil migration into airway space, and later lung fibrosis induced by bleomycin instillation. It was observed that the inflammatory response, especially the neutrophil influx, preceded the fibrotic process. Therefore, our objective was to block PMN recruitment with a CXCR2 receptor antagonist to evaluate whether CXCR2-mediated neutrophil influx could play a relevant role in the induction of the fibrotic response induced by bleomycin. CXCR2 is a very important receptor associated with neutrophil recruitment during infective or inflammatory processes (15–18). In the model of bleomycin-induced pulmonary inflammation and fibrosis, treatment with the CXCR2 antagonist diminished neutrophil transmigration into airway space, even in the presence of large concentrations of the CXCR2 ligands CXCL1/KC and CXCL2/MIP-2. These results show that blockade of CXCR2 is sufficient to prevent neutrophil influx into BAL fluid. Interestingly, the CXCR2 receptor antagonist administration did not modify the accumulation of neutrophils in lung parenchyma, as assessed by MPO measurements and confirmed by histology. The present study did not investigate in any detail mechanisms underlying this differential inhibition of accumulation in lung parenchyma or airway spaces. However, it has been demonstrated that intravascular, interstitial, and intra-alveolar accumulation of neutrophils may be differentially regulated; indeed, PMNs can enter the pulmonary interstitium without advancing to the alveolar airway space and crossing the epithelial barrier seems to be pivotal for inducing lung injury (36). Thus, blockade of CXCR2 prevented neutrophil influx into the airways but not their accumulation into lung parenchyma. Thus, although there was a good correlation between neutrophil influx into BAL and prevention of fibrosis, the presence of neutrophils in lung parenchyma and previous studies showing the lack of effect of anti-PMN antibodies in the model suggests that neutrophils may not be the major site of action for CXCR2 antagonists in the system.

Although CXCR2 has been identified as a receptor directing neutrophil migration and activation, other cell types, including lymphocytes, airway epithelial cells, and endothelial cells, express CXCR2 and may also be activated by ligands of this receptor (10, 13, 38, 39). It is, therefore, possible that blockade of CXCR2 on these other cell types may contribute to the protective effects of DF2162 on bleomycin-induced lung injury. Indeed, attenuation of alveolar wall thickness could be secondary to inhibition of CXCR2-dependent proliferation of airway epithelial cells (38). On endothelial cells, the activation of CXCR2 by CXCL1/KC or CXCL2/MIP-2 may induce angiogenesis, an effect counteracted by angiostatic CXCR3 ligands, such as CXCL9/MIG and CXCL10/IP-10 (13, 14). Interestingly, we found that blockade of CXCR2 was associated with an elevated production of CXCL9/MIG at Day 2 and CXCL9/MIG and CXCL10/IP-10 at Day 16 after bleomycin challenge. In addition, DF2162 administration led to a reduction in the expression of the endothelial cell marker vWF (25) in injured lungs. IL-8 has an important role on angiogenesis by promoting endothelial cell proliferation, survival, and migration and also the expression of matrix metalloproteinases through CXCR1 and CXCR2 signaling (27). Here, we report direct effects of DF2162 on HUVECs stimulated with

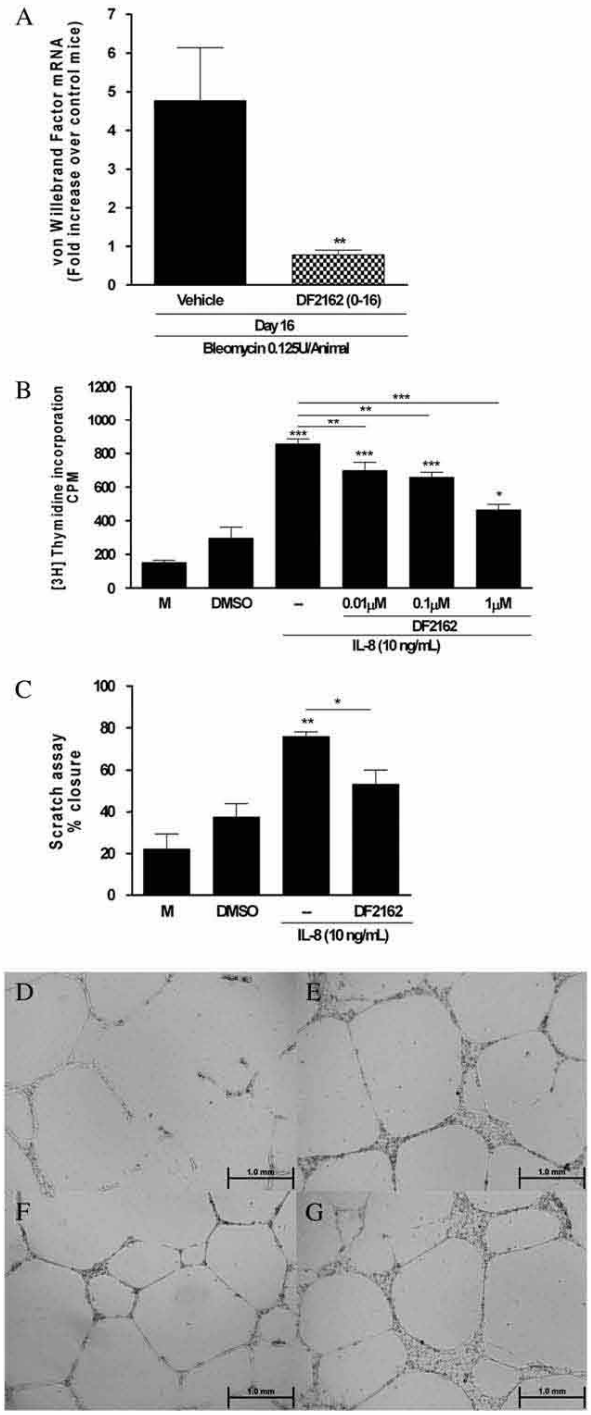


Figure 7. Effects of DF2162 on a maker of angiogenesis *in vivo* and on endothelial cells *in vitro*. Animals were given a single intratracheal challenge of bleomycin (0.125 U) (*solid bars*) or PBS (Control) and evaluated at Day 16 after challenge. DF2162 was given orally (twice daily) at the dose 6 mg/kg (*cross-hatched bar*) from Day 0 to Day 16 (0–16), and lung expression of von Willebrand Factor was measured by quantitative PCR after bleomycin challenge (*A*); results are expressed as fold increase over control mice challenged with PBS. Results are representative of one experiment and are shown as the mean ± SEM of five animals in each group. (*B*) *In vitro* human umbilical vein endothelial cells (HUVEC) proliferation induced by IL-8 (10 ng/ml), in the absence or presence of DF2162 (0.01, 0.1, and 1 μM), measured by ^{3}H-thymidine incorporation after 24 hours. (*C*) *In vitro* HUVEC scratch assay induced by IL-8 (10 ng/ml) in the absence or presence of DF2162 (0.1 μM) revealed by wound closure area after 12 hours. Results are expressed as % closure area in relation to t = 0, under an optical microscope with ×10 objective. Results are representative of two experiments and are shown as the mean ± SEM of four wells in each group. $*P < 0.05$, $**P < 0.01$, and $***P < 0.001$, respectively. Effect of DF2162 on HUVEC capillary-like organization assay induced by IL-8 (10 ng/ml). HUVEC were plated on a Matrigel-coated 24-well plate with (*D*) medium alone, (*E*) medium containing DMSO, (*F*) IL-8 alone, or (*G*) IL-8 plus DF2162 (0.1 μM). After 24 hours of incubation, plates were examined for capillary-like organization under optical microscope (*bars* = 1 mm). Each assay was done in duplicate.

IL-8 by reducing HUVEC proliferation, migration, and its ability in organizing capillary-like structures *in vitro*. Overall, these results suggest an anti-angiogenic effect of DF2162 on the setting of pulmonary fibrosis. The effects of DF2162 on angiogenesis could potentially be secondary to a direct effect of the compound on pulmonary endothelial cells or via the induction of high levels of CXCR3 agonists (CXCL9/MIG and CXCL10/IP-10), chemokines that generate a microenvironment with angiostatic characteristics.

It is noteworthy that we found that DF2162 administered mice had reduced levels of IL-10, IL-13, and active TGF-β_1 and increased GM-CSF production, although they had normal levels of IFN-γ. IL-13 is a pleiotropic cytokine produced in large quantities by stimulated CD4 Th2 cells (40), CD8 T cells (41), and airway epithelial cells in lungs during asthma (42). Recent studies in macrophages demonstrated that IL-13 is an enhancer of the production of the pro-fibrotic cytokine TGF-β_1 which play a major role in pulmonary fibrosis induced by bleomycin in mice (43). The reduction in lung collagen content was associated with lower levels of IL-13 and active TGF-β_1 in lungs of DF2162-treated animals, suggesting that blockade of CXCR2 could be preventing fibrosis in this model via control of IL-13 production and TGF-β_1 activation without change IFN-γ levels after bleomycin challenge. As CXCR2 receptors are present on activated T cells (10), inhibition of this receptor by DF2162 could prevent their *in vivo* recruitment and production of IL-13. Consistently, we found lower levels of infiltrating lymphocytes in lungs of DF2162-treated animals. DF2162-treated animals had lower levels of CCL5/RANTES, which signals through CCR5 receptor (10, 44), and is a lymphocyte chemoattractant factor that mediates T cell influx in fibrosing alveolitis (45). Thus, the blockade of CXCR2 on airway epithelial cells and lymphocytes could also contribute to the protective effects observed.

An intriguing finding was the elevated number of neutrophils in the lung interstitium of animals treated from Days 0 to 16 with DF2162 when compared with vehicle-treated mice at Day 16 after bleomycin instillation. This increase did not occurred when DF2162 was given from Day 8 to Day 16 after bleomycin. Those results are in accordance with those of Keane and coworkers, who found that the administration of anti–MIP-2/anti-CXCL2 antibodies did not reduce MPO levels (22). It is unclear, however, why neutrophils would persist for longer in the group of animals that received the CXCR2 receptor antagonist from Days 0 to 16. One possibility to explain such findings stems from the observation that there were reduced levels of IL-10 and increased levels of GM-CSF in lungs of DF2162-treated mice. As IL-10 possesses relevant anti-inflammatory and pro-apoptotic actions on neutrophils (46, 47), and GM-CSF has an opposite effect, prolonging neutrophil survival and activation (48), the balance between IL-10 and GM-CSF levels in drug-treated animals could account for the greater number of neutrophils in lung parenchyma at the later stages of DF2162-treated animals. Another putative mechanism

contributing to leukocyte clearance and eventual resolution of inflammatory response is the transmigration of cells into airway spaces. The transmigrated granulocyte can then be safely eliminated by apoptosis and subsequent phagocytosis, or be trapped by secretions and removed by mucociliary escalator mechanisms (49, 50). As the blockade of CXCR2 inhibits neutrophil transmigration into airway space, the drug would, hence, promote their arrest and interstitial accumulation after bleomycin challenge. Whatever the mechanisms underlying the enhanced number of neutrophils found in lung interstitium after DF2162 treatment, these results would suggest that it is the neutrophils' transmigration into airway space that is relevant for the induction of lung injury by bleomycin instillation. During transmigration from interstitium to airway space, activated neutrophils are able to secrete proteases, such as elastase and matrix metalloproteinases. These proteases facilitate neutrophil transmigration by digesting extracellular matrix and promoting increase in vascular permeability, thus potentially enhancing lung damage and cleavage of inactive TGF-β_1 into the active form (35, 36). We found identical levels of total TGF-β_1 when comparing DF2162- and vehicle-treated-mice at Day 16 after bleomycin. However, DF2162-treated mice displayed reduced levels of active TGF-β_1. The latter results suggest that DF2162 treatment may regulate not only the transmigration of neutrophils into airspaces but also their activation state. Further studies are necessary to confirm this possibility.

Therapeutic benefits of DF2162 administration were tested by giving the drug from day 8 after bleomycin challenge. Using this therapeutic schedule, the drug decreased the pulmonary levels of IL-13 and TGF-β_1 and pulmonary fibrosis. There were also increased levels of angiostatic chemokines and reduced angiogenic activity. In summary, our work showed that CXCR2 has an important role in mediating pulmonary fibrosis after bleomycin instillation in mice. Blockade of CXCR2 was associated with inhibition of neutrophil influx into airspaces, inhibition of the fibrogenic cytokines IL-13 and TGF-β_1 and decreased pulmonary angiogenesis and fibrosis. It is possible that CXCR2 may represent an interesting target for therapeutic intervention in idiopathic pulmonary fibrosis.

Conflict of Interest Statement: M.T. has received $10,000 for serving as consultant for Dompe. None of the other authors has a financial relationship with a commercial entity that has an interest in the subject of this manuscript.

Acknowledgments: The authors thank Valdinéria Borges and Ilma Marçal for technical assistance. The authors are grateful to Dr. Massimo Locati and Dr. Alberto Mantovani, from Istituto Clinico Humanitas (ICH), for help with experiments *in vitro* and reagents.

References

1. Coultas DB, Zumwalt RE, Black WC, Sobonya RE. The epidemiology of interstitial lung diseases. *Am J Respir Crit Care Med* 1994;150:967–972.
2. Kaminski N. Microarray analysis of idiopathic pulmonary fibrosis. *Am J Respir Cell Mol Biol* 2003;29:S32–S36.
3. Selman M. Idiopathic pulmonary fibrosis challenges for the future. *Chest* 2001;120:8–10.
4. Chen J, Stubbe J. Bleomycins. towards better therapeutics. *Nat Rev Cancer* 2005;5:102–112.
5. Einhorn LH. Chemotherapeutic and surgical strategies for germ cell tumors. *Chest Surg Clin N Am.* 2002;12:695–706.
6. Hecht SM. Bleomycin: new perspectives on the mechanism of action. *J Nat Prod* 2000;63:158–168.
7. Sleijfer S. Bleomycin-induced pneumonitis. *Chest* 2001;120:617–624.
8. Giri SN, Schwartz LW, Hollinger MA, Freywald ME, Schiedt MJ, Zuckerman JE. Biochemical and structural alterations of hamster lungs in response to intratracheal administration of bleomycin. *Exp Mol Pathol* 1980;33:1–14.
9. Giri SN. Novel pharmacological approaches to manage interstitial lung fibrosis in the twenty-first century. *Annu Rev Pharmacol Toxicol* 2003;43:73–95.
10. Murphy PM, Baggiolini M, Charo IF, Hebert CA, Horuk R, Matsushima K, Miller LH, Oppenheim JJ, Power CA. International union of pharmacology: XXII. Nomenclature for chemokine receptors. *Pharmacol Rev* 2000;52:145–176.
11. Luster AD. Chemokines-chemotactic cytokines that mediate inflammation. *N Engl J Med.* 1998;338:436–445.
12. Christopherson K II, Hromas R. Chemokine regulation of normal and pathologic immune responses. *Stem Cells* 2001;19:388–396.
13. Belperio JA, Keane MP, Arenberg DA, Addison CL, Ehlert JE, Burdick MD, Strieter RM. CXC chemokines in angiogenesis. *J Leukoc Biol* 2000;68:1–8.
14. Strieter RM, Gomperts BN, Keane MP. The role of CXC chemokines in pulmonary fibrosis. *J Clin Invest* 2007;117:549–556.
15. Bertini R, Allegretti M, Bizzarri C, Moriconi A, Locati M, Zampella G, Cervellera MN, Di Cioccio V, Cesta MC, Galliera E, *et al.* Noncompetitive allosteric inhibitors of the inflammatory chemokine receptors CXCR1 and CXCR2: prevention of reperfusion injury. *Proc Natl Acad Sci U S A.* 2004;101:11791–11796.
16. Souza DG, Bertini R, Vieira AT, Cunha FQ, Poole S, Allegretti M, Colotta F, Teixeira MM. Repertaxin, a novel inhibitor of rat CXCR2 function, inhibits inflammatory responses that follow intestinal ischaemia and reperfusion injury. *Br J Pharmacol* 2004;143:132–142.
17. Barsante MM, Cunha TM, Allegretti M, Cattani F, Policani F, Bizzarri C, Tafuri WL, Poole S, Cunha FQ, Bertini R, *et al.* Blockade of the chemokine receptor CXCR2 ameliorates adjuvant-induced arthritis in rats. *Br J Pharmacol* 2008;153:992–1002.
18. Cunha TM, Barsante MM, Guerrero AT, Verri WA Jr, Ferreira SH, Coelho FM, Bertini R, Di Giacinto C, Allegretti M, Cunha FQ, *et al.* Treatment with DF2162, a non-competitive allosteric inhibitor of CXCR1/2, diminishes neutrophil influx and inflammatory hypernociception in mice. *Br J Pharmacol* 2008;154:460–470.
19. Burg ND, Pillinger MH. The neutrophil: function and regulation in innate and humoral immunity. *Clin Immunol* 2001;99:7–17.
20. Tirouvanziam R. Neutrophilic inflammation as a major determinant in the progression of cystic fibrosis. *Drug News Perspect* 2006;19:609–614.
21. Barnes PJ. New molecular targets for the treatment of neutrophilic diseases. *J Allergy Clin Immunol* 2007;119:1055–1062.
22. Keane MP, Belperio JA, Moore TA, Moore BB, Arenberg DA, Smith RE, Burdick MD, Kunkel SL, Strieter RM. Neutralization of the CXC chemokine, Macrophage Inflammatory Protein-2, attenuates bleomycin-induced pulmonary fobrosis. *J Immunol* 1999;162:5511–5518.
23. Soares AC, Souza DG, Pinho V, Vieira AT, Nicoli JR, Cunha FQ, Mantovani A, Reis LF, Dias AA, Teixeira MM. Dual function of the long pentraxin PTX3 in resistance against pulmonary infection with Klebsiella pneumoniae in transgenic mice. *Microbes Infect* 2006;8:1321–1329.
24. Reddy GK, Enwemeka CS. A simplified method for the analysis of hydroxyproline in biological tissues. *Clin Biochem* 1996;29:225–229.
25. Wagner DD, Olmsted JB, Marder VJ. Immunolocalization of von Willebrand protein in Weibel-Palade bodies of human endothelial cells. *J Cell Biol* 1982;95:355–360.
26. Sahni A, Francis CW. Vascular endothelial growth factor binds to fibrinogen and fibrin and stimulates endothelial cell proliferation. *Blood* 2000;96:3772–3778.
27. Li A, Dubey S, Varney ML, Dave BJ, Singh RK. IL-8 directly enhanced endothelial cell survival, proliferation, and matrix metalloproteinases production and regulated angiogenesis. *J Immunol* 2003;170:3369–3376.
28. Selman M, Pardo A. Idiopathic pulmonary fibrosis: an epithelial/fibroblastic cross-talk disorder. *Respir Res* 2002;3:3.
29. Thannickal VJ, Toews GB, White ES, Lynch JP III, Martinez FJ. Mechanisms of pulmonary fibrosis. *Annu Rev Med* 2004;55:395–417.
30. Chapman HA. Disorders of lung matrix remodeling. *J Clin Invest* 2004;113:148–157.
31. Strieter RM. Con: Inflammatory mechanisms are not a minor component of the pathogenesis of idiopathic pulmonary fibrosis. *Am J Respir Crit Care Med* 2002;165:1206–1207.
32. Gauldie J. Pro: Inflammatory mechanisms are a minor component of the pathogenesis of idiopathic pulmonary fibrosis. *Am J Respir Crit Care Med* 2002;165:1205–1206.
33. Razzaque MS, Taguchi T. Pulmonary fibrosis: Cellular and molecular events. *Pathol Int* 2003;53:133–145.
34. Gauldie J, Kolb M, Sime PJ. A new direction in the pathogenesis of idiopathic pulmonary fibrosis? *Respir Res* 2002;3:1.
35. Chua F, Dunsmore SE, Clingen PH, Mutsaers SE, Shapiro SD, Segal AW, Roes J, Laurent GJ. Mice lacking neutrophil elastase are resistant to bleomycin-induced pulmonary fibrosis. *Am J Pathol* 2007;170:65–74.

36. Li Q, Park PW, Wilson CL, Parks WC. Matrilysin shedding of syndecan-1 regulates chemokine mobilization and transepithelial efflux of neutrophils in acute lung injury. *Cell* 2002;111:635–646.
37. Manoury B, Nénan S, Guénon I, Lagente V, Boichot E. Influence of early neutrophil depletion on MMPs/TIMP-1 balance in bleomycin-induced lung fibrosis. *Int Immunopharmacol* 2007;7:900–911.
38. Vanderbilt JN, Mager EM, Allen L, Sawa T, Wiener-Kronish J, Gonzalez R, Dobbs LG. CXC chemokines and their receptors are expressed in type II cells and upregulated following lung injury. *Am J Respir Cell Mol Biol* 2003;29:661–668.
39. Schraufstatter IU, Chung J, Burger M. IL-8 activates endothelial cell CXCR1 and CXCR2 through Rho and Rac signaling pathways. *Am J Physiol Lung Cell Mol Physiol* 2001;280:L1094–L1103.
40. McKenzie AN, Li X, Largaespada DA, Sato A, Kaneda A, Zurawski SM, Doyle EL, Milatovich A, Francke U, Copeland NG, Jenkins NA, Zurawski G. Structural comparison and chromosomal localization of the human and mouse IL-13 genes. *J Immunol.* 1993;150:5436–5444.
41. Miyahara N, Takeda K, Kodama T, Joetham A, Taube C, Park JW, Miyahara S, Balhorn A, Dakhama A, Gelfand EW. Contribution of antigen-primed CD8+ T cells to the development of airway hyperresponsiveness and inflammation is associated with IL-13. *J Immunol.* 2004;172:2549–2558.
42. Temann UA, Laouar Y, Eynon EE, Homer R, Flavell RA. IL9 leads to airway inflammation by inducing IL13 expression in airway epithelial cells. *Int Immunol* 2007;19:1–10.
43. Fichtner-Feigl S, Strober W, Kawakami K, Puri RK, Kitani A. IL-13 signaling through the IL-13alpha2 receptor is involved in induction of TGF-beta1 production and fibrosis. *Nat Med* 2006;12:99–106.
44. Oppermann M, Mack M, Proudfoot AE, Olbrich H. Differential effects of CC chemokines on CC chemokine receptor 5 (CCR5) phosphorylation and identification of phosphorylation sites on the CCR5 carboxyl terminus. *J Biol Chem.* 1999;274:8875–8885.
45. Petrek M, Pantelidis P, Southcott AM, Lympany P, Safranek P, Black CM, Kolek V, Weigl E, du Bois RM. The source and role of RANTES in interstitial lung disease. *Eur Respir J* 1997;10:1207–1216.
46. Cox G. IL-10 enhances resolution of pulmonary inflammation in vivo by promoting apoptosis of neutrophils. *Am J Physiol* 1996;271:L566–L571.
47. Cassatella MA. The neutrophil: one of the cellular targets of interleukin-10. *Int J Clin Lab Res* 1998;28:148–161.
48. Hamilton JA. Colony-stimulating factors in inflammation and autoimmunity. *Nat Rev Immunol* 2008;8:533–544.
49. Uller L, Persson CG, Erjefalt JS. Resolution of airway disease: removal of inflammatory cells through apoptosis, egression or both? *Trends Pharmacol Sci* 2006;27:461–466.
50. Erjefalt JS, Uller L, Malm-Erjefalt M, Persson CG. Rapid and efficient clearance of airway tissue granulocytes through transepithelial migration. *Thorax* 2004;59:136–143.

3.2. Trabalho cientifico – 2

DÉRUAZ, M.; FRAUENSCHUH, A.; ALESSANDRI, A. L.; DIAS, J. M.; COELHO, F. M.; **RUSSO, R. C.**; FERREIRA, B. R.; GRAHAM, G. J.; SHAW, J. P.; WELLS, T. N.; TEIXEIRA, M. M.; POWER, C. A.; PROUDFOOT, A. E. ***Ticks produce highly selective chemokine binding proteins with antiinflammatory activity.*** **J Exp Med.** 2008 Sep 1;205(9):2019-31.

Os objetivos específicos deste estudo foram:

1. Clonar e caracterizar uma família de proteínas ligantes de quimiocinas (CKBP) derivadas da saliva do carrapato *Rhipicephalus sanguineus,* denominadas Evasinas.

2. Determinar a seletividade de ligação às quimiocinas de cada membro da família destas Evasinas.

3. Avaliar os efeitos das Evasinas em modelos de recrutamentos celular *in vitro* e *in vivo*.

4. Estudar os efeitos anti-inflamatórios do tratamento com as Evasinas nos modelos de patologias animais dependentes da produção de quimiocinas, dentre eles, estudar os efeitos da administração de Evasina-1 (*CCL3-binding protein*) no modelo de fibrose pulmonar induzida por bleomicina.

Published August 4, 2008

JEM

ARTICLE

Ticks produce highly selective chemokine binding proteins with antiinflammatory activity

Maud Déruaz,[1] Achim Frauenschuh,[1] Ana L. Alessandri,[2] João M. Dias,[1] Fernanda M. Coelho,[2] Remo C. Russo,[2] Beatriz R. Ferreira,[3] Gerard J. Graham,[4] Jeffrey P. Shaw,[1] Timothy N.C. Wells,[1] Mauro M. Teixeira,[2] Christine A. Power,[1] and Amanda E.I. Proudfoot[1]

[1]Merck Serono Geneva Research Centre, 1202 Geneva, Switzerland
[2]Departamento de Bioquimica e Imunologia, Instituto de Ciencias Biologicas, Universidade Federal de Minas Gerais, Belo Horizonte, MG, Brazil
[3]Departamento de Bioquímica e Imunologia, Faculdade de Medicina de Ribeirão Preto, Universidade de São Paulo, SP, Brazil
[4]Division of Immunology, Infection and Inflammation, University of Glasgow, Glasgow, G12 8TA, Scotland, UK

Bloodsucking parasites such as ticks have evolved a wide variety of immunomodulatory proteins that are secreted in their saliva, allowing them to feed for long periods of time without being detected by the host immune system. One possible strategy used by ticks to evade the host immune response is to produce proteins that selectively bind and neutralize the chemokines that normally recruit cells of the innate immune system that protect the host from parasites. We have identified distinct cDNAs encoding novel chemokine binding proteins (CHPBs), which we have termed Evasins, using an expression cloning approach. These CHBPs have unusually stringent chemokine selectivity, differentiating them from broader spectrum viral CHBPs. Evasin-1 binds to CCL3, CCL4, and CCL18; Evasin-3 binds to CXCL8 and CXCL1; and Evasin-4 binds to CCL5 and CCL11. We report the characterization of Evasin-1 and -3, which are unrelated in primary sequence and tertiary structure, and reveal novel folds. Administration of recombinant Evasin-1 and -3 in animal models of disease demonstrates that they have potent antiinflammatory properties. These novel CHBPs designed by nature are even smaller than the recently described single-domain antibodies (Hollinger, P., and P.J. Hudson. 2005. *Nat. Biotechnol.* 23:1126–1136), and may be therapeutically useful as novel antiinflammatory agents in the future.

CORRESPONDENCE
Amanda E.I. Proudfoot:
amanda.proudfoot@merckserono.net
OR
Chrstine A. Power:
christine.power@merckserono.net

Abbreviations used: CHPB, chemokine binding protein; mBSA, methylated BSA; SELDI, surface enhanced laser desorption ionization; SPR, surface plasmon resonance.

Many pathogenic organisms, including viruses, have developed strategies to evade the host immune system based on interference with host cytokine and chemokine proinflammatory mediators (1–3). Inhibitory binding proteins for proinflammatory cytokines, including TBP, IFNAR, and IL-18 BP, have also been described in humans, but no secreted chemokine binding proteins (CHPBs) have so far been identified in vertebrates. However, internal and external parasites have evolved chemokine neutralization strategies that allow them to productively suppress the mammalian immune response to prolong survival on their host. Ticks are bloodsucking parasites whose role in the transmission of pathogens such as *Borrelia burgdorferi*, which causes Lyme disease, has been the subject of intensive research (4). Ticks feed on their hosts for relatively long periods of time, ranging from several days to weeks, and provided that they do not carry infectious agents, can remain essentially undetected by their hosts. To achieve this, they have evolved an arsenal of antiinflammatory, anticoagulant, and analgesic agents that are used to render the ticks invisible to the immune system (5). Little is known about the molecular nature of such agents, but the cloning and characterization of these factors may shed light on the immunoevasion mechanisms used by these organisms, as well as yield

A. Frauenschuh's present address is Novartis Pharma AG, 4056 Basel, Switzerland.

© 2008 Déruaz et al. This article is distributed under the terms of an Attribution–Noncommercial–Share Alike–No Mirror Sites license for the first six months after the publication date (see http://www.jem.org/misc/terms.shtml). After six months it is available under a Creative Commons License (Attribution–Noncommercial–Share Alike 3.0 Unported license, as described at http://creativecommons.org/licenses/by-nc-sa/3.0/).

The Rockefeller University Press $30.00
J. Exp. Med.
www.jem.org/cgi/doi/10.1084/jem.20072689

The Journal of Experimental Medicine

Downloaded from www.jem.org on August 6, 2008

novel proteins of potential therapeutic use in human inflammatory pathologies.

Successful prevention of the activity of families of small chemoattractant proteins called chemokines has been shown for several viral CHBPs (for reviews see [1, 6]), and, more recently, by a CHBP isolated from the parasitic worm *Schistosoma mansoni* (7). Deletion of the gene encoding the broad spectrum CHPB T1 from the rabbit poxvirus myxoma virus resulted in extensive leukocyte infiltration in the dermis of the infected animal, which was absent upon infection by the wild-type virus (8). This study clearly demonstrated that the virus had evolved a mechanism that prevented the recruitment of leukocytes to the site of infection.

Recently, the presence of antichemokine activities has been reported in tick saliva (9, 10). Tick salivary gland extracts were shown to contain an activity that neutralized CXCL8, and in a later study, neutralization of other chemokines was also demonstrated. Our own analyses of tick saliva harvested during feeding also demonstrated the presence of molecules that bound to CXCL8, CCL3, and CCL5. Using an expression cloning strategy to identify the protein(s) in tick saliva that bind to chemokines, we cloned a CHPB, which we called Evasin-1, that specifically binds to the CC chemokines CCL3, CCL4, and CCL18 (11). We also cloned a second protein of similar size, Evasin-2, for which the ligand remains to be elucidated. Subsequent rescreening of the tick salivary gland cDNA library with a selection of chemokines and cytokines enabled us to identify two further CHBPs. In this study, we report the cloning of a CXC CHPB named Evasin-3 and a second CC CHPB, distinct from Evasin-1, named Evasin-4. Interestingly, Evasin-3 bears no sequence homology to Evasin-1 and -4, which appear to belong to the same structural family. The three proteins are all surprisingly small compared with other chemokine and cytokine binding proteins described to date. Evasin-1 and -3 were crystallized, and their three-dimensional structures have been solved, revealing novel folds with binding modes distinct from that of viral CHBPs. Investigations of their specificity in vitro and their efficacy in vivo in animal models of chronic inflammatory diseases such as pulmonary fibrosis, arthritis, and psoriasis have demonstrated that the Evasins have potent antiinflammatory activities, providing tantalizing new insights into scaffolds evolved by nature to inhibit inflammation.

RESULTS

Evidence for the presence of CHPBs in tick saliva and their expression cloning

We analyzed the ability of saliva from *Rhipicephalus sanguineus* (common brown dog tick) to inhibit the binding of the I^{125}-labeled chemokines CCL2, CCL5, and CXCL8, as well as CCL3, to their respective receptors using a scintillation proximity assay. As shown in Fig. 1 a, inhibition of binding was achieved for CCL3, CCL5, and CXCL8, with the most potent effect on CCL3. No inhibition was observed for CCL2 although saliva harvested from another tick species, *Amblyomma cajennense*, appeared to have anti-CCL2 activity (unpublished data). The possibility that the inhibition was caused by degradation of the radiolabeled chemokines by a proteolytic activity in the saliva was addressed by incubation of the radiolabeled chemokines in saliva for 4 h. Subsequent analysis by SDS-PAGE revealed that no degradation of the chemokine had occurred (unpublished data). We next addressed the question of whether there was more than one binding protein present in the saliva by testing whether an excess of CXCL8 was able to block the activity of the CCL3 binding protein. As shown in Fig. 1 a, a 500-fold excess of CXCL8 had no effect on the ability of the saliva to inhibit CCL3 binding to CCR5, therefore suggesting the presence of at least two binding proteins.

Incubation of ^{125}I-CCL3 with tick saliva, followed by chemical cross-linking, produces a clear band shift when the reaction products were analyzed on SDS PAGE, and this method was adopted as a screening assay in our attempts to clone the tick CHBPs. We therefore used the band shift assay to screen supernatants from HEK293 cells transfected with a tick salivary gland cDNA library, to identify a cDNA encoding Evasin-1 (11). Surface plasmon resonance (SPR) performed with immobilized CCL3 and CCL5 demonstrated the presence of binding proteins for these two chemokines in tick saliva (Fig. 1 b), and surface enhanced laser desorption ionization (SELDI) identified peaks that bound to immobilized CXCL8 and CCL5 (Fig. 1 c), but surprisingly, no peak was observed for CCL3 (not depicted). The masses identified by SELDI indicated very small proteins with a mass of 7,133 Daltons binding to CXCL8 and a mass of 11,052 Daltons binding to CCL5; these masses are very close to those of the predicted protein cores, as discussed in the following section.

We therefore rescreened the cDNA library using a cocktail of chemokines and cytokines, containing iodinated CXCL8, IL-1β, and IL-2. IL-2 was included because an anti-IL-2 activity has previously been reported in tick salivary gland extracts (9). In the first round of screening, we identified a band shift in one pool of 270 clones. After deconvolution of the positive pool, and cross-linking to the individual iodinated proteins present in the cocktail, we identified a cDNA encoding a CXCL8 binding protein. As we had previously identified a putative CHBP that we named Evasin-2, the function of which remains to be elucidated, we called the CXCL8 binding protein Evasin-3 (Fig. 2 a, lane 3). Competition experiments using a panel of chemokines (CCL3, CXCL1, CXCL4, CXCL7, CXCL8, CXCL9, CXCL10, CXCL11, CXCL12, and CXCL13) indicated that only CXCL1 and CXCL8 were able to compete with radiolabeled CXCL8 for binding to Evasin-3 (unpublished data). We then screened the expression library with a second cocktail consisting of iodinated CCL5, CCL11, and CXCL10. Upon analysis of supernatants from HEK cells transfected with the pools of clones from the cDNA expression library, we observed a band shift migrating at ~50 kD in several pools. This band was almost masked by a nonspecific band migrating at ~60 kD detected in all experiments. Deconvolution of the positive pools revealed a cDNA

Downloaded from www.jem.org on August 6, 2008

Published August 4, 2008

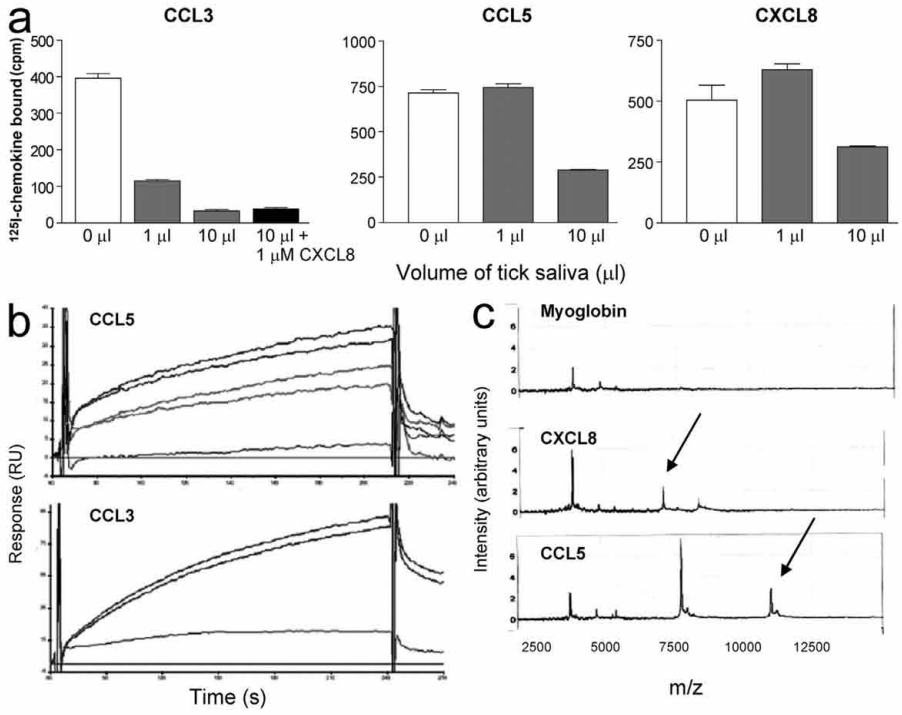


Figure 1. Chemokine binding activity in tick saliva. (a) Tick saliva inhibits the binding of CCL3, CCL5, and CXCL8 to their cognate receptors. Radiolabeled chemokines were incubated with CHO cell membranes expressing CCR1 for CCL3 and CCL5, and CXCR2 for CXCL8, in the presence of 1 µl, 10 µl, or in the absence of tick saliva. The antichemokine activity is caused by the presence of more than one binding protein because an excess of CXCL8 did not abolish the inhibition of CCL3 binding. Error bars represent the mean ± SEM. (b) Detection of CHPBs in tick saliva by SPR. Sensograms demonstrated binding to CCL5(E66A) and CCL3 immobilized on a CM4 chip. (c) Detection of distinct CHPBs to CCL5 and CXCL8 by Retentate chromatography SELDI of flight mass spectrometry (RC-SELDI-TOF-MS). Tick saliva was incubated on a PS-20 Proteinchip array coated with either CCL5 (bottom), CXCL8 (middle), or the control protein equine myoglobin (top). Specific peaks, indicated by arrows, corresponding to a protein with a mass of 11,052 Daltons binding to CCL5 and of 7,133 Daltons for the binding to CXCL8 were observed.

clone that was able to mediate cross-linking to both CCL5 and CCL11 (Fig. 2 a, lanes 4 and 5), but not CXCL10 when tested in HEK293 cells. The CCL5 and CCL11 binding protein was named Evasin-4.

Structural analyses of the Evasins

The cDNA for Evasin-3 encoded an ORF of 92 amino acids that, after signal peptide cleavage, gave rise to a mature protein of 66 amino acids with a predicted molecular mass of 7,005 Daltons. The cDNA for Evasin-4 encoded an ORF of 117 amino acids. Cleavage of the signal peptide sequence predicted that using the Signal P algorithm would generate a mature protein of 110 amino acids with a predicted molecular mass of 12,032 Daltons (Fig. 2 b). Analyses of the amino acid sequences of Evasin-3 and -4 revealed that Evasin-3 was unrelated to Evasin-1, whereas the Cys residues of the mature Evasin-4 sequence demonstrated an almost perfect alignment with those of Evasin-1 (Fig. 2 b). This indicates an identical disulfide topology, suggesting that these two proteins are structurally related, despite their relatively low level of identity at the amino acid level (27% identity over 91 amino acids). Conservation of a homologous fold, despite a low level of identity at the primary sequence level, is well known in protein families such as cytokines and chemokines.

Transient expression of C-terminal 6His tagged Evasin-3 and -4 in HEK293 cells revealed that unlike Evasin-1, these two proteins were poorly secreted. We were able to obtain a small amount of purified Evasin-3 (150 µg), which was extensively glycosylated for in vitro characterization. SPR analysis revealed that Evasin-3, similar to Evasin-1, is a highly selective CHPB in that it was only able to bind to CXCL1 and CXCL8 and their murine counterparts, KC and MIP-2 (Fig. 2 c). The kinetic parameters, as determined by SPR, are shown in Table I. It has proven difficult to produce recombinant 6His-tagged Evasin-4 in HEK293 cells, thus the identification of the N terminus of the mature protein has not yet been experimentally verified. Using the Signal P program to predict the cleavage site of the putative signal peptide sequence indicates that the mature protein sequence would commence with WLSTKC (Fig. 2 b). However, secondary structure predictions show that these amino acids are contained in a helix, suggesting that signal peptide cleavage may in fact be after Cys23, yielding an N terminus of EVPQM, as predicted by the latest version of Signal P. Nevertheless, alignment of the amino acid

Downloaded from www.jem.org on August 6, 2008

Published August 4, 2008

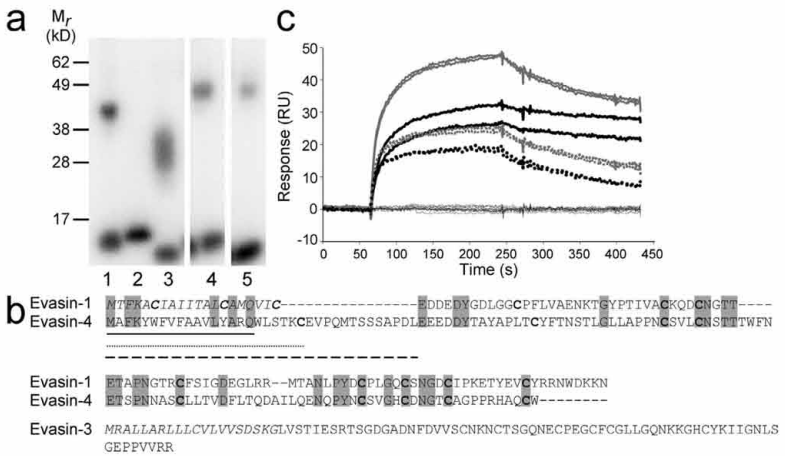


Figure 2. Identification of Evasin-3 and -4. (a) Identification of Evasin-3 and -4 by cross-linking to radiolabeled chemokine in supernatants from transfected HEK293 cells. Viral CHBP p35 incubated with [^{125}I]-CCL2 as a positive control in the presence (lane 1) or absence (lane 2) of the cross-linker BS_3; supernatant from clone 69.19.1 incubated with [^{125}I]-CXCL8 and BS_3 (lane 3); supernatant from clone 10.27.1 incubated with [^{125}I]-CCL5 and BS_3 (lane 4) or [^{125}I]-CCL11 and BS_3 (lane 5). (b) Alignment of the predicted protein sequences of Evasin-1 and -4. Conserved residues are highlighted in gray and cysteines are shown in bold type. The predicted protein sequence of Evasin-3 is shown below the alignment. The signal peptides are shown in italics. Possible signal peptides of Evasin-4 are shown as follows: based on SignalJ prediction, black underline; based on secondary structure prediction, dotted underline; based on similarity to Evasin-1, dashed line. (c) Determination of the selectivity of immobilized recombinant Evasin-3 produced in *E. coli* by surface plasmon resonance. Sensograms corresponding to CXCL8 (bold black lines) CXCL1 (dotted black lines), MIP-2 (gray lines), and KC (dotted gray lines) showed strong binding of these chemokines to Evasin-3. The sensograms corresponding to CCL1, CCL2, CCL3, CCL4, CCL5, CCL11, CCL18, CCL27, CXCL9, CXCL10, CXCL11, CXCL12, CXCL13, and CX_3CL1 (black lines) indicated no binding of these chemokines to Evasin-3.

sequences of Evasin-4 and -1 still shows that Evasin-4 has an extended N terminus compared with Evasin-1, which may be an important determinant of ligand binding specificity. We are currently testing different expression strategies to obtain sufficient Evasin-4 for N-terminal sequence verification and for in vitro and in vivo studies.

Because the yield of Evasin-3 was poor in the HEK293 expression system, we attempted expression in a prokaryotic host, *Escherichia coli*. It was very probable that Evasin-3 would be directed into inclusion bodies based on a formula predicting solubility for recombinant expression in *E. coli* (12). Surprisingly, the protein was expressed at high levels as soluble protein that could be purified to homogeneity in two chromatographic steps (unpublished data). Although the protein produced in *E. coli* is not glycosylated, it had equivalent activity to Evasin-3 produced in HEK293 cells (Table I; see also Fig. 8 a), suggesting that the glycosylation was not essential for activity.

Table I. Binding characteristics of Evasin-1 and -3 as determined by SPR

CKBP	Chemokine	$k_a \times 10^6$	$k_d \times 10^{-3}$	$K_d \times 10^{-9}$
		$M^{-1}s^{-1}$	s^{-1}	nM
Evasin-1	CCL3	13.8 ± 3.54	2.43 ± 0.61	0.12
	CCL3L1	13.2 ± 2.9	0.67 ± 0.13	0.05
	mMIP-1α	15.6 ± 16	1.18 ± 1.07	0.08
	CCL4	4.29 ± 2.58	2.2 ± 0.18	0.51
	mMIP-1β	3.84 ± 1.42	0.58 ± 0.12	0.15
Evasin-3 (HEK)	CXCL1	3.95 ± 4.23	1.42 ± 0.36	0.34
	CXCL8	0.41 ± 0.30	0.29 ± 0.14	0.7
	KC	0.64 ± 0.58	1.44 ± 0.35	2.25
	MIP-2	0.79 ± 0.9	0.33 ± 0.11	0.4
Evasin-3 (*E. coli*)	CXCL1	2.61 ± 0.69	2.22 ± 0.49	0.85
	CXCL8	0.84 ± 0.33	0.36 ± 0.05	0.43
	KC	0.32 ± 0.17	1.85 ± 0.43	5.78
	MIP-2	1.02 ± 0.56	0.65 ± 0.25	0.64

Downloaded from www.jem.org on August 6, 2008

Published August 4, 2008

Evasin-3 produced in *E. coli* crystallized readily, and the structure revealed a novel fold that was totally unrelated to that of Evasin-1 (Fig. 3). The crystallographic structure of Evasin-1, described in detail elsewhere (unpublished data), also revealed a novel protein fold (Fig. 3 a). Neither protein has a structural homologue in the Protein Data Bank database. So although Evasin-1 and -3 are of similar size and function, they are completely unrelated at the amino acid sequence level, as well as in the secondary and tertiary structure (Fig. 3, a and b). Although the mode of binding of Evasin-1 has been elucidated by the determination of the structure of the complex of Evasin-1 with CCL3 (unpublished data), the structure of the Evasin-3 complex remains to be solved. If ticks produce two very different CHPBs, with very different selectivity profiles, it is likely that they bind their substrates in very different way. The elucidation of the structure of the complex of Evasin-3 with its ligand(s) would thus greatly help to understand the selectivity of these different CHPBs.

Evasin-1 inhibits cell recruitment in vitro and in vivo

We have previously determined the binding affinities of Evasin-1 for three chemokines by surface plasmon resonance, and we have extended these analyses to include the second form of CCL3, known as CCL3L1, as well as the murine homologues of CCL3 and CCL4 (Table I). The K_d value for 0.05 nM CCL3L1 is similar to that determined for CCL3, in contrast to their very different potencies on CCR5 and CCR1 (13). Importantly, the affinities for murine MIP-1α and -1β, with K_d values of 0.08 and 0.15 nM, respectively, are similar to those for the human chemokines, allowing subsequent investigation of the antiinflammatory properties of Evasin-1 in murine models.

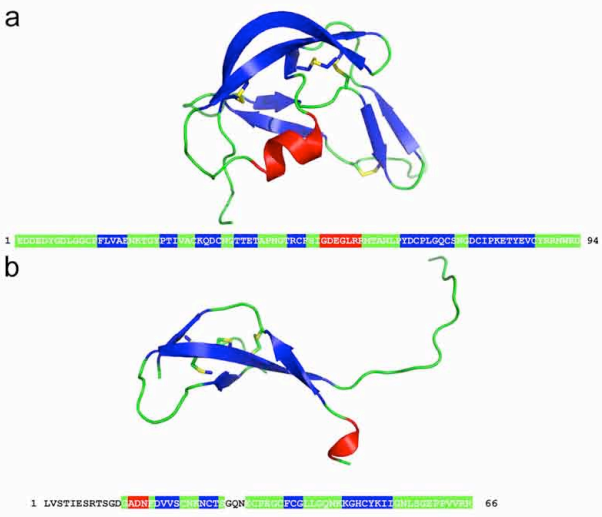


Figure 3. Crystal structures of Evasin-1 and -3. Ribbon diagram of Evasin-1 (a) and Evasin-3 (b) with the amino acid sequence depicting residues in loops (green), α-helix (red), or β-sheet (blue).

The IC_{50} values reported for the inhibition of receptor binding, 0.015 nM for CCL3 binding to CCR1 and 3 nM for CCL4 binding to CCR5 (11), are reflected by the ability of Evasin-1 to inhibit the chemotactic activity of these chemokines in vitro and in vivo. We chose the L1.2/CCR5 transfectants for these analyses because we were able to test inhibition of CCL3, CCL3L1, the high-affinity variant for this receptor, and CCL4 in the same assay system. As shown in Fig. 4 a, Evasin-1 showed potent inhibition of ligand-induced chemotaxis of the L1.2/CCR5 transfectants. Using an ED_{80} ligand concentration of 1 nM for CCL3L1 and CCL4, and 10 nM for CCL3, the IC_{50} values were 0.17 nM for CCL3L1, 2 nM for CCL3, and 4 nM for CCL4.

We then tested Evasin-1 in in vivo leukocyte recruitment models in mice. CCL3 and murine MIP-1α were administered into the peritoneal cavity, and the ability of systemically administered Evasin-1 to block leukocyte recruitment was

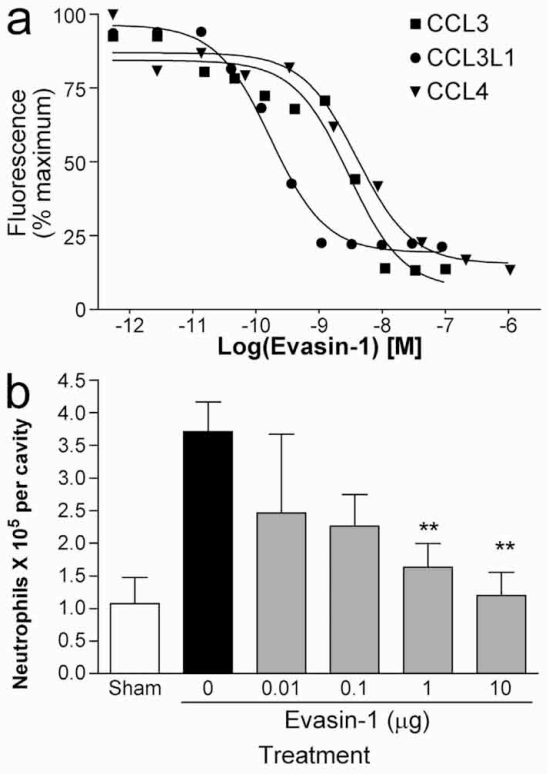


Figure 4. Evasin-1 inhibits cell recruitment in vitro and in vivo. (a) Inhibition of CCL3- (■), CCL3L1- (●) and CCL4-mediated (▲) chemotaxis of L1.2/CCR5 transfectants. The IC_{50} values are 2 nM for CCL3, 0.17 nM for CCL3L1, and 4 nM for CCL4. Data are shown as the mean ± the SD as a percentage of maximal recruitment and are representative of three to five individual experiments. (b) Evasin-1 inhibits granulocyte recruitment induced by CCL3 in mice. Evasin-1 was administered s.c. 45 min before the injection of 10 μg of CCL3 i.p. Cells in the peritoneal cavity were counted 18 h after the injection of CCL3. One representative experiment of three is shown, with 8 mice per group. **, $P < 0.01$ when compared with PBS-treated group. Error bars represent the mean ± SEM.

Downloaded from www.jem.org on August 6, 2008

Published August 4, 2008

assessed after 18 h. Evasin-1 showed dose-related inhibition of neutrophil recruitment with maximal activity at a dose of 10 µg (Fig. 4 b), with little effect on other cell types (not depicted). We therefore used this dose in subsequent studies. The inhibition of granulocyte recruitment by Evasin-1 was then further investigated in a murine model of a Th1-predominant delayed-type hypersensitivity and a Th2-predominant, late-phase reaction. In the Th1 sensitization model using methylated BSA (mBSA), recruitment of granulocytes into the pleural cavity was significantly impaired (Fig. 5 a). Although the inhibition of neutrophil recruitment was most striking, inhibition of $CD3^+$ lymphocytes was also observed, although not of $CD11b^+$ monocytes as determined by FACS (unpublished data). In the Th2 sensitization model, Evasin-1 inhibited eosinophil recruitment induced by antigen challenge into the lungs of mice immunized with *S. mansoni* eggs. An analysis of naive mice by intravital microscopy demonstrated that Evasin-1 was able to block adhesion and emigration of leukocytes induced by injection of MIP-1α (Fig. 5 b). Lastly, administration of Evasin-1 alone had no chemoattractant activity (unpublished data).

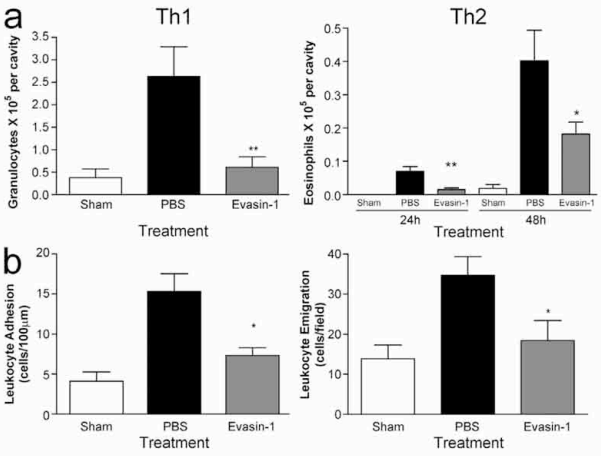


Figure 5. Evasin-1 inhibits cellular recruitment in models of Th1 and Th2 inflammation. (a) Evasin-1 inhibits granulocyte recruitment induced by antigen challenge of immunized mice in models of Th1-predominant delayed-type hypersensitivity and Th2-predominant late-phase response. In the Th1 model, 10 µg Evasin-1 was administered s.c. 45 min before intrapleural injection of 10 µg of mBSA in mice immunized with mBSA in Freund's complete adjuvant. Cells in the pleural cavity were counted 48 h after the injection of antigen. In the Th2 model, 10 µg Evasin-1 was administered s.c. 45 min before and 24 h after the intratracheal injection of 10 µg of *S. mansoni* egg antigen in mice immunized with *S. mansoni* eggs. Cells in the bronchoalveolar lavage fluid were counted 24 and 48 h after the injection of antigen. There were six mice per group in each experiment. *, $P < 0.05$; **, $P < 0.01$ when compared with PBS-treated group. (b) Evasin-1 blocks adhesion and emigration of leukocytes induced by mMIP-1α as assessed by intravital microscopy performed in the cremaster vein of C57BL/6 mice. Evasin-1 was injected s.c. in the right scrotal skin 1 h before exteriorization. Normalized data were analyzed by one-way analysis of variance, and differences between groups were assessed using Student-Newman-Keuls post-test. *, $P < 0.05$; **, $P < 0.01$. There were six mice per group in each experiment. Error bars represent the mean ± SEM.

Evasin-1 shows antiinflammatory activity in murine models of disease

The ability of Evasin-1 to prevent CCL3-/CCL4-dependent cellular recruitment translated into potent antiinflammatory effects in animal models of disease. Skin inflammation in $D6^{-/-}$ mice sensitized with TPA gives rise to a phenotype closely resembling that of the human inflammatory skin disorder, psoriasis, and has been shown to be dependent on the induction of several CC chemokines, including CCL3 and CCL4, which are high-affinity ligands for D6 (14). Evasin-1 administration resulted in a significant reduction in skin inflammation observed in these mice (Fig. 6, a and b), but not complete abrogation as observed with an anti-TNF antibody. This is in accordance with our previous observations and

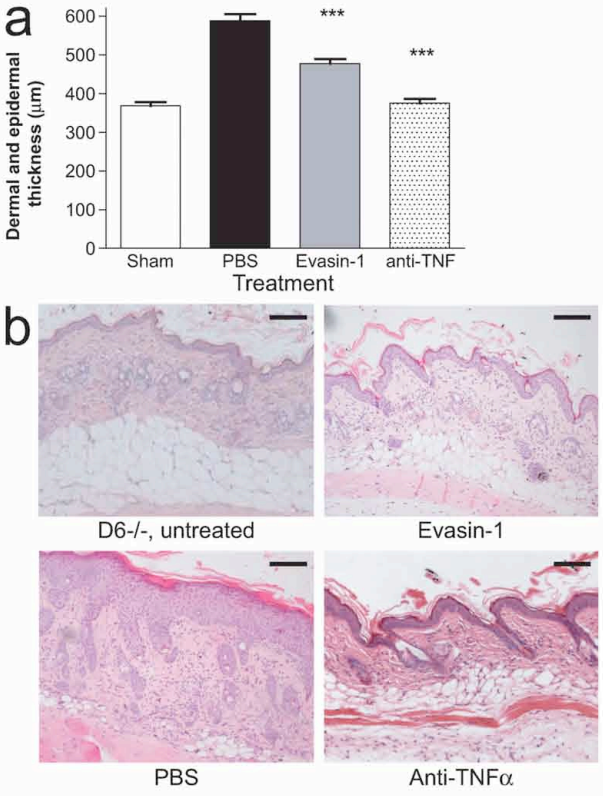


Figure 6. Evasin-1 inhibits cellular recruitment in an animal model of psoriasis. (a) Dermal and epidermal thickness of the skin of WT and D6-deficient (KO) mice after a single cutaneous application of TPA. Evasin-1 (30 µg/mouse) and anti-TNF-α were given daily, and tissues were collected on day 4 for histological assessment. One representative experiment of three is shown, with eight mice per group. ***, $P < 0.001$ when compared with PBS-treated group. Error bars represent the mean ± SEM. (b) Haematoxylin and eosin staining of sections from untreated skin of sham and TPA-injected D6-deficient mice treated with PBS, Evasin-1, or anti-TNF-α. Skin sections were obtained on day 4 after TPA application and are representative of 10 mice per group per experiment. Bars, 100 µm.

Downloaded from www.jem.org on August 6, 2008

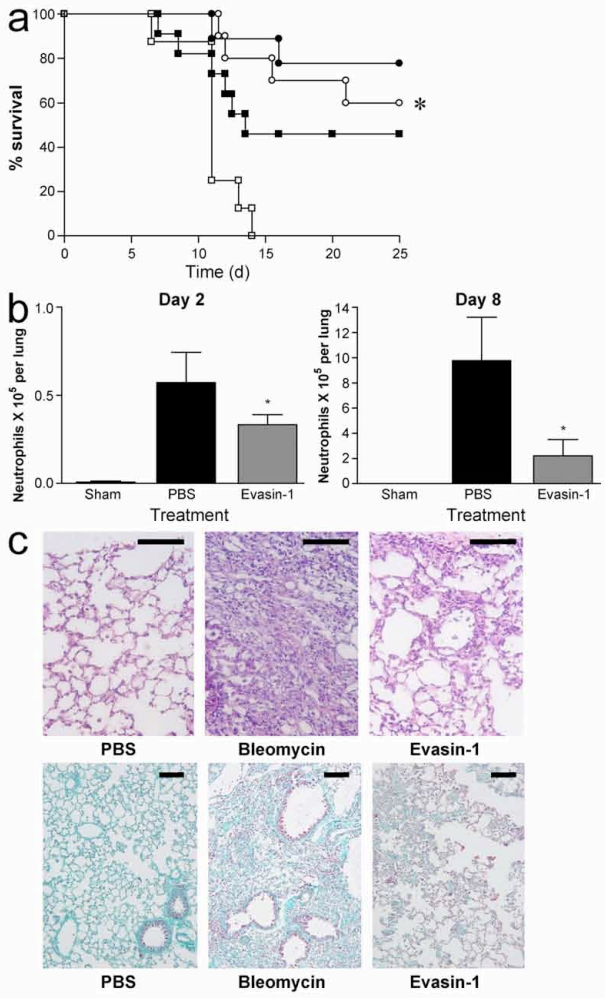


Figure 7. Evasin-1 inhibits lethality, cellular recruitment, and fibrosis in a model of bleomycin-induced pulmonary injury. (a) Evasin-1 inhibits lethality associated with pulmonary instillation of bleomycin in C57BL/6 mice. Bleomycin was instilled intratracheally at doses of 0.0625 U (circles) or 0.125 U (squares) and survival rates were evaluated for 25 d. PBS (open symbols) or Evasin-1 (10 µg per animal; closed symbols) were administered s.c. 45 min before and every 12 h after initial bleomycin instillation. There were 12 mice per group in each experiment. *, $P < 0.05$ when comparing PBS- and Evasin-1–treated animals at 0.125 U. (b) Evasin-1 inhibits neutrophil recruitment induced by bleomycin. Neutrophil recruitment was evaluated at 2 and 8 d after bleomycin (0.125 U) and Evasin-1 (10 µg per animal) was administered s.c. 45 min before and every 12 h after initial bleomycin instillation. There were six mice per group in each experiment. *, $P < 0.05$ when compared with the PBS-treated group. Error bars represent the mean ± SEM. (c) Evasin-1 inhibits pulmonary inflammation and fibrosis induced by instillation of bleomycin. Hematoxylin and eosin– (top) and Gomori's trichrome–stained (bottom) sections from animals instilled with sodium chloride (0.9% NaCl, 25 µl) or bleomycin (0.125 U). Evasin-1 (10 µg per animal) was administered as previously described and lungs were removed on day 16. Bars: (top) 100 µm; (bottom) 50 µm.

indicates that although several CC chemokines are implicated in this model, targeting CCL3 and CCL4 is sufficient to ameliorate pathology.

CCL3 has previously been demonstrated to play a role in mediating pulmonary fibrosis (15). We therefore tested the effect of Evasin-1 in a lung injury model induced by intratracheal instillation of bleomycin. Mild or severe disease was induced with 0.0625 or 0.125 U of bleomycin. Evasin-1 reduced lethality in both forms of the disease (Fig. 7 a). Reduction in lethality was associated with a decrease in neutrophil accumulation at 2 and 8 d after bleomycin challenge (Fig. 7 b), and a net decrease in the ensuing fibrosis observed at later stages after the bleomycin challenge. Histopathological analysis of lung tissue confirmed decreased leukocyte infiltration in the lung (Fig. 7 c), which was corroborated by a decrease in the number of $CD3^+CD4^+$ and $CD3^+CD8^+$ lymphocytes and $GR1^+$ leukocytes in the bronchoalveolar lavage fluid of mice challenged with bleomycin. In bleomycin-instilled mice that did not receive Evasin-1, there was a considerable deterioration of normal pulmonary architecture with loss of alveolar structure and collagen deposition (Fig. 7 c). Treatment with Evasin-1 resulted in the preservation of lung architecture and a decrease in collagen deposition. Morphometric analysis of Gomori's trichrome–stained areas showed that Evasin-1 treatment reduced collagen deposition by 40%.

Evasin-3 is a potent inhibitor of neutrophil-mediated inflammation

Evasin-3 has also been shown to have potent antiinflammatory properties. In accordance with the nanomolar affinities observed by SPR analysis (Table I), Evasin-3 produced in HEK293 cells and in *E. coli* inhibited binding of ^{125}I-CXCL8 to CXCR1 with IC_{50} values of 0.7 and 1 nM, respectively (Fig. 8 a), demonstrating that glycosylation is not necessary for binding, similar to Evasin-1 (11). CXCL8-induced chemotaxis of neutrophils in vitro was inhibited by Evasin-3 with an IC_{50} of 3.35 nM (Fig. 8 b). In vivo, Evasin-3 inhibited KC-induced neutrophil recruitment into the peritoneal cavity in a dose-dependent manner, with maximal inhibition at a dose of 1 µg per mouse (Fig. 8 c). We also tested the ability of Evasin-3 to inhibit KC recruitment into the knee joint, and found it to be even more potent in this cavity (Fig. 8 d).

Evasin-3 was then tested in a mouse model of antigen-induced arthritis. In this model, rapid up-regulation of KC and MIP-2 precedes the recruitment of neutrophils into the knee joint. This is followed by CXCR2 up-regulation and TNF-α production, culminating in synovial hyperplasia and inflammatory hypernociception (16). Administration of Evasin-3 resulted in a 50% decrease in the total number of leukocytes in the synovial cavity (Fig. 9 a). The major leukocyte populations affected were neutrophils, which were reduced by 70% in the knee joint (Fig. 9 b). Moreover, Evasin-3 treatment significantly reduced the inflammatory hypernociception associated with this model (Fig. 9 c), and interestingly, the treatment resulted in decreased local production of TNF-α (Fig. 9 d). Intravital microscopy studies of the synovial microvasculature

Downloaded from www.jem.org on August 6, 2008

Published August 4, 2008

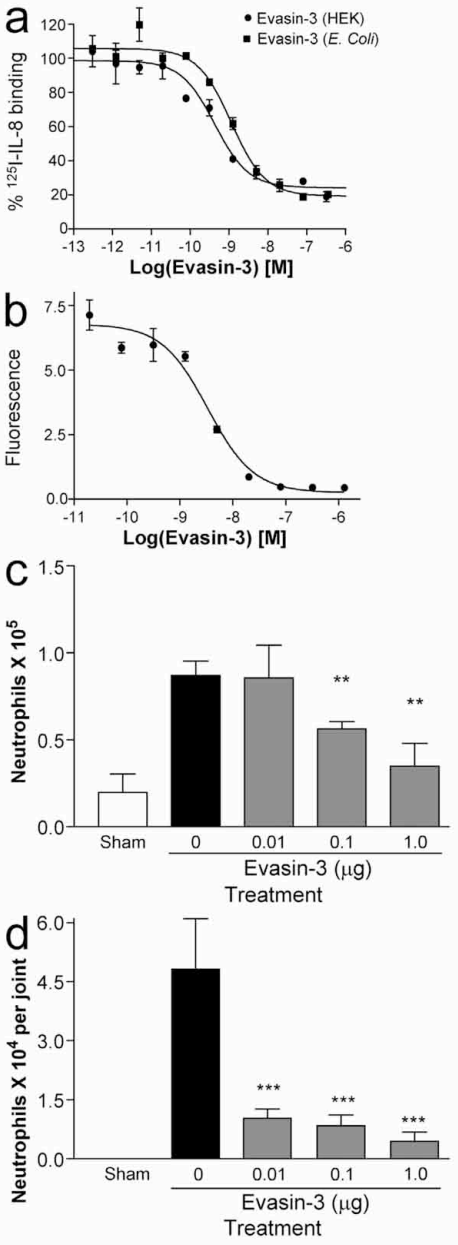


Figure 8. Evasin-3 inhibits cell recruitment in vitro and in vivo. (a) Inhibition of ^{125}I-CXCL8 binding to CXCR2 by Evasin-3 produced in HEK293 cells (●) and by Evasin-3 produced in *E. coli* (■). (b) Inhibition of CXCL8 induced neutrophil chemotaxis in vitro. (c) Inhibition of KC induced neutrophil recruitment into the peritoneal cavity (c) and into the knee joint (d). There were six mice per group in each experiment. **, $P < 0.01$; ***, $P < 0.001$ when compared with PBS-treated group. Error bars represent the mean ± SEM.

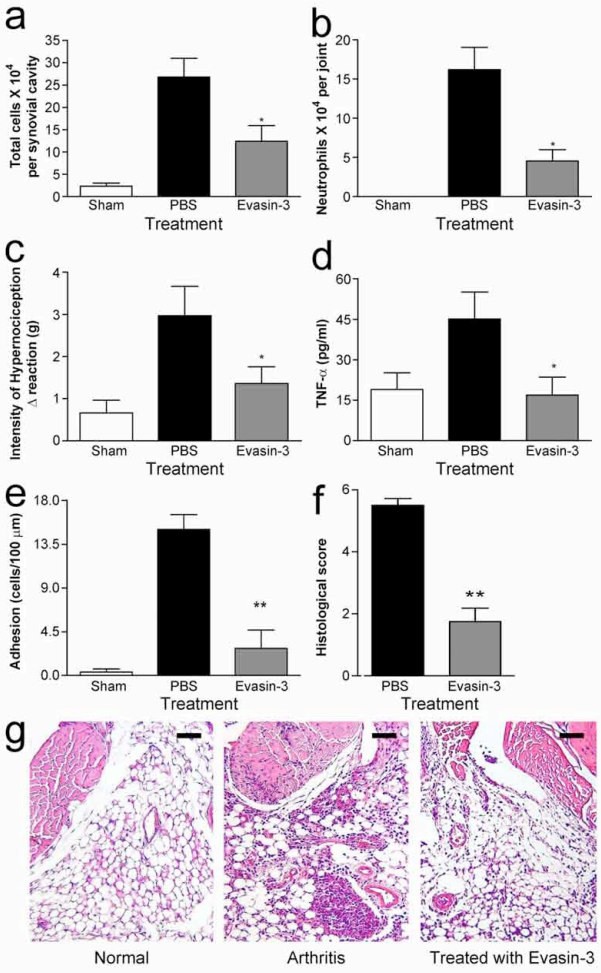


Figure 9. Evasin-3 inhibits neutrophil recruitment and ameliorates inflammation and functionality in a mouse model of antigen-induced arthritis. (a–g) Reduction of inflammation in mBSA induced arthritis by Evasin-3 (1 µg per animal). (a) Inhibition of total cell accumulation in the synovial cavity. (b) Inhibition of neutrophil infiltration into the knee joint. (c) Reduction of hypernociception induced by intraarticular antigen challenge of immunized mice. (d) Reduction of TNF-α production in periarticular tissues. (e) Inhibition of adhesion of leukocytes to synovial microvessels as assessed by intravital microscopy. (f and g) Histological evaluation of the tissue sections form the knee joint. All parameters were evaluated 24 h after antigen challenge, and there were 6 mice per group in each experiment. *, $P < 0.05$; **, $P < 0.01$. Error bars represent the mean ± SEM. Bars, 100 µm.

showed that administration of Evasin-3 prevented the adhesion of leukocytes to the synovial endothelium (Fig. 9 e), providing a direct demonstration of the efficacy of Evasin-3 in the prevention of neutrophil influx in an inflammatory setting. Consistent with the aforementioned findings, histopathological analysis of tissue demonstrated overall inhibition of leukocyte influx into the joint and periarticular tissues, decreased edema, and decreased synovial hyperplasia (Fig. 9, f and g).

Finally, we tested both proteins in the same recruitment model, chemokine-induced neutrophil in the knee joint, at the doses used in the disease models, and both Evasins were able to completely inhibit the recruitment induced by their

Downloaded from www.jem.org on August 6, 2008

respective ligand (Fig. 10 a). The effect of the Evasins was shown to be specific to chemokine inhibition because neither was able to inhibit neutrophil recruitment mediated by zymosan (Fig. 10 b), which has been shown to mediate its effects through chemoattractants such as C5a (17) and LTB4 (18). As both Evasins inhibit neutrophil recruitment mediated by different chemokines, we tested them head to head in the same model, intestinal ischemia. As shown in Fig. 10 c, Evasin-3 was more efficacious, showing significant reduction in lethality at doses of 1 and 0.1 μg, whereas Evasin-1 only showed significant efficacy at the 30 μg dose, with only a slight effect seen at the 10 μg dose.

DISCUSSION

Since the identification of the first members of chemokine family over 20 yr ago, it has become clear that the interaction of these small proteins with their cognate receptors are important targets for therapeutic intervention in several inflammatory, autoimmune, and infectious diseases. Indeed, there are currently many intense drug discovery programs in this area. Yet, although there are numerous reports of the efficacy of small molecule antagonists (19–21), neutralizing antibodies (22, 23), and other antagonists (24) in animal models of disease, it has proven to be more of a challenge to translate these molecules into medicines in the clinic. Although many molecules are currently progressing into late-stage clinical trials, it is possible that alternative approaches may be needed to successfully target the chemokine–chemokine receptor interaction. Ticks have evolved natural antichemokine strategies in the guise of CHPBs, which are able to counter the host defense systems against parasites. Unraveling the molecular nature of these CHBPs may produce novel insights into the design of therapeutically useful chemokine blocking agents.

In this study, we describe the cloning and characterization of a family of CHPBs from tick saliva. In vitro characterization of the family members identified to date indicates that these CHBPs are considerably different from the known viral CHPBs in terms of chemokine selectivity. Many of the viral CHBPs such as myxoma virus M-T7 and murine gammaherpes virus 68 M3 and the recently identified *S. mansoni* (for review see [3]) tend toward broad selectivity, binding both CC and CXC chemokines; the Evasins described here have restricted selectivity. In the studies presented here, we have shown that Evasins are able to bind and inhibit specific chemokines in vitro, and inhibit leukocyte recruitment induced by their respective ligands in simple models of leukocyte recruitment in mice. Furthermore, the antiinflammatory properties of Evasins were confirmed mechanistically by intravital microscopy where their administration both in naive and inflamed mice abrogated leukocyte adhesion to, and transmigration across, the endothelium. Together, these experiments clearly demonstrated the potential of Evasins to prevent leukocyte recruitment.

We evaluated the Evasins in more complex animal models of human disease. Evasin-1, which is highly selective for CCL3 and CCL4, reduced symptoms in a murine model of

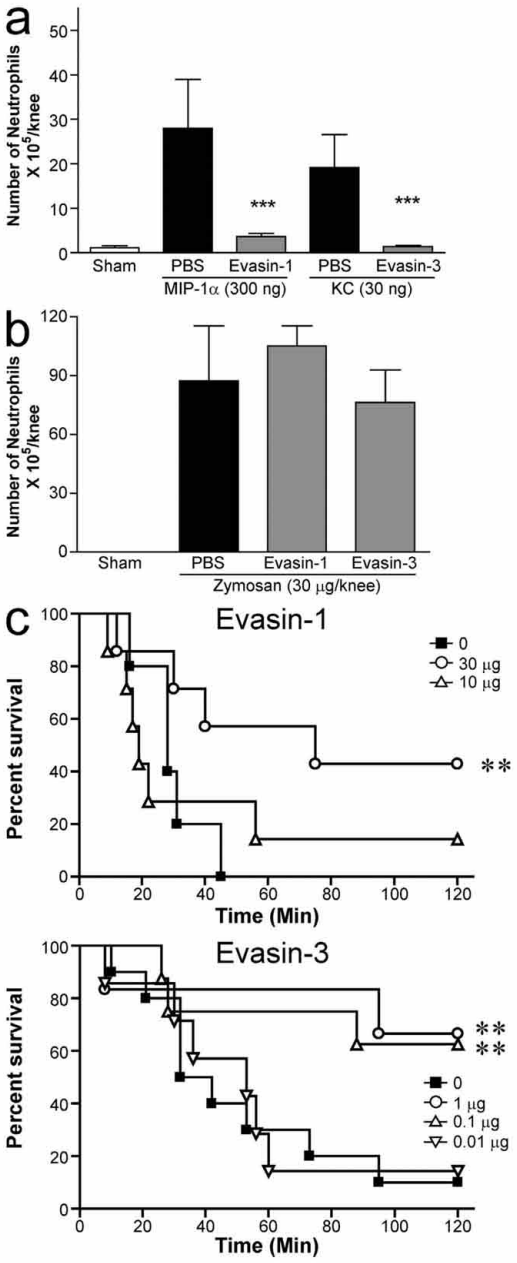


Figure 10. Direct comparison of Evasin-3 and -1. (a) Inhibition of chemokine-induced neutrophil recruitment into the knee joint induced by chemokine (a) or by Zymozan (b). Evasin-1 (10 μg) and Evasin-3 (1 μg) were administered 30 min into the knee joint before the administration of 300 ng mMIP-1α or 30 ng KC, respectively, or 30 μg Zymosan. Cells in the joint were counted 6 h after the injection of stimuli. There were five mice per group in each experiment. **, $P < 0.01$; ***, $P < 0.001$ when compared with PBS-treated group. (c) Prevention of ischemic reperfusion. Evasin-1 and -3 were administered s.c. at the doses indicated 30 min before the reperfusion of the occluded superior mesenteric artery. There were seven to eight mice in each experimental group. **, $P < 0.01$ when compared with PBS-treated group. Error bars represent the mean ± SEM.

Downloaded from www.jem.org on August 6, 2008

skin inflammation that resembles psoriasis in humans, in which several CC chemokines are implicated (14). Because both Evasin-1 and -3 were shown to prevent neutrophil influx, they were subsequently tested in disease models in which neutrophils have previously been shown to play an important role. Thus, in the CCL3-dependent bleomycin-induced lung injury, Evasin-1 reduced leukocyte influx, fibrosis, and lethality, an effect qualitatively and quantitatively similar to experiments in CCL3-deficient mice (15, 25). Blockade of CXCR2 has been reported to prevent leukocyte influx and joint damage in several models of experimental arthritis in rats and mice (26, 27). Evasin-3, which binds to both human and murine CXCR2 ligands, prevented neutrophil influx into the joint in a model of antigen-induced arthritis. Interestingly, this treatment also prevented the local production of TNF-α, a cytokine that has been shown to play an important role in the pathogenesis of arthritis, and which is associated with hypernociception or inflammatory pain in experimental animals. Indeed, blockade of TNF-α with biologicals has been successful in the treatment of rheumatoid arthritis and other rheumatologic conditions (28, 29).

Our initial expectation was that identification of CHBPs in primitive eukaryotic species such as ticks may allow us to identify orthologues in mammalian genomes, based on either primary sequence or on the three-dimensional folds of the CHBPs. However, extensive searching of public databases at both the amino acid and nucleotide sequence level have indicated that there are no human or mammalian orthologues or structural counterparts to the Evasins. On the other hand, by blast analysis of the available tick sequences, we were able to identify an EST in the cattle tick *Boophilus microplus* that may encode a potential orthologue of Evasin-1 (30% identity over 95 amino acids). Although the level of identity is low, it is comparable to that seen between Evasin-1 and -4. We are now in the process of producing the *Boophilus microplus* protein to verify if it is indeed a CHPB. It is likely that additional CHPBs from other species of tick will be identified in due course through homology searching, as the number of tick EST sequences appearing in public databases increases from tick salivary gland transcriptome sequencing projects.

Thus, it appears that ticks have specifically developed novel protective CKBPs as they adapted to their chemokine-producing vertebrate hosts. Although mammals do have molecules that can bind and block chemokine function, they are molecularly and structurally distinct from the Evasins. For example, the atypical chemokine receptors such as D6, CCX-CKR, and Duffy (30, 31) are nonsignaling GPCRs that appear to be able to function as mammalian equivalents of the soluble CKBPs expressed by pathogens and parasitic worms. This suggests that, contrary to viral chemokines and chemokine receptors that have been hijacked from the mammalian genome, pathogens have evolved CKBPs through a "convergent" evolution mechanism.

The leukocytes involved in the first line of defense against pathogens and parasites are neutrophils and eosinophils. The CHBPs described here specifically inhibit the chemokines that recruit these cell types; Evasin-1 (in rodents) and Evasin-3 prevent neutrophil accumulation, and preliminary results indicate that Evasin-4 binds the eosinophil-recruiting chemokines CCL5 and CCL11. Moreover, their selectivity profiles highlight the issue of species specificity in the chemokine system. The common brown dog tick feeds on dogs and other domestic animals, as well as rodents, deer, and humans; thus, in spite of chemokine selectivity, one would expect species cross-reactivity. We have performed our studies using human chemokines, and in some cases, their murine counterparts, and have shown that the Evasins are able to bind to chemokines in both species. The cross species reactivity may be an advantage in the development of these molecules as potential therapeutic agents, as one of the pitfalls in the development of small molecule antagonists of human chemokine receptors has been their lack of cross-reactivity with rodent chemokine receptors, which has hampered testing in animal models of disease, PK/PD, and toxicological studies. However, results obtained from in vivo testing of Evasins still needs to be interpreted with caution, as there are known differences in specific chemokine receptor expression on immune cells between the human and murine system, particularly on neutrophils. In humans, the principal mediators of neutrophil recruitment are CXC chemokines 1–8, acting through CXCR2, and CXCL8, which acts on both CXCR1 and CXCR2. On the contrary, recruitment of murine neutrophils is mediated by both CCR1 and CXCR2, and perhaps also the recently identified murine CXCR1 (32), although little is known about the role of the latter in vivo. However, CCR1 is not normally expressed on human neutrophils, although it can be induced by IFN-γ (33). Interestingly, CCL3 has been shown to recruit neutrophils when injected into human skin (34). Thus, Evasin-1 shows activity against CCL3-mediated neutrophil recruitment rather than monocyte recruitment in the mouse, whereas the ability of Evasin-3 to recruit neutrophils is predictable from its binding profile. It should also be noted that although Evasin-1 has a higher affinity for its ligands than Evasin-3, the latter is more efficacious in the murine models we have tested.

Saliva from ticks harvested at different times during their feeding periods has differential chemokine inhibitory activity, suggesting that different CHPBs are produced at different times during feeding, with the aim of selectively inhibiting specific cell populations (35). It is possible that the most potent inhibitor of neutrophil recruitment produced by the tick is Evasin-3, whereas Evasin-1 may be produced to inhibit (later) monocyte recruitment in nonrodent hosts, as well as T lymphocytes, as was observed in the bleomycin lung inflammation model. Unfortunately, the expression profile of chemokine receptors on leukocytes in the dog, which although its name implies is the preferred host, may simply be the most easily available food source, is unknown and hence we cannot substantiate this hypothesis. Lastly, the availability of recombinant Evasin-4 will enable us to address the ability of this CHBP to modulate eosinophil trafficking because both CCL5 and CCL11 have been extensively described to recruit this cell type.

Downloaded from www.jem.org on August 6, 2008

A striking feature of these proteins is their small size. Both viral and mammalian chemokine and cytokine binding proteins have been shown to be much larger, generally ~30–40 kD. On the other hand, *R. sanguineus* has developed very small, highly selective CHBPs. Interestingly, these proteins are similar in size, if not smaller, than the naturally occurring single chain antibodies such as shark V-NAR domains (15 kD) or camelid VhH domains (15 kD). Large efforts are currently being undertaken to produce small proteins known as nanobodies, minibodies, or microproteins, created by rational design in silico, which will mimic the binding properties of natural single-domain antibodies (36). The two proteins described here represent highly potent, miniaturized scaffolds that have evolved to selectively bind certain proteins, pivotal to the immune response, and which could be useful in the creation of new scaffolds, paving the way for development of these molecules as novel antiinflammatory agents.

One of the important issues surrounding the use of any protein as a potential therapeutic agent concerns immunogenicity, which could be particularly pertinent for nonhuman proteins. There are already examples of xenoproteins in the clinic (4, 37) and others are entering clinical trials. However, as these proteins are generally administered in a single dose for acute indications, potential immunogenicity is not a major concern. However, treatment of inflammatory and autoimmune diseases with therapeutic proteins such as IFN-β or antibodies, e.g., Raptiva and Etanercept, requires chronic administration, and even fully human proteins can elicit an antibody response that may reduce the efficacy of the treatment. By their very nature, antiinflammatory proteins in tick saliva do not appear to be immunogenic. It is still unclear if this is entirely caused by the inhibition of immune cell recruitment to the attachment site, or indeed whether the protein structure itself or through glycosylation minimizes exposure of antigenic epitopes. Furthermore, bioinformatic analysis of T cell epitopes on Evasins using software developed by Biovation (EMD Serono) revealed that the tick Evasins have relatively few potential immunogenic epitopes compared with other therapeutic proteins currently in the clinic, such as IFN-β. It is also interesting to note that only 1 mouse out of 6 treated for 25 d had an IgG response to Evasin-1 (unpublished data). So although immunogenicity in the murine system will not predict the outcome in humans, further evaluation of Evasins in preclinical models is warranted for their development as potential protein therapeutic agents.

Lastly, the mining of the salivary transcriptomes of the numerous species of ticks will provide a wealth of potential immunomodulatory molecules, and other pharmacologically relevant proteins, which will provide novel molecular entities to enrich the current repertoire of biotherapeutics in the future (5, 38).

MATERIALS AND METHODS

Biochemical analysis of antichemokine activity in saliva. Collection of *R. sanguineus* saliva, inhibition of receptor binding and the cross-linking assay were performed as previously described (11). SPR was performed by coating the chemokines on a CM4 chip (BIAcore), with RNaseA as negative protein control, and tick saliva injected after a 10- or 25-fold dilution in HBS-P buffer (BIAcore) for equilibration and 10 mM glycine-HCl, pH 2.5, for regeneration. The sensograms were analyzed using BIAcore 3000 evaluation software after subtraction of nonspecific binding to the control protein. Retentate chromatography SELDI mass spectrometry (RC-SELDI-TOF-MS) was used to detect distinct CHPBs in the tick saliva. CCL5, CCL3, and CXCL8 or the control protein, equine myoglobin, were diluted to 0.1 μg/μl in PBS and immobilized onto separate spots of a PS-20 ProteinChip array according to the manufacturer's instructions (Ciphergen Biosystems, Inc.). After blocking and washing of the array, frozen tick saliva was diluted fivefold in PBS and 5 μl was applied to each spot and incubated for 2 h at room temperature. After washing, the matrix, sinapinic acid, was dried onto each spot on the array and mass analysis was performed by SELDI-TOF-MS, using a calibrated ProteinChip Biology System IIc reader. Spectra were generated using an automated protocol and a positive ion mode with a laser intensity of 220 and deflector sensitivity of 10. The mass optimization range was set between 10 and 50 kD, with a mass focus set to 18 kD. To obtain quantitative data, the mass spectra from each spot were accumulated from 155 laser shots over 31 different and nonoverlapping positions.

Molecular cloning. Expression cloning was performed by transient transfection of HEK293 cells with a cDNA library constructed from the salivary glands of *R. sanguineus*, as previously described (11). Supernatants from transfected cells were screened using two cocktails of radiolabeled [I-^{125}] CXCL8, IL-1, and IL-2, or CCL5, CCL11, and CXCL10, respectively, followed by cross-linking and analysis by SDS-PAGE. After deconvolution of the cDNA pools and sequencing of the positive clones, a C-terminal 6His-tagged version of the cDNA encoding the relevant CHBP was subcloned into the mammalian cell expression vector pEAK12d (Edge Biosystems) using the Gateway cloning system (Invitrogen). The protein was purified by Ni-chelate chromatography after transient expression in 500 ml HEK293 cultures. The cDNA encoding Evasin-3 was subcloned into the pET30a vector (Novagen) for expression in *E. coli* strain BL21(DE3) and produced in a 5-liter fermenter. The protein was purified from the cytosolic fraction by cation exchange chromatography and size exclusion chromatography.

In vitro characterization. The selectivity of Evasin-3 was determined by SPR, as previously described (11). Kinetic measurements were performed to determine the binding constants. The kinetic values k_a and k_d, which are shown in Table I, are the mean of three independent experiments performed in triplicate on three different chips. The affinity constant K_d was calculated from theses mean values. Equilibrium competition receptor binding assays were performed using CHO/CXCR1 transfectants using ^{125}I-CXCL8, as previously described (39). Inhibition of chemotaxis in vitro was measured using L1.2/CCR5 transfectants for Evasin-1 or neutrophils purified from buffy coats as previously described (40).

In vivo experiments. Male BALB/c or C57BL/6 mice (18–22 g) were housed in a temperature-controlled room and had free access to food and water. All experiments received prior approval by the local animal ethics committee. To test the effect of Evasin-1 on cellular recruitment in vivo, mice were administered 0.01–10 μg Evasin-1 in 200 μl PBS s.c. 45 min before the administration of 10 μg CCL3 or 0.3 μg mMIP-1α in 200 μl PBS i.p. Cell recruitment was evaluated 18 h after the stimulus. To test the effect of Evasin-3 on neutrophil recruitment, KC (30 ng/cavity) was injected into the peritoneal cavity or the left knee joint of the mouse and recruitment was evaluated 4 h later. Evasin-3 (0.01–1 μg/mouse) was given s.c. 45 min before KC administration.

Intravital microscopy was performed in unbranched cremasteric venules (25–40 μm in diameter) of C57BL/6 mice, as previously described (41). For each experiment, 0.3 μg of human CCL3 in 100 μl of PBS was administered locally by s.c. injection beneath the right scrotal skin, 1 h before exteriorization. To test inhibition, a solution of Evasin-1 (10 μg per animal) plus CCL3 (0.3 μg) in 100 μl PBS was prepared 15 min before intrascrotal injection.

Downloaded from www.jem.org on August 6, 2008

mBSA-induced DTH reaction in the pleural cavity. C57BL/6 mice were immunized s.c. with a 1:1 emulsion of mBSA (5 mg/ml in saline) and complete Freund's adjuvant (Sigma-Aldrich), as previously described (42). 14 d after the immunization, antigen (mBSA; 10 µg per pleural cavity) or vehicle was injected into the pleural cavity, and the number of cells per cavity was evaluated 48 h after injection of antigen.

Sensitization and induction of Th2 cellular recruitment into the lungs. BALB/c mice were immunized i.p. with 2,500 isolated *S. mansoni* eggs at day 0 and 7 of the protocol, as previously described (43). On day 14, mice were given an intranasal challenge of 10 µg soluble egg antigens (SEA) in 10 µl of PBS to localize the response to the airway. Mice were then rechallenged 6 d later by intratracheal administration of 10 µg SEA in 25 µl of PBS or with PBS alone. To test inhibition, Evasin-1 (10 µg per animal) was administered s.c. 45 min before and 24 h after antigen challenge. The number of cells in the bronchoalveolar lavage fluid was evaluated at 24 and 48 h after stimulation.

Induction of skin inflammation in D6$^{-/-}$ mice. Skin inflammation was induced as previously described (14). In brief, the phorbol ester TPA was applied three times, at 24-h intervals, to the shaved dorsal skin of 6–8-wk-old D6 (−/−) mice, and the mice were left for 4 d to allow the exaggerated cutaneous inflammation to develop. In addition, mice were administered either PBS or Evasin-1 daily (30 µg/mouse pr day) by i.p. injection or were given daily doses of anti-TNF as previously described (14). Mice were killed at day 4 after TPA treatment, and the skin was harvested for histological assessment. Skin samples were collected into neutral-buffered formalin and processed for hematoxylin and eosin staining as described (14).

Bleomycin-induced lung injury. 0.0625 or 0.125 U blenoxane (Bristol-Meyers Squibb Co.) in 25 µl PBS was instilled under anesthesia into the trachea of C57BL/6j mice. Control animals received PBS alone. To test inhibition, Evasin-1 (3 or 10 µg per animal) was administered s.c. 45 min before, and every 12 h after bleomycin instillation. At 4, 8, or 25 d after instillation, the lungs were washed with 3 × 1 ml of PBS, and the number of infiltrating leukocytes were evaluated. Right lung lobes were collected and inflated with 10% formaldehyde for histological analysis of tissue sections stained with hematoxylin and eosin. For localization of collagen within the lung tissues, Gomori's trichrome-specific staining was used.

Antigen-induced arthritis. Animals were immunized intradermally (i.d.) at the base of the tail with 500 µg of methylated BSA (mBSA; Sigma-Aldrich) in 100 µl of an emulsion of saline and an equal volume of CFA (Sigma-Aldrich) on day 0, as previously described (44). Challenge of mice with 10 µg of mBSA in 10 µl sterile saline in the left knee joint was performed 14 d later. The knee cavity was washed 24 h later with PBS (2 × 5 µl), and the periarticular tissues were removed for the evaluation of TNF-α and MPO activity. Intravital microscopy was performed in the synovial microcirculation of the left mouse knee, as previously described (45).

Evaluation of mechanical hypernociception. Inflammatory hypernociception was performed as previously described (46) using an electronic pressure meter. In brief, an increasing perpendicular force is applied to the central area of the plantar surface of the hind paw to induce the dorsal flexion of the femur-tibial joint, followed by paw withdrawal. The flexion-elicited withdrawal threshold (expressed in grams) is recorded before and after the stimulus and is used to infer mechanical hypernociception.

Ischemia and reperfusion. Ischemia and reperfusion injury were performed as previously described (47). In brief, ischemia was induced by totally occluding the superior mesenteric artery for 60 min. Reperfusion was reestablished, and death was monitored during the indicated time periods.

Animal experimentation. Skin inflammation experiments in D6$^{-/-}$ mice were approved by a Glasgow ethical review committee and performed under licence number 60/3415 granted by the UK Home Office. Bleomycin-induced lung injury, antigen-induced arthritis, and ischemia and reperfusion injury experiments were evaluated and approved by the Animal Ethics committee of the Universidade Federal de Minas Gerais, Brazil.

Histological assessment. Sections were graded as previously described (48). In brief, the histological score (0–8) was the sum of the synovial hyperplasia, cellular exudate, and cartilage depletion/bone erosion ranging from 0 (normal) to 3 (severe), and the degree of synovial infiltrate ranging from 0 (normal) to 5 (severe).

Statistical analysis. All results are presented as the mean ± SEM. Normalized data were analyzed by one-way ANOVA, and differences between groups were assessed using the Student-Newman-Keuls post test. A P value < 0.05 was considered to be significant.

We thank M. de Tiani, S. Jaconi, F. Borlat, V. Dechavanne, L. Glez, L. Friedli, F. Bollin, C. Losberger, and L. Chevalet for advice in protein expression and purification.

This work was supported by the European Union FP6 (INNOCHEM, grant number LSHB-CT-2005-518167 to A.E.I. Proudfoot and M.M. Teixeira).

The authors have no conflicting financial interests.

Submitted: 19 December 2007
Accepted: 1 July 2008

REFERENCES

1. Alcami, A. 2003. Viral mimicry of cytokines, chemokines and their receptors. *Nat. Rev. Immunol.* 3:36–50.
2. McFadden, G., A. Lalani, H. Everett, P. Nash, and X. Xu. 1998. Virus-encoded receptors for cytokines and chemokines. *Semin. Cell Dev. Biol.* 9:359–368.
3. Fallon, P.G., and A. Alcami. 2006. Pathogen-derived immunomodulatory molecules: future immunotherapeutics? *Trends Immunol.* 27:470–476.
4. Hovius, J.W., A.P. van Dam, and E. Fikrig. 2007. Tick-host-pathogen interactions in Lyme borreliosis. *Trends Parasitol.* 23:434–438.
5. Ribeiro, J.M. 1995. Blood-feeding arthropods: live syringes or invertebrate pharmacologists? *Infect. Agents Dis.* 4:143–152.
6. Lucas, A., and G. McFadden. 2004. Secreted immunomodulatory viral proteins as novel biotherapeutics. *J. Immunol.* 173:4765–4774.
7. Smith, P., R.E. Fallon, N.E. Mangan, C.M. Walsh, M. Saraiva, J.R. Sayers, A.N. McKenzie, A. Alcami, and P.G. Fallon. 2005. *Schistosoma mansoni* secretes a chemokine binding protein with antiinflammatory activity. *J. Exp. Med.* 202:1319–1325.
8. Lalani, A.S., J. Masters, K. Graham, L.Y. Liu, A. Lucas, and G. McFadden. 1999. Role of the myxoma virus soluble CC-chemokine inhibitor glycoprotein, M-T1, during myxoma virus pathogenesis. *Virology.* 256:233–245.
9. Hajnicka, V., P. Kocakova, M. Slavikova, M. Slovak, J. Gasperik, N. Fuchsberger, and P.A. Nuttall. 2001. Anti-interleukin-8 activity of tick salivary gland extracts. *Parasite Immunol.* 23:483–489.
10. Hajnicka, V., I. Vancova, P. Kocakova, M. Slovak, J. Gasperik, M. Slavikova, R.S. Hails, M. Labuda, and P.A. Nuttall. 2005. Manipulation of host cytokine network by ticks: a potential gateway for pathogen transmission. *Parasitology.* 130:333–342.
11. Frauenschuh, A., C.A. Power, M. Deruaz, B.R. Ferreira, J.S. Silva, M.M. Teixeira, J.M. Dias, T. Martin, T.N. Wells, and A.E. Proudfoot. 2007. Molecular cloning and characterization of a highly selective chemokine-binding protein from the tick Rhipicephalus sanguineus. *J. Biol. Chem.* 282:27250–27258.
12. Wilkinson, D.L., and R.G. Harrison. 1991. Predicting the solubility of recombinant proteins in *Escherichia coli*. *Biotechnology (N. Y.).* 9:443–448.
13. Nibbs, R.J., J. Yang, N.R. Landau, J.H. Mao, and G.J. Graham. 1999. LD78beta, a non-allelic variant of human MIP-1alpha (LD78alpha), has enhanced receptor interactions and potent HIV suppressive activity. *J. Biol. Chem.* 274:17478–17483.
14. Jamieson, T., D.N. Cook, R.J. Nibbs, A. Rot, C. Nixon, P. McLean, A. Alcami, S.A. Lira, M. Wiekowski, and G.J. Graham. 2005. The chemokine receptor D6 limits the inflammatory response in vivo. *Nat. Immunol.* 6:403–411.

Downloaded from www.jem.org on August 6, 2008

15. Smith, R.E., R.M. Strieter, S.H. Phan, N.W. Lukacs, G.B. Huffnagle, C.A. Wilke, M.D. Burdick, P. Lincoln, H. Evanoff, and S.L. Kunkel. 1994. Production and function of murine macrophage inflammatory protein-1 alpha in bleomycin-induced lung injury. *J. Immunol.* 153:4704–4712.
16. Grespan, R., S.Y. Fukada, H.P. Lemos, S.M. Vieira, M.H. Napimoga, M.M. Teixeira, A.R. Fraser, F.L. Liew, I.B. McInnes, and F.D. Cunha. 2008. *Arthritis Rheum.* 58:2030–2040.
17. Mullaly, S.C., and P. Kubes. 2007. Mast cell-expressed complement receptor, not TLR2, is the main detector of zymosan in peritonitis. *Eur. J. Immunol.* 37:224–234.
18. Rao, N.L., P.J. Dunford, X. Xue, X. Jiang, K.A. Lundeen, F. Coles, J.P. Riley, K.N. Williams, C.A. Grice, J.P. Edwards, et al. 2007. Anti-inflammatory activity of a potent, selective leukotriene A4 hydrolase inhibitor in comparison with the 5-lipoxygenase inhibitor zileuton. *J. Pharmacol. Exp. Ther.* 321:1154–1160.
19. Liang, M., C. Mallari, M. Rosser, H.P. Ng, K. May, S. Monahan, J.G. Bauman, I. Islam, A. Ghannam, B. Buckman, et al. 2000. Identification and characterization of a potent, selective, and orally active antagonist of the CC chemokine receptor-1. *J. Biol. Chem.* 275:19000–19008.
20. Anders, H.J., V. Vielhauer, M. Frink, Y. Linde, C.D. Cohen, S.M. Blattner, M. Kretzler, F. Strutz, M. Mack, H.J. Grone, et al. 2002. A chemokine receptor CCR-1 antagonist reduces renal fibrosis after unilateral ureter ligation. *J. Clin. Invest.* 109:251–259.
21. Brodmerkel, C.M., R. Huber, M. Covington, S. Diamond, L. Hall, R. Collins, L. Leffet, K. Gallagher, P. Feldman, P. Collier, et al. 2005. Discovery and pharmacological characterization of a novel rodent-active CCR2 antagonist, INCB3344. *J. Immunol.* 175:5370–5378.
22. Kennedy, K.J., R.M. Strieter, S.L. Kunkel, N.W. Lukacs, and W.J. Karpus. 1998. Acute and relapsing experimental autoimmune encephalomyelitis are regulated by differential expression of the CC chemokines macrophage inflammatory protein-1 alpha and monocyte chemotactic protein-1. *J. Neuroimmunol.* 92:98–108.
23. Lloyd, C.M., M.E. Dorf, A. Proudfoot, D.J. Salant, and J.C. Gutierrez-Ramos. 1997. Role of MCP-1 and RANTES in inflammation and progression to fibrosis during murine crescentic nephritis. *J. Leukoc. Biol.* 62:676–680.
24. Proudfoot, A.E. 2002. Chemokine receptors: multifaceted therapeutic targets. *Nat. Rev. Immunol.* 2:106–115.
25. Ishida, Y., A. Kimura, T. Kondo, T. Hayashi, M. Ueno, N. Takakura, K. Matsushima, and N. Mukaida. 2007. Essential roles of the CC chemokine ligand 3-CC chemokine receptor 5 axis in bleomycin-induced pulmonary fibrosis through regulation of macrophage and fibrocyte infiltration. *Am. J. Pathol.* 170:843–854.
26. Barsante, M.M., T.M. Cunha, M. Allegretti, F. Cattani, F. Policani, C. Bizzarri, W.L. Tafuri, S. Poole, F.Q. Cunha, R. Bertini, and M.M. Teixeira. 2008. Blockade of the chemokine receptor CXCR2 ameliorates adjuvant-induced arthritis in rats. *Br. J. Pharmacol.* 153:992–1002.
27. Cunha, T.M., M.M. Barsante, A.T. Guerrero, W.A. Verri, Jr., S.H. Ferreira, F.M. Coelho, R. Bertini, C. Di Giacinto, M. Allegretti, F.Q. Cunha, and M.M. Teixeira. 2008. Treatment with DF 2162, a non-competitive allosteric inhibitor of CXCR1/2, diminishes neutrophil influx and inflammatory hypernociception in mice. *Br. J. Pharmacol.* 154: 460–470.
28. Vilcek, J., and M. Feldmann. 2004. Historical review: cytokines as therapeutics and targets of therapeutics. *Trends Pharmacol. Sci.* 25:201–209.
29. Tarner, I.H., U. Muller-Ladner, and S. Gay. 2007. Emerging targets of biologic therapies for rheumatoid arthritis. *Nat. Clin. Pract. Rheumatol.* 3:336–345.
30. Nibbs, R., G. Graham, and A. Rot. 2003. Chemokines on the move: control by the chemokine "interceptors" Duffy blood group antigen and D6. *Semin. Immunol.* 15:287–294.
31. Mantovani, A., R. Bonecchi, and M. Locati. 2006. Tuning inflammation and immunity by chemokine sequestration: decoys and more. *Nat. Rev. Immunol.* 6:907–918.
32. Fan, X., A.C. Patera, A. Pong-Kennedy, G. Deno, W. Gonsiorek, D.J. Manfra, G. Vassileva, M. Zeng, C. Jackson, L. Sullivan, et al. 2007. Murine CXCR1 is a functional receptor for GCP-2/CXCL6 and interleukin-8/CXCL8. *J. Biol. Chem.* 282:11658–11666.
33. Bonecchi, R., N. Polentarutti, W. Luini, A. Borsatti, S. Bernasconi, M. Locati, C.A. Power, A.E.I. Proudfoot, T.N.C. Wells, C. Mackay, et al. 1999. Up-regulation of CCR1 and CCR3 and induction of chemotaxis to CC chemokines by IFN-gamma in human neutrophils. *J. Immunol.* 162:474–479.
34. Lee, S.C., M.E. Brummet, S. Shahabuddin, T.G. Woodworth, S.N. Georas, K.M. Leiferman, S.C. Gilman, C. Stellato, R.P. Gladue, R.P. Schleimer, and L.A. Beck. 2000. Cutaneous injection of human subjects with macrophage inflammatory protein-1 alpha induces significant recruitment of neutrophils and monocytes. *J. Immunol.* 164:3392–3401.
35. Vancova, I., M. Slovak, V. Hajnicka, M. Labuda, L. Simo, K. Peterkova, R.S. Hails, and P.A. Nuttall. 2007. Differential anti-chemokine activity of *Amblyomma variegatum* adult ticks during blood-feeding. *Parasite Immunol.* 29:169–177.
36. Holliger, P., and P.J. Hudson. 2005. Engineered antibody fragments and the rise of single domains. *Nat. Biotechnol.* 23:1126–1136.
37. Barnett, A. 2007. Exenatide. *Expert Opin. Pharmacother.* 8:2593–2608.
38. Ribeiro, J.M., F. Alarcon-Chaidez, I.M. Francischetti, B.J. Mans, T.N. Mather, J.G. Valenzuela, and S.K. Wikel. 2006. An annotated catalog of salivary gland transcripts from *Ixodes scapularis* ticks. *Insect Biochem. Mol. Biol.* 36:111–129.
39. van Riper, G., D.W. Nicholson, M.P. Scheid, P.A. Fischer, M.S. Springer, and H. Rosen. 1994. Induction, characterization, and functional coupling of the high affinity chemokine receptor for RANTES and macrophage inflammatory protein-1 alpha upon differentiation of an eosinophilic HL-60 cell line. *J. Immunol.* 152:4055–4061.
40. Proudfoot, A.E., T.M. Handel, Z. Johnson, E.K. Lau, P. LiWang, I. Clark-Lewis, F. Borlat, T.N. Wells, and M.H. Kosco-Vilbois. 2003. Glycosaminoglycan binding and oligomerization are essential for the in vivo activity of certain chemokines. *Proc. Natl. Acad. Sci. USA.* 100:1885–1890.
41. Cara, D.C., and P. Kubes. 2004. Intravital microscopy as a tool for studying recruitment and chemotaxis. *Methods Mol. Biol.* 239:123–132.
42. Teixeira, M.M., A. Talvani, W.L. Tafuri, N.W. Lukacs, and P.G. Hellewell. 2001. Eosinophil recruitment into sites of delayed-type hypersensitivity reactions in mice. *J. Leukoc. Biol.* 69:353–360.
43. Lukacs, N.W., T.J. Standiford, S.W. Chensue, R.G. Kunkel, R.M. Strieter, and S.L. Kunkel. 1996. C-C chemokine-induced eosinophil chemotaxis during allergic airway inflammation. *J. Leukoc. Biol.* 60:573–578.
44. Healy, A.M., E. Izmailova, M. Fitzgerald, R. Walker, M. Hattersley, M. Silva, E. Siebert, J. Terkelsen, D. Picarella, M.D. Pickard, et al. 2006. PKC-theta-deficient mice are protected from Th1-dependent antigen-induced arthritis. *J. Immunol.* 177:1886–1893.
45. Veihelmann, A., G. Szczesny, D. Nolte, F. Krombach, H.J. Refior, and K. Messmer. 1998. A novel model for the study of synovial microcirculation in the mouse knee joint in vivo. *Res. Exp. Med. (Berl.).* 198:43–54.
46. Cunha, T.M., W.A. Verri Jr., G.G. Vivancos, I.F. Moreira, S. Reis, C.A. Parada, F.Q. Cunha, and S.H. Ferreira. 2004. An electronic pressure-meter nociception paw test for mice. *Braz. J. Med. Biol. Res.* 37:401–407.
47. Souza, D.G., A.C. Soares, V. Pinho, H. Torloni, L.F. Reis, M.M. Teixeira, and A.A. Dias. 2002. Increased mortality and inflammation in tumor necrosis factor-stimulated gene-14 transgenic mice after ischemia and reperfusion injury. *Am. J. Pathol.* 160:1755–1765.
48. Williams, A.S., P.J. Richards, E. Thomas, S. Carty, M.A. Nowell, R.M. Goodfellow, C.M. Dent, B.D. Williams, S.A. Jones, and N. Topley. 2007. Interferon-gamma protects against the development of structural damage in experimental arthritis by regulating polymorphonuclear neutrophil influx into diseased joints. *Arthritis Rheum.* 56:2244–2254.

Downloaded from www.jem.org on August 6, 2008

3.3. Trabalho cientifico – 3

RUSSO, R. C.; ALESSANDRI, A. L.; GARCIA, C. C.; PINHO, V.; CASSALI, D. G.; PROUDFOOT, A. E. I.; TEIXEIRA, M. M. ***Therapeutic effects of Evasin-1, a CCL3-Binding Protein, in bleomycin-induced lung fibrosis in mice.*** **Am J Respir Cell Mol Biol.** 2009. *(submetido)*.

Os objetivos específicos deste estudo foram:

1. Estudar e comparar os efeitos inibitórios da administração de Evasina-1 (*CCL3-binding portein*) e da ausência de CCL3 usando animais geneticamente deficientes, durante a inflamação e fibrose pulmonar induzida por bleomicina *in vivo*.

2. Avaliar e comparar os efeitos nos regimes preventivo e terapêutico de tratamento com Evasina-1 durante a fibrose pulmonar induzida por bleomicina *in vivo.*

American Journal of Respiratory Cell and Molecular Biology/AJRCMB

Therapeutic Effects of Evasin-1, a CCL3-Binding Protein, in Bleomycin-Induced Lung Fibrosis in Mice

Journal:	*American Journal of Respiratory Cell and Molecular Biology*
Manuscript ID:	Red-2009-0406OC
Manuscript Type:	OC - Original Contribution
Date Submitted by the Author:	06-Nov-2009
Complete List of Authors:	Russo, Remo; Universidade Federal De Minas Gerais (UFMG), Departamento de Bioquímica e Imunologia Alessandri, Ana; Universidade Federal De Minas Gerais (UFMG), Departamento de Bioquímica e Imunologia Garcia, Cristiana; Universidade Federal De Minas Gerais (UFMG), Departamento de Bioquímica e Imunologia Pinho, Vanessa; Universidade Federal De Minas Gerais (UFMG), Departamento de Bioquímica e Imunologia Cassali, Geovanni; Universidade Federal De Minas Gerais (UFMG), Departamento de Bioquímica e Imunologia Proudfoot, Amanda; Merck Serono Geneva Research Centre TEIXEIRA, MAURO; Universidade Federal De Minas Gerais (UFMG), Departamento de Bioquímica e Imunologia
Key Words:	Chemokine, Lung Inflammation, Pulmonary Fibrosis, Bleomycin, Evasin-1

scholarONE Manuscript Central

Therapeutic Effects of Evasin-1, a CCL3-Binding Protein, in Bleomycin-Induced Lung Fibrosis in Mice

Remo C. Russo[1#], Ana L. Alessandri[1#], Cristiana C. Garcia[1], Vanessa Pinho[2], Geovanni D. Cassali[3], Amanda E. I. Proudfoot[4] and Mauro M. Teixeira[1].

[1]Laboratório de Imunofarmacologia, Departamento de Bioquímica e Imunologia, Instituto de Ciências Biológicas, Universidade Federal de Minas Gerais, Belo Horizonte, MG, Brazil.

[2]Departamento de Morfologia, Instituto de Ciências Biológicas, Universidade Federal de Minas Gerais, Belo Horizonte, MG, Brazil.

[3]Departamento de Patologia Geral, Instituto de Ciências Biológicas, Universidade Federal de Minas Gerais, Belo Horizonte, MG, Brazil.

[4]Merck Serono Geneva Research Centre, 1202 Geneva, Switzerland.

[#]These authors contributed equally to this work.

Grant Support: This investigation received financial support from the Coordenação de Aperfeiçoamento de Pessoal de Nível Superior (CAPES/Brazil), Fundação de Amparo a Pesquisa do Estado de Minas Gerais (FAPEMIG/Brazil), Conselho Nacional de Desenvolvimento Científico e Tecnológico (CNPq/Brazil) and the European Union's Sixth Framework Programme (INNOCHEM project grant LSHBCT2005518167).

Corresponding Author: Mauro Martins Teixeira (also for reprint requests).

Laboratório de Imunofarmacologia. Departamento de Bioquímica e Imunologia. Instituto de Ciências Biológicas – Universidade Federal de Minas Gerais. Avenida Antônio Carlos, 6627. CEP 30882-650 - Pampulha. Belo Horizonte, MG – Brazil. Phone/FAX: 55 31 3409 2651. mmtex@icb.ufmg.br.

Running head: *Evasin-1 reduces pulmonary fibrosis.*

For Review Only

Abstract:

CC chemokines play an important role in the pathogenesis of idiopathic pulmonary fibrosis (IPF). Few studies have evaluated the efficacy of therapeutically targeting CC chemokines and their receptors during interstitial lung diseases. In the present study, the therapeutic effects of Evasin-1, a tick-derived Chemokine-Binding Protein that has high affinity for CCL3, was investigated in a murine model of bleomycin-induced lung fibrosis.

CCL3 concentrations in lung homogenates increased significantly with time after bleomycin challenge and this was accompanied by increased number of leukocytes and elevated levels of CCL2, CCL5, TNF-α and TGF-β_1 and pulmonary fibrosis. Evasin-1 administration, in a preventive (from the day of bleomycin administration) or therapeutic (from day 8 after bleomycin) schedule, decreased number of leukocytes in the lung, reduced levels of TNF-α and TGF-β_1 and attenuated lung fibrosis.

In conclusion, targeting CCL3 is beneficial in the context of bleomycin-induced lung injury event when treatment is started days after the insult. Modulation of CCL3 function by Evasin-1 could represent a potential therapy for IPF.

Keywords: *Chemokine, Lung Inflammation, Pulmonary Fibrosis, Bleomycin, Evasin-1.*

For Review Only

Introduction:

Bleomycins are members of glycopeptide antibiotics clinically used as anti-neoplasic drugs for a variety of human cancers (1). An important side effect of these compounds is the induction of lung fibrosis. In addition, bleomycin-induced pulmonary injury and fibrosis in mice is an animal model widely used to investigate the biochemical, cellular, and morphological mechanisms associated with pathogenesis of lung inflammation and repair, as it resembles some aspects of human Idiopathic Pulmonary Fibrosis (IPF) (2). IPF is a progressive-degenerative lethal disease that comprises a group of conditions characterized by chronic lung inflammation, disruption of alveolar structure, interstitial fibroblast proliferation, and excessive extracellular matrix synthesis and deposition (3). Although causes of pulmonary fibrosis remain unclear and controversial (4, 5), available evidences suggest that leukocyte infiltration plays an important role during exacerbation of pulmonary injury and also regulates subsequent lung fibrosis by secretion of pro-inflammatory and pro-fibrogenic factors as TNF-α and TGF-β_1, respectively (6). The coordinated recruitment of neutrophils, macrophages, lymphocytes and fibroblasts into injured lungs is correlated to different patterns of chemokine and cytokine expression during each phase of lung fibrosis, which are classically described as acute and chronic lung inflammation, tissue repair and scarring (7). There is no effective treatment for IPF.

Chemokines are small molecules that signal through seven-transmembrane G protein-coupled receptors which are expressed on both hematopoietic and non-hematopoietic cells. The functions of chemokines are diverse and include chemoattraction and proliferative effects on diverse cell types (8). Clinical studies and animal models of pulmonary fibrosis have shown a correlation between certain chemokines with lung inflammation and fibrosis (5-7, 9). For example, CCL2 production is required for lung fibrosis and acts on the chemokine receptor CCR2, expressed by macrophages and fibroblasts (10). It has also been shown that CCL3 and CCL5 contribute to an exacerbated lung injury (11, 12). More recently, Yshida and colleagues

For Review Only

demonstrated that the CCL3–CCR5 axis is involved in recruitment of bone marrow-derived fibrocytes, TGF-β_1 producing fibroblast precursors, in bleomycin-induced pulmonary fibrosis (12).

Chemokine binding-proteins (CHBPs) are pathogen-derived factors which may be used by virus, helminthes and arthropods, to evade the host immune response (13). We have recently cloned and characterized a new family of proteins isolated from the saliva of the tick *Rhipicephalus sanguineus*, evasins (14). Evasins have potent chemokine-binding activity *in vitro*, which reflects in potent anti-inflammatory effects *in vivo* (14, 15). One of these proteins, Evasin-1, has high affinity to CCL3 and may also bind to CCL4 and CCL18 at higher concentrations (14, 15). Treatment of mice with Evasin-1 from the time of bleomycin administration significantly decreased pulmonary inflammation and fibrosis caused by bleomycin (15). The aims of the present study were to extend the previous observation to a more chronic model of lung fibrosis (using a lower dose of bleomycin) and to examine the therapeutic effects of Evasin-1 administered 8 days after bleomycin instillation. For this purpose, we evaluated the efficacy of Evasin-1 given in preventive (from day 0 to 25) or therapeutic (from day 8 to 25) regimens and we also assessed the effects of bleomycin instillation in CCL3-deficient (CCL3 -/-) mice for comparison.

For Review Only

Material and Methods:

Animals, drugs and reagents.

In the present study, 8 to 10 weeks old male C57Bl/6J (WT) obtained from Centro de Bioterismo (CEBIO) of the Universidade Federal de Minas Gerais (UFMG, Brazil) and CCL3 -/- mice (16) were bred and obtained from the animal facility of the Centro de Pesquisas René Rachou. Animals were maintained with filtered water, food *ad libitum* and in a controlled environment. All experiments were conducted under conditions prior approved by the local animal ethics committee, CETEA/UFMG (Protocol number 146/06). Bleomycin sulfate (Blenoxane; Bristol-Meyers Squibb); Ketamine (Dopalen®/Vetbrands); xylazine (Calmiun®/Agener, União); PBS (phosphate buffered saline, pH 7.4). Evasin-1 (Ev-1) was produced as previously described (14).

Bleomycin induced-lung injury and fibrosis in mice.

Animals were anesthetized intraperitonealy with a ketamine and xylazine solution (3.2 mg/Kg e 0.16 mg/Kg, respectively) prior to tracheotomy. The lethal (severe disease) protocol of bleomycin-induced lung fibrosis (0.125U/animal) was used to study acute inflammation and the sub-lethal (milder disease) protocol of bleomycin-induced lung fibrosis (0.0625U/animal) was used to study the chronic effects of Evasin-1 treatment during the pulmonary inflammation and fibrosis development. A single 25µL injection containing 0.0625U or 0.125U of bleomycin diluted in PBS or PBS only (control group) was instilled intratracheally using Hamilton syringes. In each time-point after bleomycin or PBS administration, animals were sacrificed by a lethal dose of ketamine and xylazine, in order to perform bronchoalveolar lavage and collect lung samples for biochemical and histological analysis.

For Review Only

Evasin-1 treatment schedules.

Bleomycin-instilled mice received BID (twice a day) treatment with vehicle or Evasin-1 (10 μg/animal). Evasin-1 was given by subcutaneous injection diluted in 100 μl of PBS. The vehicle group received 100μL of PBS only. In the preventive schedule (Figure 1A), Evasin-1 was given 45 minutes before bleomycin injection and then twice a day from day 0 to 25. Lung inflammation and fibrosis were evaluated at days 4, 8 and 25 after bleomycin challenge. In the therapeutic schedule, administration of Evasin-1 was from day 8 to 25 (Figure 1B), lung inflammation and fibrosis were evaluated at day 25 after bleomycin challenge.

Bronchoalveolar lavage and lung samples.

Bronchoalveolar lavage (BAL) was performed as previously described (17) to obtain leukocytes from alveolar spaces. Total number of leukocytes was determined by counting cells in a modified Neubauer chamber and the percentage of neutrophils, eosinophils and mononuclears counts on a May-Grünwald-Giemsa-stained cytospin (Shandon III) slide. After BAL, the pulmonary vasculature was perfused with 5 mL of PBS through the right ventricle. The organ was removed and frozen at -70°C and used at a later stage to measure chemokines and cytokines, and for quantification of neutrophil and macrophage accumulation in lung tissue.

Quantification of neutrophil and macrophage accumulation into the lung tissue by myeloperoxidase (MPO) and N-acetylglucosaminidase (NAG) activity measurement.

The extent of neutrophil accumulation in lung tissue was measured by assaying myeloperoxidase activity, as previously described (17). Briefly, lung tissue was homogeneized using 0.5% hexadecyl-trimethylammonium bromide and MPO activity, an index of tissue neutrophil influx, assayed using 3,3'-5,5'-tetramethylbenzidine. Neutrophil number in each sample was calculated from a standard curve of neutrophils obtained from the peritoneal cavity

For Review Only

of 5% casein-treated animals and processed in the same way. The results were expressed as relative number of neutrophils per 100 mg of wet tissue.

Macrophage accumulation in tissues was inferred, as previously described (18), by assaying N-acetylglucosaminidase activity in homogeneized lung samples. One hundred milligrams of lung tissue were homogenized in 2 mL of saline solution (0.9%) containing 0.1% v/v Triton X-100, and centrifuged at 4°C for 10 minutes at 1,500g. The supernatants were used for NAG assay. The reaction was started at 37°C for 10 min in 96 wells microplate by addition of 100 μL of *p*-nitrophenyl-N-acetyl-*β*-D-glucosaminide (Sigma) in citrate/phosphate buffer (0.1 M citric acid, 0.1 M Na_2HPO_4; pH 4.5) in final concentration of 2.24 mM, to 100 μL supernatant from tissue sample processed, diluted in citrate/phosphate buffer. The reaction was stopped by the addition of 100 μL 0.2 M glycine buffer (pH 10.6) and quantified at 405 nm in spectrophotometer (Emax – Molecular Devices). The macrophage content was calculated from a standard curve based on NAG activity expressed as absorbance increase at 405 nm from 3% thioglycollate peritoneal-induced macrophages assayed in parallel. The results were expressed in relative number of macrophages per 100 mg of wet tissue. MPO and NAG assays performed under these conditions are specific for neutrophils and macrophages, respectively.

ELISA assay for assessment of cytokines and chemokines concentrations in lungs.

The concentration of the cytokines TNF-α and active TGF-β_1, and the chemokines CCL2, CCL3 and CCL5 were measured in lung tissue homogenates by ELISA, according to the instructions provided by the manufacturer (DuoSet kits, R&D Systems; Minneapolis). Tissues were processed as previously described (17).

Histopathological and Morphometric analysis.

The left lung was removed and fixed in 10% neutral phosphate buffered formalin (pH 7.4). The tissues were dehydrated gradually in ethanol, embedded in paraffin, cut into 4-μm

For Review Only

sections stained with Gomori's Trichrome, and examined under light microscopy. Slides with lung sections stained with Gomori's Trichrome were analyzed by a pathologist in a blind manner.

For the quantitative analysis of Gomori's Trichrome area, images covering 326.000 μm^2 of lung sections were captured with a digital camera (Optronics DEI-470) connected to a microscope (Olympus IX70) with a magnification of 200x and collagen (green areas) measured in the software Image Pro-Plus, as previously described (17). At least 20 images, covering all lung slide area, were obtained for each animal, with n=6 per group. Results were expressed as the mean green area per μm^2. This morphometrical index was used to describe lung collagen deposition.

Statistical analysis.

All results are presented as the mean ± SEM. Normalized data were analyzed by one-way ANOVA and differences between groups were assessed using the Student-Newman-Keuls post hoc test, using Software GraphPad Prism 4.0. Differences were considered significant at $P<0.05$.

For Review Only

Results

Effects of Evasin-1 on bleomycin-induced pulmonary inflammation.

Using the severe disease protocol, our preliminary studies confirmed that CCL3 was produced rapidly after bleomycin administration (0.125U/animal) and that levels of CCL3 were high at least until day 25 (Figure 2A). We have previously shown that Evasin-1 inhibited CCL3-induced granulocyte recruitment into the peritoneal cavity with maximal inhibition at 10 μg/mice (15). Treatment with Evasin-1 (10 μg/mice BID) using a preventive schedule (Figure 1A) reduced CCL3 levels in lungs of wild type mice at 8 days after bleomycin (0.125U/animal) instillation (Figure 2B). There was also decreased neutrophil influx into the airways and reduced production of active TGF-β_1 in Evasin-1 treated mice (Figure 2C and D, respectively). In agreement with a previous study (12), there was reduced neutrophil numbers in BAL and low levels of active TGF-β_1 (Figure 2C and D, respectively) in CCL3-deficient mice exposed to bleomycin.

Thereafter, to evaluate the effects of chronic Evasin-1 administration, we used a milder disease protocol of bleomycin-induced lung fibrosis (0.0625U/animal) on subsequent experiments. Daily treatment with Evasin-1 (10 μg/mice BID) from the day of instillation (preventive schedule; Figure 1A) led to a significant reduction of total leukocyte number in BAL (Figure 3A), with inhibition of neutrophil recruitment at days 4 and 8 (Figure 3B), and reduced mononuclear cell numbers at days 8 and 25 (Figure 3C). Preventive treatment with Evasin-1 also decreased neutrophil accumulation in lung tissues at days 8 and 25, as evaluated by myeloperoxidase assay (Figure 4A). NAG levels, an index of macrophage accumulation in the lungs, were decreased at day 8 but not at day 24 after bleomycin instillation (Figure 4B).

Treatment with Evasin-1 from day 8 after bleomycin instillation (Therapeutic schedule, Figure 1B) significantly decreased the total cell influx in the BAL fluid at day 25 (Figure 3A),

For Peer Review Only

mostly due to inhibition of the influx of mononuclear cells (Figure 3C). The therapeutic treatment with Evasin-1 failed to decrease MPO or NAG levels in the lung at day 25 (Figure 4).

Effects of Evasin-1 on bleomycin-induced on pulmonary levels of cytokines and chemokines.

Levels of the pro-inflammatory cytokine TNF-α were significantly increased in lungs of vehicle-treated mice after bleomycin administration. In contrast, treatment with Evasin-1 in preventive or therapeutic manner induced a marked reduction of TNF-α levels at all time points evaluated (Figure 5A). There was a significant increase in lung levels of active TGF-β_1 at days 8 and 25, but not at day 4, after bleomycin instillation (Figure 5B). Preventive treatment with Evasin-1 did not affect the levels of this pro-fibrogenic cytokine at day 8, but both preventive and therapeutic administration of Evasin-1 decreased the active TGF-β_1 levels at day 25 (Figure 5B).

Levels of CCL2 and CCL3 were increased from day 4 till 25 in lungs of vehicle-treated mice after bleomycin instillation. Treatment with Evasin-1 partially decreased pulmonary levels of CCL2 at days 4 and 25 after bleomycin instillation when the drug was given in a preventive manner (Figure 6A). Therapeutic administration of Evasin-1 failed to modify pulmonary levels of CCL2 at day 25 (Figure 6A). Both regimens of Evasin-1 administration drastically reduced levels of CCL3, the specific target of Evasin-1 (Figure 6B). The production of CCL5 was greater in bleomycin-instilled mice only at day 25 after challenge. Whereas the preventive treatment with Evasin-1 decreased, the therapeutic schedule had no effect on pulmonary levels of CCL5 levels (Figure 6C).

Effects of Evasin-1 on bleomycin-induced pulmonary fibrosis.

Histopathological analysis of lungs revealed pronounced lung damage, diffuse and dense fibrosis with loss of architecture at day 25 after bleomycin challenge (Figure 7B). In bleomycin-

For Review Only

instilled mice treated with Evasin-1 in preventive manner, there was moderate wall thickening with preserved lung architecture, reduced damage and areas of attenuated fibrosis (Figure 7C). Similarly, therapeutic administration of Evasin-1 also reduced pulmonary damage, wall thickening and fibrosis, and caused preservation of lung structure after bleomycin instillation (Figure 7D). We also evaluated lung collagen deposition by morphometry. There was increased collagen area (μm^2) at day 25 after bleomycin instillation (Figure 7E). Treatment with Evasin-1 significantly diminished collagen deposition both in the preventive (Prev-Ev-1) and therapeutic (Ther-Ev-1) regimens (Figure 7E).

For Review Only

Discussion:

The major findings of the present study can be summarized as follows: (i) preventive treatment with Evasin-1 reduced neutrophil and mononuclear migration into the lungs, reduced chemokine, TNF-α and active TGF-β_1 production and reduced pulmonary fibrosis; (ii) therapeutic treatment with Evasin-1 from day 8, at the peak of neutrophil influx, significantly reduced subsequent mononuclear cell migration, TNF-α and active TGF-β_1 production and reduced pulmonary fibrosis. Overall, administration of Evasin-1 mimicked the findings observed in $CCL3^{-/-}$ mice exposed to bleomycin, including reduced neutrophil influx into the airways and reduction of pulmonary levels of active TGF-β_1.

Several studies have now shown that chemokines, including CCL2, CCL3, CCL5, CXCL1, CXCL2, CXCL9, CXCL10 and their receptors, contribute to the pathogenesis of chronic inflammation and pulmonary fibrosis induced by the instillation of bleomycin in the murine lung (5, 6, 10-12, 17, 19). For example, it has been shown that anti-CCL3 antibodies reduced leukocyte accumulation and subsequent pulmonary fibrosis in bleomycin-instilled mice (20). Similarly, our studies using CCL3-deficient mice demonstrate a role for this chemokine in mediating inflammation and fibrosis after bleomycin instillation. Consistent with these studies in animal models, the analysis of bronchoalveolar fluid and biopsies of patients with IPF demonstrated higher levels of CCL3 than in samples from healthy volunteers (21). In addition, increased levels of CCL2, CCL3 and CCL4 were found in bronco-alveolar lavage fluid obtained from IPF patients when compared to healthy volunteers (22, 23). In the present study, we evaluated the effect of a chemokine binding-protein, Evasin-1, which has high selectivity for CCL3, as well as CCL4, and have shown that it reduced bleomycin-induced pulmonary inflammation and fibrosis in mice. Importantly, we show that treatment with Evasin-1 was effective even when started at day 8 after bleomycin instillation, at a time when neutrophil influx was maximal.

The acute inflammatory process in response to bleomycin instillation is characterized by the initial presence of neutrophils in the lung interstitium and airway space followed by the influx of mononuclear cells, especially macrophages. The latter cell types characterize the chronification of this lung inflammatory process (17). Neutrophils are thought to be major effector leukocytes in the context of IPF and are mostly found in bronco-alveolar lavage fluid from sick patients (24). Experimentally, the blockade of neutrophil recruitment into airway through CXCR2 receptor antagonism but not early neutrophil depletion by antibodies decreases bleomycin-induced lung injury (17, 25). The preventive treatment with Evasin-1 reduced neutrophil influx in alveolar and lung parenchyma at all times after bleomycin instillation. As preventive treatment started at day 8, at the time neutrophil accumulation is maximal (17), there was no effect on total MPO activity in the lungs at day 25. Altogether, these results suggest that, although inhibition of neutrophil influx is relevant for the development of fibro sis (12, 17, 26), it is unlikely that an inhibitory effect of Evasin-1 on neutrophil influx could account for the inhibition of fibrosis after bleomycin instillation.

Preventive treatment with Evasin-1 also reduced mononuclear cell numbers in the airway space but had a minor effect on total NAG activity, an index of macrophage influx, in the lung. A similar effect was observed when the drug was given from day 8 after bleomycin instillation. In both situations and in agreement with its mechanism of action (CCL3 binding), Evasin-1 greatly decreased CCL3 levels in lungs. These results would suggest that binding to and inhibition of CCL3 function is important for the influx of mononuclear cells, especially macrophages to the alveolar spaces but less important to the arrival of these cells in lung parenchyma. In addition, we also observed some inhibition of CCL2 and CCL5 production, especially when the drug was given as a preventive treatment. Inhibition of CCL2 and CCL5 may be secondary to the inhibition of the migration and activation of both macrophages and neutrophils, which are potential sources of these chemokines. In addition, it is possible that CCL3 can act on epithelial cells to promote chemokine release (12, 27). Regardless of the

mechanism by which Evasin-1 leads to an indirect inhibition of CCL2 and CCL5, it is of note that Evasin-1 given from day 8 prevented lung fibrosis without affecting CCL2 and CCL5 levels significantly. Therefore, it appears that a major effect of Evasin-1 in our model is to decrease levels and function of CCL3.

TNF-α is expressed by lung macrophages and suggested to play an important role in bleomycin-induced pulmonary fibrosis (28). In our study, preventive and therapeutic treatment with Evasin-1 greatly reduced TNF-α levels induced by bleomycin instillation. Smith and colleagues (1998) have suggested that epithelial cells and resident alveolar macrophages are major sources of IL-6 and TNF-α following bleomycin instillation. These cytokines act synergistically to stimulate CCL3 expression by alveolar cells (29). The released CCL3 can then recruit macrophages and neutrophils that can release further TNF-α, CCL3 and other chemokines, including CCL2 (30). Together, these cytokines and chemokines cooperate to activate macrophages and lymphocytes in the lungs and contribute to tissue injury. Administration of the Evasin-1 blocks the action of CCL3, hence preventing the positive feedback cycle among leukocytes, CCL3 and TNF-α which culminate in lung injury and fibrosis.

In addition to TNF-α, bleomycin exposure results in upregulated expression of TGF-β_1 mRNA and TGF-β_1 expression appears to be dependent on TNF-α receptor activation (28). Anti-TGF-β_1 antibodies have been shown to reduce bleomycin-induced pulmonary fibrosis (31). In our study, preventive or therapeutic treatment with Evasin-1 greatly reduced bleomycin-induced TGF-β_1 levels. This is consistent with the study by Ishida and colleagues (2007), which showed that CCL3 and CCR5 deficient mice had reduced macrophages and fibrocyte influx, and lower TGF-β_1 expression (12). Therefore, the ability of Evasin-1 to prevent CCL3 action leads to a decreased leukocyte influx and reduced TNF-α expression. The latter mechanisms may account for the reduced TGF-β_1 expression and reduced pulmonary fibrosis.

In conclusion, our results show that preventive or therapeutic administration of Evasin-1 is efficient in reducing progression of pulmonary injury and fibrosis induced by bleomycin in mice. Therefore, targeting CCL3 with Evasin-1 may be useful therapeutically for the treatment of inflammatory and fibrogenic lung diseases, such as idiopathic pulmonary fibrosis (IPF) treatment.

Acknowledgements:

We are grateful to Valdinéria Borges and Ilma Marçal for technical assistance. This work was supported by grants from Coordenação de Aperfeiçoamento de Pessoal de Nível Superior (CAPES/Brazil), Conselho Nacional de Desenvolvimento Científico e Tecnológico (CNPq/Brazil), Fundação de Amparo a Pesquisa do Estado de Minas Gerais (FAPEMIG/Brazil) and the European Union's Sixth Framework Programme (INNOCHEM project grant LSHBCT2005518167).

For Review Only

References:

1. Chen J, Stubbe J. Bleomycins: Towards better therapeutics. *Nat Rev Cancer* 2005;5(2):102-112.

2. Giri SN, Schwartz LW, Hollinger MA, Freywald ME, Schiedt MJ, Zuckerman JE. Biochemical and structural alterations of hamster lungs in response to intratracheal administration of bleomycin. *Exp Mol Pathol* 1980;33(1):1-14.

3. Sleijfer S. Bleomycin-induced pneumonitis. *Chest* 2001;120(2):617-624.

4. Gauldie J. Pro: Inflammatory mechanisms are a minor component of the pathogenesis of idiopathic pulmonary fibrosis. *Am J Respir Crit Care Med* 2002;165(9):1205-1206.

5. Strieter RM. Con: Inflammatory mechanisms are not a minor component of the pathogenesis of idiopathic pulmonary fibrosis. *Am J Respir Crit Care Med* 2002;165(9):1206-1207; discussion 1207-1208.

6. Phan SH, Kunkel SL. Lung cytokine production in bleomycin-induced pulmonary fibrosis. *Exp Lung Res* 1992;18(1):29-43.

7. Razzaque MS, Taguchi T. Pulmonary fibrosis: Cellular and molecular events. *Pathol Int* 2003;53(3):133-145.

8. Locati M, Otero K, Schioppa T, Signorelli P, Perrier P, Baviera S, Sozzani S, Mantovani A. The chemokine system: Tuning and shaping by regulation of receptor expression and coupling in polarized responses. *Allergy* 2002;57(11):972-982.

9. Selman M, Pardo A, Barrera L, Estrada A, Watson SR, Wilson K, Aziz N, Kaminski N, Zlotnik A. Gene expression profiles distinguish idiopathic pulmonary fibrosis from hypersensitivity pneumonitis. *Am J Respir Crit Care Med* 2006;173(2):188-198.

10. Gharaee-Kermani M, McCullumsmith RE, Charo IF, Kunkel SL, Phan SH. Cc-chemokine receptor 2 required for bleomycin-induced pulmonary fibrosis. *Cytokine* 2003;24(6):266-276.

For Review Only

11. Tokuda A, Itakura M, Onai N, Kimura H, Kuriyama T, Matsushima K. Pivotal role of ccr1-positive leukocytes in bleomycin-induced lung fibrosis in mice. *J Immunol* 2000;164(5):2745-2751.

12. Ishida Y, Kimura A, Kondo T, Hayashi T, Ueno M, Takakura N, Matsushima K, Mukaida N. Essential roles of the CC chemokine ligand 3-CC chemokine receptor 5 axis in bleomycin-induced pulmonary fibrosis through regulation of macrophage and fibrocyte infiltration. *Am J Pathol* 2007;170(3):843-854.

13. Fallon PG, Alcami A. Pathogen-derived immunomodulatory molecules: Future immunotherapeutics? *Trends Immunol* 2006;27(10):470-476.

14. Frauenschuh A, Power CA, Deruaz M, Ferreira BR, Silva JS, Teixeira MM, Dias JM, Martin T, Wells TN, Proudfoot AE. Molecular cloning and characterization of a highly selective chemokine-binding protein from the tick rhipicephalus sanguineus. *J Biol Chem* 2007;282(37):27250-27258.

15. Deruaz M, Frauenschuh A, Alessandri AL, Dias JM, Coelho FM, Russo RC, Ferreira BR, Graham GJ, Shaw JP, Wells TN, et al. Ticks produce highly selective chemokine binding proteins with antiinflammatory activity. *J Exp Med* 2008;205(9):2019-2031.

16. Cook DN, Beck MA, Coffman TM, Kirby SL, Sheridan JF, Pragnell IB, Smithies O. Requirement of mip-1 alpha for an inflammatory response to viral infection. *Science* 1995;269(5230):1583-1585.

17. Russo RC, Guabiraba R, Garcia CC, Barcelos LS, Roffe E, Souza AL, Amaral FA, Cisalpino D, Cassali GD, Doni A, et al. Role of the chemokine receptor cxcr2 in bleomycin-induced pulmonary inflammation and fibrosis. *Am J Respir Cell Mol Biol* 2009;40(4):410-421.

18. Barcelos LS, Talvani A, Teixeira AS, Vieira LQ, Cassali GD, Andrade SP, Teixeira MM. Impaired inflammatory angiogenesis, but not leukocyte influx, in mice lacking tnfr1. *J Leukoc Biol* 2005;78(2):352-358.

For Review Only

19. Jiang D, Liang J, Hodge J, Lu B, Zhu Z, Yu S, Fan J, Gao Y, Yin Z, Homer R, et al. Regulation of pulmonary fibrosis by chemokine receptor cxcr3. *J Clin Invest* 2004;114(2):291-299.

20. Smith RE, Strieter RM, Phan SH, Lukacs NW, Huffnagle GB, Wilke CA, Burdick MD, Lincoln P, Evanoff H, Kunkel SL. Production and function of murine macrophage inflammatory protein-1 alpha in bleomycin-induced lung injury. *J Immunol* 1994;153(10):4704-4712.

21. Standiford TJ, Rolfe MW, Kunkel SL, Lynch JP, 3rd, Burdick MD, Gilbert AR, Orringer MB, Whyte RI, Strieter RM. Macrophage inflammatory protein-1 alpha expression in interstitial lung disease. *J Immunol* 1993;151(5):2852-2863.

22. Capelli A, Di Stefano A, Gnemmi I, Donner CF. Ccr5 expression and cc chemokine levels in idiopathic pulmonary fibrosis. *Eur Respir J* 2005;25(4):701-707.

23. Suga M, Iyonaga K, Ichiyasu H, Saita N, Yamasaki H, Ando M. Clinical significance of mcp-1 levels in balf and serum in patients with interstitial lung diseases. *Eur Respir J* 1999;14(2):376-382.

24. Obayashi Y, Yamadori I, Fujita J, Yoshinouchi T, Ueda N, Takahara J. The role of neutrophils in the pathogenesis of idiopathic pulmonary fibrosis. *Chest* 1997;112(5):1338-1343.

25. Manoury B, Nenan S, Guenon I, Lagente V, Boichot E. Influence of early neutrophil depletion on mmps/timp-1 balance in bleomycin-induced lung fibrosis. *Int Immunopharmacol* 2007;7(7):900-911.

26. Zemans RL, Colgan SP, Downey GP. Transepithelial migration of neutrophils: Mechanisms and implications for acute lung injury. *Am J Respir Cell Mol Biol* 2009;40(5):519-535.

27. Abonyo BO, Lebby KD, Tonry JH, Ahmad M, Heiman AS. Modulation of eotaxin-3 (ccl26) in alveolar type ii epithelial cells. *Cytokine* 2006;36(5-6):237-244.

For Review Only

28. Ortiz LA, Lasky J, Hamilton RF, Jr., Holian A, Hoyle GW, Banks W, Peschon JJ, Brody AR, Lungarella G, Friedman M. Expression of tnf and the necessity of tnf receptors in bleomycin-induced lung injury in mice. *Exp Lung Res* 1998;24(6):721-743.

29. Smith RE, Strieter RM, Phan SH, Lukacs N, Kunkel SL. Tnf and il-6 mediate mip-1alpha expression in bleomycin-induced lung injury. *J Leukoc Biol* 1998;64(4):528-536.

30. Tsuda Y, Takahashi H, Kobayashi M, Hanafusa T, Herndon DN, Suzuki F. Three different neutrophil subsets exhibited in mice with different susceptibilities to infection by methicillin-resistant staphylococcus aureus. *Immunity* 2004;21(2):215-226.

31. Giri SN, Hyde DM, Hollinger MA. Effect of antibody to transforming growth factor beta on bleomycin induced accumulation of lung collagen in mice. *Thorax* 1993;48(10):959-966.

For Review Only

Figure legends:

Figure 1: Evasin-1 treatment schedules. Animals were given a single intratracheal challenge of bleomycin (0.0625U) or PBS and evaluated 4, 8 and 25 days after challenge. The following parameters were evaluated at days 4, 8 and 25: BAL and lung leukocytes influx, lung cytokine and chemokine levels. Fibrosis was accessed only at day 25 post-bleomycin. (A) Preventive schedule - 10 μg/animal of Evasin-1 was given subcutaneously 45 minutes before bleomycin injection then twice a day, from day 0 to 25. (B) Therapeutic schedule - 10 μg/animal of Evasin-1 was given subcutaneously twice a day starting from day 8 to 25.

Figure 2: Comparison of the effects of preventive treatment with Evasin-1 and results in CCL3-deficient instilled with bleomycin. (A) Kinetics of CCL3 production in the lungs in response to bleomycin challenge; (B) pulmonary levels of CCL3, (C) neutrophil numbers in bronchoalveolar lavage fluid and (D) active TGF-β_1 levels in lungs of wild type mice, CCL3$^{-/-}$ mice and mice treated with Evasin-1 (10 μg/animal) in a preventive schedule,. Animals were given a single intratracheal challenge of bleomycin (0.125U) (white columns) or PBS (Control, black columns) and parameters were evaluated 8 days after challenge. Results are representative of two experiments and are shown as the mean ± SEM of seven to eight animals in each group. *, ** and *** for $P < 0.05$, 0.01 and 0.001, respectively, when comparing to vehicle-given bleomycin-challenged mice, or to PBS instilled mice, as indicated.

Figure 3: Effects of preventive and therapeutic treatment with Evasin-1 on bleomycin-induced leukocyte influx into the airway space. The following parameters were evaluated in bronco-alveolar lavage (BAL): (A) total number of leukocytes, (B) number of neutrophils and (C) mononuclears. Animals were given a single intratracheal challenge of bleomycin (0.0625U) (white columns) or PBS (Control, black columns) and leukocytes evaluated 4, 8 and 25 days after challenge. Results are representative of two experiments and are shown as the mean ± SEM of seven to eight animals in each group. *, ** and *** for $P < 0.05$, 0.01 and 0.001, respectively, when comparing to vehicle-given bleomycin-challenged mice, or to PBS instilled mice, as indicated.

Figure 4: Effects of preventive and therapeutic treatment with Evasin-1 on bleomycin-induced lung neutrophil (A) and macrophage (B) accumulation. Lung neutrophils and macrophage were evaluated by determining of myeloperoxidase (MPO) and N-acetylglucosaminidase activities, respectively, in lung homogenates. Animals were given a single intratracheal challenge of bleomycin (0.0625U) (white columns) or PBS (Control, black columns) and lung tissue evaluated 4, 8 and 25 days after challenge. Results are representative of two experiments and are shown as the mean ± SEM of seven to eight animals in each group. *, ** and *** for $P < 0.05$, 0.01 and 0.001, respectively, when comparing to vehicle-given bleomycin-challenged mice, or to PBS instilled mice, as indicated.

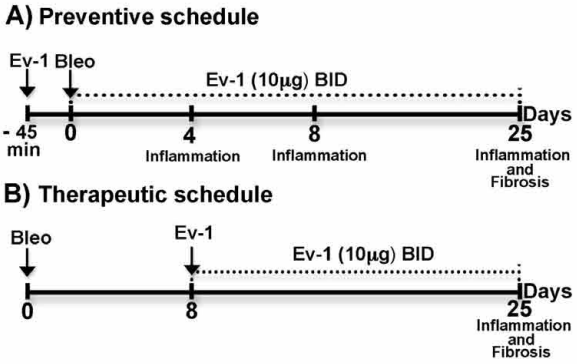
Figure 5: Effects of preventive and therapeutic treatment with Evasin-1 on bleomycin-induced pulmonary levels of TNF-α and TGF-β_1. Animals were given a single intratracheal challenge of bleomycin (0.0625U) (white columns) or PBS (Control, black columns) and pulmonary levels of (A) TNF-α and (B) active TGF-β_1 evaluated at 4, 8 and 25 days after challenge. Results are representative of two experiments and are shown as the mean ± SEM of seven to eight animals in each group. *, ** and *** for $P < 0.05$, 0.01 and 0.001, respectively, when comparing to vehicle-given bleomycin-challenged mice, or to PBS instilled mice, as indicated.

Figure 6: Effects of preventive and therapeutic treatment with Evasin-1 on bleomycin-induced lung chemokine production. The following soluble mediators were evaluated by ELISA in lung tissue: (A) CCL2, (B) CCL3, (C) CCL5. Animals were given a single intratracheal challenge of bleomycin (0.0625U) (white columns) or PBS (Control, black columns) and chemokines evaluated 4, 8 and 25 days after challenge. Results are representative of two experiments and are shown as the mean ± SEM of seven to eight animals in each group. *, ** and *** for $P < 0.05$, 0.01 and 0.001, respectively, when comparing to vehicle-given bleomycin-challenged mice, or to PBS instilled mice, as indicated.

Figure 7: Effects of preventive and therapeutic treatment with Evasin-1 on bleomycin-induced lung fibrosis. Animals were given a single intratracheal challenge of bleomycin (0.0625U) and fibrosis evaluated 25 days after challenge. Representative sections of Gomori's trichrome-stained lungs after PBS administration (A). Bleomycin-challenged (B-D) animals are also shown. Note the large areas of collagen deposition (green stained areas) at day 25 (B) after bleomycin instiallation. Preventive (Prev-Ev-1, C) or therapeutic (Thre-Ev-1, D) treatment with Evasin-1 decreased the amount and modified the pattern of collagen deposition at day 25 after challenge. Bars represents 50μm. In (E), lung collagen deposition was assessed by morphometric analysis of Gomori´s trichrome stained areas. Bleomycin-challenged (white columns) or PBS instilled (Control, black columns) mice are shown. Results are representative of two experiments and are shown as the mean ± SEM of seven to eight animals in each group. *, ** and *** for $P < 0.05$, 0.01 and 0.001, respectively, when comparing to vehicle-given bleomycin-challenged mice, or to PBS instilled mice, as indicated.

For Review Only

Figure 1



For Review Only

Figure 2

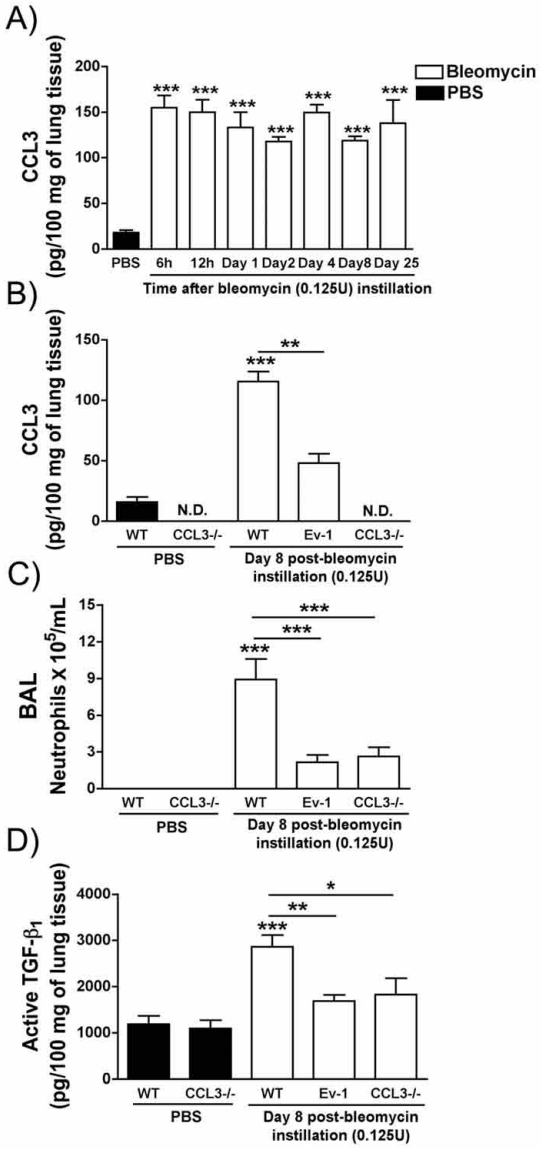

A)
CCL3 (pg/100 mg of lung tissue)
Bleomycin
PBS
PBS
6h
12h
Day 1
Day2
Day 4
Day8
Day 25
Time after bleomycin (0.125U) instillation
B)
CCL3 (pg/100 mg of lung tissue)
N.D.
N.D.
WT
CCL3-/-
WT
Ev-1
CCL3-/-
PBS
Day 8 post-bleomycin instillation (0.125U)
C)
BAL Neutrophils X 10^5/mL
WT
CCL3-/-
WT
Ev-1
CCL3-/-
PBS
Day 8 post-bleomycin instillation (0.125U)
D)
Active TGF-β1 (pg/100 mg of lung tissue)
WT
CCL3-/-
WT
Ev-1
CCL3-/-
PBS
Day 8 post-bleomycin instillation (0.125U)

Figure 3

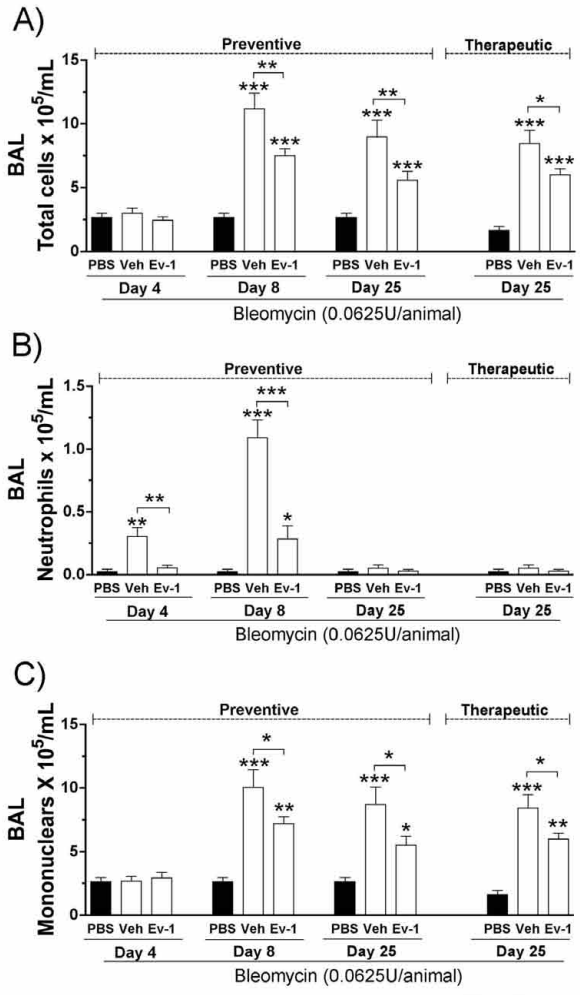
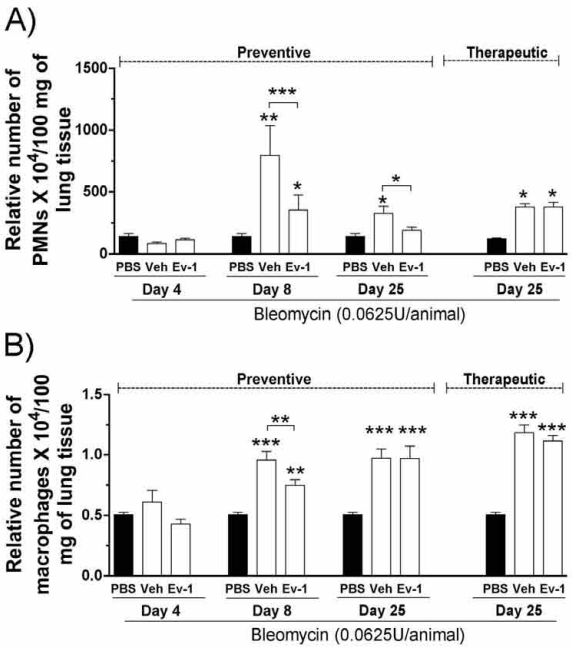
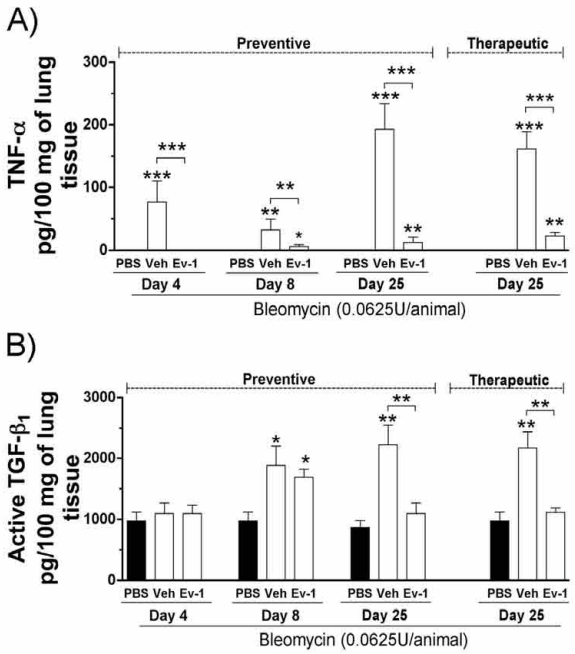

A)
Preventive
Therapeutic
BAL
Total cells x 10^5/mL
PBS Veh Ev-1
Day 4
Day 8
Day 25
Day 25
Bleomycin (0.0625U/animal)
B)
BAL
Neutrophils x 10^5/mL
C)
BAL
Mononuclears X 10^5/mL

Figure 4



For Peer Review Only

Figure 5



For Review Only

Figure 6

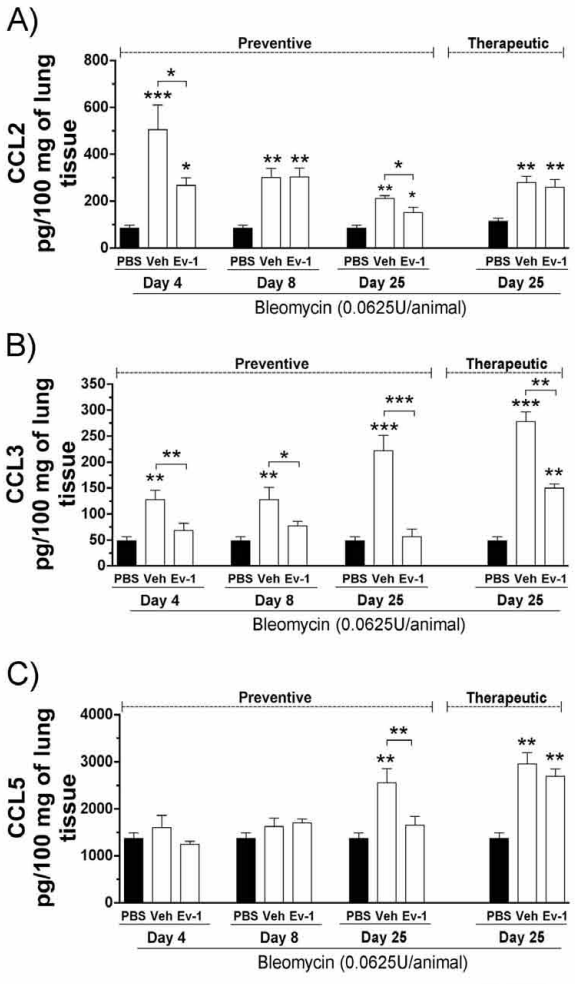
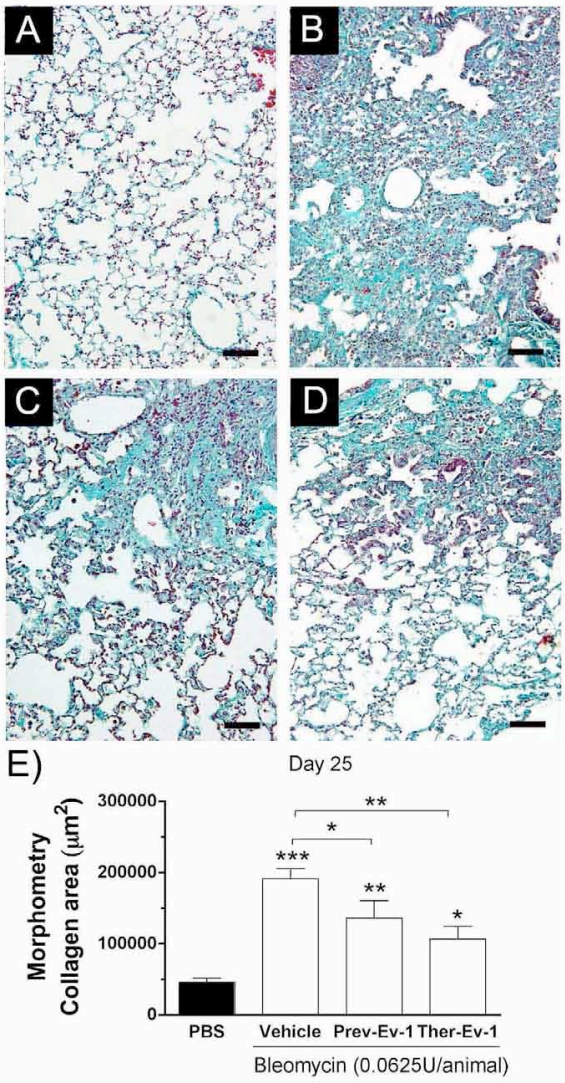

A)
CCL2 pg/100 mg of lung tissue
Preventive
Therapeutic
PBS Veh Ev-1
Day 4
Day 8
Day 25
Day 25
Bleomycin (0.0625U/animal)
B)
CCL3 pg/100 mg of lung tissue
Preventive
Therapeutic
PBS Veh Ev-1
Day 4
Day 8
Day 25
Day 25
Bleomycin (0.0625U/animal)
C)
CCL5 pg/100 mg of lung tissue
Preventive
Therapeutic
PBS Veh Ev-1
Day 4
Day 8
Day 25
Day 25
Bleomycin (0.0625U/animal)

Figure 7


A
B
C
D
E)
Day 25
Morphometry
Collagen area (μm²)
300000
200000
100000
0
***
**
*
**
*
PBS
Vehicle
Prev-Ev-1
Ther-Ev-1
Bleomycin (0.0625U/animal)

3.4. Trabalho cientifico – 4

RUSSO, R. C.; GARCIA, C. C.; BARCELOS, L. S.; GUABIRABA, R.; SOUSA, L. P.; ROFFÊ, E.; SOUZA, A. L. S.; CASSALI, D. G.; MIROLO, M.; DONI, A.; PINHO, V.; LOCATI, M.; TEIXEIRA, M. M. ***PI3K-γ plays a critical role enhancing pulmonary injury and fibrosis induced by bleomycin in mice.*** **Am. J. Respir. Crit. Care Med.** 2009. *(submetido)*.

Os objetivos específicos deste estudo foram:

1. Caracterizar os efeitos da ausência da isoforma γ da PI3K, utilizando animais geneticamente deficientes, sobre a inflamação e fibrose pulmonar induzida por bleomicina *in vivo*.
2. Avaliar os efeitos da administração do inibidor especifico da isoforma γ da PI3K, AS605240, sobre as funções sobre células endoteliais humanas e fibroblastos pulmonares murinos estimuladas com quimiocinas *in vitro*.

American Journal of Respiratory and Critical Care Medicine/AJRCCM

PI3Kγ plays a critical role enhancing pulmonary injury and fibrosis induced by bleomycin in mice

Journal:	*American Journal of Respiratory and Critical Care Medicine*
Manuscript ID:	Blue-200912-1790OC
Manuscript Type:	OC - Original Contribution
Date Submitted by the Author:	01-Dec-2009
Complete List of Authors:	Russo, Remo; UNIVERSIDADE FEDERAL DE MINAS GERAIS, DEPARTMENTO DE BIOQUIMICA E IMUNOLOGIA Garcia, Cristiana; UNIVERSIDADE FEDERAL DE MINAS GERAIS, DEPARTMENTO DE BIOQUIMICA E IMUNOLOGIA Barcelos, Luciola; UNIVERSIDADE FEDERAL DE MINAS GERAIS, DEPARTMENTO DE BIOFISICA Guabiraba, Rodrigo; UNIVERSIDADE FEDERAL DE MINAS GERAIS, DEPARTMENTO DE BIOQUIMICA E IMUNOLOGIA Sousa, Lirlandia; UNIVERSIDADE FEDERAL DE MINAS GERAIS, DEPARTMENTO DE BIOQUIMICA E IMUNOLOGIA Roffê, Ester; UNIVERSIDADE FEDERAL DE MINAS GERAIS, DEPARTMENTO DE BIOQUIMICA E IMUNOLOGIA Souza, Adriano; UNIVERSIDADE FEDERAL DE MINAS GERAIS, DEPARTMENTO DE BIOQUIMICA E IMUNOLOGIA Cassali, Geovanni; UNIVERSIDADE FEDERAL DE MINAS GERAIS, DEPARTMENTO DE PATOLOGIA GERAL Mirolo, Massimiliano; ISTITUTO CLINICO HUMANITAS, TRANSLATIONAL MEDICINE Doni, Andrea; ISTITUTO CLINICO HUMANITAS, TRANSLATIONAL MEDICINE Pinho, Vanessa; UNIVERSIDADE FEDERAL DE MINAS GERAIS, DEPARTMENTO DE MORFOLOGIA Locati, Massimo; ISTITUTO CLINICO HUMANITAS, TRANSLATIONAL MEDICINE TEIXEIRA, MAURO; UNIVERSIDADE FEDERAL DE MINAS GERAIS, DEPARTMENTO DE BIOQUIMICA E IMUNOLOGIA
Key Words:	Chemokine, Lung Injury, Pulmonary Fibrosis, PI3Kγ, Bleomycin

PI3Kγ plays a critical role enhancing pulmonary injury and fibrosis induced by bleomycin in mice

Remo C. Russo[1], Cristiana C. Garcia[1], Lucíola S. Barcelos[1,2], Rodrigo Guabiraba[1], Lirlândia P. Sousa[1,3], Ester Roffê[1], Adriano L. S. Souza[1], Geovanni D. Cassali[4], Massimiliano Mirolo[5], Andrea Doni[5], Vanessa Pinho[1,6], Massimo Locati[5] and Mauro M. Teixeira[1].

[1]Laboratório de Imunofarmacologia, Departamento de Bioquímica e Imunologia, Instituto de Ciências Biológicas, Universidade Federal de Minas Gerais, Belo Horizonte, MG, Brazil. [2]Departamento de Biofísica, Instituto de Ciências Biológicas, Universidade Federal de Minas Gerais, Belo Horizonte, MG, Brazil. [3]Setor de Patologia Clínica, Colégio Técnico, Universidade Federal de Minas Gerais, Belo Horizonte, MG, Brazil. [4]Departamento de Patologia Geral, Instituto de Ciências Biológicas, Universidade Federal de Minas Gerais, Belo Horizonte, MG, Brazil. [5]Laboratory of Leukocyte Biology, Istituto Clinico Humanitas (ICH), IRCCS, Department of Immunology and Inflammation, Rozzano, MI, Italy. [5]Departamento de Morfologia, Instituto de Ciências Biológicas, Universidade Federal de Minas Gerais, Belo Horizonte, MG, Brazil.

Corresponding Author: Mauro Martins Teixeira. Laboratório de Imunofarmacologia. Departamento de Bioquímica e Imunologia, Instituto de Ciências Biológicas – Universidade Federal de Minas Gerais. Avenida Antônio Carlos, 6627. CEP 30882-650 - Pampulha. Belo Horizonte, MG – Brazil. Phone/FAX: 55 31 3409 2651. mmtex@icb.ufmg.br.

Grant Support: This investigation received financial support from the Coordenação de Aperfeiçoamento de Pessoal de Nível Superior (CAPES/Brazil), Fundação de Amparo a Pesquisa do Estado de Minas Gerais (FAPEMIG/Brazil), Conselho Nacional de Desenvolvimento Científico e Tecnológico (CNPq/Brazil) and the European Union's Sixth Framework Programme (INNOCHEM project grant LSHBCT2005518167).

A short running head: *PI3Kγ enhances pulmonary fibrosis.*

Descriptor number: 7.3-Animal Models of Airway Fibrosis. 5.01-Chemokines: Immune Effects.

This article has an online data supplement, which is accessible from this issue's table of content online at www.atsjournals.org.

For Review Only

ABSTRACT

Rationale: PI3Kγ is a central signalling element in diverse arrays of cellular functions and inflammation. Idiopathic Pulmonary Fibrosis is associated with intense pulmonary inflammation and deposition of collagen and is modelled by instillation of bleomycin.

Objectives: To evaluate the role of PI3Kγ in mediating bleomycin-induced pulmonary inflammation and fibrosis in mice.

Methods: WT or PI3Kγ KO mice were instilled with bleomycin and leukocyte subtype influx, cytokine and chemokine levels, and tissue fibrosis were evaluated at various times in the lung. The activation of lung-derived leukocytes and fibroblasts were evaluated *in vitro*. The relevance of PI3Kγ for endothelial cell function was evaluated in human umbilical vein endothelial cells.

Measurements and Main Results: PI3Kγ KO mice had greater survival, weight recovery and less fibrosis than WT mice after bleomycin instillation. This was associated with decreased production of TGF-β_1 and CCL2, and increased production of IFNγ and IL-10. There was reduced expression of collagen, Fibronectin, α-SMA and von Willebrand factor. In lungs of PI3Kγ KO mice, there were decreased numbers and activation of leukocytes, enhanced number of apoptotic events and decreased phosphorylation of AKT and IκB-α. *In vitro*, treatment of human endothelial cells with the PI3Kγ inhibitor AS605240 decreased proliferation, migration and formation of capillary-like structures. AS605240 also decreased production of collagen by murine lung-derived fibroblasts.

Conclusions: PI3Kγ deficiency confers protection against bleomycin-induced pulmonary injury and fibrosis via modulation of the function of leukocytes, fibroblasts and endothelial cells. Inhibitors of PI3Kγ may be beneficial for the treatment of pulmonary fibrosis.

Keywords: Chemokine, Lung Injury, Pulmonary Fibrosis, PI3Kγ, Bleomycin.

For Review Only

INTRODUCTION:

Phosphatidylinositol 3-kinases (PI3Ks) are a subfamily of lipid kinases, that play an important role in intracellular signaling and are involved in many homeostatic mechanisms including cell growth, differentiation, tissue morphogenesis, metabolism and immune function (1). The PI3K family is divided into three classes that mediate distinct functions correlated to their cell distribution. Class I PI3K is the best characterized class that is further subdivided into two subclasses, IA and IB. The three members of subclass IA, PI3Kα, PI3Kβ and PI3Kδ, are primarily activated by tyrosine kinase receptors (2). PI3Kγ, the unique member of class IB, is activated by G protein-coupled receptors (GPCRs) via binding to βγ subunits. PI3Kγ activation mediates subsequent PIP_3 production that may trigger AKT activation and, consequently, enhance IκB kinase (IKK) phosphorylation and NF-κB activation in a wide range of cells (2). PI3Ks are thought to be relevant for several leukocyte functions, including actin-rearrangement and polarization, influx and migration into inflamed tissues and survival (2-6). PI3Kγ is expressed on leukocytes but also on other cell types, including endothelial cells and fibroblasts (3, 4, 7, 8), and may regulate the influx of leukocytes into the lung (9-11). The involvement of PI3Kγ in the context of pulmonary fibrosis remains uncharacterized.

Fibrotic lung diseases, including idiopathic pulmonary fibrosis (IPF), characterized by excessive and progressive lung parenchymal collagen deposition, represent a group of fatal lung diseases without effective therapeutic treatment (12). The etiology and pathogenesis of IPF are not completely understood. Bleomycin instillation induces lung injury and fibrosis in mice and is used as an animal model to investigate potential patho-physiological mechanisms which may be relevant in the context of human IPF (13). Bleomycin instillation results in oxidative damage to alveolar epithelium DNA, promoting chemokine release with subsequent cellular activation, expansion and airway recruitment. Leukocyte transmigration into airways

For Review Only

contributes to the maintenance of inflammatory process by cytokine production that enhances the initial injury (14), triggering fibroblast proliferation and excessive collagen deposition, leading to pulmonary fibrosis (15, 16). The chemokine system plays a central role in the pathogenesis of pulmonary fibrosis (12, 15-19) representing an attractive therapeutic target in this disease context (20).

The present study evaluated the role of PI3Kγ during pulmonary fibrosis induced by bleomycin. Our results indicate that pulmonary fibrosis and lethality induced by bleomycin is clearly attenuated in PI3Kγ-deficient mice. Mechanistically, absence of PI3Kγ was associated with reduced phosphorylation of AKT and translocation of NF-κB and consequent reduction of leukocyte influx and activation, enhanced apoptosis of inflammatory cells in the lungs, decreased expression of fibrosis-inducing genes, and decreased endothelial cell and fibroblast activation.

For Review Only

MATERIAL AND METHODS:

For detailed methods, see the online supplement.

Bleomycin-induced lung injury and fibrosis in mice.

C57Bl/6j (WT) and PI3Kγ deficient (PI3Kγ KO) mice (5), bred in our animal facility at Instituto de Ciências Biológicas, were maintained with filtered water, food *ad libitum* and in a controlled environment. Eight to 10-week-old male mice were injected with 0.125U/mouse of bleomycin as previously described (19). All experiments were conducted under conditions prior approved by the local animal ethics committee (CETEA/UFMG, *Protocol number: 146/06*).

Bronchoalveolar lavage analysis.

Leukocytes from airways were recovered by bronchoalveolar lavage (BAL) and the differential counts performed on cytospin preparations stained with May-Grunwald-Giemsa, as previously described (19). Protein amounts were quantified in BAL fluid samples using Bradford assay (21).

FACS analysis: BAL single cell suspensions were stained with fluorescent-labeled monoclonal antibodies CD3, CD4, CD8, Ly6G and CXCR2 and were acquired in FACScan cytometer for posterior analysis using FlowJo software.

Cytokine and chemokine measurement.

Cytokine and chemokine (IFN-γ, IL-10, active TGF-β_1, CXCL1, CXCL9 and CCL2) levels were quantified in lungs and BAL fluid using DuoSet ELISA kits (R&D Systems), in

For Review Only

accordance to the manufacturer's instructions. Tissues were processed as previously described (19).

Lung analysis

Fibrosis measurements.

Lung fragments were removed for hydroxyproline quantification as previously described (19). Lung sections stained with Hematoxilin & Eosin or Gomori's Trichrome were examined under light microscope, and the quantitative analysis was performed by morphometry, as previously described (19). *In vitro* total soluble collagen content was quantified by Sircol collagen-dye binding assay kit (Biocolor Dye Science, N. Ireland).

Quantitative Real-Time PCR.

Mice lungs were removed for analysis of Collagen1α1, Collagen1α2, Fibronectin, α-Smooth Muscle Actin, von Willebrand Factor mRNAs expression by quantitative RT-PCR (19). The primers and probes used are presented on Table-1. Results were normalized for 18S housekeeping gene, and expressed as transcript fold change over control mice.

Neutrophil and macrophage quantification: The accumulation into the lungs was measured in processed tissues by assaying myeloperoxidase (MPO) and N-acetylglucosaminidase (NAG) activities as previously described (19, 22).

Western blot: Lung cell extracts were used for quantify the AKT and IκB-α phosphorilation as previous described (21).

Apoptosis assay: Lung apoptosis was quantified performing the TUNEL assay in according to the manufacturer's instructions (TdT-FragEL™ DNA Fragmentation Kit, Calbiochem).

For Review Only

Lung collagenase digestion: Leukocytes were recovered from lungs processed with collagenase as previously described (23).

Lung leukocyte activation: Lung cells were used for evaluation of cell respiratory burst induced by unopsonized zymosan using a luminol-enhanced chemiluminescence assay as previous described (23).

***In Vitro* Experiments.**

Primary endothelial cells were obtained from human umbilical veins (HUVECs) and cultured for proliferation, scratch and capillary-like structure formation assays, as previously described (19). Isolation of mouse lung primary fibroblasts was performed as a previous described (24).

Statistical analysis.

All data are presented as the mean ± SEM and were analyzed by one-way ANOVA and differences between groups were assessed using the Student-Newman-Keuls post hoc test or Log-rank test. Graphs and analysis were performed using GraphPad Prism 4 software. Differences were considered significant at $P<0.05$.

For Review Only

RESULTS:

PI3K-γ deficiency protects mice against lethality and fibrosis induced by bleomycin.

Instillation of bleomycin (0.125U/nimal) in the lungs was associated with significant clinical disease, as seen by changes in weight and lethality rate that reached around 60% at day 16. In contrast, instillation of bleomycin in PI3Kγ KO mice was associated with only 15% lethality (Figure-1 A). WT mice lost weight progressively after bleomycin administration, with a more pronounced loss after day 5 which persisted till day 16. On the other hand, PI3Kγ KO mice had lower weight loss peak, which was accompanied by weight recovery from day 4 (Figure-1 B). There was an increased pulmonary fibrosis at day 16 after bleomycin instillation in WT mice, as assayed by hydroxyproline quantification and morphometric analysis in lung samples (Figure-1). PI3Kγ KO mice had reduced content of lung hydroxyproline (OH-proline) (Figure-1 C) and reduced collagen deposition, as assessed by morphometric analysis (Figure-1 D). There was no difference in lung morphology of WT (Figure-1 E) and PI3Kγ KO mice (Figure-1 F) after PBS instillation. Following bleomycin instillation, there was a dense and diffuse interstitial lung fibrosis with loss of pulmonary architecture in WT mice (Figure-1 G). In PI3Kγ KO mice, there was focal and less pronounced fibrosis with areas of preserved lung parenchyma after bleomycin (Figure-1 H).

PI3Kγ deficiency decreases cytokine production and expression of genes associated with fibrosis.

Because of the decreased fibrosis in PI3Kγ KO mice, we evaluated levels of inflammatory mediators and genes associated with lung fibrogenesis in lung homogenates. Levels of IFN-γ decreased markedly by instillation of bleomycin in WT mice. In PI3Kγ KO, the decrease of IFN-γ was less intense when compared to WT mice (Figure-2 A). Pulmonary

For Review Only

levels of IL-10 were enhanced by bleomycin and this increase was greater in PI3Kγ KO than WT at day 16 (Figure-2 B). In contrast, bleomycin enhanced pulmonary levels of CCL2 and active TGF-β_1 in WT mice instilled with bleomycin, but this increase was blunted in PI3Kγ KO mice (Figure-2 C and D).

Bleomycin challenge induced significant enhancement of mRNA expression, as assayed by real-time PCR, for several markers of pulmonary fibrosis, including genes that code for collagen-1α1, collagen-1α2 and fibronectin, at day 8 after bleomycin instillation in WT mice. There was also an increase in mRNA expression of α-Smooth Muscle Actin (α-SMA), a marker of fibroblast differentiation into myofibroblast. Of interest, mRNA expression of these genes was greatly decreased in PI3Kγ KO mice (Figure-2 E). A series of experiments were undertaken to examine why there was decreased production of fibrogenic mediators and fibrosis in PI3Kγ KO mice instilled with bleomycin

PI3Kγ deficiency decreases leukocyte infiltration induced by bleomycin.

Instillation of bleomycin in WT mice induced significant recruitment of leukocyte in the lungs, as assessed by counting cells in BAL fluid and in lung homogenates (Figures-3 and 4). In BAL fluid, there was a 6-fold increase in total number of leukocytes after bleomycin instillation in WT mice (Figure-3 A). Neutrophils predominated at day 8 and macrophages at day 16 after instillation (Figure-3 B and C). There was also an increase in number of $CD3^+CD4^+$ and $CD3^+CD8^+$ lymphocytes at day 8 (Figure-3 D and E). Infiltration of these leukocytes was associated with an increase in BAL fluid levels of chemokines, including CXCL1, CXCL9 and CCL2 (Figure-3 F-H), and lung damage, as shown by an increase in protein levels in BAL (Figure-3 I). In lung tissue, there was also an increase in leukocyte influx (Figure-4). Indeed, neutrophil numbers, as assessed by MPO assay, and macrophage numbers, as assessed by NAG activity, were greatly enhanced after bleomycin challenge

For Review Only

(Figure-4 A and B). Consistent with the latter changes, histological analysis of lung sections showed enhanced cellularity and damage after bleomycin challenge (Figure 4 C and E).

Parallel experiments in PI3Kγ KO mice showed that total influx of leukocytes, neutrophils, macrophages and lymphocytes in BAL fluid was lower than that found in WT mice after bleomycin challenge (Figure-3 A-E). Levels of total protein in BAL, a marker of lung damage and vascular permeability, were also lower in PI3Kγ KO than WT mice instilled with bleomycin (Figure-3 I). Despite the decrease in leukocyte influx and proteins into BAL fluid, overall, levels of chemokines were not decreased in PI3Kγ KO mice (Figure-3 F-H). In lung tissue, there was decreased macrophage accumulation (Figure-4 B), a finding that concurred with histological evaluation of lung sections (Figure-4 D and F). Number of neutrophils in lung tissue was not modified in PI3Kγ KO mice instilled with bleomycin, as assessed by MPO assay (Figure-4 A) and by evaluation of the percentage of Ly6G+CXCR2+ cells in lungs by FACS analysis (Day 8 - WT 6.2±1.6% vs. PI3Kγ KO 5.3±0.7 % of total lung cells, n= 6).

PI3Kγ deficiency is associated with greater number of apoptotic events after bleomycin instillation.

In addition to playing a role in mediating leukocyte influx into tissues, several studies have now shown that PI3Kγ is also important for leukocyte survival *in vivo* (25). PI3Kγ may regulate leukocyte survival via activation of AKT and consequent induction of NF-κB translocation (25, 26). As seen in Figure-5 A, instillation of bleomycin in WT mice induced phosphorylation of AKT and translocation of NF-κB, as demonstrated by enhanced phosphorylation of IκB-α. Experiments in PI3Kγ KO mice, showed that AKT and IκB-α were less phosphorylated than WT mice subjected to bleomycin-induced lung injury (Figure-5 A and B). There was no difference in the number of apoptotic events in WT (Figure-5 D) or

For Review Only

PI3Kγ KO mice (Figure-5 E), as assessed by TUNEL, after PBS instillation. In agreement with the decreased activation of AKT and IκB-α and their role in promoting leukocyte survival, there was greater number of apoptotic events in PI3Kγ KO than WT mice instilled with bleomycin (Figure-5 C, and F-G). These results suggest that decreased PI3Kγ-dependent leukocyte survival may account for the decreased accumulation of leukocytes observed in PI3Kγ KO mice instilled with bleomycin.

PI3Kγ regulates activation of lung-derived leukocytes.

Several studies have shown that leukocyte activation may be dependent on the function of PI3Kγ (27, 28). Addition of zymosan to leukocytes recovered from WT mice 8 days after bleomycin instillation induced a respiratory burst that could be measured in a luminol-enhanced chemiluminescence assay (Figure 6). Basal chemoluminescence of leukocytes recovered from PI3Kγ KO was similar to those of WT mice, but stimulation of the leukocytes with zymosan induced a respiratory burst that was approximately 40% lower (Figure 6). Therefore, there is decreased overall leukocyte activation, as assessed by their ability to produce reactive oxygen species, in PI3Kγ KO instilled with bleomycin.

PI3Kγ regulates endothelial cell function and angiogenesis

In addition to modifying the function of leukocytes, it has been shown that PI3Kγ may be expressed and be important for the function of endothelial cells (6, 27, 29). Of interest, there was lower mRNA expression of von Willebrand factor (vWF), a marker of endothelial cells activation/proliferation, in PI3Kγ KO than WT mice after bleomycin instillation (Figure-2 E). To confirm the relevance of PI3Kγ expression for the proliferation of endothelial cells, a series of experiments were conducted with a selective PI3Kγ inhibitor, AS605240, in a model of CXCL8-induced HUVEC proliferation. Previous studies have shown a crucial role of

For Review Only

CXCR1/2, to which IL-8 and other ELR^+ CXC chemokines bind, in bleomycin-induced lung injury (19). Cell proliferation induced by CXCL8 was significantly reduced in dose-dependent manner by AS605240, with maximal inhibition of 85% observed at 10 μM (Figure-7 A). Next, we examined the relevance of PI3Kγ for HUVEC migration using a scratch assay. HUVEC migration and scratch closure induced by CXCL8 (10 ng/ml) was significantly decreased in the presence of AS605240 (1 μM) after 12 hours of incubation (Figure-7 B). AS605240 (1 μM) also decreased the formation of capillary-like structures induced by CXCL8 in matrigel assay (Figure-7 C). Therefore, these results suggest that CXCL8-induced functional changes on human endothelial cells are dependent on PI3Kγ, an effect that may account for the decreased expression of vWF after bleomycin instillation in PI3Kγ KO mice.

PI3Kγ regulates activation of lung-derived fibroblasts.

Fibroblasts secrete collagen and may play a crucial role in the context of pulmonary fibrosis (16). To test whether PI3Kγ mediates chemokines-induced collagen production, lung explants from WT mice were taken for fibroblasts isolation and primary culture. We found, *in vitro*, that CXCL1 and CCL2 induced secretion of soluble collagen by lung fibroblasts, as quantified by Sircol assay (Figure-8), 24 hours after chemokine stimulation. However, when fibroblasts were treated with AS605240 (1 μM), there was a marked decrease in the production of chemokine-induced soluble collagen, compared to DMSO-treated fibroblasts (Figure-8), suggesting that the fibrogenesis is mediated by PI3Kγ activity.

For Review Only

Discussion:

The present study provides the first evidence that mice-lacking PI3Kγ are resistant to bleomycin-induced pulmonary injury and fibrosis, supporting a central role of PI3Kγ for lung fibrogenesis. The major findings of our study can be summarized as follows: (i) Bleomycin-exposed PI3Kγ KO mice had reduced weight loss, greater survival, reduced collagen deposition and reduced expression of pro-fibrogenic and pro-angiogenic genes; (ii) there was decreased accumulation of leukocyte in lungs of PI3Kγ KO, (iii) decreased phosphorylation of AKT and IκB-α and enhanced number of apoptotic events in the lungs. Moreover, (iv) there was decreased leukocyte activation, as shown by decreased production of reactive oxygen species. Finally, i*n vitro* studies showed that (v) PI3Kγ mediated collagen secretion by fibroblasts and controlled endothelial cell function, including proliferation, migration and capillary-like formation of HUVEC induced by chemokine, and angiogenesis *in vivo*.

The development of lung fibrosis is believed to be associated with aberrant tissue injury and repair, but is incompletely understood (12, 16, 30, 31). Pulmonary fibrogenesis is characterized by increased production and deposition of extracellular matrix (ECM) proteins into the lung parenchyma (12, 16). After bleomycin instillation, PI3Kγ KO mice displayed decreased lethality and pulmonary fibrogenesis and lower up-regulation of collagens and fibronectin mRNAs transcripts. Associated to this less pronounced pulmonary fibrosis, PI3Kγ KO mice had reduced lung production of active TGF-β_1 and CCL2, which are notorious pro-fibrogenic factors (32). These factors can activate and differentiate fibroblast into myofibroblast, which expresses α-SMA and are effectors cells during pulmonary fibrosis, responsible for the deposition of extracellular matrix components (33). Among these extracellular matrix components, fibronectin is necessary for wound healing and for fibroblast activation and expression of α-SMA during pulmonary fibrosis (34). In addition, there was also enhanced α-SMA mRNA transcription expression together with increased active TGF-

For Review Only

β_1, CCL2 and fibronectin levels in lungs WT mice. These results indicated that fibroblast differentiation into myofibroblast occurred in WT but was really reduced in PI3Kγ KO mice. IFN-γ is a cytokine with anti-fibrotic proprieties, which may act in the context of lung fibrosis as a negative regulator of TGF-β_1 production and action (35). IFN-γ was elevated in PI3Kγ KO but not in WT mice after bleomycin, a finding that may contribute for generation of a lung anti-fibrogenic microenvironment. Altogether, these results show that PI3Kγ KO mice are protected from lethality induced by bleomycin and suggest that down regulation of the development of pulmonary fibrosis may account for this overall protective effect of PI3Kγ deficiency.

The accumulation of leukocytes in the lungs is a critical event for the development of fibrosis after bleomycin instillation in mice (36). Efficient trafficking of leukocytes to sites of inflammation requires expression of PI3Kγ and PI3Kδ on leukocytes and endothelial cells (7, 8, 37). In models of acute lung inflammation, recruitment of leukocytes into airway spaces depends on PI3Kγ whereas recruitment into lung parenchyma is mostly PI3Kγ-independent (7, 38). In our model, there was reduced influx of neutrophils, lymphocytes and macrophages into airway spaces. Indeed, leukocyte migration into airways is an important event that triggers lung damage by secretion of leukocyte-derived toxic products and its consequences are the contribution to chronic lung injury and repair (14). There was also reduced accumulation of macrophages, but not neutrophils, in lung parenchyma of PI3Kγ deficient mice. This is in agreement with other studies which show that neutrophil accumulation in this compartment (lung parenchyma) is PI3Kγ-independent (7, 38). Reduced influx of leukocytes occurred in presence of significant levels of chemokines, suggesting that reduced influx of cells was not due to a decreased production of chemoattractants molecules, but rather secondary to decreased PI3Kγ-dependent influx of leukocytes. Activation of the PI3K-AKT-NF-κB cascade also regulates leukocyte survival *in vivo* (39), and several studies have shown

For Review Only

that PI3Kγ KO mice have disease amelioration associated with increased apoptosis. For example, the genetic ablation of the gene expression or enzymatic activity of PI3Kγ attenuates lung functional and morphologic alterations associated to ventilator-induced lung injury model, through the enhancement of pulmonary apoptosis (10). Our results showed that AKT and IκB-α were less phosphorylated and apoptotic events greater in PI3Kγ KO mice than WT mice subjected to bleomycin-induced lung injury. Therefore, decreased PI3Kγ-dependent influx of leukocytes and decreased AKT-NF-κB-dependent survival may have accounted for the decreased overall leukocyte influx observed after instillation of bleomycin in PI3Kγ KO mice. Moreover, decreased leukocyte accumulation may explain, at least in part, the decreased production of pro-fibrogenic cytokines, fibrosis and death associated with instillation of bleomycin.

In addition to its role in mediating leukocyte migration, previous studies have shown that PI3Kγ plays an important role in modulating leukocyte function triggered by chemoattractant molecules, such as chemokines (2, 5, 27, 28). For example, activation of leukocytes by chemokines induced generation of ROS which was dependent on the function of PI3Kγ (40). Here, we show that there was reduced production of ROS by lung-derived leukocytes activated with zymosan. This demonstrates reduced leukocyte activation in our system that could be secondary to the reduced translocation of NF-κB and enhanced expression of anti-inflammatory cytokine IL-10 (41). As ROS generation may have fibrogenic effects (3, 42), the observed inhibition of ROS production by leukocytes *ex vivo* may contribute to the observed protective phenotype of PI3Kγ mice.

Angiogenesis is required for pulmonary healing in response to tissue injury (43, 44). PI3Kγ has been shown to play a significant role in angiogenesis (6, 45). We observed reduced expression of von Willebrand factor, a marker of endothelial cell proliferation and angiogenesis (19), in PI3Kγ mice instilled with bleomycin. We have previously shown that

For Review Only

activation of CXCR2 to play a crucial role in the development of bleomycin-induced lung injury, an effect greatly dependent on activation of CXCR2 on endothelial cells (19). A few studies have shown that CXCR2 may activate endothelial cells via PI3Kγ (29). In our system, activation of HUVEC by CXCL8 induced endothelial cell proliferation, migration and formation of capillary-like structures that was PI3Kγ-dependent. Taken together with our previous study showing a role for CXCR2 in the context of bleomycin-induced lung injury, these data indicate that absence of PI3Kγ on endothelial cells may contribute to the protection against pulmonary fibrosis afforded by the absence of PI3Kγ in bleomycin-instilled mice.

Chemokines may induce fibrocyte migration and directly activate myofibroblasts to induce production of collagen into scar tissues (46-48). These two functions may contribute to fibrogenesis induced by various stimuli, including bleomycin. Skin fibroblasts recovered from patients with diffuse cutaneous scleroderma, but not normal subjects, express CXCR2 and CCR2 (49). Likewise, CXCR2 expression was restricted to fibroblasts and myofibroblast from keloid but not in healthy tissues (50). Using fibroblasts obtained from animals instilled with bleomycin, we found significant production of collagen after stimulation with CXCL1 and CCL2. Interestingly, addition of a PI3Kγ inhibitor prevented collagen production in response to both chemokines. Therefore, PI3Kγ is important on fibroblasts for their capacity to respond to chemokines, suggesting that absence of PI3Kγ on fibroblasts may contribute to the protection against pulmonary fibrosis afforded by the absence of PI3Kγ in bleomycin-instilled mice

Chemokines play a major role in driving tissue inflammation and fibrosis after bleomycin instillation (15, 17, 18). Several of the functions of chemokines are signaled via PI3Kγ. Here, we demonstrate a critical contribution of PI3Kγ in driving tissue inflammation, angiogenesis, fibrosis and lung injury after bleomycin instillation in mice. Mechanistically, PI3Kγ regulates chemokine-induced leukocyte activation, migration and survival. In addition,

For Review Only

PI3Kγ is necessary for chemokine-induced endothelial cell and fibroblast function. It is suggested that further studies should define the therapeutic value of inhibiting PI3Kγ in patients with idiopathic pulmonary fibrosis.

Acknowledgements:

The authors thank Valdinéria Borges and Ilma Marçal for technical assistance. The authors are grateful to Prof. Alberto Mantovani, from Istituto Clinico Humanitas (ICH), for help with experiments *in vitro* and reagents.

For Review Only

References:

1. Rameh LE, Cantley LC. The role of phosphoinositide 3-kinase lipid products in cell function. *J Biol Chem* 1999;274:8347-8350.

2. Kok K, Geering B, Vanhaesebroeck B. Regulation of phosphoinositide 3-kinase expression in health and disease. *Trends Biochem Sci* 2009;34:115-127.

3. Lu Y, Azad N, Wang L, Iyer AK, Castranova V, Jiang BH, Rojanasakul Y. Phosphatidylinositol-3-kinase/akt regulates bleomycin-induced fibroblast proliferation and collagen production. *Am J Respir Cell Mol Biol* 2009.

4. Pinho V, Souza DG, Barsante MM, Hamer FP, De Freitas MS, Rossi AG, Teixeira MM. Phosphoinositide-3 kinases critically regulate the recruitment and survival of eosinophils in vivo: Importance for the resolution of allergic inflammation. *J Leukoc Biol* 2005;77:800-810.

5. Hirsch E, Katanaev VL, Garlanda C, Azzolino O, Pirola L, Silengo L, Sozzani S, Mantovani A, Altruda F, Wymann MP. Central role for g protein-coupled phosphoinositide 3-kinase gamma in inflammation. *Science* 2000;287:1049-1053.

6. Madeddu P, Kraenkel N, Barcelos LS, Siragusa M, Campagnolo P, Oikawa A, Caporali A, Herman A, Azzolino O, Barberis L, et al. Phosphoinositide 3-kinase gamma gene knockout impairs postischemic neovascularization and endothelial progenitor cell functions. *Arterioscler Thromb Vasc Biol* 2008;28:68-76.

7. Pinho V, de Castro Russo R, Amaral FA, de Sousa LP, Barsante MM, de Souza DG, Alves-Filho JC, Cara DC, Hayflick JS, Rommel C, et al. Tissue- and stimulus-dependent role of phosphatidylinositol 3-kinase isoforms for neutrophil recruitment induced by chemoattractants in vivo. *J Immunol* 2007;179:7891-7898.

For Review Only

8. Puri KD, Doggett TA, Huang CY, Douangpanya J, Hayflick JS, Turner M, Penninger J, Diacovo TG. The role of endothelial pi3kgamma activity in neutrophil trafficking. *Blood* 2005;106:150-157.

9. Doukas J, Eide L, Stebbins K, Racanelli-Layton A, Dellamary L, Martin M, Dneprovskaia E, Noronha G, Soll R, Wrasidlo W, et al. Aerosolized phosphoinositide 3-kinase gamma/delta inhibitor tg100-115 [3-[2,4-diamino-6-(3-hydroxyphenyl)pteridin-7-yl]phenol] as a therapeutic candidate for asthma and chronic obstructive pulmonary disease. *J Pharmacol Exp Ther* 2009;328:758-765.

10. Lionetti V, Lisi A, Patrucco E, De Giuli P, Milazzo MG, Ceci S, Wymann M, Lena A, Gremigni V, Fanelli V, et al. Lack of phosphoinositide 3-kinase-gamma attenuates ventilator-induced lung injury. *Crit Care Med* 2006;34:134-141.

11. Takeda M, Ito W, Tanabe M, Ueki S, Kato H, Kihara J, Tanigai T, Chiba T, Yamaguchi K, Kayaba H, et al. Allergic airway hyperresponsiveness, inflammation, and remodeling do not develop in phosphoinositide 3-kinase gamma-deficient mice. *J Allergy Clin Immunol* 2009;123:805-812.

12. American thoracic society. Idiopathic pulmonary fibrosis: Diagnosis and treatment. International consensus statement. American thoracic society (ats), and the european respiratory society (ers). *Am J Respir Crit Care Med* 2000;161:646-664.

13. Giri SN, Schwartz LW, Hollinger MA, Freywald ME, Schiedt MJ, Zuckerman JE. Biochemical and structural alterations of hamster lungs in response to intratracheal administration of bleomycin. *Exp Mol Pathol* 1980;33:1-14.

14. Zemans RL, Colgan SP, Downey GP. Transepithelial migration of neutrophils: Mechanisms and implications for acute lung injury. *Am J Respir Cell Mol Biol* 2009;40:519-535.

For Review Only

15. Shimabukuro DW, Sawa T, Gropper MA. Injury and repair in lung and airways. *Crit Care Med* 2003;31:S524-531.

16. Wilson MS, Wynn TA. Pulmonary fibrosis: Pathogenesis, etiology and regulation. *Mucosal Immunol* 2009;2:103-121.

17. Strieter RM, Gomperts BN, Keane MP. The role of cxc chemokines in pulmonary fibrosis. *J Clin Invest* 2007;117:549-556.

18. Smith RE, Strieter RM, Zhang K, Phan SH, Standiford TJ, Lukacs NW, Kunkel SL. A role for c-c chemokines in fibrotic lung disease. *J Leukoc Biol* 1995;57:782-787.

19. Russo RC, Guabiraba R, Garcia CC, Barcelos LS, Roffe E, Souza AL, Amaral FA, Cisalpino D, Cassali GD, Doni A, et al. Role of the chemokine receptor cxcr2 in bleomycin-induced pulmonary inflammation and fibrosis. *Am J Respir Cell Mol Biol* 2009;40:410-421.

20. Ruckle T, Schwarz MK, Rommel C. Pi3kgamma inhibition: Towards an 'aspirin of the 21st century'? *Nat Rev Drug Discov* 2006;5:903-918.

21. Souza DG, Fagundes CT, Amaral FA, Cisalpino D, Sousa LP, Vieira AT, Pinho V, Nicoli JR, Vieira LQ, Fierro IM, et al. The required role of endogenously produced lipoxin a4 and annexin-1 for the production of il-10 and inflammatory hyporesponsiveness in mice. *J Immunol* 2007;179:8533-8543.

22. Barcelos LS, Talvani A, Teixeira AS, Vieira LQ, Cassali GD, Andrade SP, Teixeira MM. Impaired inflammatory angiogenesis, but not leukocyte influx, in mice lacking tnfr1. *J Leukoc Biol* 2005;78:352-358.

23. Amaral FA, Fagundes CT, Guabiraba R, Vieira AT, Souza AL, Russo RC, Soares MP, Teixeira MM, Souza DG. The role of macrophage migration inhibitory factor in the cascade of events leading to reperfusion-induced inflammatory injury and lethality. *Am J Pathol* 2007;171:1887-1893.

For Review Only

24. Vittal R, Zhang H, Han MK, Moore BB, Horowitz JC, Thannickal VJ. Effects of the protein kinase inhibitor, imatinib mesylate, on epithelial/mesenchymal phenotypes: Implications for treatment of fibrotic diseases. *J Pharmacol Exp Ther* 2007;321:35-44.

25. Yang KY, Arcaroli J, Kupfner J, Pitts TM, Park JS, Strasshiem D, Perng RP, Abraham E. Involvement of phosphatidylinositol 3-kinase gamma in neutrophil apoptosis. *Cell Signal* 2003;15:225-233.

26. Sousa LP, Carmo AF, Rezende BM, Lopes F, Silva DM, Alessandri AL, Bonjardim CA, Rossi AG, Teixeira MM, Pinho V. Cyclic amp enhances resolution of allergic pleurisy by promoting inflammatory cell apoptosis via inhibition of pi3k/akt and nf-kappab. *Biochem Pharmacol* 2009;78:396-405.

27. Barberis L, Hirsch E. Targeting phosphoinositide 3-kinase gamma to fight inflammation and more. *Thromb Haemost* 2008;99:279-285.

28. Fruman DA, Bismuth G. Fine tuning the immune response with pi3k. *Immunol Rev* 2009;228:253-272.

29. Gavard J, Hou X, Qu Y, Masedunskas A, Martin D, Weigert R, Li X, Gutkind JS. A role for a cxcr2/phosphatidylinositol 3-kinase gamma signaling axis in acute and chronic vascular permeability. *Mol Cell Biol* 2009;29:2469-2480.

30. Gauldie J. Pro: Inflammatory mechanisms are a minor component of the pathogenesis of idiopathic pulmonary fibrosis. *Am J Respir Crit Care Med* 2002;165:1205-1206.

31. Strieter RM. Con: Inflammatory mechanisms are not a minor component of the pathogenesis of idiopathic pulmonary fibrosis. *Am J Respir Crit Care Med* 2002;165:1206-1207; discussion 1207-1208.

32. Murray LA, Argentieri RL, Farrell FX, Bracht M, Sheng H, Whitaker B, Beck H, Tsui P, Cochlin K, Evanoff HL, et al. Hyper-responsiveness of ipf/uip fibroblasts: Interplay between tgfbeta1, il-13 and ccl2. *Int J Biochem Cell Biol* 2008;40:2174-2182.

For Review Only

33. Gharaee-Kermani M, McCullumsmith RE, Charo IF, Kunkel SL, Phan SH. Cc-chemokine receptor 2 required for bleomycin-induced pulmonary fibrosis. *Cytokine* 2003;24:266-276.

34. Muro AF, Moretti FA, Moore BB, Yan M, Atrasz RG, Wilke CA, Flaherty KR, Martinez FJ, Tsui JL, Sheppard D, et al. An essential role for fibronectin extra type iii domain a in pulmonary fibrosis. *Am J Respir Crit Care Med* 2008;177:638-645.

35. Leask A, Abraham DJ. Tgf-beta signaling and the fibrotic response. *FASEB J* 2004;18:816-827.

36. Jones HA, Schofield JB, Krausz T, Boobis AR, Haslett C. Pulmonary fibrosis correlates with duration of tissue neutrophil activation. *Am J Respir Crit Care Med* 1998;158:620-628.

37. Liu L, Puri KD, Penninger JM, Kubes P. Leukocyte pi3kgamma and pi3kdelta have temporally distinct roles for leukocyte recruitment in vivo. *Blood* 2007;110:1191-1198.

38. Reutershan J, Saprito MS, Wu D, Ruckle T, Ley K. Phosphoinositide-3 kinase {gamma} required for lps-induced transepithelial neutrophil trafficking in the lung. *Eur Respir J* 2009.

39. Duronio V. The life of a cell: Apoptosis regulation by the pi3k/pkb pathway. *Biochem J* 2008;415:333-344.

40. Fu H, Bylund J, Karlsson A, Pellme S, Dahlgren C. The mechanism for activation of the neutrophil nadph-oxidase by the peptides formyl-met-leu-phe and trp-lys-tyr-met-val-met differs from that for interleukin-8. *Immunology* 2004;112:201-210.

41. Cox G. Il-10 enhances resolution of pulmonary inflammation in vivo by promoting apoptosis of neutrophils. *Am J Physiol* 1996;271:L566-571.

For Review Only

42. Hagiwara SI, Ishii Y, Kitamura S. Aerosolized administration of n-acetylcysteine attenuates lung fibrosis induced by bleomycin in mice. *Am J Respir Crit Care Med* 2000;162:225-231.

43. Keane MP. Angiogenesis and pulmonary fibrosis: Feast or famine? *Am J Respir Crit Care Med* 2004;170:207-209.

44. McDonald DM. Angiogenesis and remodeling of airway vasculature in chronic inflammation. *Am J Respir Crit Care Med* 2001;164:S39-45.

45. Heller R, Chang Q, Ehrlich G, Hsieh SN, Schoenwaelder SM, Kuhlencordt PJ, Preissner KT, Hirsch E, Wetzker R. Overlapping and distinct roles for pi3kbeta and gamma isoforms in s1p-induced migration of human and mouse endothelial cells. *Cardiovasc Res* 2008;80:96-105.

46. Ishida Y, Kimura A, Kondo T, Hayashi T, Ueno M, Takakura N, Matsushima K, Mukaida N. Essential roles of the cc chemokine ligand 3-cc chemokine receptor 5 axis in bleomycin-induced pulmonary fibrosis through regulation of macrophage and fibrocyte infiltration. *Am J Pathol* 2007;170:843-854.

47. Lama VN, Phan SH. The extrapulmonary origin of fibroblasts: Stem/progenitor cells and beyond. *Proc Am Thorac Soc* 2006;3:373-376.

48. Mehrad B, Burdick MD, Strieter RM. Fibrocyte cxcr4 regulation as a therapeutic target in pulmonary fibrosis. *Int J Biochem Cell Biol* 2009;41:1708-1718.

49. Carulli MT, Ong VH, Ponticos M, Shiwen X, Abraham DJ, Black CM, Denton CP. Chemokine receptor ccr2 expression by systemic sclerosis fibroblasts: Evidence for autocrine regulation of myofibroblast differentiation. *Arthritis Rheum* 2005;52:3772-3782.

50. Nirodi CS, Devalaraja R, Nanney LB, Arrindell S, Russell S, Trupin J, Richmond A. Chemokine and chemokine receptor expression in keloid and normal fibroblasts. *Wound Repair Regen* 2000;8:371-382.

For Review Only

Figure Legends:

Figure-1: Lethality, weight loss and pulmonary fibrosis after bleomycin instillation in WT and PI3Kγ KO mice. Lethality (A) and weight loss (B), were monitored daily after intra-tracheal bleomycin instillation (0.125U/animal, n=13-16 mice for each group). After 16 days, mice were sacrificed for fibrosis assessment by Hydroxyproline quantification (C) and morphometry of lung collagen area under Gomori's Trichrome staining (D). Representative photomicrography of Gomori's Trichrome stained lungs 16 days post-bleomycin instillation (E-H). Bars represent 1000μm. PBS-instilled WT mice (E) and PI3Kγ KO mice (F) presented normal lung architecture. Histopathology shows a dense and diffuse interstitial lung fibrosis with loss of pulmonary architecture in WT mice bleomycin-challenged (G), whereas there was a focal and less pronounced fibrosis with preserved areas of lung parenchyma in PI3Kγ KO mice (H). Results are representative of two experiments and are shown as the mean ± SEM of seven to eight animals in each group. *, ** and *** for $P < 0.05$, 0.01 and 0.001, respectively, when comparing to WT-given bleomycin-challenged mice and instilled-PI3Kγ KO mice, as indicated.

Figure-2: Levels of cytokines and mRNA expression of fibrosis-associated genes after bleomycin instillation in WT and PI3Kγ KO mice. Animals were given a single intratracheal challenge of bleomycin (0.125U) or PBS and pulmonary levels of IFN-γ (A), IL-10 (B), CCL2 (C), and active TGF-β_1 (D) evaluated by ELISA at days 8 and 16 after challenge. Total lung mRNA expression using quantitative real time PCR (E) 8 days after bleomycin instillation. Primers (Table-1) used targeted genes for Collagen 1α1 (Col1α1), Collagen 1α2 (Col1α2), Fibronectin, α-Smooth Muscle Actin (α-SMA) and von Willebrand factor (vWF) transcription. Results are representative of two experiments and are shown as the mean ± SEM of seven to eight animals in each group. *, ** and *** for $P < 0.05$, 0.01 and 0.001, respectively, when comparing to WT-given bleomycin-challenged mice and instilled-PI3Kγ KO mice, as indicated.

Figure-3: Number of leukocytes in bronco-alveolar lavage (BAL) fluid after bleomycin instillation in WT and PI3Kγ KO mice. analysis. Animals were given a single intratracheal challenge of bleomycin (0.125U) or PBS, and leukocyte influx into the airway space (A-E) was quantified using citospin preparations (A-C) or FACS analysis (D and E). The following cell types were evaluated: total number of leukocytes (A), neutrophils (B), macrophages (C), CD3+CD4+ lymphocytes (D), CD3+CD8+ lymphocytes (E) and. BAL levels of CXCL1 (F), CXCL9 (G) and CCL2 (H) were quantified by ELISA and BAL protein (I) were quantified by Bradford assay. Results are representative of two experiments and are shown as the mean ± SEM of seven to eight animals in each group. *, ** and *** for $P < 0.05$, 0.01 and 0.001, respectively, when comparing to WT-given bleomycin-challenged mice and instilled-PI3Kγ KO mice, as indicated.

For Review Only

Figure-4: Inflammatory changes in lung parenchyma after bleomycin instillation in WT and PI3Kγ KO mice. Animals were given a single intratracheal challenge of bleomycin (0.125U) or PBS, and neutrophil and macrophage accumulation into lung parenchyma quantified by mieloperoxidase activity (A) and N-acetyglucosaminidase activity (B), respectively. InC-F, representative Hematoxilin & Eosin stained lung photomicrography 8 days after bleomycin instillation. Bars represent 50μm. PBS-instilled WT mice (C) and PI3Kγ KO mice (D) presented normal lung architecture. Histopathology shows increased lung damage with alveolar disorganization and interstitial edema in response to bleomycin in WT mice (E), whereas there was a reduced injury and alveolar edema in PI3Kγ KO mice (F). Results are representative of two experiments and are shown as the mean ± SEM of seven to eight animals in each group. *, ** and *** for $P < 0.05$, 0.01 and 0.001, respectively, when comparing to WT-given bleomycin-challenged mice and instilled-PI3Kγ KO mice, as indicated.

Figure-5: Expression of phosphorylated AKT and IκB-α and number of apoptotic events after bleomycin instillation in WT and PI3Kγ KO mice. Lung levels of P-AKT and P-IκB-α in WT and PI3Kγ KO mice after bleomycin induced lung injury by Western Blot (A). Samples were collected 8 days post-bleomycin instillation and processed for protein extraction for Western blot analysis. Lung extracts (40 mg) were fractioned on 10% SDS-PAGE, transferred onto nitrocellulose membrane, and then probed with anti-Phospho-AKT$^{Ser\ 473}$ (**top row**), anti-Phospho-IκB-α (**middle row**) or anti-β-actin (**bottom row**) antibodies, for loading control. Densitometric analysis (B) by using LabImage software and results are presented as a fold increased over PBS-instilled mice. Apoptosis by TUNEL assay (C-G). Quantification of apoptosis was determined by calculating the average percentage of TUNEL-positive nuclei relative to total nuclei of pulmonary cells on inflammatory locus (C). Representative photomicrography of stained lungs 8 days post-bleomycin instillation: WT (D) and PI3Kγ KO mice (E) PBS-instilled. Bleomycin induced apoptosis was found in WT mice (F) and it was enhanced in PI3Kγ KO mice (G). Note that TUNEL-positive cells are brown stained; bars represent 100μm. Results are representative of two experiments and are shown as the mean ± SEM of seven to eight animals in each group. *, ** and *** for $P < 0.05$, 0.01 and 0.001, respectively, when comparing to WT-given bleomycin-challenged mice and instilled-PI3Kγ KO mice, as indicated.

Figure-6: Production of reactive oxygen species by lung-derived leukocytes after bleomycin instillation in WT and PI3Kγ KO mice. Time course of luminol-enhanced chemiluminescence in leukocytes obtained from lungs of WT and PI3Kγ KO mice undergoing bleomycin induced injury. Leukocytes (3×10^5cells/well), pooled from lungs of seven mice after 8 days of bleomycin exposure were left unstimulated (basal) or were stimulated with zymosan (20 particles/cell). The relative luminescence units (RLUs) were assayed in triplicate and results are representative of two different experiments. Results are representative of two experiments and are shown as the mean ± SEM of seven to eight animals in each group. *, ** and *** for $P < 0.05$, 0.01 and 0.001, respectively, when comparing to WT-given bleomycin-challenged mice and instilled-PI3Kγ KO mice, as indicated.

For Review Only

Figure-7: Effects of a PI3Kγ inhibitor, AS605240, on the function of human umbilical vein endothelial cells in vitro. Proliferation of human umbilical vein endothelial cells (HUVEC) induced by CXCL8 (10 ng/ml) (A) in the absence or presence of AS605240 (0.1, 1, and 10 mM) was measured by 3H-thymidine incorporation after 24 hours. (B) HUVEC migration induced by CXCL8 (10 ng/ml) in the absence or presence of AS605240 (0.1 mM) was assessed using a scratch assay. Results are expressed as % closure in relation to t= 0, under an optical microscope with x10 objective. Results are representative of two experiments and are shown as mean ± SEM of five wells in each group. *, ** and *** for $P < 0.05$, 0.01 and 0.001, respectively. In C-F, effects of the treatment with AS605240 on HUVEC capillary-like organization induced by CXCL8 (10 ng/ml). HUVEC were plated on a Matrigel-coated 24-well plate with (C) medium alone, (D) medium containing DMSO, (E) IL-8 alone, or (F) IL-8 plus AS605240 (1 mM). After 24 hours of incubation, plates were examined for capillary-like organization under optical microscope (bars =1 mm). Each assay was done in duplicate.

Figure-8: Effects of a PI3Kγ inhibitor, AS605240, on the production of soluble collagen by chemokine-stimulated fibroblasts. Lung-derived fibroblasts (1 x 10^6/well) were cultured from lung explants of bleomycin instilled mice and were stimulated for 24 hour with 10 ng/mL of CXCL1 or CCL2 in presence or absence of AS605240 (1 μM). The supernatants were collected and the total soluble collagen quantified using the Sircol collagen-dye binding assay kit. Results are representative of two experiments and are shown as the mean ± SEM of 5-6 wells in each group. *, ** and *** for $P < 0.05$, 0.01 and 0.001, respectively.

For Review Only

Tables:

Table – 1. Primers used for Quantitative Real-Time-PCR.

Gene target	Name	Primer	Sequence	Probe
Collagen-1α1	Col1α1	5'-ATGTTCAGCTTTGTGGACCTC-3' 5'-GCAGCTGACTTCAGGGATGT-3'	*Forward* *Reverse*	15
Collagen-1α2	Col1α2	5'-GCAGGTTCACCTACTCTGTCCT-3' 5'-CTTGCCCCATTCATTTGTCT-3'	*Forward* *Reverse*	46
Fibronectin	FN	5'-CGGAGAGAGTGCCCCTACTA-3' 5'-CGATATTGGTGAATCGCAGA-3'	*Forward* *Reverse*	52
α-Smooth muscle actin	α-SMA	5'-TGGAGCAGGACTTGGAGGT-3' 5'-CCTCCAGCACCATACTTAGCA-3'	*Forward* *Reverse*	70
Von Willebrand Factor	vWF	5'-CAGGGGGCTGCAGTTATC-3' 5'-CTCATTCTCTTGCCATCTTGG-3'	*Forward* *Reverse*	20
18S	18S	5'-CTCAACACGGGAAACCTCAC-3' 5'-CGCTCCACCAACTAAGAACG-3'	*Forward* *Reverse*	77

For Review Only

Figure – 1

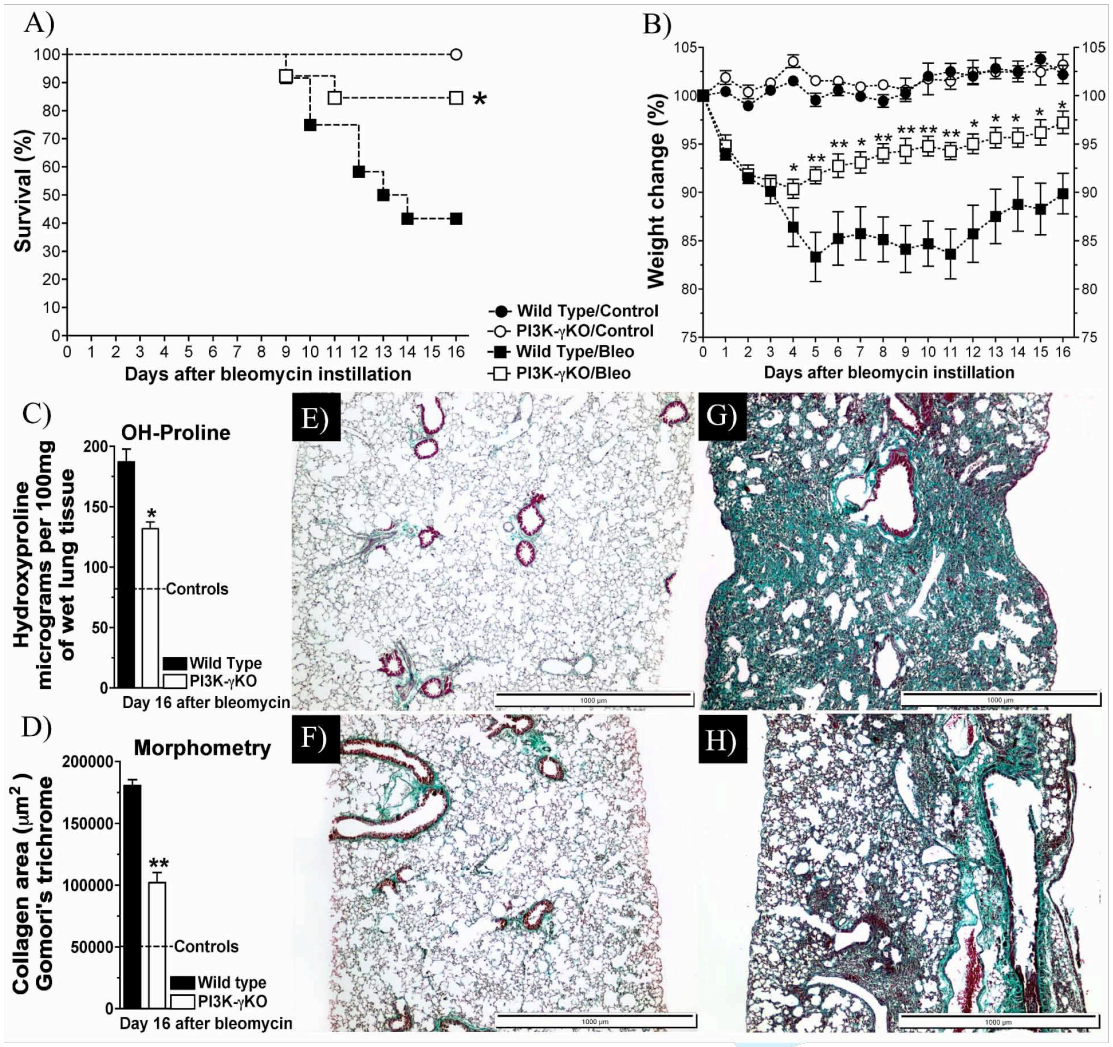

A)
Survival (%)
Days after bleomycin instillation
Wild Type/Control
PI3K-γKO/Control
Wild Type/Bleo
PI3K-γKO/Bleo
B)
Weight change (%)
Days after bleomycin instillation
C)
OH-Proline
Hydroxyproline micrograms per 100mg of wet lung tissue
Controls
Wild Type
PI3K-γKO
Day 16 after bleomycin
D)
Morphometry
Collagen area (μm²) Gomori's trichrome
Controls
Wild type
PI3K-γKO
Day 16 after bleomycin
E)
F)
G)
H)

Figure – 2

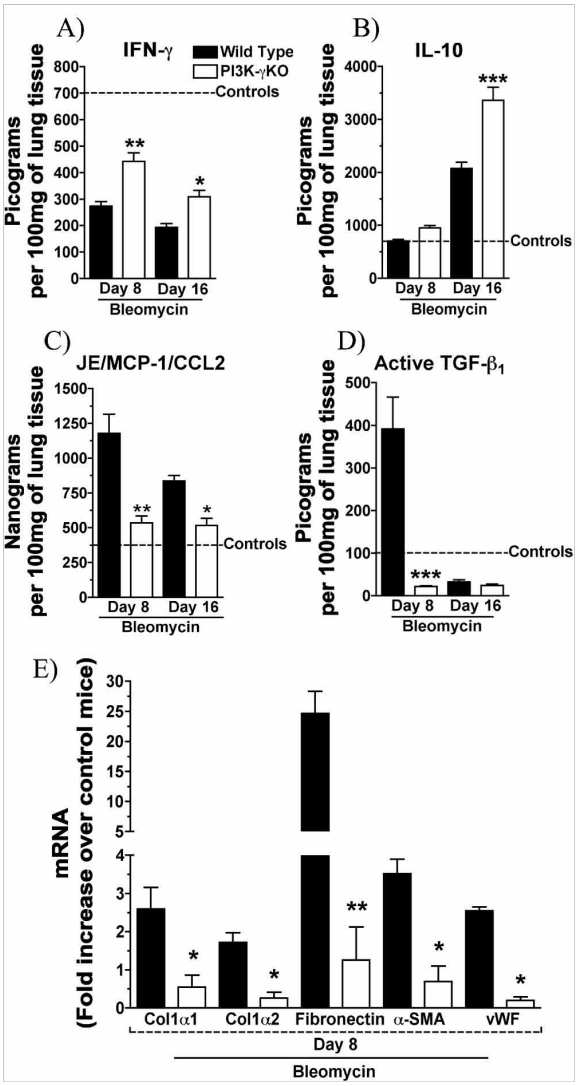
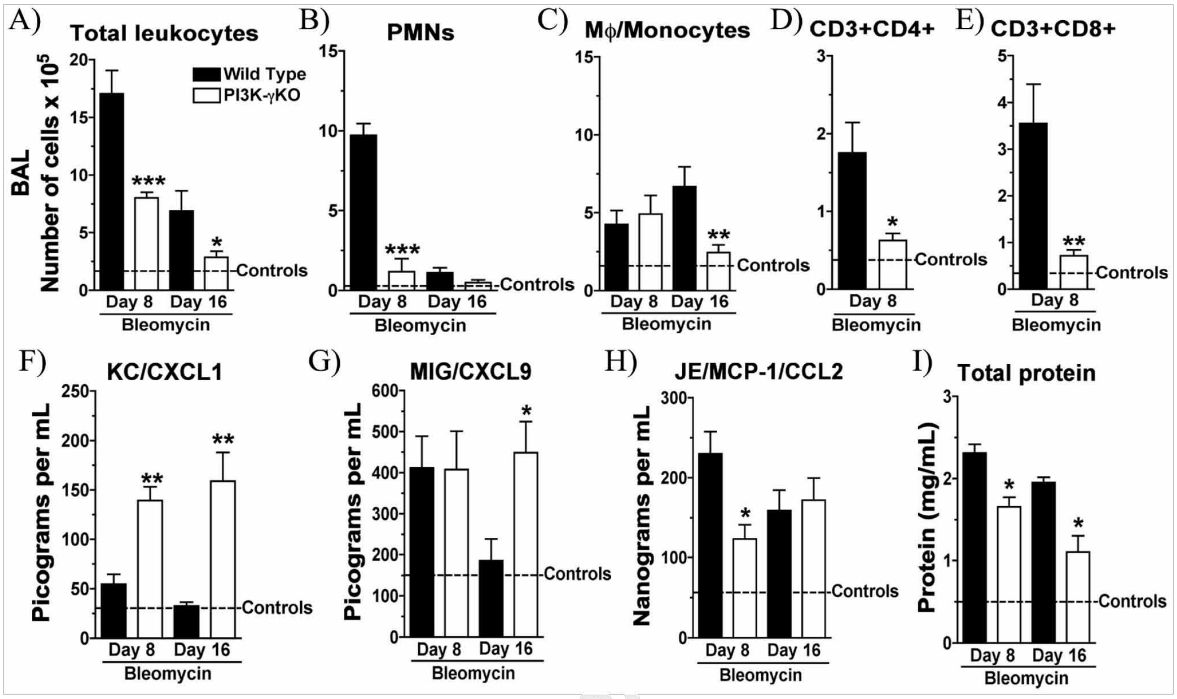

A)
IFN-γ
Wild Type
PI3K-γKO
Controls
Picograms per 100mg of lung tissue
Day 8
Day 16
Bleomycin
B)
IL-10
Picograms per 100mg of lung tissue
Controls
C)
JE/MCP-1/CCL2
Nanograms per 100mg of lung tissue
D)
Active TGF-β1
E)
mRNA (Fold increase over control mice)
Col1α1
Col1α2
Fibronectin
α-SMA
vWF

Figure – 3



For Review Only

Figure – 4

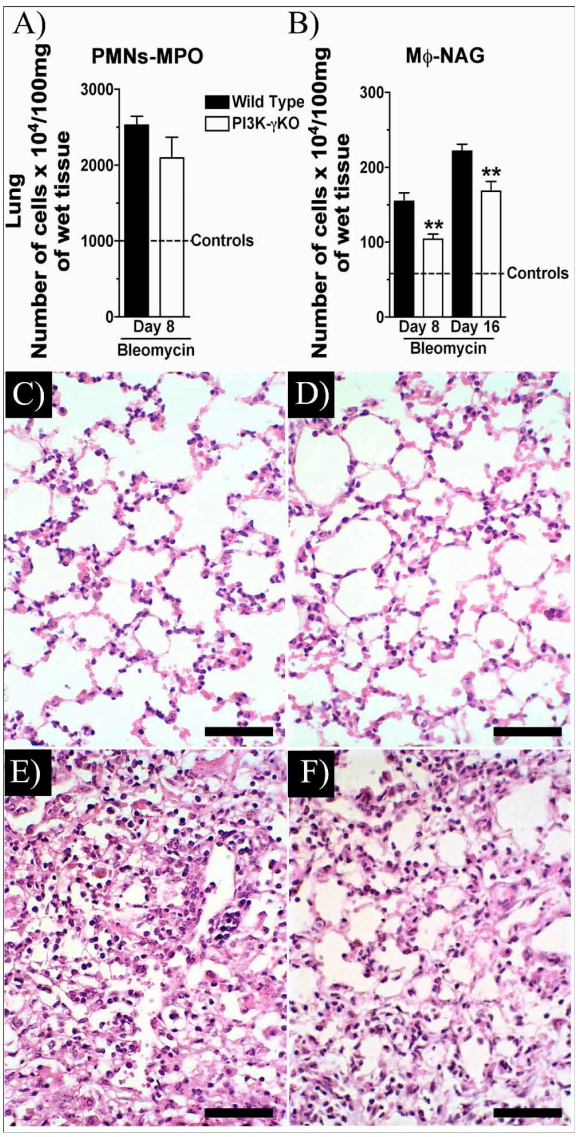

A)
PMNs-MPO
Lung
Number of cells x 10^4/100mg of wet tissue
3000
2000
1000
0
Wild Type
PI3K-γKO
Controls
Day 8
Bleomycin
B)
Mϕ-NAG
Number of cells x 10^4/100mg of wet tissue
300
200
100
0
**
**
Controls
Day 8
Day 16
Bleomycin
C)
D)
E)
F)

Figure – 5

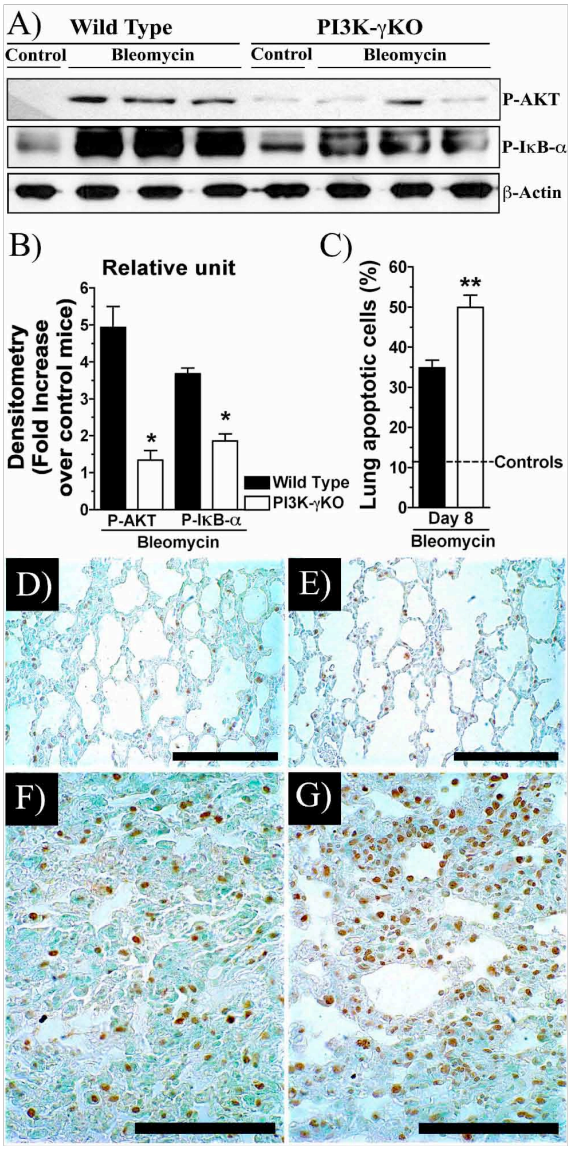
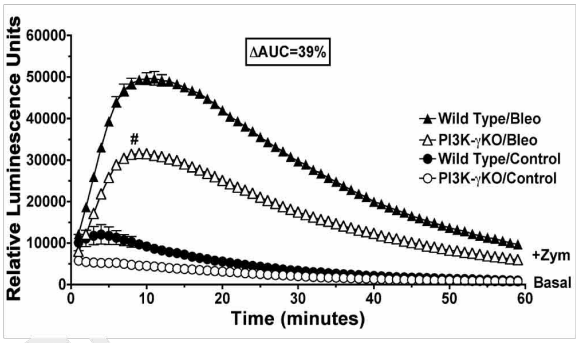

A)
Wild Type
PI3K-γKO
Control
Bleomycin
Control
Bleomycin
P-AKT
P-IκB-α
β-Actin
B)
Relative unit
Densitometry (Fold Increase over control mice)
Wild Type
PI3K-γKO
P-AKT
P-IκB-α
Bleomycin
C)
Lung apoptotic cells (%)
Controls
Day 8
Bleomycin
D)
E)
F)
G)

Figure – 6



For Review Only

Figure – 7

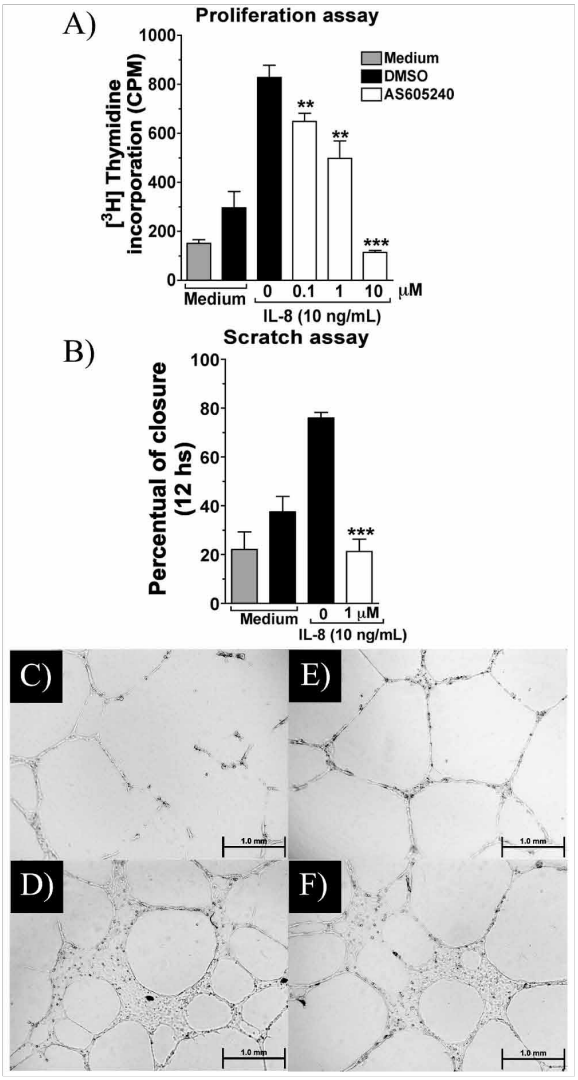
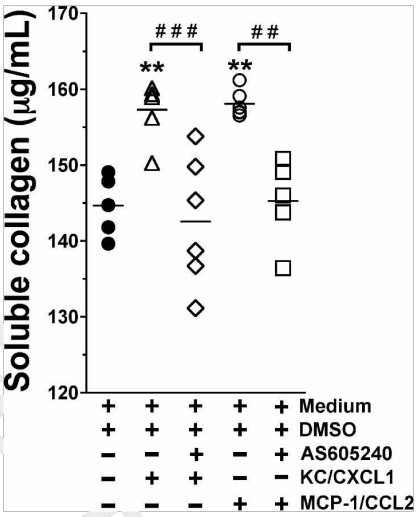

A)
Proliferation assay
[3H] Thymidine incorporation (CPM)
1000
800
600
400
200
0
Medium
DMSO
AS605240
**
**
***
Medium
0
0.1
1
10
μM
IL-8 (10 ng/mL)
B)
Scratch assay
Percentual of closure (12 hs)
100
80
60
40
20
0
***
Medium
0
1 μM
IL-8 (10 ng/mL)
C)
E)
D)
F)
1.0 mm

Figure – 8



For Review Only

Supplementary Material and Methods:

Drugs and reagents.

Recombinant human CXCL8, recombinant mouse CXCL1 and CCL2 (R&D Systems, Minneapolis, MN); endothelial cell basal medium-2 (EBM-2; Cambrex BioScience, Walkersville, MD); Growth factor-reduced Matrigel matrix (BD Bioscience, Bedford, MA); AS605240 (Echelon Biosciences Inc, Salt Lake City, UT); Bradford assay reagent from Bio-Rad (Bio-Rad, USA); Collagenase IV (Sigma); Monoclonal antibodies CD3, CD4, CD8, Ly6G (BD Pharmigen TM) and CXCR2 (R&D Systems);

Quantification of neutrophil and macrophage accumulation into the lung tissue by myeloperoxidase (MPO) and N-acetylglucosaminidase (NAG) activity measurement.

The extent of neutrophil accumulation in lung tissue was measured by assaying myeloperoxidase activity, as previously described (1). Briefly, lung tissue was homogeneized using 0.5% hexadecyl-trimethylammonium bromide and MPO activity, an index of tissue neutrophil influx, assayed using 3,3'-5,5'-tetramethylbenzidine. Neutrophil number in each sample was calculated from a standard curve of neutrophils obtained from the peritoneal cavity of 5% casein-treated animals and processed in the same way. The results were expressed as relative number of neutrophils per 100 mg of wet tissue.

Macrophage accumulation in tissues was inferred, as previously described (2), by assaying N-acetylglucosaminidase activity in homogenized lung samples. One hundred milligrams of lung tissue were homogenized in 2 mL of saline solution (0.9%) containing 0.1% v/v Triton X-100, and centrifuged at 4°C for 10 minutes at 1,500g. The supernatants were used for NAG assay. The reaction was started at 37°C for 10 min in 96 wells microplate by addition of 100 µL of *p*-nitrophenyl-N-acetyl-β-D-glucosaminide (Sigma) in citrate/phosphate buffer (0.1 M citric acid, 0.1 M Na_2HPO_4; pH 4.5) in final concentration of

For Review Only

2.24 mM, to 100 μL supernatant from tissue sample processed, diluted in citrate/phosphate buffer. The reaction was stopped by the addition of 100 μL 0.2 M glycine buffer (pH 10.6) and quantified at 405 nm in spectrophotometer (Emax – Molecular Devices). The macrophage content was calculated from a standard curve based on NAG activity expressed as absorbance increase at 405 nm from 3% thioglycollate peritoneal-induced macrophages assayed in parallel. The results were expressed in relative number of macrophages per 100 mg of wet tissue. MPO and NAG assays performed under these conditions are specific for neutrophils and macrophages, respectively.

FACS of BAL.

Leukocytes recovered from BALF were stained with fluorescent-labeled monoclonal antibodies CD3, CD4, CD8, Ly6G (BD Pharmigen TM) and CXCR2 (R&D Systems). Stained cells were acquired in FACScan cytometer and analyzed in FlowJo (Tree Star) software.

We performed BAL in WT and PI3Kγ KO mice groups as a previously described (1) using 2 mL of incomplete RPMI 1640 (Cultilab), 3x each mL. BALF cells were subjected to hypotonic lyses of residual erythrocytes. We used $5x10^5$ lung cells in staining. Before antibodies staining, cells suspensions were incubated with Fc Block antibodies. Cells were fixed after staining with 4% paraformaldehyde and 100 thousands events were acquired in BALF samples. Isotypes controls to PE and FITC staining were conducted prior to sample acquisition. Analysis in FlowJo software took into account size and granularity of populations. The populations to a specific marker were determined in histograms of the constitutive marker. Frequency in percentage of analyzed population in front of total acquired events was used in construction of graphs. The number of cells collected by BAL was adjusted with the total cell counts.

For Review Only

Detection of apoptotic cells.

Paraffin embedded tissue sections (4 mm) were examined by the terminal deoxynucleotidyl transferase-mediated deoxyuridine nick end-labeling (TUNEL) assay performed according to the manufacturer's instructions (TdT-FragEL™ DNA Fragmentation Kit, Calbiochem). The 3'-OH ends of fragmented nucleosomal DNA of apoptotic cells were specifically labeled using exogenous terminal deoxynucleotidyl transferase (TdT) and biotin-labeled dNTP, then detected using a streptavidin-horseradish peroxidase (HRP) conjugate and Diaminobenzidine (DAB). Nuclei were counterstained with Methyl Green. There were three animals per group and each animal had three serial brain sections analysed by two blind and independent investigators. Digital images were collected using an Olympus digital camera. Apoptosis was evaluated by calculating the percentage of TUNEL-positive nuclei relative to total nuclei of cells infiltrating in the meninges and in the perivascular space (at 600x magnification). Data are expressed as apoptosis index, which means the average percentage of apoptotic nuclei.

Western Blot Analysis.

Whole cell extracts were obtained from homogenized lungs by using a lysis buffer (1% Triton X-100, 100 mM Tris/HCl, pH 8.0, 10% glycerol, 5 mM EDTA, 200 mM NaCl, 1 mM DTT, 1 mM PMSF, 25mM NaF, 2.5 mg/ml leupeptin, 5 mg/ml aprotinin, and 1 mM sodium orthovanadate). Lysates were centrifuged at 13,000g for 10 min at 4^{o}C and quantified using the Bradford assay reagent from Bio-Rad (Hercules, CA). Extracts (40mg) were separated by electrophoresis on a denaturing 10% polyacrylamide-SDS gel and transferred onto nitrocellulose membranes, as previously described (4). Membranes were blocked overnight at 4°C with PBS containing 5% (w/v) nonfat dry milk and 0.1% Tween-20, washed three times with PBS containing 0.1% Tween-20, and then incubated with specific antibodies

For Review Only

(1:1000) (rabbit anti-Phospho-Akt$^{Ser\ 473}$ or mouse anti-phospho-IkB-α) - both from Cell Signaling Technology- Beverly MA, USA), in phosphate-buffered saline containing 5% (w/v) BSA and 0.1% Tween-20. After washing, membranes were incubated with appropriated horseradish peroxidase-conjugated secondary antibody (1:3000). Immunoreactive bands were visualized by using an enhanced chemiluminescence detection system, as described by the manufacturer (GE Healthcare, Piscataway, NJ). The levels of P-Akt and P-IkB-a were quantified by using densitometric analysis software (LabImage, leipzig, Germany), and the levels were normalized to the levels of b-actin in the same sample. Changes in protein levels with respect to controls values were estimated and the results were expressed as P-Akt and P-IkB-α to-β-actin ratio measured in arbitrary units.

Quantitative RT-PCR analysis.

For RT-PCR, total RNA obtained using Trizol (Invitrogen) was treated with DNAse1 and reverse transcribed using the cDNA Achieve kit (Applied Biosystems). Real-time PCR was performed in triplicate using 100 ng cDNA on the DNA Engine Opticon 2 System (MJ Research) using the FastStart Taqman Probe Master Mix (Roche Molecular Biochemicals), 100 nM Universal Probe Library probes (Roche Molecular Biochemicals) and 300 nM primers designed using the ProbeFinder 2.20 software (Roche Molecular Biochemicals). The primers and probes used are shown in Table 1. The samples were amplified by means of one cycle at 95°C for 10 min and 39 cycles at 95°C for 15 sec and 60°C for 1 min. Results were normalized on the 18S housekeeping gene, and expressed as transcript fold change over control mice.

In vitro experiments.

Cell culture.

For Review Only

Primary endothelial cells were obtained from human umbilical veins (HUVEC) as described previously (1). HUVEC was seeded on 0.2% wt/vol gelatin-coated 25-cm^2 tissue culture flasks and cultured in endothelial cell basal medium-2 (EBM-2) containing 20% fetal calf serum (FCS), 50 mg/mL endothelial cell growth supplement (ECGS) (Collaborative Research, Inc, Bedford, MA), and 100 mg/mL heparin (Sigma) until they reached confluence. Cells were passaged up to 2 times before use and then placed in suspension by trypsinization.

Cell proliferation assay.

The proliferation assay was performed as described previously (1). Briefly, 96-well culture plates were with 0.2% wt/vol gelatin. Approximately 5 X 10^3 HUVECs were plated in EBM-2 supplemented with 20% FCS, 50 µg/mL ECGS and 100 µg/mL heparin in gelatin-precoated 96-well, and allowed to adhere for 6 hours. The medium was then removed and the cells were washed twice with serum-free medium. Serum-free EBM-2 containing 1% Nutridoma (Roche diagnostics GmbH, Mannheim, Germany), ECGS, heparin and 0.037MBq/mL (1µCi/mL) methyl 3(3H)-thymidine (GE Healthcare GmbH, Milan, Italy) in the presence or absence of human recombinant IL-8 (10 ng/mL) and/or AS605240 (as described bellow) was then added to the wells and left incubating for 24 h at 37°C in the presence of 5% CO_2. After incubation time, non-adherent cells were removed by washing twice with ice-cold PBS. Then, 50 µL 10% ice-cold trichloroacetic acid (TCA) was added to each well and the precipitates were collected on a filter using a filtration manifold. Filters were extensively washed with distilled water and then suspended in scintillation fluid. Counts per minute (CPM) were quantified using a scintillator counter. For the inhibition approach, AS605240 was diluted in EBM-2 medium containing 0.01% of DMSO (Dimethyl sulfoxide, Sigma) to three different final concentrations, 0.1, 1 and 10 µM. The cells were pretreated for 1 h with either vehicle (EBM-2+DMSO) or AS605240 prior to the addition of human IL-8.

For Review Only

Scratch assays

For the scratch assay (1), 5 X 10^5 HUVECs were plated in gelatin-precoated 24-wells culture plate and incubated in EBM-2 medium supplemented with 20% FCS, 50 µg/mL ECGS, and 100 µg/mL heparin for 24 hours at 37°C in presence of CO_2 5%. The confluent cells were starved for 1 h in EBM-2 medium with 5% FCS before starting the experiments. Confluent cell monolayer was then scraped with a yellow pipette tip to generate scratch wounds and rinsed twice with serum-free EBM-2 to remove debris. EBM-2 medium with 5% FCS was added to the cells which had been pretreated for 1 h with vehicle (0.01% DMSO in EBM-2) or AS605240 (1 µM) prior to the addition of human IL-8 (10 ng/mL). The cells were then incubated at 37°C in presence of 5% CO_2. Scratchs were photographed immediately and 12 h after the scraping. Images were obtained using a Nikon digital camera coupled to a 10x objective on a Zeiss Axiovert microscope (Zeiss, Thornwood, NY) and the wound area was measured using the software NIH ImageJ.

HUVEC capillary-like structure formation assay

An in vitro capillary-like structure formation assay was performed as described earlier (1). Briefly, forty-eight-well culture plate (Nunc, Nalge Europe; Neerijse, Belgium) were coated with 150 µL of Growth factor-reduced Matrigel matrix was then allowed to solidify at 37°C for 30 minutes. HUVECs, 5 X 10^4 per well, were suspended in EBM-2 medium supplemented with 20% FCS, 50 µg/mL ECGS and 100 µg/mL heparin and seeded on the Matrigel-coated plates. The cells had been pretreated for 1 h with either vehicle (0.01% DMSO in EBM-2) or AS605240 (1 µM) prior to the addition of human IL-8 (10 ng/mL). The plates were incubated for 24 hours at 37°C in presence of 5% CO_2 and the wells were then photographed using a Nikon digital camera coupled to a 10x objective on a Zeiss Axiovert microscope (Zeiss,

For Review Only

Thornwood, NY) to determine qualitative influence of AS605240 on the ability of the HUVECs to form capillary-like structures.

Isolation and culture of primary lung fibroblasts from mice.

Isolation of mouse lung primary fibroblasts was performed as a previous described (5). Briefly, whole lungs of C57Bl/6j (WT) were removed sterilely and cut into small 2- to 3-mm slices and allowed to adhere on tissue culture plastic. These lung tissue explants were maintained in medium consisting of Dulbecco's modified Eagle's medium (GIBCO, Grand Island, NY) supplemented with 10% fetal bovine serum (FBS; Sigma), 100 U/ml penicillin/streptomycin (Sigma), and Fungizone (GIBCO). Fibroblasts grown from explant tissues were isolated by trypsinization and passaging (typically 7–10 days after initial explant). Cell supernatants were obtained for collagen quantification at passage 2 and at a confluence of 90 to 100%. Fibroblasts, 1 X 10^6, were plated in 48-wells culture plate and incubated in DMEM supplemented with 10% FCS, 100 U/ml penicillin/streptomycin, and Fungizone for stabilization during 24 hours at 37°C in presence of CO_2 5%. AS605240 was diluted in DMEM containing 0.01% of DMSO (Dimethyl sulfoxide, Sigma) to the final concentration of 1 µM. The cells were pretreated for 1 h with either vehicle (DMEM+DMSO) or AS605240 prior to the addition of mouse recombinant CXCL1 or CCL2 (10 ng/mL). The total amount of soluble collagen production was quantified by Sircol assay, using fibroblasts supernatant culture 24 hours after chemokine or chemokine plus AS605240 administration.

Sircol assay for collagen quantification

In vitro total soluble collagen content was quantified by Sircol collagen-dye binding assay kit (Biocolor Dye Science, N. Ireland). Briefly, Sirius red dye reagent (900 µl) and supernatants (100 µl) were mixed for 30 min (at r.t.) and centrifuged at 13,000 g for 10 min. Pellets (bead-dye-collagen complex) were then dissolved in 1 ml alkali reagent (0.5 M NaOH), and the

For Review Only

amount of collagen was quantified using a standard curve for collagen standard provided by the manufacturer.

References:

1. Russo RC, Guabiraba R, Garcia CC, Barcelos LS, Roffe E, Souza AL, Amaral FA, Cisalpino D, Cassali GD, Doni A, et al. Role of the chemokine receptor cxcr2 in bleomycin-induced pulmonary inflammation and fibrosis. *Am J Respir Cell Mol Biol* 2009;40:410-421.

2. Barcelos LS, Talvani A, Teixeira AS, Vieira LQ, Cassali GD, Andrade SP, Teixeira MM. Impaired inflammatory angiogenesis, but not leukocyte influx, in mice lacking tnfr1. *J Leukoc Biol* 2005;78:352-358.

3. Amaral FA, Fagundes CT, Guabiraba R, Vieira AT, Souza AL, Russo RC, Soares MP, Teixeira MM, Souza DG. The role of macrophage migration inhibitory factor in the cascade of events leading to reperfusion-induced inflammatory injury and lethality. *Am J Pathol* 2007;171:1887-1893.

4. Souza DG, Fagundes CT, Amaral FA, Cisalpino D, Sousa LP, Vieira AT, Pinho V, Nicoli JR, Vieira LQ, Fierro IM, et al. The required role of endogenously produced lipoxin a4 and annexin-1 for the production of il-10 and inflammatory hyporesponsiveness in mice. *J Immunol* 2007;179:8533-8543.

5. Vittal R, Zhang H, Han MK, Moore BB, Horowitz JC, Thannickal VJ. Effects of the protein kinase inhibitor, imatinib mesylate, on epithelial/mesenchymal phenotypes: Implications for treatment of fibrotic diseases. *J Pharmacol Exp Ther* 2007;321:35-44.

For Review Only

4. DISCUSSÃO E CONCLUSÕES GLOBAIS

Dada a grande morbidade e mortalidade associadas à fibrose pulmonar idiopática (IPF), além da ausência de terapias efetivas no seu tratamento, uma ampla rede de ensaios clínicos e farmacológicos, associados ao crescente desenvolvimentos de anti-inflamatórios e anti-fibróticos, está em atividade. Porém, infelizmente os fármacos já desenvolvidos se mostram pouco eficazes no tratamento da IPF. Atualmente são utilizados tratamentos baseados na administração crônica de corticosteróides, com ou sem a adição de agentes imunossupressores, tais como azatioprina, ciclofosfamida, ciclosporina e metrotexato, mas o aparecimento de efeitos adversos durante o período de tratamento limitam a sua terapêutica (141, 142). Novas técnicas têm sido desenvolvidas e os testes clínicos correntes têm se baseado no uso de antagonistas dos receptores de endotelina-1 (Bosentan), CTGF (FG-3019), e PDGF (Imatinib mesilato), anticorpos anti-TNF-α (Etanercept) e administração de IFN-γ recombinante, sendo estes estudos ainda inconclusivos (79, 142, 143).

Embora descritas originalmente com funções associadas ao sistema imune (21), sendo principalmente responsáveis pelo recrutamento de leucócitos, quimiocinas têm sido associadas a funções tais como as regulações dos processos de angiogênese e fibrose pulmonar (59). Os trabalhos aqui reunidos corroboram a literatura e apresentam novos mecanismos relacionados com a modulação farmacológica do sistema quimiocinas durante o desenvolvimento da fibrose pulmonar experimental.

Após a instilação intra-traqueal de bleomicina em camundongos, observamos uma correlação direta entre o desenvolvimento da fibrose pulmonar e o aumento precoce dos níveis das quimiocinas CXCL1, CXCL2, CCL2, CCL3 e CCL5 concomitante com o influxo de neutrófilos, macrófagos e linfócitos para o pulmão e produção de citocinas pró-fibrogênicas, tais como IL-13 e TGF-β_1. Estas observações nos levaram à hipótese de que a modulação negativa da atividade inflamatória das quimiocinas, neste modelo, poderia proteger os animais contra a fibrose pulmonar.

O influxo acentuado de neutrófilos é característico deste modelo, ocorrendo durante a primeira semana após a administração de bleomicina, nos levando a perguntar se a inibição dos receptores CXCR1/2, o receptor quimiotático preferencial de neutrófilos, poderia atenuar a inflamação e conseqüentemente a fibrose. Nossos resultados mostraram que o antagonista de receptores CXCR1/2 causava redução no influxo neutrofílico, apresentando menor dano pulmonar e menor deposição de colágeno no parênquima pulmonar associados a baixos níveis de IL-13 e TGF-β_1. Esta redução do colágeno pulmonar esteve associada aos efeitos angiostáticos da administração do DF2162, causados pelo aumento nos níveis das quimiocinas agonistas CXCR3 (CXCL9 e CXCL10) e pelo bloqueio do receptor CXCR1/2 em células endoteliais pulmonares, efeitos semelhantes aos já relatados na literatura causados pela administração de anticorpos recombinantes anti-CXCL2 (117). De fato, o mecanismo responsável por este efeito protetor durante o tratamento com DF2162 parece ser causada pelos efeitos inibitórios sobre a angiogênese, podendo até ser de natureza dual, por inibição da transmigração neutrofílica para as vias aéreas (Figura-7a).

Em um contexto geral, CXCR1/2 participa como um mediador crítico nos mais diversos tipo de respostas imunes pulmonares dependentes de infecção, inflamação e angiogênese. É responsável pelo controle da resposta neutrofílica contra bactérias, representando um mediador inato durante infecções patogênicas (134, 135). CXCR1/2 também exerce um importante papel na rejeição de transplantes e tumorogênese, regulando os processos angiogênicos necessários para o desenvolvimento destas patologias pulmonares (133, 136). A migração CXCR1/2 dependente de neutrófilos para o pulmão é uma característica de doenças inflamatórias responsáveis pelos danos causados à estrutura pulmonar, assim como ocorre na lesão pulmonar aguda (ALI), lesão pulmonar induzida pelo ventilador mecânico (VILI) e enfisema pulmonar (COPD) causado pela fumaça do cigarro (144-146). Aqui, nós demonstramos que a fibrose pulmonar induzida por bleomicina é dependente das funções de CXCR1/2 sobre a angiogênese e migração neutrofílica, e que a

intervenção farmacológica sobre este receptor acarretou proteção. Estes dados, juntos às evidências apresentadas na literatura, sugerem que o fármaco inibidor de receptores CXCR1/2, utilizado em nosso estudo, também poderia ser aplicado como terapia para outras doenças pulmonares como ALI, VILI, câncer, COPD e síndrome de bronquiolite obliterante (BOS).

É atribuído a CCL3 um papel importante no desenvolvimento da fibrose pulmonar, sendo responsável também de forma dual, pelo controle da inflamação pulmonar via recrutamento de leucócitos e da fibrogênese pela migração de fibrócitos, responsáveis pela produção de TGF-β_1 e colágeno (97). Da mesma maneira, nós demonstramos que a neutralização de CCL3 através da utilização da *CCL3-binding protein*, Evasina-1 ou deficiência na produção de CCL3, causa redução da fibrose pulmonar, associada a um menor infiltrado neutrofílico e macrofágico, e da produção de TNF-α e TGF-β_1 pulmonar. Assim, uma menor inflamação pulmonar causaria uma menor lesão e conseqüentemente menor remodelamento. Também acreditamos que mecanismos alheios a este apontado sobre a inflamação, tais como redução na migração de fibrócitos, podem estar relacionados à menor fibrose pulmonar apresentada pelos animais tratados com Evasina-1 (Figura-7b).

Sobre a complexidade do sistema quimiocinas aqui discutidas, a promiscuidade deste sistema poderia ser explorada pela determinação de fármacos com efeitos amplos, sobre elementos *downstream* de ativação dos receptores de quimiocina. Neste caso, uma inibição de elementos redundantes de sinalização gerados pela formação do complexo ligantes:receptores, como por exemplo a ativação da PI3Kγ, seria uma boa estratégia para burlar o problema da ativação promíscua de múltiplos receptores de quimiocinas (37). De fato, isso se aplica também aos demais GPCRs, como demonstrado anteriormente pelo nosso grupo (147) (Anexo-1). O recrutamento de neutrófilos *in vivo* dependente de CXCL1-CXCR2 é controlado pelas isoformas γ e δ da PI3K, mas a migração induzida por C5a ou fMLP

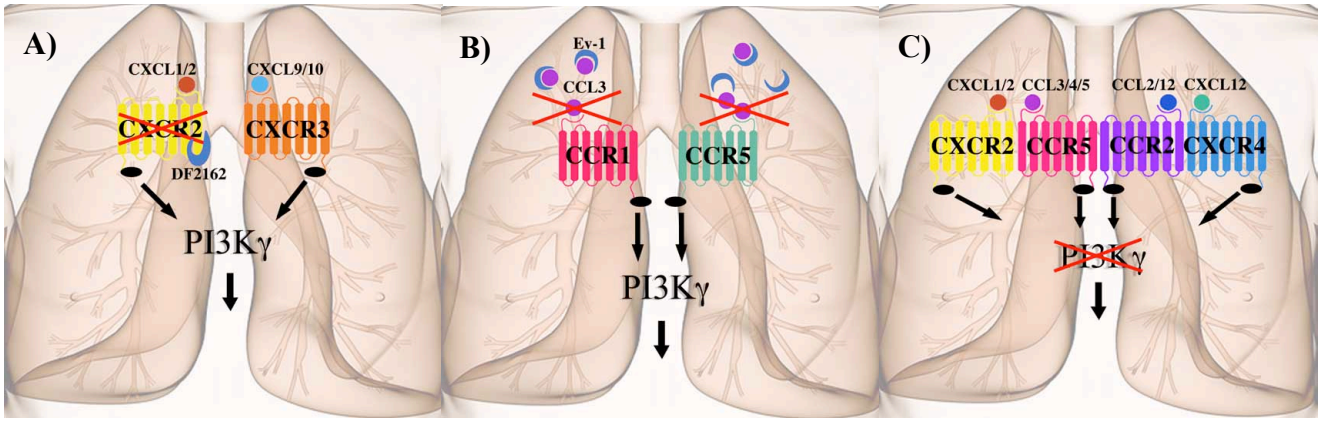
dependem apenas da isoforma γ, demonstrando uma redundância funcional da PI3Kγ durante o influxo de neutrófilos causado pela administração de agonistas de GPCRs nas vias aéreas. Estes resultados suportam que PI3Kγ é um importante alvo para desenvolvimento de novos anti-inflamatórios.

Partindo da premissa de que a inibição da PI3Kγ possui propriedades anti-inflamatórias, decidimos estudar o seu papel na fibrose pulmonar experimental. Animais deficientes em PI3Kγ foram protegidos das ações deletérias causada pela administração de bleomicina. A deficiência para PI3Kγ causou atenuação da fibrose e aumento na sobrevida dos animais, além de apresentarem redução no influxo pulmonar de neutrófilos, macrófagos, linfócitos e baixos níveis de TGF-β_1. Mecanisticamente, a ausência de PI3Kγ resultou em menor influxo celular nas vias aéreas e aumento da apoptose, causadas pela menor ativação da cascata PI3Kγ-AKT-NF-κB. De fato, efeitos similares foram encontrados nos tratamentos com DF2162 e Evasina-1, sugerindo um papel redundante da PI3Kγ no controle das atividades dos receptores de quimiocina. Na presença destas moléculas, a inibição da PI3Kγ também gerou modificações funcionais em células endoteliais e fibroblastos *in vitro*, sugerindo que PI3Kγ participa do processo de angiogênese e na secreção de colágeno por fibroblastos. Portanto, assim como as quimiocinas, a PI3Kγ exerce múltiplos papéis no desenvolvimento da fibrose pulmonar, coordenando a inflamação, angiogênese, resolução e fibrogênese (Figura-7c). Estes resultados reforçam a idéia de que estratégias bloqueadoras da atividade da PI3Kγ são benéficas para o desenvolvimento de patologias pulmonares, como por exemplo, a asma, COPD, ALI e VILI (148-151).

Foi apresentado, desta forma, um grupo de evidências acerca do papel das quimiocinas no desenvolvimento da fibrose pulmonar, sua complexa regulação e implicações nos fenômenos patofisiológicos, além de novas possibilidades terapêuticas. De forma geral, a intervenção farmacológica no sistema quimiocina teve efeitos positivos, ocasionando redução

da fibrose pulmonar, seja por proteínas neutralizantes de quimiocinas, bloqueadores de receptores ou ausência de sua sinalização intracelular. Também é importante ressaltar que os tratamentos tardios com DF2162 ou Evasina-1, mesmo quando administrados de forma terapêutica (do dia 8 em diante), preveniu o desenvolvimento da fibrose pulmonar. Em conjunto, estes dados não apenas demonstram uma passível modulação do sistema quimiocinas no contexto de patologias inflamatórias pulmonares, mas principalmente oferecem novos fármacos como candidatos para o tratamento da fibrose pulmonar. Futuros ensaios clínicos poderão validar seu uso terapêutico.

Figura-7: Mecanismo proposto. *Intervenção no sistema quimiocina como alvo para tratamento da fibrose pulmonar induzida por bleomicina. Três formas são apresentadas: A) O bloqueio de receptores CXCR2 por antagonista alostérico (DF2162) promove potencialização dos sinais angiostáticos (CXCR3), causam redução na angiogênese e menor influxo neutrofílico no BAL, atenuando a lesão e reparo pulmonar; B) A proteína ligadora de quimiocina (Evasin-1 – Ev-1) neutraliza a função de CCL3 sobre os receptores CCR5 e CCR1, causando menor inflamação e producao de citocinas , reduzindo a lesão e a cicatrização execessiva pulmonar; C) A ausência da PI3Kγ (deficiência genética) causa redução da fibrose pulmonar por controlar processos angiogênicos, influxo de leucócitos no BAL, apoptose e ativação de células no parênquima pulmonar, reduzindo a atividade de todos os receptores de quimiocinas envolvidos da fibrose pulmonar.*



↓ Angiogênese	↓ Leucócitos no BAL	↓ Angiogênese
↓ Neutrófilos no BAL	↓ Citocinas pró-inflamatórias	↓ Citocinas pró-inflamatórias
↓ Citocinas pró-fibrogênicas	↓ Citocinas pró-fibrogênicas	↓ Citocinas pró-fibrogênicas
	↓ Influxo de fibrócitos??	↓ Influxo de fibrócitos??
		↓ Deposição de colágeno
		↑ Apoptose
		↓ Ativação leucocitária
FIBROSE PULMONAR	**FIBROSE PULMONAR**	**FIBROSE PULMONAR**

5. REFERÊNCIAS BIBLIOGRÁFICAS

1. Katzenstein AL, Myers JL. Idiopathic pulmonary fibrosis: Clinical relevance of pathologic classification. *Am J Respir Crit Care Med* 1998;157:1301-1315.
2. Nathan C. Points of control in inflammation. *Nature* 2002;420:846-852.
3. Cara DC, Negrao-Correa D, Teixeira MM. Mechanisms underlying eosinophil trafficking and their relevance in vivo. *Histol Histopathol* 2000;15:899-920.
4. Butcher EC. Leukocyte-endothelial cell recognition: Three (or more) steps to specificity and diversity. *Cell* 1991;67:1033-1036.
5. Scapini P, Lapinet-Vera JA, Gasperini S, Calzetti F, Bazzoni F, Cassatella MA. The neutrophil as a cellular source of chemokines. *Immunol Rev* 2000;177:195-203.
6. Burns AR, Smith CW, Walker DC. Unique structural features that influence neutrophil emigration into the lung. *Physiol Rev* 2003;83:309-336.
7. Burg ND, Pillinger MH. The neutrophil: Function and regulation in innate and humoral immunity. *Clin Immunol* 2001;99:7-17.
8. Chertov O, Yang D, Howard OM, Oppenheim JJ. Leukocyte granule proteins mobilize innate host defenses and adaptive immune responses. *Immunol Rev* 2000;177:68-78.
9. D'Ambrosio D, Iellem A, Colantonio L, Clissi B, Pardi R, Sinigaglia F. Localization of th-cell subsets in inflammation: Differential thresholds for extravasation of th1 and th2 cells. *Immunol Today* 2000;21:183-186.
10. van Rooijen N, Sanders A. Elimination, blocking, and activation of macrophages: Three of a kind? *J Leukoc Biol* 1997;62:702-709.
11. Danese S, Dejana E, Fiocchi C. Immune regulation by microvascular endothelial cells: Directing innate and adaptive immunity, coagulation, and inflammation. *J Immunol* 2007;178:6017-6022.
12. Rosenkilde MM, Schwartz TW. The chemokine system -- a major regulator of angiogenesis in health and disease. *APMIS* 2004;112:481-495.
13. Gilroy DW, Lawrence T, Perretti M, Rossi AG. Inflammatory resolution: New opportunities for drug discovery. *Nat Rev Drug Discov* 2004;3:401-416.
14. Lingen MW. Role of leukocytes and endothelial cells in the development of angiogenesis in inflammation and wound healing. *Arch Pathol Lab Med* 2001;125:67-71.
15. Carroll MC. The role of complement and complement receptors in induction and regulation of immunity. *Annu Rev Immunol* 1998;16:545-568.
16. Margolius HS. Theodore cooper memorial lecture. Kallikreins and kinins. Some unanswered questions about system characteristics and roles in human disease. *Hypertension* 1995;26:221-229.
17. Martin T, Losa JE, Garcia-Salgado MJ, Perez-Arellano JL. The role of platelet-activating factor (paf) in interstitial pulmonary disease. *J Investig Allergol Clin Immunol* 1994;4:149-157.
18. Fialkow L, Wang Y, Downey GP. Reactive oxygen and nitrogen species as signaling molecules regulating neutrophil function. *Free Radic Biol Med* 2007;42:153-164.
19. Borish LC, Steinke JW. 2. Cytokines and chemokines. *J Allergy Clin Immunol* 2003;111:S460-475.
20. Steinke JW, Borish L. 3. Cytokines and chemokines. *J Allergy Clin Immunol* 2006;117:S441-445.
21. Murphy PM. The molecular biology of leukocyte chemoattractant receptors. *Annu Rev Immunol* 1994;12:593-633.
22. Wynn TA. Cellular and molecular mechanisms of fibrosis. *J Pathol* 2008;214:199-210.
23. Luster AD. Chemokines--chemotactic cytokines that mediate inflammation. *N Engl J Med* 1998;338:436-445.

24. Locati M, Otero K, Schioppa T, Signorelli P, Perrier P, Baviera S, Sozzani S, Mantovani A. The chemokine system: Tuning and shaping by regulation of receptor expression and coupling in polarized responses. *Allergy* 2002;57:972-982.
25. Mantovani A. The chemokine system: Redundancy for robust outputs. *Immunol Today* 1999;20:254-257.
26. Dorner BG, Dorner MB, Zhou X, Opitz C, Mora A, Guttler S, Hutloff A, Mages HW, Ranke K, Schaefer M, et al. Selective expression of the chemokine receptor xcr1 on cross-presenting dendritic cells determines cooperation with cd8(+) t cells. *Immunity* 2009.
27. Mantovani A, Bonecchi R, Locati M. Tuning inflammation and immunity by chemokine sequestration: Decoys and more. *Nat Rev Immunol* 2006;6:907-918.
28. Thelen M, Stein JV. How chemokines invite leukocytes to dance. *Nat Immunol* 2008;9:953-959.
29. Allen SJ, Crown SE, Handel TM. Chemokine: Receptor structure, interactions, and antagonism. *Annu Rev Immunol* 2007;25:787-820.
30. Johnson Z, Proudfoot AE, Handel TM. Interaction of chemokines and glycosaminoglycans: A new twist in the regulation of chemokine function with opportunities for therapeutic intervention. *Cytokine Growth Factor Rev* 2005;16:625-636.
31. Proudfoot AE, Handel TM, Johnson Z, Lau EK, LiWang P, Clark-Lewis I, Borlat F, Wells TN, Kosco-Vilbois MH. Glycosaminoglycan binding and oligomerization are essential for the in vivo activity of certain chemokines. *Proc Natl Acad Sci U S A* 2003;100:1885-1890.
32. Ludwig A, Weber C. Transmembrane chemokines: Versatile 'special agents' in vascular inflammation. *Thromb Haemost* 2007;97:694-703.
33. Ogilvie P, Bardi G, Clark-Lewis I, Baggiolini M, Uguccioni M. Eotaxin is a natural antagonist for ccr2 and an agonist for ccr5. *Blood* 2001;97:1920-1924.
34. Ogilvie P, Paoletti S, Clark-Lewis I, Uguccioni M. Eotaxin-3 is a natural antagonist for ccr2 and exerts a repulsive effect on human monocytes. *Blood* 2003;102:789-794.
35. Petkovic V, Moghini C, Paoletti S, Uguccioni M, Gerber B. I-tac/cxcl11 is a natural antagonist for ccr5. *J Leukoc Biol* 2004;76:701-708.
36. Petkovic V, Moghini C, Paoletti S, Uguccioni M, Gerber B. Eotaxin-3/ccl26 is a natural antagonist for cc chemokine receptors 1 and 5. A human chemokine with a regulatory role. *J Biol Chem* 2004;279:23357-23363.
37. Ruckle T, Schwarz MK, Rommel C. Pi3kgamma inhibition: Towards an 'aspirin of the 21st century'? *Nat Rev Drug Discov* 2006;5:903-918.
38. Cardona AE, Sasse ME, Liu L, Cardona SM, Mizutani M, Savarin C, Hu T, Ransohoff RM. Scavenging roles of chemokine receptors: Chemokine receptor deficiency is associated with increased levels of ligand in circulation and tissues. *Blood* 2008;112:256-263.
39. Mantovani A, Locati M. Housekeeping by chemokine scavenging. *Blood* 2008;112:215-216.
40. Neel NF, Schutyser E, Sai J, Fan GH, Richmond A. Chemokine receptor internalization and intracellular trafficking. *Cytokine Growth Factor Rev* 2005;16:637-658.
41. Marchese A. Ubiquitination of chemokine receptors. *Methods Enzymol* 2009;460:413-422.
42. Thelen M, Munoz LM, Rodriguez-Frade JM, Mellado M. Chemokine receptor oligomerization: Functional considerations. *Curr Opin Pharmacol* 2009.
43. Mantovani A, Locati M, Vecchi A, Sozzani S, Allavena P. Decoy receptors: A strategy to regulate inflammatory cytokines and chemokines. *Trends Immunol* 2001;22:328-336.

44. Locati M, Torre YM, Galliera E, Bonecchi R, Bodduluri H, Vago G, Vecchi A, Mantovani A. Silent chemoattractant receptors: D6 as a decoy and scavenger receptor for inflammatory cc chemokines. *Cytokine Growth Factor Rev* 2005;16:679-686.
45. Comerford I, Nibbs RJ. Post-translational control of chemokines: A role for decoy receptors? *Immunol Lett* 2005;96:163-174.
46. Pruenster M, Mudde L, Bombosi P, Dimitrova S, Zsak M, Middleton J, Richmond A, Graham GJ, Segerer S, Nibbs RJ, et al. The duffy antigen receptor for chemokines transports chemokines and supports their promigratory activity. *Nat Immunol* 2009;10:101-108.
47. Martinez de la Torre Y, Buracchi C, Borroni EM, Dupor J, Bonecchi R, Nebuloni M, Pasqualini F, Doni A, Lauri E, Agostinis C, et al. Protection against inflammation- and autoantibody-caused fetal loss by the chemokine decoy receptor d6. *Proc Natl Acad Sci U S A* 2007;104:2319-2324.
48. Whitehead GS, Wang T, DeGraff LM, Card JW, Lira SA, Graham GJ, Cook DN. The chemokine receptor d6 has opposing effects on allergic inflammation and airway reactivity. *Am J Respir Crit Care Med* 2007;175:243-249.
49. Jamieson T, Cook DN, Nibbs RJ, Rot A, Nixon C, McLean P, Alcami A, Lira SA, Wiekowski M, Graham GJ. The chemokine receptor d6 limits the inflammatory response in vivo. *Nat Immunol* 2005;6:403-411.
50. Di Liberto D, Locati M, Caccamo N, Vecchi A, Meraviglia S, Salerno A, Sireci G, Nebuloni M, Caceres N, Cardona PJ, et al. Role of the chemokine decoy receptor d6 in balancing inflammation, immune activation, and antimicrobial resistance in mycobacterium tuberculosis infection. *J Exp Med* 2008;205:2075-2084.
51. McKimmie CS, Fraser AR, Hansell C, Gutierrez L, Philipsen S, Connell L, Rot A, Kurowska-Stolarska M, Carreno P, Pruenster M, et al. Hemopoietic cell expression of the chemokine decoy receptor d6 is dynamic and regulated by gata1. *J Immunol* 2008;181:8171-8181.
52. Graham GJ. D6 and the atypical chemokine receptor family: Novel regulators of immune and inflammatory processes. *Eur J Immunol* 2009;39:342-351.
53. Fallon PG, Alcami A. Pathogen-derived immunomodulatory molecules: Future immunotherapeutics? *Trends Immunol* 2006;27:470-476.
54. Frauenschuh A, Power CA, Deruaz M, Ferreira BR, Silva JS, Teixeira MM, Dias JM, Martin T, Wells TN, Proudfoot AE. Molecular cloning and characterization of a highly selective chemokine-binding protein from the tick rhipicephalus sanguineus. *J Biol Chem* 2007;282:27250-27258.
55. Degryse B, de Virgilio M. The nuclear protein hmgb1, a new kind of chemokine? *FEBS Lett* 2003;553:11-17.
56. Yang D, Chertov O, Bykovskaia SN, Chen Q, Buffo MJ, Shogan J, Anderson M, Schroder JM, Wang JM, Howard OM, et al. Beta-defensins: Linking innate and adaptive immunity through dendritic and t cell ccr6. *Science* 1999;286:525-528.
57. Bernhagen J, Krohn R, Lue H, Gregory JL, Zernecke A, Koenen RR, Dewor M, Georgiev I, Schober A, Leng L, et al. Mif is a noncognate ligand of cxc chemokine receptors in inflammatory and atherogenic cell recruitment. *Nat Med* 2007;13:587-596.
58. Weathington NM, van Houwelingen AH, Noerager BD, Jackson PL, Kraneveld AD, Galin FS, Folkerts G, Nijkamp FP, Blalock JE. A novel peptide cxcr ligand derived from extracellular matrix degradation during airway inflammation. *Nat Med* 2006;12:317-323.
59. Wilson MS, Wynn TA. Pulmonary fibrosis: Pathogenesis, etiology and regulation. *Mucosal Immunol* 2009;2:103-121.

60. Shimabukuro DW, Sawa T, Gropper MA. Injury and repair in lung and airways. *Crit Care Med* 2003;31:S524-531.
61. Pardo A, Selman M. Matrix metalloproteases in aberrant fibrotic tissue remodeling. *Proc Am Thorac Soc* 2006;3:383-388.
62. Parks WC, Wilson CL, Lopez-Boado YS. Matrix metalloproteinases as modulators of inflammation and innate immunity. *Nat Rev Immunol* 2004;4:617-629.
63. Ward PA, Hunninghake GW. Lung inflammation and fibrosis. *Am J Respir Crit Care Med* 1998;157:S123-129.
64. Wynn TA. Fibrotic disease and the t(h)1/t(h)2 paradigm. *Nat Rev Immunol* 2004;4:583-594.
65. Mucida D, Salek-Ardakani S. Regulation of th17 cells in the mucosal surfaces. *J Allergy Clin Immunol* 2009;123:997-1003.
66. Aujla SJ, Kolls JK. Il-22: A critical mediator in mucosal host defense. *J Mol Med* 2009;87:451-454.
67. Traves SL, Donnelly LE. Th17 cells in airway diseases. *Curr Mol Med* 2008;8:416-426.
68. Takatsu K, Nakajima H. Il-5 and eosinophilia. *Curr Opin Immunol* 2008;20:288-294.
69. Tamachi T, Maezawa Y, Ikeda K, Iwamoto I, Nakajima H. Interleukin 25 in allergic airway inflammation. *Int Arch Allergy Immunol* 2006;140 Suppl 1:59-62.
70. Barlow JL, McKenzie AN. Il-25: A key requirement for the regulation of type-2 immunity. *Biofactors* 2009;35:178-182.
71. Lloyd CM, Hawrylowicz CM. Regulatory t cells in asthma. *Immunity* 2009;31:438-449.
72. Barnes PJ. Role of gata-3 in allergic diseases. *Curr Mol Med* 2008;8:330-334.
73. Wynn TA. Common and unique mechanisms regulate fibrosis in various fibroproliferative diseases. *J Clin Invest* 2007;117:524-529.
74. Thannickal VJ, Toews GB, White ES, Lynch JP, 3rd, Martinez FJ. Mechanisms of pulmonary fibrosis. *Annu Rev Med* 2004;55:395-417.
75. Giri SN. Novel pharmacological approaches to manage interstitial lung fibrosis in the twenty-first century. *Annu Rev Pharmacol Toxicol* 2003;43:73-95.
76. McDonald DM. Angiogenesis and remodeling of airway vasculature in chronic inflammation. *Am J Respir Crit Care Med* 2001;164:S39-45.
77. White ES, Lazar MH, Thannickal VJ. Pathogenetic mechanisms in usual interstitial pneumonia/idiopathic pulmonary fibrosis. *J Pathol* 2003;201:343-354.
78. American thoracic society. Idiopathic pulmonary fibrosis: Diagnosis and treatment. International consensus statement. American thoracic society (ats), and the european respiratory society (ers). *Am J Respir Crit Care Med* 2000;161:646-664.
79. Frankel SK, Schwarz MI. Update in idiopathic pulmonary fibrosis. *Curr Opin Pulm Med* 2009;15:463-469.
80. Maher TM, Wells AU, Laurent GJ. Idiopathic pulmonary fibrosis: Multiple causes and multiple mechanisms? *Eur Respir J* 2007;30:835-839.
81. Raghu G, Weycker D, Edelsberg J, Bradford WZ, Oster G. Incidence and prevalence of idiopathic pulmonary fibrosis. *Am J Respir Crit Care Med* 2006;174:810-816.
82. Gauldie J. Pro: Inflammatory mechanisms are a minor component of the pathogenesis of idiopathic pulmonary fibrosis. *Am J Respir Crit Care Med* 2002;165:1205-1206.
83. Strieter RM. Con: Inflammatory mechanisms are not a minor component of the pathogenesis of idiopathic pulmonary fibrosis. *Am J Respir Crit Care Med* 2002;165:1206-1207; discussion 1207-1208.
84. Selman M, Pardo A. The epithelial/fibroblastic pathway in the pathogenesis of idiopathic pulmonary fibrosis. *Am J Respir Cell Mol Biol* 2003;29:S93-97.

85. Selman M, Pardo A, Kaminski N. Idiopathic pulmonary fibrosis: Aberrant recapitulation of developmental programs? *PLoS Med* 2008;5:e62.
86. Willis BC, duBois RM, Borok Z. Epithelial origin of myofibroblasts during fibrosis in the lung. *Proc Am Thorac Soc* 2006;3:377-382.
87. Selman M, Pardo A. Role of epithelial cells in idiopathic pulmonary fibrosis: From innocent targets to serial killers. *Proc Am Thorac Soc* 2006;3:364-372.
88. Guarino M, Tosoni A, Nebuloni M. Direct contribution of epithelium to organ fibrosis: Epithelial-mesenchymal transition. *Hum Pathol* 2009;40:1365-1376.
89. Brody JS, Williams MC. Pulmonary alveolar epithelial cell differentiation. *Annu Rev Physiol* 1992;54:351-371.
90. Willis BC, Borok Z. Tgf-beta-induced emt: Mechanisms and implications for fibrotic lung disease. *Am J Physiol Lung Cell Mol Physiol* 2007;293:L525-534.
91. Razzaque MS, Taguchi T. Pulmonary fibrosis: Cellular and molecular events. *Pathol Int* 2003;53:133-145.
92. Roberts CR, Walker DC, Schellenberg RR. Extracellular matrix. *Clin Allergy Immunol* 2002;16:143-178.
93. Thannickal VJ, Horowitz JC. Evolving concepts of apoptosis in idiopathic pulmonary fibrosis. *Proc Am Thorac Soc* 2006;3:350-356.
94. Kuwano K. Epithelial cell apoptosis and lung remodeling. *Cell Mol Immunol* 2007;4:419-429.
95. Kuwano K. Involvement of epithelial cell apoptosis in interstitial lung diseases. *Intern Med* 2008;47:345-353.
96. Strieter RM, Gomperts BN, Keane MP. The role of cxc chemokines in pulmonary fibrosis. *J Clin Invest* 2007;117:549-556.
97. Ishida Y, Kimura A, Kondo T, Hayashi T, Ueno M, Takakura N, Matsushima K, Mukaida N. Essential roles of the cc chemokine ligand 3-cc chemokine receptor 5 axis in bleomycin-induced pulmonary fibrosis through regulation of macrophage and fibrocyte infiltration. *Am J Pathol* 2007;170:843-854.
98. Moore BB, Kolodsick JE, Thannickal VJ, Cooke K, Moore TA, Hogaboam C, Wilke CA, Toews GB. Ccr2-mediated recruitment of fibrocytes to the alveolar space after fibrotic injury. *Am J Pathol* 2005;166:675-684.
99. Murray LA, Argentieri RL, Farrell FX, Bracht M, Sheng H, Whitaker B, Beck H, Tsui P, Cochlin K, Evanoff HL, et al. Hyper-responsiveness of ipf/uip fibroblasts: Interplay between tgfbeta1, il-13 and ccl2. *Int J Biochem Cell Biol* 2008;40:2174-2182.
100. Carre PC, Mortenson RL, King TE, Jr., Noble PW, Sable CL, Riches DW. Increased expression of the interleukin-8 gene by alveolar macrophages in idiopathic pulmonary fibrosis. A potential mechanism for the recruitment and activation of neutrophils in lung fibrosis. *J Clin Invest* 1991;88:1802-1810.
101. Keane MP, Arenberg DA, Lynch JP, 3rd, Whyte RI, Iannettoni MD, Burdick MD, Wilke CA, Morris SB, Glass MC, DiGiovine B, et al. The cxc chemokines, il-8 and ip-10, regulate angiogenic activity in idiopathic pulmonary fibrosis. *J Immunol* 1997;159:1437-1443.
102. Ziegenhagen MW, Zabel P, Zissel G, Schlaak M, Muller-Quernheim J. Serum level of interleukin 8 is elevated in idiopathic pulmonary fibrosis and indicates disease activity. *Am J Respir Crit Care Med* 1998;157:762-768.
103. Andersson-Sjoland A, de Alba CG, Nihlberg K, Becerril C, Ramirez R, Pardo A, Westergren-Thorsson G, Selman M. Fibrocytes are a potential source of lung fibroblasts in idiopathic pulmonary fibrosis. *Int J Biochem Cell Biol* 2008;40:2129-2140.

104. Antoniades HN, Neville-Golden J, Galanopoulos T, Kradin RL, Valente AJ, Graves DT. Expression of monocyte chemoattractant protein 1 mrna in human idiopathic pulmonary fibrosis. *Proc Natl Acad Sci U S A* 1992;89:5371-5375.
105. Yogo Y, Fujishima S, Inoue T, Saito F, Shiomi T, Yamaguchi K, Ishizaka A. Macrophage derived chemokine (ccl22), thymus and activation-regulated chemokine (ccl17), and ccr4 in idiopathic pulmonary fibrosis. *Respir Res* 2009;10:80.
106. Kodama N, Yamaguchi E, Hizawa N, Furuya K, Kojima J, Oguri M, Takahashi T, Kawakami Y. Expression of rantes by bronchoalveolar lavage cells in nonsmoking patients with interstitial lung diseases. *Am J Respir Cell Mol Biol* 1998;18:526-531.
107. Capelli A, Di Stefano A, Lusuardi M, Gnemmi I, Donner CF. Increased macrophage inflammatory protein-1alpha and macrophage inflammatory protein-1beta levels in bronchoalveolar lavage fluid of patients affected by different stages of pulmonary sarcoidosis. *Am J Respir Crit Care Med* 2002;165:236-241.
108. Capelli A, Di Stefano A, Gnemmi I, Donner CF. Ccr5 expression and cc chemokine levels in idiopathic pulmonary fibrosis. *Eur Respir J* 2005;25:701-707.
109. Pierce EM, Carpenter K, Jakubzick C, Kunkel SL, Evanoff H, Flaherty KR, Martinez FJ, Toews GB, Hogaboam CM. Idiopathic pulmonary fibrosis fibroblasts migrate and proliferate to cc chemokine ligand 21. *Eur Respir J* 2007;29:1082-1093.
110. Moore BB, Hogaboam CM. Murine models of pulmonary fibrosis. *Am J Physiol Lung Cell Mol Physiol* 2008;294:L152-160.
111. Chen J, Stubbe J. Bleomycins: Towards better therapeutics. *Nat Rev Cancer* 2005;5:102-112.
112. Lira SA. Genetic approaches to study chemokine function. *J Leukoc Biol* 1996;59:45-52.
113. Keane MP, Belperio JA, Arenberg DA, Burdick MD, Xu ZJ, Xue YY, Strieter RM. Ifn-gamma-inducible protein-10 attenuates bleomycin-induced pulmonary fibrosis via inhibition of angiogenesis. *J Immunol* 1999;163:5686-5692.
114. Burdick MD, Murray LA, Keane MP, Xue YY, Zisman DA, Belperio JA, Strieter RM. Cxcl11 attenuates bleomycin-induced pulmonary fibrosis via inhibition of vascular remodeling. *Am J Respir Crit Care Med* 2005;171:261-268.
115. Tager AM, Kradin RL, LaCamera P, Bercury SD, Campanella GS, Leary CP, Polosukhin V, Zhao LH, Sakamoto H, Blackwell TS, et al. Inhibition of pulmonary fibrosis by the chemokine ip-10/cxcl10. *Am J Respir Cell Mol Biol* 2004;31:395-404.
116. Jiang D, Liang J, Hodge J, Lu B, Zhu Z, Yu S, Fan J, Gao Y, Yin Z, Homer R, et al. Regulation of pulmonary fibrosis by chemokine receptor cxcr3. *J Clin Invest* 2004;114:291-299.
117. Keane MP, Belperio JA, Moore TA, Moore BB, Arenberg DA, Smith RE, Burdick MD, Kunkel SL, Strieter RM. Neutralization of the cxc chemokine, macrophage inflammatory protein-2, attenuates bleomycin-induced pulmonary fibrosis. *J Immunol* 1999;162:5511-5518.
118. Russo RC, Guabiraba R, Garcia CC, Barcelos LS, Roffe E, Souza AL, Amaral FA, Cisalpino D, Cassali GD, Doni A, et al. Role of the chemokine receptor cxcr2 in bleomycin-induced pulmonary inflammation and fibrosis. *Am J Respir Cell Mol Biol* 2009;40:410-421.
119. Inoshima I, Kuwano K, Hamada N, Hagimoto N, Yoshimi M, Maeyama T, Takeshita A, Kitamoto S, Egashira K, Hara N. Anti-monocyte chemoattractant protein-1 gene therapy attenuates pulmonary fibrosis in mice. *Am J Physiol Lung Cell Mol Physiol* 2004;286:L1038-1044.
120. Okuma T, Terasaki Y, Kaikita K, Kobayashi H, Kuziel WA, Kawasuji M, Takeya M. C-c chemokine receptor 2 (ccr2) deficiency improves bleomycin-induced pulmonary fibrosis

by attenuation of both macrophage infiltration and production of macrophage-derived matrix metalloproteinases. *J Pathol* 2004;204:594-604.
121. Gharaee-Kermani M, McCullumsmith RE, Charo IF, Kunkel SL, Phan SH. Cc-chemokine receptor 2 required for bleomycin-induced pulmonary fibrosis. *Cytokine* 2003;24:266-276.
122. Moore BB, Murray L, Das A, Wilke CA, Herrygers AB, Toews GB. The role of ccl12 in the recruitment of fibrocytes and lung fibrosis. *Am J Respir Cell Mol Biol* 2006;35:175-181.
123. Hashimoto N, Jin H, Liu T, Chensue SW, Phan SH. Bone marrow-derived progenitor cells in pulmonary fibrosis. *J Clin Invest* 2004;113:243-252.
124. Xu J, Mora A, Shim H, Stecenko A, Brigham KL, Rojas M. Role of the sdf-1/cxcr4 axis in the pathogenesis of lung injury and fibrosis. *Am J Respir Cell Mol Biol* 2007;37:291-299.
125. Phillips RJ, Burdick MD, Hong K, Lutz MA, Murray LA, Xue YY, Belperio JA, Keane MP, Strieter RM. Circulating fibrocytes traffic to the lungs in response to cxcl12 and mediate fibrosis. *J Clin Invest* 2004;114:438-446.
126. Mehrad B, Burdick MD, Strieter RM. Fibrocyte cxcr4 regulation as a therapeutic target in pulmonary fibrosis. *Int J Biochem Cell Biol* 2009;41:1708-1718.
127. Belperio JA, Dy M, Murray L, Burdick MD, Xue YY, Strieter RM, Keane MP. The role of the th2 cc chemokine ligand ccl17 in pulmonary fibrosis. *J Immunol* 2004;173:4692-4698.
128. Trujillo G, O'Connor EC, Kunkel SL, Hogaboam CM. A novel mechanism for ccr4 in the regulation of macrophage activation in bleomycin-induced pulmonary fibrosis. *Am J Pathol* 2008;172:1209-1221.
129. Huaux F, Gharaee-Kermani M, Liu T, Morel V, McGarry B, Ullenbruch M, Kunkel SL, Wang J, Xing Z, Phan SH. Role of eotaxin-1 (ccl11) and cc chemokine receptor 3 (ccr3) in bleomycin-induced lung injury and fibrosis. *Am J Pathol* 2005;167:1485-1496.
130. Tokuda A, Itakura M, Onai N, Kimura H, Kuriyama T, Matsushima K. Pivotal role of ccr1-positive leukocytes in bleomycin-induced lung fibrosis in mice. *J Immunol* 2000;164:2745-2751.
131. Allegretti M, Bertini R, Bizzarri C, Beccari A, Mantovani A, Locati M. Allosteric inhibitors of chemoattractant receptors: Opportunities and pitfalls. *Trends Pharmacol Sci* 2008;29:280-286.
132. Viola A, Luster AD. Chemokines and their receptors: Drug targets in immunity and inflammation. *Annu Rev Pharmacol Toxicol* 2008;48:171-197.
133. Keane MP, Belperio JA, Xue YY, Burdick MD, Strieter RM. Depletion of cxcr2 inhibits tumor growth and angiogenesis in a murine model of lung cancer. *J Immunol* 2004;172:2853-2860.
134. Tsai WC, Strieter RM, Mehrad B, Newstead MW, Zeng X, Standiford TJ. Cxc chemokine receptor cxcr2 is essential for protective innate host response in murine pseudomonas aeruginosa pneumonia. *Infect Immun* 2000;68:4289-4296.
135. Mehrad B, Strieter RM, Moore TA, Tsai WC, Lira SA, Standiford TJ. Cxc chemokine receptor-2 ligands are necessary components of neutrophil-mediated host defense in invasive pulmonary aspergillosis. *J Immunol* 1999;163:6086-6094.
136. Belperio JA, Keane MP, Burdick MD, Gomperts B, Xue YY, Hong K, Mestas J, Ardehali A, Mehrad B, Saggar R, et al. Role of cxcr2/cxcr2 ligands in vascular remodeling during bronchiolitis obliterans syndrome. *J Clin Invest* 2005;115:1150-1162.

137. Luciani MG, Stoppacciaro A, Peri G, Mantovani A, Ruco LP. The monocyte chemotactic protein a (mcp-1) and interleukin 8 (il-8) in hodgkin's disease and in solid tumours. *Mol Pathol* 1998;51:273-276.
138. Wells TN, Power CA, Shaw JP, Proudfoot AE. Chemokine blockers--therapeutics in the making? *Trends Pharmacol Sci* 2006;27:41-47.
139. Medina-Tato DA, Watson ML, Ward SG. Leukocyte navigation mechanisms as targets in airway diseases. *Drug Discov Today* 2006;11:866-879.
140. Chapman RW, Phillips JE, Hipkin RW, Curran AK, Lundell D, Fine JS. Cxcr2 antagonists for the treatment of pulmonary disease. *Pharmacol Ther* 2009;121:55-68.
141. Thannickal VJ, Flaherty KR, Hyzy RC, Lynch JP, 3rd. Emerging drugs for idiopathic pulmonary fibrosis. *Expert Opin Emerg Drugs* 2005;10:707-727.
142. Bouros D, Antoniou KM. Current and future therapeutic approaches in idiopathic pulmonary fibrosis. *Eur Respir J* 2005;26:693-702.
143. Scotton CJ, Chambers RC. Molecular targets in pulmonary fibrosis: The myofibroblast in focus. *Chest* 2007;132:1311-1321.
144. Zarbock A, Allegretti M, Ley K. Therapeutic inhibition of cxcr2 by reparixin attenuates acute lung injury in mice. *Br J Pharmacol* 2008;155:357-364.
145. Belperio JA, Keane MP, Burdick MD, Londhe V, Xue YY, Li K, Phillips RJ, Strieter RM. Critical role for cxcr2 and cxcr2 ligands during the pathogenesis of ventilator-induced lung injury. *J Clin Invest* 2002;110:1703-1716.
146. Thatcher TH, McHugh NA, Egan RW, Chapman RW, Hey JA, Turner CK, Redonnet MR, Seweryniak KE, Sime PJ, Phipps RP. Role of cxcr2 in cigarette smoke-induced lung inflammation. *Am J Physiol Lung Cell Mol Physiol* 2005;289:L322-328.
147. Pinho V, de Castro Russo R, Amaral FA, de Sousa LP, Barsante MM, de Souza DG, Alves-Filho JC, Cara DC, Hayflick JS, Rommel C, et al. Tissue- and stimulus-dependent role of phosphatidylinositol 3-kinase isoforms for neutrophil recruitment induced by chemoattractants in vivo. *J Immunol* 2007;179:7891-7898.
148. Takeda M, Ito W, Tanabe M, Ueki S, Kato H, Kihara J, Tanigai T, Chiba T, Yamaguchi K, Kayaba H, et al. Allergic airway hyperresponsiveness, inflammation, and remodeling do not develop in phosphoinositide 3-kinase gamma-deficient mice. *J Allergy Clin Immunol* 2009;123:805-812.
149. Doukas J, Eide L, Stebbins K, Racanelli-Layton A, Dellamary L, Martin M, Dneprovskaia E, Noronha G, Soll R, Wrasidlo W, et al. Aerosolized phosphoinositide 3-kinase gamma/delta inhibitor tg100-115 [3-[2,4-diamino-6-(3-hydroxyphenyl)pteridin-7-yl]phenol] as a therapeutic candidate for asthma and chronic obstructive pulmonary disease. *J Pharmacol Exp Ther* 2009;328:758-765.
150. Ong E, Gao XP, Predescu D, Broman M, Malik AB. Role of phosphatidylinositol 3-kinase-gamma in mediating lung neutrophil sequestration and vascular injury induced by e. Coli sepsis. *Am J Physiol Lung Cell Mol Physiol* 2005;289:L1094-1103.
151. Lionetti V, Lisi A, Patrucco E, De Giuli P, Milazzo MG, Ceci S, Wymann M, Lena A, Gremigni V, Fanelli V, et al. Lack of phosphoinositide 3-kinase-gamma attenuates ventilator-induced lung injury. *Crit Care Med* 2006;34:134-141.

6. ANEXOS

A presente Tese de doutoramento possui um formato alternativo de apresentação de acordo com o permitido pelo Art. 50 do regulamento do Curso de Pós-gradução em Bioquímica e Imunologia da Universidade Federal de Minas Gerais. O formato apresentado compreende uma introdução abrangente sobre o objeto de estudo da Tese, um conjunto de trabalhos científicos (dois publicados e dois submetidos) com contribuição original e relevante na área de estudo, o qual foi seguido por uma seção de conclusões globais.

Como parte das exigências do regulamento, seguem, em anexo, outros trabalhos científicos já publicados, correlatos ao presente estudo e que abordam mecanismos inflamatórios pulmonares, mas com objetivos alheios aos objetivos deste, e dos quais sou co-autor. Esses trabalhos representam apenas documentos comprobatórios da publicação de artigos científicos durante o período do meu doutoramento (necessários para a apresentação no formato alternativo) não constituindo, portanto, objeto de análise da presente Tese.

Remo de Castro Russo

6.1. Anexo – 1

PINHO, V.; **RUSSO, R. C.**; AMARAL, F. A.; SOUSA, L. P.; BARSANTE, M. M.; SOUZA, D. G.; ALVES-FILHO, J. C.; CARA, D. C.; HAYFLICK, J. S.; ROMMEL, C.; RUCKLE, T.; ROSSI, A. G.; TEIXEIRA, M. M. ***Tissue- and stimulus-dependent role of phosphatidylinositol 3-kinase isoforms for neutrophil recruitment induced by chemoattractants in vivo.*** **J Immunol.** 2007 Dec 1;179(11):7891-8.

Tissue- and Stimulus-Dependent Role of Phosphatidylinositol 3-Kinase Isoforms for Neutrophil Recruitment Induced by Chemoattractants In Vivo[1]

Vanessa Pinho,[2†] Remo de Castro Russo,* Flávio A. Amaral,* Lirlândia P. de Sousa,* Michele M. Barsante,* Danielle G. de Souza,[§] José C. Alves-Filho,[¶] Denise C. Cara,[‡] Joel S. Hayflick,[‖] Christian Rommel,[#] Thomas Ruckle,[#] Adriano G. Rossi, and Mauro M. Teixeira***

PI3K plays a fundamental role in regulating neutrophil recruitment into sites of inflammation but the role of the different isoforms of PI3K remains unclear. In this study, we evaluated the role of PI3Kγ and PI3Kδ for neutrophil influx induced by the exogenous administration or the endogenous generation of the chemokine CXCL1. Administration of CXCL1 in PI3K$\gamma^{-/-}$ or wild-type (WT) mice induced similar increases in leukocyte rolling, adhesion, and emigration in the cremaster muscle when examined by intravital microscopy. The induction of neutrophil recruitment into the pleural cavity or the tibia-femoral joint induced by the injection of CXCL1 was not significantly different in PI3K$\gamma^{-/-}$ or WT mice. Neutrophil influx was not altered by treatment of WT mice with a specific PI3Kδ inhibitor, IC87114, or a specific PI3Kγ inhibitor, AS605240. The administration of IC87114 prevented CXCL1-induced neutrophil recruitment only in presence of the PI3Kγ inhibitor or in PI3K$\gamma^{-/-}$ mice. Ag challenge of immunized mice induced CXCR2-dependent neutrophil recruitment that was inhibited by wortmannin or by blockade of and PI3Kδ in PI3K$\gamma^{-/-}$ mice. Neutrophil recruitment to bronchoalveolar lavage induced by exogenously added or endogenous production of CXCL1 was prevented in PI3K$\gamma^{-/-}$ mice. The accumulation of the neutrophils in lung tissues was significantly inhibited only in PI3K$\gamma^{-/-}$ mice treated with IC87114. Neutrophil recruitment induced by exogenous administration of C5a or fMLP appeared to rely solely on PI3Kγ. Altogether, our data demonstrate that there is a tissue- and stimulus-dependent role of PI3Kγ and PI3Kδ for neutrophil recruitment induced by different chemoattractants in vivo. ***The Journal of Immunology*****, 2007, 179: 7891–7898.**

Phosphatidylinositol 3-kinases are a family of proteins that catalyze the phosphorylation of the 3′-OH position of the inositol ring of phosphatidylinositols (PtdIns)[3] resulting in the formation of PtdIns(3)P, PtdIns(3,4)P2, and PtdIns(3,4,5)P3, collectively termed 3′-PtdIns lipids (1, 2). These molecules work as second messengers and are important in regulation of various cellular responses, including proliferation, transformation, survival, superoxide production, adhesion, and cell migration (3). There are different isoforms of PI3Ks that can be divided into three main classes. The class I PI3Ks are heterodimers consisting of a catalytic subunit and an adaptor/regulatory subunit present mainly in the cytosol of cells and can be subdivided into two subclasses: class IA enzymes may have one of three catalytic isoforms (p110α, p110β, or p110δ) associated to five regulatory isoforms and signal downstream of tyrosine kinases; class IB enzymes are constituted by a unique catalytic subunit (p110γ) associated with a regulatory subunit p101 and signal downstream of heterotrimeric G protein-coupled receptors (GPCRs) (1, 2). There is also a class II PI3K, characterized by the presence of a C2 domain, and a class III PI3K, which uses only PtdIns as a substrate (1, 2).

Neutrophils, a major type of blood leukocytes, are indispensable for host defense of bacterial and fungal infections (4). This activity depends on the stimulation of various functions after activation of specific receptors, including the formyl methionyl leucyl peptide, chemotactic factor, and TLRs (5–10). Neutrophil migration is dependent on their activation by chemotactic stimuli, including chemokines, complement fragments, and lipid mediators, which enable these cells to enter the site of infection and destroy the invading pathogens. Chemotactic factors bind to seven-transmembrane domain receptors and activate heterotrimeric G proteins (5, 6, 11, 12). Downstream of these proteins a complex interrelated signaling network is activated and may result in the activation of PI3K isoforms (12–15). Involvement of PI3Ks in neutrophil activation has been demonstrated using the inhibitors of class I PI3K, wortmannin and LY294002, which block neutrophil activation and PtdIns(3,4,5)P3 generation, a main product of PI3K activation (16, 17). Studies using mice lacking the p110 catalytic subunit of PI3Kγ have demonstrated the importance of this PI3K isoform for

*Departamento de Bioquímica e Imunologia, †Departamento de Morfologia, ‡Departamento de Patologia, and §Departamento de Microbiologia, Instituto de Ciências Biológicas, Universidade Federal de Minas Gerais, Belo Horizonte, Brazil; ¶Departmento de Farmacologia, Escola de Medicina de Ribeirão Preto, Universidade de São Paulo, São Paulo, Brazil; ‖ICOS Corporation, Bothell, WA 98021; #Merck Serono International, Geneva, Switzerland; and **Medical Research Council Centre for Inflammation Research, Queen's Medical Research Institute, University of Edinburgh, Edinburgh, United Kingdom

Received for publication March 27, 2007. Accepted for publication September 20, 2007.

The costs of publication of this article were defrayed in part by the payment of page charges. This article must therefore be hereby marked *advertisement* in accordance with 18 U.S.C. Section 1734 solely to indicate this fact.

[1] This work was supported by Conselho Nacional de Desenvolvimento Científico e Tecnológico (Brazil), Fundação de Amparo a Pesquisas do Estado de Minas Gerais (Brazil).

[2] Address correspondence and reprint requests to Dr. Vanessa Pinho, Imunofarmacologia, Departamento de Bioquímica e Imunologia, Departamento de Morfologia, Instituto de Ciências Biológicas, Universidade Federal de Minas Gerais, Avenida Antonio Carlos, 6627 Pampulha, 31270-901, Belo Horizonte, MG, Brazil. E-mail address: vpinho@icb.ufmg.br

[3] Abbreviations used in this paper: PtdIns, phosphatidylinositol; GPCR, G protein-coupled receptor; WT, wild type; i.pl., intrapleural; BAL, bronchoalveolar lavage; MPO, myeloperoxidase.

Copyright © 2007 by The American Association of Immunologists, Inc. 0022-1767/07/$2.00

chemokine-regulated recruitment of neutrophils in vitro (18, 19). Furthermore, PI3Kγ-deficient neutrophils exhibited severe defects in GPCR-induced respiratory burst and produced less PtdIns(3,4,5)P3 after stimulation of cells with C5a, fMLP, and CXCL8 (IL-8) (19). It has been recently suggested that PI3Kδ may also modulate the activity and recruitment of neutrophils in vivo (20, 21). However, the exact extent to which PI3Kγ participates in the process of neutrophil recruitment in vivo is not known.

The present study was conducted initially to investigate the role of PI3Kγ in modulating neutrophil rolling, adhesion, and transmigration induced by the chemokine CXCL1 in the mouse cremaster. However, as PI3Kγ appeared not to be directly involved with CXCL1-induced neutrophil influx, further studies were conducted to investigate whether the enzyme was relevant for the neutrophil recruitment in other sites of inflammation and that induced by more complex inflammatory stimuli, including Ag challenge or bleomycin administration. We also evaluated the relevance of PI3Kγ for neutrophil influx induced by other chemoattractant molecules and whether PI3Kδ played a role in CXCL1-induced neutrophil influx. We demonstrate that the involvement of PI3Kγ on neutrophil recruitment depends on the chemotactic stimulus and on the tissue in which the inflammatory stimulation is occurring. PI3Kδ and PI3Kγ have a redundant role in mediating exogenously added or endogenously generated CXCL1-induced neutrophil recruitment.

Materials and Methods

Animals

PI3Kγ-deficient male C57BL/6 $\times$ sv129 mice and their wild-type (WT) littermate control mice (+/+) (18–22 g) were used throughout these experiments. PI3K$\gamma^{-/-}$ mice (in a C57BL/6 $\times$ sv129 background) were generated as previously described (18). The mice were a gift of Dr. J. M. Penninger (Institute of Molecular Biotechnology of the Austrian Academy of Sciences, Vienna, Austria) and supplied by Taconic Farms. *PI3Kγ* gene deletion was confirmed by PCR using specific primers (WT primers: sense, 5-TCAGGC TCGGAGATTAGGTA-3; antisense, 5-GCCCAATCGGTGGTAGAACT-3; *PI3K$\gamma^{-/-}$* primers: sense, 5-GGACACGGCTTTGATTACAATC-3; antisense primer, 5-GGGGTGGGATTAGATAAATG-3 as previously described (18). Animals were bred and housed in a temperature-controlled room with free access to water and food. All experimental protocols have been subjected to evaluation and were approved by the local animal ethics committee.

Drugs and reagents

Recombinant murine CXCL1 was purchased from PeproTech. CXCL1 was dissolved in water, diluted further in PBS (pH 7.4) containing 0.01% BSA and stored at −70°C until use. OVA was purchased from Sigma-Aldrich and C5a and wortmannin were purchased from Calbiochem. Wortmannin was diluted in DMSO and stored at −70°C until use. LY294002 was purchased from Alamone Laboratories, diluted in DMSO, and stored at −70°C until use. Bleomycin (blenoxane; Bristol-Meyers) was commercially available. The PI3Kδ inhibitor IC87114 was a gift of the ICOS Corporation and stored at −20°C until use. The PI3Kγ inhibitor AS605240 was a gift of Serono and was stored at −20°C until use.

Intravital microscopy

The mouse cremaster preparation was used to study the behavior of leukocytes in the microcirculation and adjacent connective tissue, as previously described (22). Briefly, an incision was made in the scrotal skin to expose the left cremaster muscle, which was then carefully removed from the associated fascia. A lengthwise incision was made on the ventral surface of the cremaster muscle using a cautery. The testicle and the epididymis were separated from the underlying muscle and were moved into the abdominal cavity. The muscle was then spread out over an optically clear viewing pedestal and was secured along the edges with a 4-0 suture. The exposed tissue was superfused with warm bicarbonate-buffered saline (pH 7.4). An intravital microscope (Olympus BX50F4) with a $\times$20 objective lens and a $\times$10 eyepiece was used to examine the cremasteric microcirculation. A video camera (5100 HS; Panasonic) was used to project the images onto a monitor, and the images were recorded for playback analysis using a conventional videocassette recorder.

Single, unbranched cremasteric venules (25–40 μm in diameter) were selected and, to minimize variability, the same section of cremasteric venule was observed throughout the experiment. The number of rolling, adherent, and emigrated leukocytes was determined offline during video playback analysis. Rolling leukocytes were defined as those cells moving at a velocity less than that of erythrocytes within a given vessel. The flux of rolling cells was measured as the number of rolling cells passing by a given point in the venule per minute. A leukocyte was considered to be adherent if it remained stationary for at least 30 s, and total leukocyte adhesion was quantified as the number of adherent cells within a 100-μm length of venule. Leukocyte emigration was defined as the number of cells in the extravascular space within an area of 50 μm of distance from the venule. Only cells adjacent to and clearly outside the vessel under study were counted as emigrated.

Experimental protocols

For each experiment, 500 ng of murine rCXCL1 in 0.2 ml of saline was administered locally by s.c. injection beneath the right scrotal skin using a 30-G needle, 2 h before exteriorization. The left cremaster was then prepared for intravital microscopy. Leukocyte kinetics was investigated, as described above, and at the end of each experiment whole blood was drawn by cardiac puncture. Total cell counts were performed in a modified Neubauer chamber using Turk's stain.

Histology

At the end of each intravital microscopy experiment, the cremaster muscles were removed and fixed in 10% neutral-buffered formalin. The tissues were dehydrated gradually in ethanol, embedded in paraffin, cut into 4-μm sections, stained with H&E, and examined under direct light microscopy.

Sensitization

Animals were immunized with OVA adsorbed to aluminum hydroxide gel as previously described (23). Briefly, mice were injected s.c. on days 1 and 8 with 0.2 ml of a solution containing 100 μg of OVA and 70 μg of aluminum hydroxide (Reheiss).

Leukocyte migration into the pleural cavity induced by Ag and chemoattractant agent

Sensitized WT or PI3K$\gamma^{-/-}$ mice were challenged by intrapleural (i.pl.) administration of Ag (OVA) or PBS. In addition, to investigate the leukocyte migration into the pleural cavity induced by a chemoattractant agent, WT or PI3K$\gamma^{-/-}$ mice were injected into the pleural cavity with CXCL1 (30–100 ng/cavity), C5a (100 ng/cavity), and fMLP (200 ng/cavity). These were optimal doses to induce leukocyte recruitment in preliminary experiments (data not shown). The cells present in the pleural cavity were harvested 6 h after Ag challenge or chemoattractant agent administration by injecting 2 ml of PBS and total cell counts performed in a modified Neubauer chamber using Turk's stain. This time was shown to be optimal for neutrophil recruitment in preliminary kinetics experiments. Differential cell counts were performed on cytospin preparations (Shandon III) stained with May-Grünwald-Giemsa using standard morphologic criteria to identify cell types. The results are presented as the number of cells per cavity.

Leukocyte migration into the lung induced by chemoattractant agent or bleomycin

WT or PI3K$\gamma^{-/-}$ mice were injected intratracheally with 500 ng of murine rCXCL1 or 0.125 U of bleomycin. The stimulus was given in 50 μl of sterile PBS. The control mice received PBS alone. The cells present in the alveolar space and the lung were harvested 6 h after CXCL1 administration or 48 h after bleomycin administration.

Bronchoalveolar lavage (BAL)

BAL was performed to obtain leukocytes in the alveolar spaces. The trachea was exposed and a 1.7-mm outside-diameter polyethylene catheter was inserted. BAL was performed by instilling three 1-ml aliquots of PBS and ~2 ml of fluid was retrieved per mouse. The number of total leukocytes was determined by counting leukocytes in a modified Neubauer chamber after staining with Turk's solution. Differential counts were obtained from cytospin preparations by evaluating the percentage of each leukocyte on a slide stained with May-Grünwald-Giemsa.

Quantification of neutrophil accumulation in lung tissue by myeloperoxidase (MPO) activity measurement

The extent of neutrophil accumulation in the lung tissue was measured by assaying MPO activity as previously described (24). Using the conditions

described below, this methodology is very selective for the determination of neutrophils over macrophages (data not shown). Before lung removal, the pulmonary vasculature was perfused with 3 ml of PBS via the right ventricle. Upon thawing, the tissue (0.1 g of tissue per 1.9 ml of buffer) was homogenized in pH 4.7 buffer (0.1 M NaCl, 0.02 M $NaPO_4$, 0.015 M sodium EDTA), centrifuged at 3000 × *g* for 10 min and the pellet was subjected to hypotonic lyses (1.5 ml of 0.2% NaCl solution followed 30 *s* later by addition of an equal volume of a solution containing 1.6% NaCl and 5% glucose). After a further centrifugation, the pellet was resuspended in 0.05 M $NaPO_4$ buffer (pH 5.4) containing 0.5% hexadecyl-trimethyl-ammonium bromide and rehomogenized. One-milliliter aliquots of the suspension were transferred into 1.5-ml Eppendorf tubes followed by three freeze-thaw cycles using liquid nitrogen. The aliquots were then centrifuged for 15 min at 3000 × *g* to perform the assay. MPO activity in the resuspended pellet was assayed by measuring the change in $OD_{450\ nm}$ using tetramethylbenzidine (1.6 mM) and H_2O_2 (0.5 mM). The reaction was stopped by adding 100 μl of 4 M H_2SO_4 and was quantified at 450 nm in a spectrophotometer (Emax; Molecular Devices). The neutrophil content was calculated from a standard curve based on MPO activity expressed as absorbance increase at 450 nm from 5% casein peritoneal-induced neutrophils assayed in parallel. The results were expressed in relative number of neutrophils per milligram of wet tissue.

Leukocyte migration into an articular cavity

The role of PI3Kγ for neutrophil recruitment was also investigated after administration of CXCL1 in articular cavity. WT or PI3Kγ$^{-/-}$ mice were injected into the tibia-femoral articulation with an optimal dose of murine rCXCL1 (30 ng/cavity). The stimulus was given in 5 μl of sterile PBS and control mice received PBS alone. The cells present in the tibia-femoral articulation were harvested 6 h after chemoattractant agent administration by washing the cavity with 30 μl of PBS. The number of total leukocytes was determined by counting leukocytes in a modified Neubauer chamber after staining with Turk's solution. Differential counts were obtained from cytospin preparations by evaluating the percentage of each leukocyte on a slide stained with May-Grünwald-Giemsa.

Treatment with inhibitors of PI3K

The role of PI3K on neutrophils recruitment was also investigated by using selective inhibitors of PI3K, wortmannin and LY294002; the selective inhibitor of PI3Kδ, IC87114; and selective inhibitor of PI3Kγ, AS605240. Wortmannin or LY294002 were administered systemically (i.p.) at the dose of 1.0 mg/kg 60 min before the i.pl. administration of OVA or chemoattractant agent. This dose was shown to be effective in other experimental systems (25). Moreover, preliminary experiments showed the dose of 1.0 mg/kg to be maximally effective at inhibiting eosinophil recruitment in a similar model (26). IC87114, a highly selective inhibitor of PI3Kδ (20), was administered orally at the dose of 25 mg/kg 60 min before administration of chemoattractant agents. This dose was shown to be effective and selective in another model of leukocyte influx (21). AS605240, a highly selective inhibitor of PI3Kγ (27), was administered orally at the dose of 50 mg/kg 60 min before administration of chemoattractant agents. This dose was shown to be effective and selective in vivo (27). Wortmannin and LY294002 were dissolved in DMSO and further diluted in PBS. IC87114 and AS605240 was suspended in 0.1% methylcellulose solution and ground in a homogenizer to ensure a uniform suspension. Control animals received drug vehicle.

Preparation of bone marrow neutrophils

The femurs and tibias from both hind limbs were removed of mice and freed of soft tissue attachments, and the extreme distal tip of each extremity was cut off. HBSS (without Ca^{2+} and Mg^{2+}) was forced through the bone by using a 5-ml syringe with a 22-gauge needle. After dispersing cell clumps and removing the debris, the bone marrow cells were suspended in 2 ml of HBSS and laid on top of a two-layer Percoll gradient of 72 and 65% Percoll (Sigma-Aldrich) diluted in HBSS (100% Percoll = nine parts Percoll and one part 10× HBSS) and centrifuged (1200 × *g*, 30 min, room temperature) without braking. The enriched neutrophil fraction was recovered at the interface between 65 and 72% Percoll. After washing twice with HBSS, 5.0 ± 1.0 × 10^6 cells were obtained per mouse, 95% neutrophils, identified by staining the nuclei with Turk reagent (Merck).

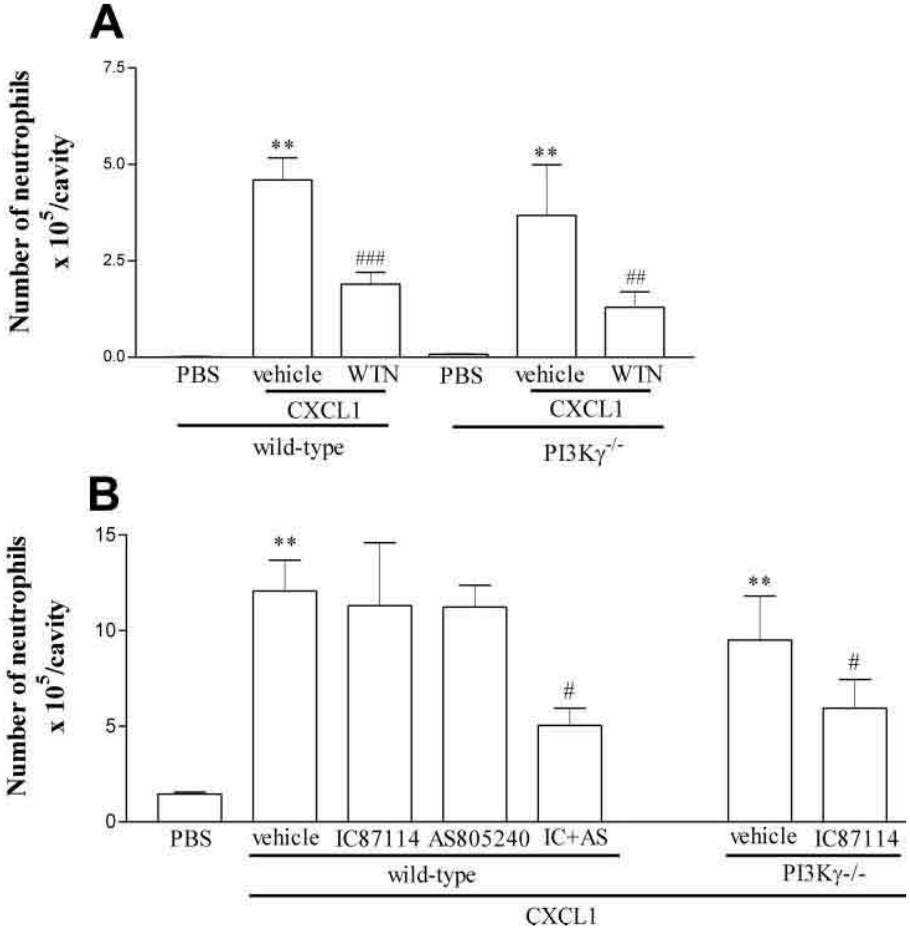


FIGURE 1. Effects of the pretreatment with the nonselective PI3K inhibitor (*A*), wortmannin, and PI3Kδ-selective inhibitor (*B*), IC87114, and PI3Kγ-selective inhibitor, AS605240, on the recruitment of neutrophils induced by CXCL1 in WT and PI3Kγ$^{-/-}$ mice. Wortmannin (1.0 mg/kg), IC87114 (25 mg/kg), and AS605240 (50 mg/kg) was administered 60 min before CXCL1 (100 ng/cavity) i.pl. administration. Neutrophil recruitment was assessed 6 h after chemokine injection. Results are expressed as the means ± SEM of five mice in each group. *, $p < 0.01$ when compared with PBS-injected mice; #, $p < 0.01$ when compared with vehicle-treated CXCL1-injected mice.

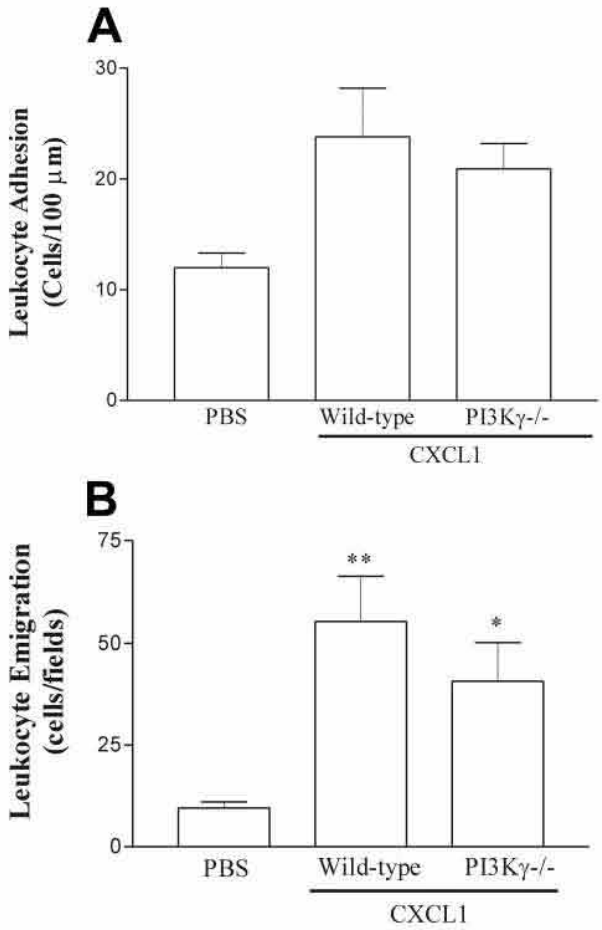


FIGURE 2. Neutrophil adhesion (*A*) and emigration (*B*) in the cremaster muscle of WT and PI3K$\gamma^{-/-}$ mice 2 h after intrascrotal administration of CXCL1 (500 ng/animal). Control mice were injected with PBS. Results are expressed as the means ± SEM of four to five mice in each group. *, $p <$ 0.01 when compared with PBS-injected mice.

Neutrophil chemotaxis

A modified Boyden chamber assay to examine the neutrophil chemoattractant response to CXCL-1 and C5a was performed using a 48-well microchamber (Neuro Probe). Murine bone marrow neutrophils were isolated as above described and resuspended in running buffer (1× HBSS, 2 mg/ml BSA, 10 mM HEPES, 1 mM $CaCl_2$, and 1 mM $MgCl_2$). C5a (10 nM) and recombinant mouse CXCL-1 (20 ng/ml) diluted in running buffer (for wells containing neutrophils) or appropriate buffer control was added to the lower chambers of the apparatus. A 5-μm-pore polycarbonate membrane (Neuro Probe) was placed between the upper and lower chambers, and 5×10^4 cells in a volume of 50 μl were added to the top chambers of the apparatus. Cells were allowed to migrate into the membrane for 1 h per treatment at 37°C with 5% CO_2. Following incubation, the chamber was disassembled and the membrane was scraped and washed three times in PBS to remove nonadherent cells before being fixed in methanol and stained using the Diff-Quik system (Dade Behring). Each well-associated membrane area was scored using light microscopy to count the intact cells present in five random fields. The results are expressed as the number of neutrophils per field.

Table I. *Circulating leukocyte counts and venular diameter in untreated mice and mice treated intrascrotally with CXCL1 (500 ng)*[a]

Animal	Treatment	Circulating Leukocyte (10^6/ml)	Venular Diameter (μm)
WT + PI3K$\gamma^{-/-}$	PBS	6.3 ± 2.2	30.9 ± 2.3
WT	CXCL1 (500 ng)	8.5 ± 2.1	33.4 ± 1.7
PI3K$\gamma^{-/-}$	CXCL1 (500 ng)	6.8 ± 1.3	33.5 ± 3.0

[a] Murine rCXCL1 in 0.2 ml of saline was administered locally by s.c. injection beneath the right scrotal skin 2 h before exteriorization of cremaster muscle. The left cremaster was then prepared for intravital microscopy. Venular diameter was verified and circulating leukocyte kinetics were assessed in whole blood drawn by cardiac puncture. Total cell counts were performed in a modified Neubauer chamber using Turk's stain. Results are expressed as the means ± SEM of five mice in each group.

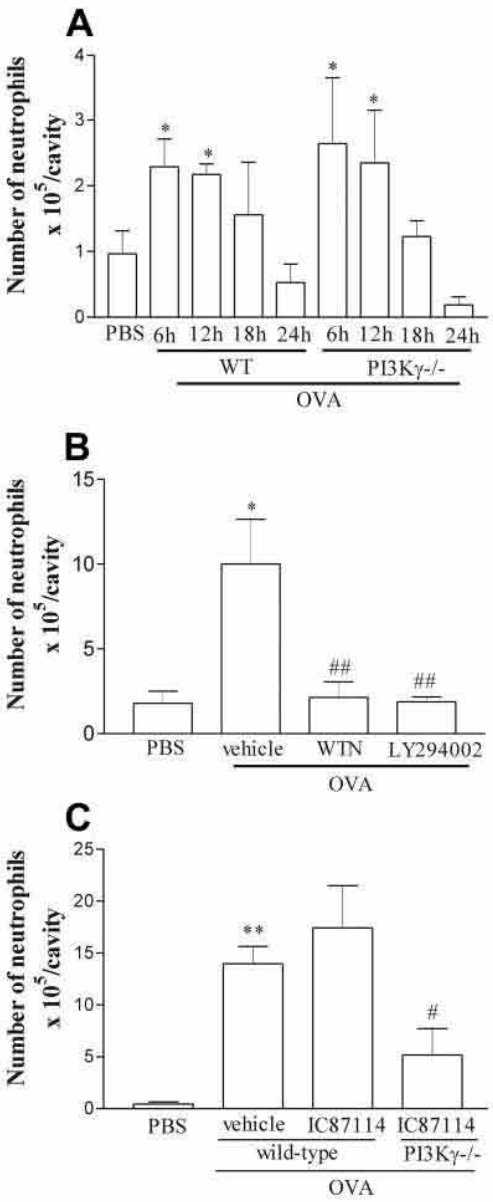


FIGURE 3. Role of PI3K in neutrophil accumulation induced by Ag challenge of sensitized PI3K$\gamma^{-/-}$ and WT mice. Neutrophil accumulation was assessed after 6 h in immunized WT or PI3K$\gamma^{-/-}$ mice and challenged with an i.pl. injection of OVA (1 μg/cavity) or PBS at the time point described in the figure (*A*). Effects of the pretreatment with the nonselective PI3K inhibitors (*B*), wortmannin (1.0 mg/kg), and LY294002 (1.0 mg/kg), and PI3Kδ-selective inhibitor (*C*), IC87114 (25 mg/kg), in the neutrophil accumulation induced by Ag were also verified. Results are expressed as the means ± SEM of five mice in each group. *, $p < 0.05$ when compared with PBS-injected mice; #, $p < 0.05$ when compared with vehicle-treated OVA-injected WT mice.

Statistical analysis

All results are presented as the mean ± SEM. Normalized data were analyzed by one-way ANOVA, and differences between groups were assessed using the Student-Newman-Keuls posttest. A p value <0.05 was considered significant.

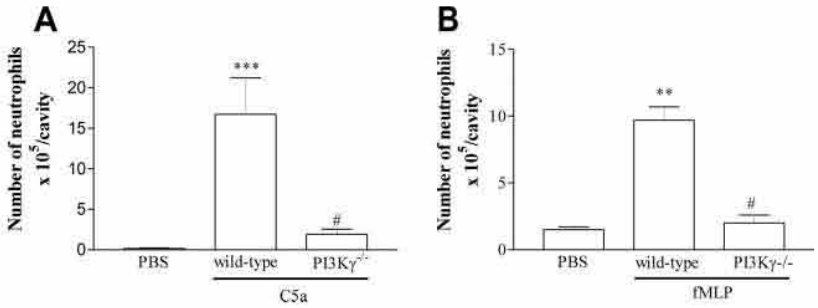


FIGURE 4. Role of PI3K in neutrophil accumulation induced by C5a and fMLP in PI3K$\gamma^{-/-}$ and WT mice. *A*, C5a (100 ng/cavity) or, *B*, fMLP (200 ng/cavity) were injected in pleural cavity and neutrophil accumulation was assessed 6 h later. Results are expressed as the means ± SEM of five mice in each group. *, $p < 0.01$ when compared with PBS-injected mice; #, $p < 0.01$ when compared with OVA-injected WT mice.

Results

Neutrophil recruitment induced by the i.pl. administration of 100 ng of CXCL1 was similar in PI3K$\gamma^{-/-}$ and WT mice (Fig. 1*A*). Neutrophil recruitment induced by lower doses (30 ng/cavity) of CXCL1 was also similar in PI3K$\gamma^{-/-}$ and WT mice (WT mice: $3.1 \pm 0.6 \times 10^5$ neutrophils/cavity; PI3K$\gamma^{-/-}$ mice: $2.1 \pm 0.4 \times 10^5$ neutrophils/cavity). Similar results were obtained using intravital microscopy in the CXCL1-treated cremaster muscle of PI3K$\gamma^{-/-}$ or WT mice. The dose of CXCL1 used in these experiments was based in preliminary experiments and previous studies (28). Intrascrotal administration of 500 ng of CXCL1 induced similar increases in leukocyte rolling (WT mice: 50.6 ± 4.3 cell/min; PI3K$\gamma^{-/-}$ mice: 75.6 ± 8.0 cell/min), adhesion, and emigration in PI3K$\gamma^{-/-}$ or WT mice (Fig. 2). To identify the type of cells that had been recruited to the site of inflammation at this time point, H&E staining was performed on the tissues after the experiment. Neutrophils were the majority of the cells attached to endothelial cells or recruited to the cremaster muscle sections of both PI3K$\gamma^{-/-}$ or WT mice (data not shown). The circulating leukocyte counts were not different in these mice after administration of PBS or CXCL1 (Table I).

The next series of experiments were conducted in the pleural cavity for ease of performance. Despite the similar neutrophil recruitment in PI3K$\gamma^{-/-}$ and WT mice, treatment with the isoform nonselective PI3K inhibitor wortmannin (1.0 mg/kg) inhibited CXCL1-induced neutrophil recruitment both in PI3K$\gamma^{-/-}$ and WT mice (Fig. 1*A*). The latter results suggested that a PI3K was indeed relevant for chemokine-induced neutrophil influx. Treatment of WT mice with IC87114, a PI3Kδ inhibitor, or AS605240, a PI3Kγ inhibitor, alone failed to affect the neutrophil recruitment induced by CXCL1 (Fig. 1*B*). However, the treatment of PI3K$\gamma^{-/-}$ mice with IC87114 and the concomitant treatment with both IC87114 and AS605240 significantly inhibited CXCL1-induced neutrophil recruitment (Fig. 1*B*). In vitro, the chemotaxis of bone marrow-derived neutrophils obtained from PI3K$\gamma^{-/-}$ mice was decreased in comparison to their WT control (basal chemotaxis: WT, 5.0 ± 0.4 neutrophils/field; PI3K$\gamma^{-/-}$, 4.3 ± 0.5 neutrophils/field; CXCL1-induced chemotaxis: WT, 18.5 ± 0.2 neutrophils/field; PI3K$\gamma^{-/-}$, 10.5 ± 0.4 neutrophils/field, $p < 0.05$).

We then examined whether PI3Kγ deficiency might alter the neutrophil recruitment induced by endogenously generated CXCL1, i.e., after Ag challenge (OVA, 1 μg/cavity) of sensitized mice. The i.pl. injection of OVA in sensitized WT mice induced a maximal neutrophil recruitment that occurred between 6 and 12 h and had dropped to baseline levels 24 h later (Fig. 3*A*). The neutrophil accumulation after Ag challenge was not altered in PI3Kγ-deficient mice (Fig. 3*A*). Treatment of sensitized WT mice with a CXCR2 antagonist greatly reduced OVA-induced neutrophil accumulation (PBS, $1.8 \pm 0.7 \times 10^5$ neutrophil/cavity; OVA, $10.0 \pm 2.6 \times 10^5$ neutrophils/cavity; OVA + CXCR2 antagonist, $2.9 \pm 1.6 \times 10^5$ neutrophils/cavity, $n = 5$, $p < 0.05$), demonstrating that the

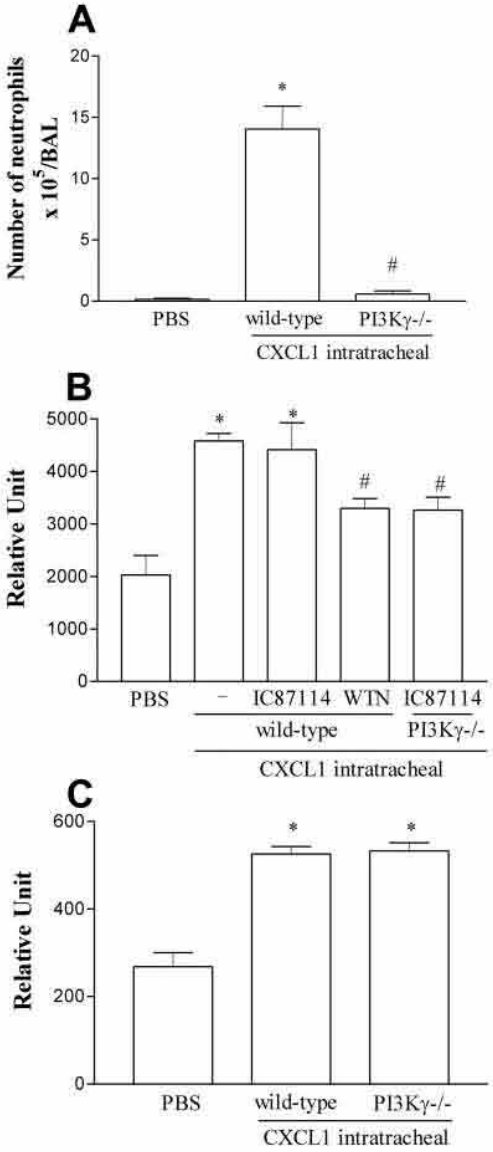


FIGURE 5. Role of PI3K in neutrophil recruitment to lung after intratracheal administration of CXCL1. CXCL1 (500 ng/animal) was administered intratracheally in WT and PI3K$\gamma^{-/-}$ mice. The BAL and lung removal was performed 6 h after chemokine administration. *A*, Neutrophil influx to alveolar spaces; *B*, CXCL1-induced recruitment of neutrophil to lung tissues assessed by measuring tissue MPO content; and *C*, CXCL1-induced recruitment of neutrophil to lung tissues assessed by measuring tissue MPO content after IC87114 treatment. Results are expressed as the means ± SEM of five mice in each group. *, $p < 0.01$ when compared with PBS-injected mice; #, $p < 0.01$ when compared with CXCL1-injected WT mice.

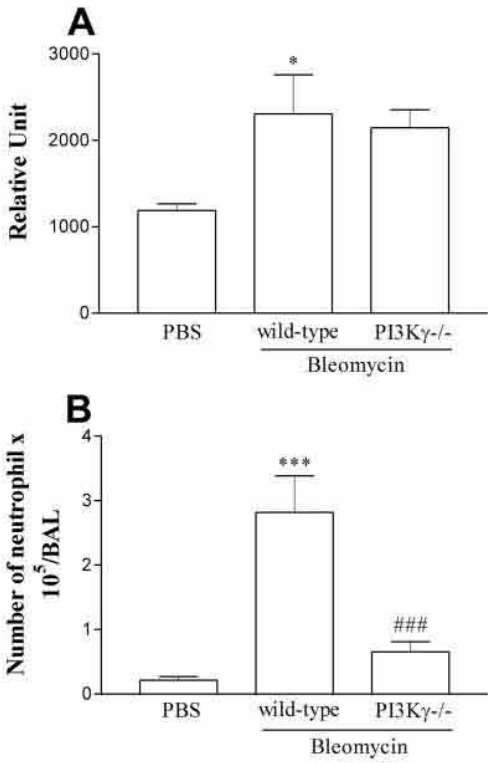


FIGURE 6. Role of PI3K in neutrophil recruitment to lung after intratracheal administration of bleomycin. Bleomycin (0.125 U/animal) was administered intratracheally in WT and PI3K$\gamma^{-/-}$ mice. Lung removal was performed 48 h after bleomycin administration. *A*, Neutrophil influx to alveolar spaces and, *B*, bleomycin-induced recruitment of neutrophil to lung tissues assessed by measuring tissue MPO content. Results are expressed as the means ± SEM of five mice in each group. *, $p < 0.01$ when compared with PBS-injected mice; #, $p < 0.01$ when compared with OVA-injected WT mice.

neutrophil recruitment induced by Ag challenge of sensitized mice depended mainly on CXC chemokine production and CXCR2 activation. Treatment with wortmannin or LY294002, two structurally distinct PI3K inhibitors, diminished the accumulation of neutrophils induced by Ag challenge (Fig. 3*B*). Treatment of WT mice with IC87114 did not affect the neutrophil recruitment induced by Ag challenge of sensitized mice. However, the treatment of PI3K$\gamma^{-/-}$ mice with IC87114 diminished the influx of neutrophils into the pleural cavity (Fig. 3*C*).

Using an in vitro chemotaxis assay, it has been previously shown that C5a-induced chemotaxis is impaired in neutrophils from PI3K$\gamma^{-/-}$ mice (19). In experiments with bone marrow-derived neutrophils, C5a-induced chemotaxis was partially diminished in PI3K$\gamma^{-/-}$ mice vs WT (basal chemotaxis: WT, 5.0 ± 0.4 neutrophils/field; PI3K$\gamma^{-/-}$, 4.3 ± 0.5 neutrophils/field; C5a-induced chemotaxis: WT, 17.8 ± 1.2 neutrophils/field; PI3K$\gamma^{-/-}$, 11.4 ± 1.2 neutrophils/field, $p < 0.05$). In our in vivo experiments, the recruitment of neutrophils induced by i.pl. administration of C5a was abrogated in PI3K$\gamma^{-/-}$ mice (Fig. 4*A*). Similarly, neutrophil recruitment induced by the administration of the chemoattractant molecule fMLP was abrogated in PI3K$\gamma^{-/-}$ mice as compared with their WT controls (Fig. 4*B*).

The recruitment of neutrophils to lung tissue and BAL fluid was evaluated after instillation of CXCL1 or bleomycin. Neutrophil influx to alveolar spaces was totally prevented in PI3Kγ-deficient mice (Fig. 5*A*). In contrast, the deficiency of PI3Kγ had no effect on CXCL1-induced recruitment of neutrophils to lung tissues of mice, as assessed by measuring tissue MPO content (Fig. 5*B*). Treatment of WT mice with IC87114 failed to affect CXCL1-induced recruitment of neutrophils to lung tissues (Fig. 5*C*). However, the amount of neutrophils in lung tissues was significantly inhibited in PI3K$\gamma^{-/-}$ mice treated with IC87114 (Fig. 5*C*).

Bleomycin-induced neutrophil influx depends of the release of CXCL1 into the alveolar space and activation of CXCR2 receptors (R. de Castro Russo and M. M. Teixeira, unpublished data). In agreement with the findings after CXCL1 administration, neutrophil influx to alveolar space after bleomycin administration was markedly diminished in PI3K$\gamma^{-/-}$ as compared with WT mice (Fig. 6*A*) and the recruitment of neutrophils to lung tissues was unaltered in PI3K$\gamma^{-/-}$ mice given bleomycin (Fig. 6*B*).

Furthermore, the role of PI3Kγ in neutrophil recruitment induced by CXCL1 was further confirmed in another model of neutrophil recruitment using the tibia-femoral joint. Neutrophil influx into the tibia-femoral joint was not significantly affected in PI3Kγ-deficient mice (number of neutrophils × 10^6/cavity: WT mice: PBS, 1.2 ± 0.9; CXCL1, 12.8 ± 5.9; PI3K$\gamma^{-/-}$ mice: PBS, 0.2 ± 0.1; CXCL1, 12.4 ± 6.4, $n = 5$, $p > 0.05$ when comparing WT vs PI3K$\gamma^{-/-}$ mice).

Discussion

The present study investigated the role of PI3Kγ and PI3Kδ for neutrophil influx induced by the exogenous administration or the endogenous generation of the chemokine CXCL1. Overall, administration of CXCL1 induced leukocyte migration that was similar in PI3K$\gamma^{-/-}$ or WT mice, or in mice treated with a specific PI3Kδ inhibitor, IC87114, or a specific PI3Kγ inhibitor, AS605240. CXCR2-dependent neutrophil recruitment was only inhibited when there was concomitant inhibition of both PI3Kδ and PI3Kγ. In contrast, neutrophil recruitment into alveolar space or in response to exogenous administration of C5a or fMLP appeared to rely solely on PI3Kγ.

We demonstrated that PI3Kγ deficiency did not interfere significantly with CXCL1-induced rolling, adhesion, and transmigration of neutrophil in cremaster muscle. Recently, it was shown that PI3Kγ-deficient mice presented a decrease in CXCL1-induced leukocyte adhesion in venules of the exteriorized mouse cremaster muscle (29). However, the experimental conditions used by the authors differ from ours in an important point. Although the chemotactic stimulus was injected i.v. and leukocyte adhesion was counted 1 min after the administration of CXCL1, CXCL1 was given locally (i.e., into the tissue) in our experiments and rolling, adhesion, and emigration were evaluated 2 h later. Thus, whereas in our experiments the inflammatory stimulus was present in the tissues where they are usually generated, in the previous study (29), the chemokine was given i.v. In the latter case, there may be stimulation (activation) of leukocytes before they migrate into tissue permitting leukocyte adherence in vessels but not their migration into tissue. Leukocyte activation may mimic the situation of chemotaxis in vitro and neutrophil chemotaxis induced by chemotactic agents is dependent on PI3Kγ (Ref. 30 and our results). In contrast, injection of stimulus in the tissue was PI3Kγ independent and correlated better with the PI3Kγ-independent chemokinetic activity of neutrophils (30, 31). More recently, Liu et al. (38) showed that neutrophil emigration in response to CXCL1 was PI3Kγ dependent at least up to 90 min after the addition of stimulus and was PI3Kγ independent thereafter. The results in later time points are consistent with the PI3Kγ-independent neutrophil influx in response to Ag and CXCL1 in our systems. Further studies are certainly needed to understand in greater detail the relevance of these in vitro phenomena (chemotaxis vs chemokinesis) for neutrophil recruitment in vivo and how the whole process is modulated by PI3Kγ.

Although CXCL1-induced accumulation of neutrophils into the pleural cavity was similar in PI3Kγ-deficient and WT mice, treatment with an isoform nonselective PI3K inhibitor, wortmannin, inhibited neutrophil accumulation induced by CXCL1. Wortmannin was capable of preventing neutrophil influx both in WT and PI3K$\gamma^{-/-}$ mice. Previous studies have demonstrated that activation of PI3K/Akt is required for the induction of human neutrophil migration in response to CXCL8 (a homolog of murine CXCL1) (6, 32). Thus, although CXC chemokine-induced neutrophil recruitment appears to be PI3K dependent, it appears that sole blockade (or absence) of PI3Kγ is not sufficient to prevent neutrophil influx induced by CXCL1. In contrast to our findings, Hirsch et al. (19) demonstrated that neutrophil influx induced by IL-8 was partially inhibited in PI3K$\gamma^{-/-}$ mice. One possibility to explain the discrepancies between those and our findings could be the need for the stimulation of intermediate cells and molecules for human IL-8 to induce recruitment of neutrophils in rodents (33, 34).

Recent reports have also suggested a role for PI3Kδ in promoting neutrophil trafficking in a mouse model of TNF-α-induced inflammation and in a model of acute pulmonary inflammation induced by LPS in rats (20, 21). Treatment with a PI3Kδ inhibitor, IC87114, did not affect CXCL1-induced neutrophil recruitment into the pleural cavity of WT mice at a dose previously shown to be effective in vivo (21). However, the data with wortmannin still suggested that the recruitment of neutrophils induced by CXCL1 would still depend on the activation of other PI3K isoforms or of the joint action of diverse isoforms. Sadhu et al. (15) have proposed that different PI3K isoforms may be activated in response to in vitro stimulation of GPCRs leading to human neutrophil migration. In our experiments, we demonstrated that inhibition of PI3Kδ in PI3K$\gamma^{-/-}$ mice or treatment with inhibitors of both enzymes was accompanied by significant inhibition of neutrophil migration induced by exogenous administration of CXCL1. This result suggests that neutrophil recruitment following triggering of CXCR2 depends on the function of both PI3Kγ and PI3Kδ. In human neutrophils, PI3Kγ and PI3Kδ act together to amplify PIP3 production leading to cell polarization and chemotaxis (15). In accordance with the latter finding, PI3Kγ/PI3K$\delta^{-/-}$ mice have a profound reduction of T cell development (35).

It has been shown that PI3Kγ deficiency affected the ability of the endothelium to adhere neutrophils, most likely due to a reduction in E-selectin-mediated rolling (36). However, deficiency in p110γ and p110δ catalytic subunits of PI3K in the venular endothelium had an additive effect in the ability of this cell type to recruit neutrophils in response to TNF-α stimulation (36). More recent studies from the same group show that PI3Kγ and PI3Kδ have temporally distinct roles in mediating leukocyte recruitment in vivo (31). Thus, PI3Kγ and PI3Kδ mediate neutrophil influx in a kinetic- (31), tissue-, and stimulus- (this study) dependent manner.

A series of experiments were then conducted to examine the role of PI3Kγ and PI3Kδ for the recruitment of neutrophils induced by administration of Ag to immunized mice. In this model, we show that neutrophil recruitment is totally dependent on the endogenous release of CXCR2-acting chemokines. As such, Ag-induced neutrophil recruitment was unchanged in PI3Kγ-deficient mice but was abrogated by treatment with PI3K-nonselective inhibitors. Administration of the PI3Kδ inhibitor failed to alter neutrophil recruitment in WT mice. In contrast, the PI3Kδ inhibitor greatly prevented neutrophil recruitment in Ag-challenged PI3Kγ-deficient mice. Altogether, the latter results demonstrate that endogenous CXCR2-acting chemokines, such as CXCL1, are necessary for Ag-induced neutrophil influx and work via activation of both PI3Kγ and PI3Kδ.

Neutrophil infiltration into BAL fluid after intranasal administration of CXCL1 was greatly diminished in PI3Kγ-deficient mice, an effect consistent with other studies (37). However, neutrophil influx into pulmonary tissue was not dependent on PI3Kγ. It has been demonstrated that intravascular, interstitial, and intra-alveolar accumulation of neutrophils may be differentially regulated; indeed, polymorphonuclear neutrophils can enter the pulmonary interstitium without advancing to the alveolar airway space and crossing the epithelial barrier (38). Thus, the differential mechanisms used by neutrophils to cross endothelial and epithelial cells may explain the differential use of PI3Kγ for neutrophil influx into lung tissues and alveolar spaces. However, the latter possibility needs to be investigated in more detail.

We also demonstrated in a model of bleomycin-induced pulmonary injury that deficiency of PI3Kγ inhibited neutrophil influx into the alveolar space but did not interfere with neutrophil recruitment to lung tissue. In this model of pulmonary inflammation, neutrophil recruitment is associated with endogenous production and action of CXCL1 on CXCR2 receptors (R. de Castro Russo and M. M. Teixeira, unpublished data). Therefore, CXCL1-dependent neutrophil transmigration through lung endothelial cells depends on the cooperative action of both PI3Kγ and PI3Kδ. In contrast, migration through epithelial cells is totally dependent on PI3Kγ.

There is evidence that GPCRs are able to activated class IA PI3K (39, 40). How might PI3Kδ be activated by GPCRs? It is proposed that an initial burst of PIP3 induced by PI3Kγ activation could activate Rac and Src family tyrosine kinases that could then activate PI3Kδ (15). It is not clear whether the latter hypothesis would be functional in our experiments, as one would expect complete blockade of migration once PI3Kγ or PI3Kδ were blocked. Additional experiments are necessary to understand the interplay (or functional relationships) between these two isoforms in vivo.

We also evaluated the importance of PI3Kγ for neutrophil recruitment to the pleural cavity induced by the complement fragment C5a and the bacterial-derived chemotactic peptide fMLP. C5a is a potent chemoattractant for neutrophils, basophils, eosinophils, monocytes, and macrophages and is released after complement activation at sites of inflammation (41, 42). The role of PI3Kγ to C5a-induced neutrophil migration is supported by previous studies demonstrating the inhibition of PtdIns(3,4,5)P3 production and chemotaxis after in vitro stimulation of neutrophil with C5a in PI3K$\gamma^{-/-}$ neutrophils (19). It is well-known also that neutrophil recruitment in response to Gram-negative infection involves bacterial-derived chemotactic factors such as *N*-formyl peptides (fMLP) and that, in the absence of PI3K neutrophils, cannot migrate toward fMLP (5, 19, 43, 44). In agreement with these previous data, the recruitment of neutrophils induced by C5a and fMLP was prevented in PI3K$\gamma^{-/-}$ mice.

In conclusion, we demonstrate there is differential usage of PI3Kγ when neutrophil recruitment is induced by different chemoattractant molecules (CXCL1, C5a, and FMLP) and whether recruitment occurs across endothelial or epithelial barriers. Whereas C5a and fMLP appear to rely entirely on PI3Kγ for induction of neutrophil influx, CXCL1-mediated effects largely depend on the redundant role of PI3Kγ and PI3Kδ. Neutrophil emigration across the epithelium also relies on PI3Kγ expression. The redundant role of and cooperation between signaling molecules and enzymes may be fundamental in providing additional specificity and complexity to signals initiated after seven-transmembrane receptor activation.

Acknowledgments

We thank Valdinéria Borges and Ilma Marçal for technical assistance.

Disclosures

Joel S. Hayflick is an employee of ICOS Corporation and Christian Rommel and Thomas Ruckle are employees of Merck Serono. These companies have commercial interest in developing PI3K-selective inhibitors for the treatment of inflammatory disease. The other authors declare no financial conflict of interest.

References

1. Kapeller, R., and L. C. Cantley. 1994. Phosphatidylinositol 3-kinase. *BioEssays* 16: 565–576.
2. Vanhaesebroeck, B., and M. D. Waterfield. 1999. Signaling by distinct classes of phosphoinositide 3-kinases. *Exp. Cell Res.* 253: 239–254.
3. Toker, A., and L. C. Cantley. 1997. Signalling through the lipid products of phosphoinositide-3-OH kinase. *Nature* 387: 673–676.
4. Lehrer, R. I., T. Ganz, M. E. Selsted, B. M. Babior, and J. T. Curnutte. 1988. Neutrophils and host defense. *Ann. Intern. Med.* 109: 127–142.
5. Le, Y., P. M. Murphy, and J. M. Wang. 2002. Formyl-peptide receptors revisited. *Trends Immunol.* 23: 541–548.
6. Heit, B., S. Tavener, E. Raharjo, and P. Kubes. 2002. An intracellular signaling hierarchy determines direction of migration in opposing chemotactic gradients. *J. Cell Biol.* 159: 91–102.
7. Godaly, G., G. Bergsten, L. Hang, H. Fischer, B. Frendeus, A. C. Lundstedt, M. Samuelsson, P. Samuelsson, and C. Svanborg. 2001. Neutrophil recruitment, chemokine receptors, and resistance to mucosal infection. *J. Leukocyte Biol.* 69: 899–906.
8. Jeyaseelan, S., H. W. Chu, S. K. Young, M. W. Freeman, and G. S. Worthen. 2005. Distinct roles of pattern recognition receptors CD14 and Toll-like receptor 4 in acute lung injury. *Infect. Immun.* 73: 1754–1763.
9. Netea, M. G., C. A. Van Der Graaf, A. G. Vonk, I. Verschueren, J. W. Van Der Meer, and B. J. Kullberg. 2002. The role of Toll-like receptor (TLR) 2 and TLR4 in the host defense against disseminated candidiasis. *J. Infect. Dis.* 185: 1483–1489.
10. Baggiolini, M., F. Boulay, J. A. Badwey, and J. T. Curnutte. 1993. Activation of neutrophil leukocytes: chemoattractant receptors and respiratory burst. *FASEB J.* 11: 1004–1010.
11. Cicchetti, G., P. G. Allen, and M. Glogauer. 2002. Chemotactic signaling pathways in neutrophils: from receptor to actin assembly. *Crit. Rev. Oral Biol. Med.* 13: 220–228.
12. Niggli, V. 2003. Signaling to migration in neutrophils: importance of localized pathways. *Int. J. Biochem. Cell Biol.* 35: 1619–1638.
13. Curnock, A. P., M. K. Logan, and S. G. Ward. 2002. Chemokine signalling: pivoting around multiple phosphoinositide 3-kinases. *Immunology* 105: 125–136.
14. Fruman, D. A., and L. C. Cantley. 2002. Phosphoinositide 3-kinase in immunological systems. *Semin. Immunol.* 14: 7–18.
15. Sadhu, C., B. Masinovsky, K. Dick, C. G. Sowell, and D. E. Staunton. 2003. Essential role of phosphoinositide 3-kinase δ in neutrophil directional movement. *J. Immunol.* 170: 2647–2654.
16. Stephens, L., A. Smrcka, F. T. Cooke, T. R. Jackson, P. C. Sternweis, and P. T. Hawkins. 1994. A novel phosphoinositide 3 kinase activity in myeloid-derived cells is activated by G protein $\beta\gamma$ subunits. *Cell* 77: 83–93.
17. Yum, H. K., J. Arcaroli, J. Kupfner, R. Shenkar, J. M. Penninger, T. Sasaki, K. Y. Yang, J. S. Park, and E. Abraham. 2001. Involvement of phosphoinositide 3-kinases in neutrophil activation and the development of acute lung injury. *J. Immunol.* 167: 6601–6608.
18. Sasaki, T., J. Irie-Sasaki, R. G. Jones, A. J. Oliveira-Dos-Santos, W. L. Stanford, B. Bolon, A. Wakeham, A. Itie, D. Bouchard, I. Kozieradzki, et al. 2000. Function of PI3Kγ in thymocyte development, T cell activation, and neutrophil migration. *Science* 287: 1040–1046.
19. Hirsch, E., V. L. Katanaev, C. Garlanda, O. Azzolino, L. Pirola, L. Silengo, S. Sozzani, A. Mantovani, F. Altruda, and M. P. Wymann. 2000. Central role for G protein-coupled phosphoinositide 3-kinase γ in inflammation. *Science* 287: 1049–1053.
20. Sadhu, C., K. Dick, W. T. Tino, and D. E. Staunton. 2003. Selective role of PI3K δ in neutrophil inflammatory responses. *Biochem. Biophys. Res. Commun.* 308: 764–769.
21. Puri, K. D., T. A. Doggett, J. Douangpanya, Y. Hou, W. T. Tino, T. Wilson, T. Graf, E. Clayton, M. Turner, J. S. Hayflick, and T. G. Diacovo. 2004. Mechanisms and implications of phosphoinositide 3-kinase δ in promoting neutrophil trafficking into inflamed tissue. *Blood* 103: 3448–3456.
22. Kanwar, S., D. C. Bullard, M. J. Hickey, C. W. Smith, A. L. Beaudet, B. A. Wolitzky, and P. Kubes. 1997. The association between α_4-integrin, P-selectin, and E-selectin in an allergic model of inflammation. *J. Exp. Med.* 185: 1077–1087.
23. Klein, A., A. Talvani, D. C. Cara, K. L. Gomes, N. W. Lukacs, and M. M. Teixeira. 2000. Stem cell factor plays a major role in the recruitment of eosinophils in allergic pleurisy in mice via the production of leukotriene B4. *J. Immunol.* 164: 4271–4276.
24. De Matos, I. M., D. G. Souza, D. G. Seabra, L. Freire-Maia, and M. M. Teixeira. 1999. Effects of tachykinin NK1- or PAF-receptor blockade on the lung injury induced by scorpion venom. *Eur. J. Pharmacol.* 376: 293–300.
25. Ezeamuzie, C. I., J. Sukumaran, and E. Philips. 2001. Effects of wortmannin on human eosinophil response in vitro and on bronchial inflammation and airway hyperresponsiveness in guinea pigs in vivo. *Am. J. Respir. Crit. Care Med.* 164: 1633–1639.
26. Pinho, V., D. G. Souza, M. M. Barsante, F. P. Hamer, M. S. De Freitas, A. G. Rossi, and M. M. Teixeira. 2005. Phosphoinositide-3 kinases critically regulate the recruitment and survival of eosinophils in vivo: importance for the resolution of allergic inflammation. *J. Leukocyte Biol.* 77: 800–810.
27. Camps, M., T. Ruckle, H. Ji, V. Ardissone, F. Rintelen, J. Shaw, C. Ferrandi, C. Chabert, C. Gillieron, B. Francon, et al. 2005. Blockade of PI3Kγ suppresses joint inflammation and damage in mouse models of rheumatoid arthritis. *Nat. Med.* 11: 936–943.
28. Zhang, X. W., Q. Liu, Y. Wang, and H. Thorlacius. 2001. CXC chemokines, MIP-2 and KC, induce P-selectin-dependent neutrophil rolling and extravascular migration in vivo. *Br. J. Pharmacol.* 133: 413–421.
29. Smith, D. F., T. L. Deem, A. C. Bruce, J. Reutershan, D. Wu, and K. Ley. 2006. Leukocyte phosphoinositide-3 kinase γ is required for chemokine-induced, sustained adhesion under flow in vivo. *J. Leukocyte Biol.* 80: 1491–1499.
30. Ferguson, G. J., L. Milne, S. Kulkarni, T. Sasaki, S. Walker, S. Andrews, T. Crabbe, P. Finan, G. Jones, S. Jackson, et al. 2007. PI3Kγ has an important context-dependent role in neutrophil chemokinesis. *Nat. Cell. Biol.* 9: 86–91.
31. Liu, L., K. D. Puri, J. M. Penninger, and P. Kubes. 2007. Leukocyte PI3Kγ and PI3Kδ have temporally distinct roles for leukocyte recruitment in vivo. *Blood* 110: 1191–1198.
32. Knall, C., G. S. Worthen, and G. L. Johnson. 1997. Interleukin 8-stimulated phosphatidylinositol-3-kinase activity regulates the migration of human neutrophils independent of extracellular signal-regulated kinase and p38 mitogen-activated protein kinases. *Proc. Natl. Acad. Sci. USA.* 94: 3052–3057.
33. Ribeiro, R. A., C. A. Flores, F. Q. Cunha, and S. H. Ferreira. 1991. IL-8 causes in vivo neutrophil migration by a cell-dependent mechanism. *Immunology* 73: 472–477.
34. Ramos, C. D., N. E. Heluy-Neto, R. A. Ribeiro, S. H. Ferreira, and F. Q. Cunha. 2003. Neutrophil migration induced by IL-8-activated mast cells is mediated by CINC-1. *Cytokine* 7: 214–223.
35. Webb, L. M., E. Vigorito, M. P. Wymann, E. Hirsch, and M. Turner. 2005. Cutting edge: T cell development requires the combined activities of the p110γ and p110δ catalytic isoforms of phosphatidylinositol 3-kinase. *J. Immunol.* 175: 2783–2787.
36. Puri, K. D., T. A. Doggett, C. Y. Huang, J. Douangpanya, J. S. Hayflick, M. Turner, J. Penninger, and T. G. Diacovo. 2005. The role of endothelial PI3Kγ activity in neutrophil trafficking. *Blood* 106: 150–157.
37. Thomas, M. J., A. Smith, D. H. Head, L. Milne, A. Nicholls, W. Pearce, B. Vanhaesebroeck, M. P. Wymann, E. Hirsch, A. Trifilieff, et al. 2005. Airway inflammation: chemokine-induced neutrophilia and the class I phosphoinositide 3-kinases. *Eur. J. Immunol.* 35: 1283–1291.
38. Li, Q., P. W. Park, C. L. Wilson, and W. C. Parks. 2002. Matrilysin shedding of syndecan-1 regulates chemokine mobilization and transepithelial efflux of neutrophils in acute lung injury. *Cell* 111: 635–646.
39. Curnock, A. P., Y. Sotsios, K. L. Wright, and S. G. Ward. 2003. Optimal chemotactic responses of leukemic T cells to stromal cell-derived factor-1 requires the activation of both class IA and IB phosphoinositide 3-kinases. *J. Immunol.* 170: 4021–4030.
40. Vicente-Manzanares, M., M. Rey, D. R. Jones, D. Sancho, M. Mellado, J. M. Rodriguez-Frade, M. A. del Pozo, M. Yanez-Mo, A. M. de Ana, C. Martinez-A, et al. 1999. Involvement of phosphatidylinositol 3-kinase in stromal cell-derived factor-1 α-induced lymphocyte polarization and chemotaxis. *J. Immunol.* 163: 4001–4012.
41. Allegretti, M., A. Moriconi, A. R. Beccari, R. Di Bitondo, C. Bizzarri, R. Bertini, and F. Colotta. 2005. Targeting C5a: recent advances in drug discovery. *Curr. Med. Chem.* 12: 217–236.
42. Guo, R. F., and P. A. Ward. 2005. Role of C5a in inflammatory responses. *Annu. Rev. Immunol.* 23: 821–852.
43. Marasco, W. A., S. H. Phan, H. Krutzsch, H. J. Showell, D. E. Feltner, R. Nairn, E. L. Becker, and P. A. Ward. 1984. Purification and identification of formyl-methionyl-leucyl-phenylalanine as the major peptide neutrophil chemotactic factor produced by *Escherichia coli*. *J. Biol. Chem.* 259: 5430–5439.
44. Hannigan, M., L. Zhan, Z. Li, Y. Ai, D. Wu, and C. K. Huang. 2002. Neutrophils lacking phosphoinositide 3-kinase γ show loss of directionality during *N*-formyl-Met-Leu-Phe-induced chemotaxis. *Proc. Natl. Acad. Sci. USA* 19: 3603–3608.

6.2. Anexo – 2

BORRONI, E. M.; BURACCHI, C.; SAVINO, B.; PASQUALINI, F.; **RUSSO, R. C.**; NEBULONI, M.; BONECCHI, R.; MANTOVANI, A.; LOCATI, M. ***Role of the chemokine scavenger receptor D6 in balancing inflammation and immune activation.*** **Methods Enzymol.** *2009;460:231-43*.

CHAPTER ELEVEN

Role of the Chemokine Scavenger Receptor D6 in Balancing Inflammation and Immune Activation

Elena M. Borroni,* Chiara Buracchi,* Benedetta Savino,* Fabio Pasqualini,* Remo C. Russo,*,† Manuela Nebuloni,‡ Raffaella Bonecchi,* Alberto Mantovani,§ *and* Massimo Locati§

Contents

1. Introduction 232
2. Methods 232
   2.1. Immunohistochemistry 232
   2.2. TB infection model 233
   2.3. Chemokine neutralization *in vivo* 233
   2.4. Cell transfection 233
   2.5. Immunofluorescence and confocal microscopy analysis 234
   2.6. Chemokine scavenging assay 234
3. Results 235
4. Discussion 236
References 241

Abstract

Chemokines play a major role in the induction of inflammatory reactions and development of an appropriate immune response by coordinating leukocyte recruitment. The appropriate control of the chemokine system involves several chemokine decoy receptors, with distinct specificity and tissue distribution, defined as nonactivating chemokine receptors able to bind the ligands and target them to degradation. The best-characterized representative of these receptors is D6, which is located on lymphatic endothelium and controls most inflammatory CC chemokines. Here we will discuss the expression and

* Laboratory of Leukocyte Biology, Department of Translational Medicine, University of Milan, IRCCS Istituto Clinico Humanitas, Italy
† Department of Biochemistry and Immunology, Instituto de Ciencias Biologicas, Universidade Federal de Minas Gerais, Belo Horizonte, Brazil
‡ Pathology Unit, L. Sacco Institute of Medical Sciences, University of Milan, Milan, Italy
§ Department of Translational Medicine, University of Milan, IRCCS Istituto Clinico Humanitas, Via Manzoni, Rozzano (Milano), Italia

Methods in Enzymology, Volume 460
ISSN 0076-6879, DOI: 10.1016/S0076-6879(09)05211-2
© 2009 Elsevier Inc.
All rights reserved.

regulation of D6 during challenge with the pathogen, and its role in dampening inflammation in tissues and draining lymph nodes and in the organization of a protective immune response.

1. Introduction

Leukocyte trafficking is a key element in the orientation of innate and adaptive immunity, and it is mainly controlled by chemokines, small secreted proteins with chemotactic and cytokine-like activities (Mantovani, 1999). These molecules are classified according to structural properties related to the number and position of conserved cysteine residues in two major (CXC and CC) and two minor (C and CX_3C) subfamilies, and according to their production in homeostatic (i.e., produced constitutively) and inflammatory (i.e., produced in response to inflammatory or immunological stimuli) chemokines (Charo and Ransohoff, 2006). Chemokine biological activities are mediated by chemokine receptors, a distinct subfamily of G protein–coupled receptors that mainly transduce intracellular signals through the activation of heterotrimeric $G\alpha_i$ proteins. A distinct subfamily of chemoattractant receptors unable to sustain signaling activities, which includes the chemokine receptors D6, Duffy antigen receptor for chemokines (DARC, also known as the Duffy antigen), and CCX-CKR, has recently been identified (Mantovani *et al.*, 2006).

The D6 molecule recognizes an unusual broad spectrum of ligands, being able to interact with most agonists at inflammatory CC chemokine receptors from CCR1 through CCR5, while homeostatic CC chemokines, agonists at CCR6 to CCR10, are not recognized, nor are chemokines belonging to other subfamilies. While the ligand-binding profile is unusually broad, its expression is fairly restricted, D6 being detectable only in placenta and on endothelial cells of lymphatic afferent vessels in skin, gut, and lung (Martinez de la Torre *et al.*, 2007; Nibbs *et al.*, 1997, 2001). *In vivo* results in several models, including challenge with complete Freund adjuvant, have clearly demonstrated that D6 and its scavenger function are mandatory for controlling the outcome of an inflammatory reaction (Liu *et al.*, 2006; Martinez de la Torre *et al.*, 2005). Here we focus on how D6 is regulated during the development of an immune response, and on its role in balancing the inflammatory and protective adaptive immune response after challenge with *Mycobacterium tuberculosis* (TB).

2. Methods

2.1. Immunohistochemistry

D6 expression was analyzed in human lung lymph nodes obtained from patients with pulmonary tuberculosis. Tissues were selected on the basis of the presence of giant cell–associated necrotic granulomas, and the tubercular

etiology was confirmed by histochemical and biomolecular methods. Consecutive sections of 3 μm width from formalin-fixed, paraffin-embedded tissues were dewaxed in xylene, rehydrated in a progressive ethanol scale, and pretreated in a microwave oven (two cycles of 5 min at 780 W, in 0.25 m*M* EDTA buffer, pH 8.0) for antigen retrieval. Slides were incubated for 2 h at room temperature (RT) in a humid chamber with a rat antihuman D6 monoclonal antibody (1:100; R&D Systems) or a mouse anti human CD68 monoclonal antibody (1:1500; Dako, Denmark) to detect macrophages. The reactions were revealed by nonbiotin, mouse-on-rat, HRP-polymer kit (Biocare Medical), and MACH 4^{TM} Universal HRP-polymer kit (Biocare Medical), respectively, with 3,3′ diaminobenzidine free base as chromogen (brown staining).

2.2. TB infection model

D6-null mice were generated as previously described (Jamieson *et al.*, 2005). Homogeneous populations were established by backcrossing heterozygous mice to C57BL/6J (WT) mice for more than eight generations. WT and D6-null mice were bred in a specific pathogen-free/viral antibody–free barrier facility and used in accordance with institutional guidelines in compliance with national and international law and policies. Mice were infected via the intranasal (IN) route with the TB H37Rv strain (2×10^3 CFU in 20 μl), resulting in the reproducible delivery of 50 to 100 viable CFU. Each experimental group consisted of 7 to 10 mice.

2.3. Chemokine neutralization *in vivo*

To block inflammatory chemokines, mice were treated with a mixture of goat antibodies to the CC chemokines CCL2/MCP-1, CCL3/MIP-1α, and CCL4/MIP-1β), and a monoclonal antibody to CCL5/RANTES purchased lyophilized from R&D Systems, resuspended in sterile phosphate-buffered saline (PBS), and mixed as previously described (Martinez de la Torre *et al.*, 2005, 2007). Mice were given intraperitoneal (IP) injections of 200 μl of the mixture, equivalent to 100 μg of each antibody. Alternatively, mice were treated with 400 μg of individual antibodies specific to a single CC chemokine. On the same days, control mice received IP injections equivalent to 400 μg of irrelevant antibodies (normal goat IgG, Sigma-Aldrich) in 200 μl PBS. Mice were injected weekly, starting from the 3rd week after infection with TB.

2.4. Cell transfection

CHO-K1/D6 cells were transiently transfected (80% confluency) with the Rab11-S25N/pEGFP plasmid by using Lipofectamine 2000 (Invitrogen) protocol as follow. Twenty microliters of Lipofectamine were added to

500 μl OptiMEM medium (Gibco) and incubated for 5 min at RT. Lipofectamine was then combined with (8 μg) DNA, mixed gently, and incubated at RT for 20 min to allow DNA-Lipofectamine complexes to form. DNA-Lipofectamine complexes were added to T25 flasks and incubated at 37 °C in a CO_2 incubator for 24 h.

2.5. Immunofluorescence and confocal microscopy analysis

CHO-K1/D6 (1×10^5) cells were seeded onto glass dishes in 24-well plates and grown at 37 °C for 18 h. Cells were stimulated with 100 n*M* CCL2 in DMEM-F12, supplemented with 1% bovine serum albumin and fixed with 4% paraformaldehyde for 15 min, permeabilized with 0.3% Triton X-100 in PBS for 5 min, and incubated with 10% normal goat serum (Dako, Glostrup, Denmark) for 30 min. Fixed cells were incubated with primary antibodies for 2 h at RT. After washing three times with 0.05% Tween 20 in PBS (pH 7.4), coverslips were incubated with secondary antibodies for 1 h, extensively washed, and incubated with DAPI for 5 min. Specimens were mounted in FluoSave (Calbiochem; San Diego, CA) and high-resolution images (1024 × 1024 pixels) were acquired sequentially with a 60×1.4 N.A. Plan-Apochromat oil immersion objective by using a FV1000 laser-scanning confocal microscope (Olympus, Hamburg, Germany). For z-stack analysis, high-resolution images (1.024 × 1.024 pixels) corresponding to $n = 50$ optical sections (slice = 100 nm) were sequentially acquired as described above. Differential interference contrast (DIC) (Nomarski technique) was also used. Images were assembled and cropped using the Photoshop software (Adobe Systems, San Jose, CA). Quantitative colocalization and statistical analysis were performed using ImarisColoc software, version 4.2 (Bitplane AG, Zurich, Switzerland).

2.6. Chemokine scavenging assay

CHO-K1/D6 cells were plated the day before the experiment in 96-well dishes at the concentration of 3×10^4 cells/well. Cells were then incubated at 37 °C for 4 h in 60 μl of DMEM-F12 supplemented with 1% bovine serum albumin, 0.1 n*M* of ^{125}I-CCL2 or ^{125}I-CCL4, and indicated concentrations of unlabeled CCL2/CCL4 or 10 n*M* CCL2/CCL4 for indicated time points. Proteins in the supernatants were precipitated with 12.5% trichloroacetic acid (Carlo Erba Reagents, Milan, Italy) at 4 °C for 15 min, and the radioactivity present in both soluble and insoluble fractions was measured with a WIZARD automatic γ counter (Perkin Elmer, Waltham, MA). Degradation rate curves were obtained by data fitting with nonlinear regression and interpolation with Michaelis-Menten equations using Prism4 software (GraphPad Software, San Diego, CA).

3. Results

Expression of the D6 receptor during TB infection was investigated by immunohistochemistry on lung lymph nodes from patients with pulmonary tuberculosis. As shown in Fig. 11.1A, D6 expression was prominent in lymphatic endothelial cells, while CD68-positive macrophages did not stain for D6, both within and around granulomas.

To better define the role of D6 in this pathological setting, D6-null mice were infected via the IN route with TB. At the dosage used, WT mice resisted to the infection, while D6-null mice showed significant mortality (Fig. 11.1B). Interestingly, the exaggerated susceptibility of D6-null mice to TB infection was not due to impaired control of the infectious agent, as the bacterial loads in the lung, liver, and spleen were not different in WT and D6-null mice. Conversely, a prominent inflammation-driven tissue damage was observed in several tissue districts, including lung, liver, and kidney, in D6-null animals, as compared to WT mice (data not shown) (Di Liberto *et al.*, 2008). We therefore investigated the role of individual inflammatory CC chemokines by treating TB-infected D6-null mice with monoclonal antibodies blocking

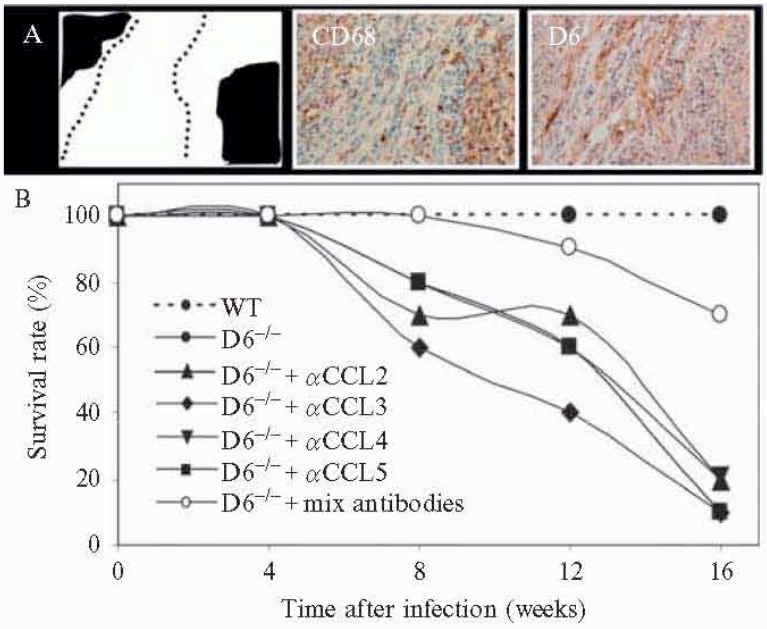


Figure 11.1 D6 expression and role of CC chemokines during TB infection. Panel A shows two serial sections of lung lymph nodes stained for D6 (right panel) and CD68 to detect macrophages (middle panel). Two granulomas with a high number of macrophages are present (indicated by filled areas in the left panel), while the D6 positivity is restricted to lymphatic vessels (indicated by dotted lines in the left panel). Panel B shows survival rate of WT and D6-null mice after IN exposure in the presence of blocking monoclonal antibodies to inflammatory CC chemokines, administered alone or in combination.

the inflammatory CC chemokines under D6 control CCL2, CCL3, CCL4, and CCL5. As shown in Fig. 11.1B, none of the monoclonal antibodies provided individually was able to reverse the exaggerated D6 susceptibility to TB. On the contrary, a cocktail of monoclonal antibodies blocking all four inflammatory CC chemokines provided a partial but significant reversion of this phenotype. These results indicate that the induction of inflammatory chemokines after TB challenge is required to induce a protective immune response, and that D6 clearance of CC chemokines is needed to contain the immune response and prevent excessive tissue damage.

As D6 provides a nonredundant negative regulator of the chemokine system, it was particularly relevant to investigate its regulation during the development of the infection. However, consistently with results previously obtained in *in vitro* settings, we have been unable to detect any significant change in D6 transcript levels in the liver, spleen, and lungs (data not shown). After ligand engagement, chemokine receptors undergo rapid internalization and recycling, allowing targeting of the ligand to lysosome and its degradation. Different from signaling chemokine receptors, we observed that D6 expression of the cell membrane was significantly upregulated in response to receptor engagement by its ligand CCL2. Receptor upregulation was particularly evident for elevated concentrations of the ligands (Bonecchi *et al.*, 2008), and this increased expression correlated with an increased efficacy in ligand degradation (Fig. 11.2A and B). To better understand the ligand-dependent induction of receptor upregulation, D6 localization in the cell was investigated by confocal microscopy. Under resting conditions, most of the receptor was stored in perinuclear compartments, whereas ligand engagement induced relocation of a significant fraction of the receptor to the cell membrane. Concomitantly, the strong colocalization of D6 with the recycling endosome marker Rab11 observed under resting conditions was significantly reduced after ligand engagement (Fig. 11.3A and B). To investigate the molecular mechanisms responsible for the ligand-induced increased expression of D6, we overexpressed a GFP-tagged, Rab11, dominant negative mutant (Rab11-S25N-EGFP), and evaluated D6 expression and colocalization after CCL2 engagement. As shown in Fig. 11.3C and D, a causative role of Rab11 in this process was demonstrated by the observation that the Rab11 dominant negative mutant was able to largely prevent receptor redistribution on the cell membrane. The colocalization of signals from the endogenous Rab11 and the transfected Rab11-S25N-EGFP demonstrated the specificity of the analysis (Fig. 11.3E and F).

4. Discussion

D6 is the best-described chemokine decoy receptor and plays a crucial role in controlling leukocyte recruitment in inflamed tissues and the levels of inflammatory chemokines in draining lymph nodes (Borroni *et al.*, 2006).

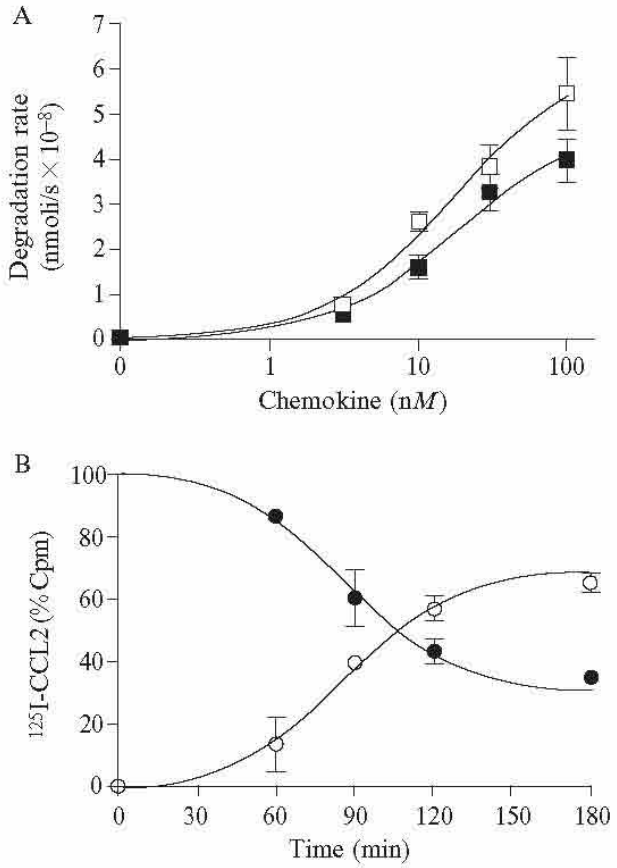


Figure 11.2 D6 increased its scavenging rate upon ligand stimulation. (A) CHO-K1/D6 cells were incubated for 4 h at 37 °C with 0.1 n*M* of ^{125}I-CCL4or ^{125}I-CCL2 and 1 to 100 n*M* of CCL4 (□) or CCL2 (■); (B) CHO-K1/D6 cells were incubated with 0.1 n*M* of ^{125}I-CCL2 and 10 n*M* CCL2 for the indicated time points. Data are representative of (A) the degradation rate (nmoli/s) of TCA soluble fraction of supernatants or (B) the percentage of radioactivity counted (cpm) over CHO-K1 cells in the TCA soluble (○) and TCA insoluble (●) fractions of the supernatants. Results (mean ± standard error) are from triplicates of one representative experiment of three performed.

This atypical CC chemokine receptor shares 30 to 35% sequence identity to conventional (i.e., signaling) chemokine receptors but lacks sequence motifs that are critical for the activation of $G\alpha_i$. Consistent with this, D6 does not support G-protein–dependent signaling functions usually activated by chemokine receptors (Bonecchi *et al.*, 2004; Fra *et al.*, 2003; Nibbs *et al.*, 1997), but appears to be structurally adapted to perform chemokine scavenging being constitutively internalized and recycled back to cell surface and not downregulated after chemokine engagement (Galliera *et al.*, 2004; Weber *et al.*, 2004).

The role of D6 as a regulator of inflammatory chemokines in *in vivo* settings has been investigated in different models of local inflammation using D6-null mice. Of relevance, D6-null mice showed an exacerbated inflammatory response in a model of inflammation induced by phorbol

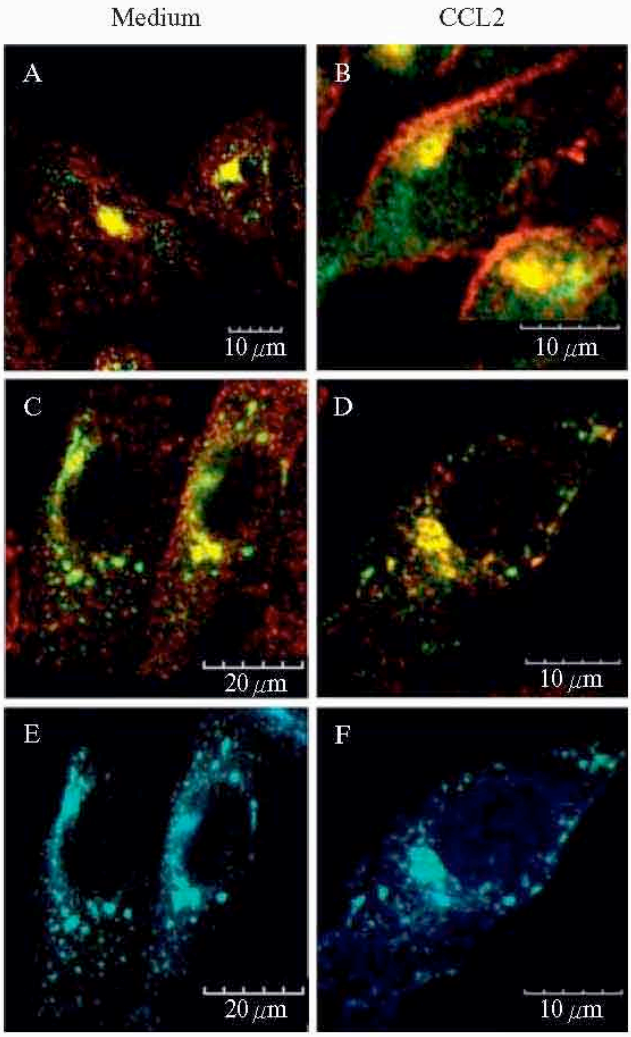


Figure 11.3 D6 constitutive and ligand-induced recycling is supported by a Rab11-dependent mechanism. Confocal images of immunofluorescence stained CHO-K1/D6 cells. Panels show representative experiments of the double staining of D6 (red) with endogenous Rab11 (green) (A, B); D6 (red) with exogenous Rab11-S25N/pEGFP (green) (C, D); colocalization of endogenous Rab11 (blue) with transfected Rab11-S25N/pEGFP (green) (E, F).

ester skin painting and in a model of skin inflammation induced by subcutaneous injection of complete Freund adjuvant (Jamieson *et al.*, 2005; Martinez de la Torre *et al.*, 2005). In particular, in this second model a significant percentage of D6-null animals also developed macroscopic granuloma-like lesions, which were evident only in a minority of WT littermates. In both models, increased levels of inflammatory CC chemokines were detected locally, and pretreatment with chemokine receptors blocking antibodies was able to prevent development of lesions, demonstrating that the increased inflammatory response was caused by an inefficient control of the chemokine system in the absence of D6.

Although the specific roles of individual CC chemokines in the recruitment of various leukocyte populations have not been defined, both reports described an imbalance restricted to inflammatory CC chemokines, consistent with the D6-binding profile. In summary, the two models highlighted a nonredundant role of D6 in the control of local inflammation in skin, although molecular mechanisms involved are still not defined and deserve further investigation, as well as the evaluation of a similar role of D6 in other tissues.

The increased inflammatory response observed in D6-null mice after injection of complete Freund adjuvant, which contains inactivated TB, prompted us to evaluate its role after challenge with the living pathogen (Di Liberto *et al.*, 2008). As compared to WT littermates, D6-null mice preserved their ability to control the infectious agent, as shown by the comparable number of TB CFU. On the contrary, D6-null mice showed an increase in inflammatory infiltrate in lung and lymph nodes, in the levels of proinflammatory cytokines (TNFα, Il-1β, IFNγ) in bronchoalveolar lavage and serum, and in the mortality rate. Given the role of D6 to act as chemokine scavenger and the detection of increased concentrations of CC chemokines (CCL2, CCL3, CCL4, and CCL5) in D6-null mice, a causative role of unbalanced chemokine concentrations was hypothesized. Blocking individual CC chemokines did not reverse the increased mortality observed in D6-null animals, indicating a redundant role of CC chemokines and the need to control the chemokine system in its entirety to properly resolve the inflammatory response, but the block of most CC inflammatory chemokines of relevance for this experimental model (CCL2, CCL3, CCL4, CCL5) using a cocktail of antibodies partially reversed the inflammatory phenotype and the increased lethality observed in D6-null mice. Interestingly, however, this approach also led to less-controlled growth of TB. Thus, during TB infection the survival of the host requires the action of inflammatory chemokines to coordinate an adequate protective immune response and control the pathogen, but the control of inflammatory CC chemokines by the D6 decoy receptor is mandatory for the resolution of the inflammatory reaction (Fig. 11.4).

The expression of D6 on afferent lymphatic vessels supports the hypothesis that this receptor could be at least in part responsible for the well-known role of this compartment as active disposal system for inflammatory chemokines (Fra *et al.*, 2003; Nibbs *et al.*, 2001; Palframan *et al.*, 2001). Consistently with this, D6 expression was detected on lymphatic vessels and not in granuloma-associated macrophages in human tuberculotic lymph nodes. As for other scavenger receptors, D6 has recently been shown to be regulated by soluble inflammatory mediators (McKimmie *et al.*, 2008). Moreover, we recently reported that chemokine stimulation increased D6 membrane expression through its rapid mobilization from a Rab11-positive

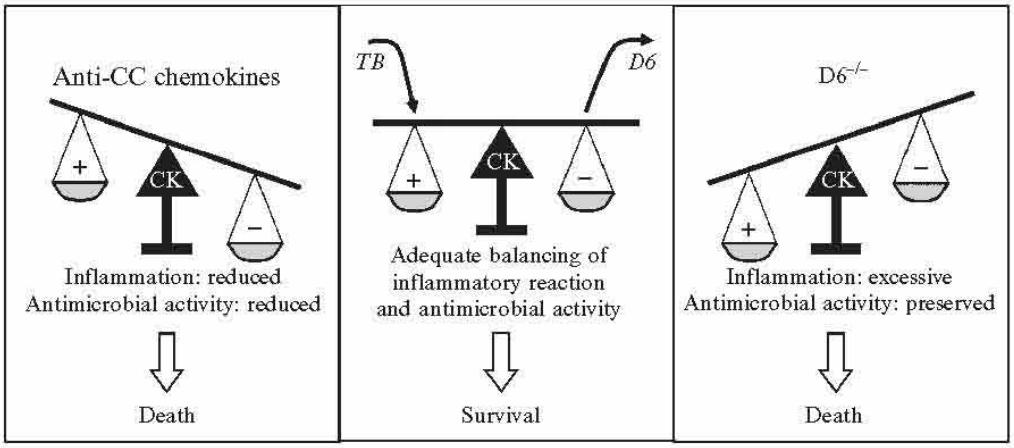


Figure 11.4 Role of D6 in the immune response to TB infection. Survival to TB challenge requires a balanced inflammatory response supporting a protective antimicrobial response without extensive tissue damage. Chemokines are key to this balance, with D6 playing a crucial role in chemokine removal (middle panel). In the absence of chemokines the inflammatory response is blunted and as a consequence an inefficient antimicrobial response lead to host death (left panel). Conversely, the absence of D6 does not significantly impact on antimicrobial response, but an excess in chemokine concentrations leads to host death for extensive tissue damage (right panel).

compartment and improves its efficiency in chemokine scavenging in a time- and ligand-dependent manner (Bonecchi *et al.*, 2008). This behavior is not observed with signaling chemokine receptors, and resembles the activity of enzymes, which catalyze chemical conversion of specific substrates into related products. Indeed, D6 is able to mediate a time-dependent conversion of intact ligand (substrate) into degraded fragments (product) and to improve its degradation rate upon increasing the concentration of ligand. Moreover, similar to what was previously described for D6 (Fra *et al.*, 2003; Galliera *et al.*, 2004; Weber *et al.*, 2004), certain enzymatic pathways undergo constitutive cycling, a phenomenon also referred to as a "futile cycle" because it is an energy-expensive process without energy gain. It has been proposed that this energy cost is necessary for extremely sensitive systems because small changes in the rate of one of these reactions causes a rapid change in net flux, avoiding the lengthy process of protein synthesis and allowing large changes in cells signaling to occur on a rapid time scale (Royle and Murrell-Lagnado, 2003).

Constitutive cycling has also been demonstrated for several transmembrane proteins, such as receptors at mammalian-synapse (Park *et al.*, 2004) adhesion molecules, ion channels, and transporters (Dugani and Klip, 2005; Royle and Murrell-Lagnado, 2003). Interestingly, the macrophage scavenger receptor for modified lipoproteins stabilin-1 (Prevo *et al.*, 2004) and the macrophage scavenger receptor for hemoglobin CD163 (Schaer *et al.*, 2006)

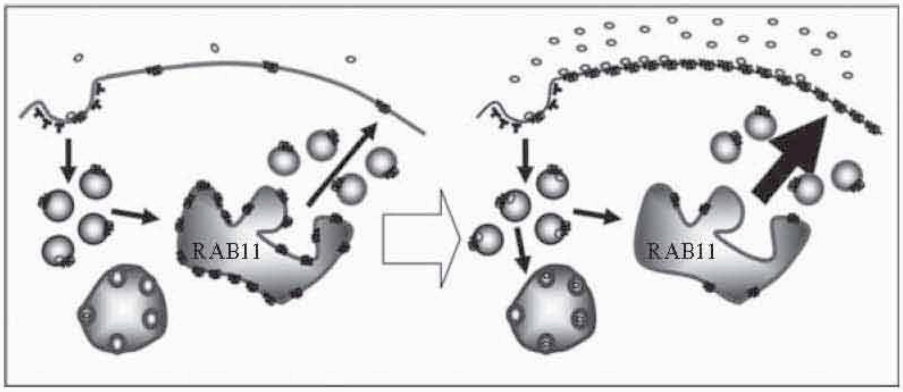


Figure 11.5 Regulation of D6 activity under homeostatic and inflammatory conditions. Under homeostatic conditions, inflammatory chemokines are barely detectable, most D6 is mostly retained in a Rab11-positive intracellular compartment, few receptors constitutively cycle from the cell membrane, and no ligand scavenging activity is detectable (figure to the left). After inflammation is triggered, significant levels of chemokines are induced, D6 engagement induces the redistribution of the stored pool from the Rab11-positive compartment to the cell membrane, and a significant increase in ligand-scavenging activity is detected (right panel).

also undergo a constitutive internalization and recycling process that is significantly increased in response to ligand binding. Similarly, D6 displays enhanced scavenging activity after ligand engagement (Bonecchi *et al.*, 2008), providing further demonstration that its activity is quite similar to the catalytic function of enzymes. Thus, it is tempting to speculate that constitutive cycling and ligand-dependent receptor upregulation might represent mechanisms used by several receptors, including D6, to rapidly modulate ligand uptake and degradation depending on the immediate needs of the tissue (Fig. 11.5).

REFERENCES

Bonecchi, R., Borroni, E. M., Anselmo, A., Doni, A., Savino, B., Mirolo, M., Fabbri, M., Jala, V. R., Haribabu, B., Mantovani, A., and Locati, M. (2008). Regulation of D6 chemokine scavenging activity by ligand- and Rab11-dependent surface up-regulation. *Blood* **112,** 493–503.

Bonecchi, R., Locati, M., Galliera, E., Vulcano, M., Sironi, M., Fra, A. M., Gobbi, M., Vecchi, A., Sozzani, S., Haribabu, B., Van Damme, J., and Mantovani, A. (2004). Differential recognition and scavenging of native and truncated macrophage-derived chemokine (macrophage-derived chemokine/CC chemokine ligand 22) by the D6 decoy receptor. *J. Immunol.* **172,** 4972–4976.

Borroni, E. M., Buracchi, C., de la Torre, Y. M., Galliera, E., Vecchi, A., Bonecchi, R., Mantovani, A., and Locati, M. (2006). The chemoattractant decoy receptor D6 as a negative regulator of inflammatory responses. *Biochem. Soc. Trans.* **34,** 1014–1017.

Charo, I. F., and Ransohoff, R. M. (2006). The many roles of chemokines and chemokine receptors in inflammation. *N. Engl. J. Med.* **354,** 610–621.

Di Liberto, D., Locati, M., Caccamo, N., Vecchi, A., Meraviglia, S., Salerno, A., Sireci, G., Nebuloni, M., Caceres, N., Cardona, P. J., Dieli, F., and Mantovani, A. (2008). Role of the chemokine decoy receptor D6 in balancing inflammation, immune activation, and antimicrobial resistance in *Mycobacterium tuberculosis* infection. *J. Exp. Med.* **205,** 2075–2084.

Dugani, C. B., and Klip, A. (2005). Glucose transporter 4: Cycling, compartments and controversies. *EMBO Rep.* **6,** 1137–1142.

Fra, A. M., Locati, M., Otero, K., Sironi, M., Signorelli, P., Massardi, M. L., Gobbi, M., Vecchi, A., Sozzani, S., and Mantovani, A. (2003). Cutting edge: Scavenging of inflammatory CC chemokines by the promiscuous putatively silent chemokine receptor D6. *J. Immunol.* **170,** 2279–2282.

Galliera, E., Jala, V. R., Trent, J. O., Bonecchi, R., Signorelli, P., Lefkowitz, R. J., Mantovani, A., Locati, M., and Haribabu, B. (2004). Beta-Arrestin-dependent constitutive internalization of the human chemokine decoy receptor D6. *J. Biol. Chem.* **279,** 25590–25597.

Jamieson, T., Cook, D. N., Nibbs, R. J., Rot, A., Nixon, C., McLean, P., Alcami, A., Lira, S. A., Wiekowski, M., and Graham, G. J. (2005). The chemokine receptor D6 limits the inflammatory response *in vivo*. *Nat. Immunol.* **6,** 403–411.

liu, L., Graham, G. J., Damodaran, A., Hu, T., Lira, S. A., Sasse, M., Canasto-Chibuque, C., Cook, D. N., and Ransohoff, R. M. (2006). Cutting edge: The silent chemokine receptor D6 is required for generating T cell responses that mediate experimental autoimmune encephalomyelitis. *J. Immunol.* **177,** 17–21.

Mantovani, A. (1999). The chemokine system: Redundancy for robust outputs. *Immunol. Today* **20,** 254–257.

Montovani, A., Bonecchi, R., and Locati, M. (2006). Tuning inflammation and immunity by chemokine sequestration: Decoys and more. *Nat. Rev. Immunol.* **6,** 907–918.

Martinez de la Torre, Y., Buracchi, C., Borroni, E. M., Dupor, J., Bonecchi, R., Nebuloni, M., Pasqualini, F., Doni, A., Lauri, E., Agostinis, C., Bulla, R., Cook, D. N., *et al.* (2007). Protection against inflammation- and autoantibody-caused fetal loss by the chemokine decoy receptor D6. *Proc. Natl. Acad. Sci. USA* **104,** 2319–2324.

Martinez de la Torre, Y., Locati, M., Buracchi, C., Dupor, J., Cook, D. N., Bonecchi, R., Nebuloni, M., Rukavina, D., Vago, L., Vecchi, A., Lira, S. A., and Mantovani, A. (2005). Increased inflammation in mice deficient for the chemokine decoy receptor D6. *Eur. J. Immunol.* **35,** 1342–1346.

McKimmie, C. S., Fraser, A. R., Hansell, C., Gutiérrez, L., Philipsen, S., Connell, L., Rot, A., Kurowska-Stolarska, M., Carreno, P., Pruenster, M., Chu, C. C., Lombardi, G., *et al.* (2008). Hemopoietic cell expression of the chemokine decoy receptor D6 is dynamic and regulated by GATA1. *J. Immunol.* **181,** 3353–3363.

Nibbs, R. J., Kriehuber, E., Ponath, P. D., Parent, D., Qin, S., Campbell, J. D., Henderson, A., Kerjaschki, D., Maurer, D., Graham, G. J., and Rot, A. (2001). The beta-chemokine receptor D6 is expressed by lymphatic endothelium and a subset of vascular tumors. *Am. J. Pathol.* **158,** 867–877.

Nibbs, R. J., Wylie, S. M., Yang, J., Landau, N. R., and Graham, G. J. (1997). Cloning and characterization of a novel promiscuous human beta-chemokine receptor D6. *J. Biol. Chem.* **272,** 32078–32083.

Palframan, R. T., Jung, S., Cheng, G., Weninger, W., Luo, Y., Dorf, M., Littman, D. R., Rollins, B. J., Zweerink, H., Rot, A., and von Andrian, U. H. (2001). Inflammatory chemokine transport and presentation in HEV: A remote control mechanism for monocyte recruitment to lymph nodes in inflamed tissues. *J. Exp. Med.* **194,** 1361–1373.

Park, M., Penick, E. C., Edwards, J. G., Kauer, J. A., and Ehlers, M. D. (2004). Recycling endosomes supply AMPA receptors for LTP. *Science* **305,** 1972–1975.

Prevo, R., Banerji, S., Ni, J., and Jackson, D. G. (2004). Rapid plasma membrane-endosomal trafficking of the lymph node sinus and high endothelial venule scavenger receptor/homing receptor stabilin-1 (FEEL-1/CLEVER-1). *J. Biol. Chem.* **279,** 52580–52592.

Royle, S. J., and Murrell-Lagnado, R. D. (2003). Constitutive cycling: A general mechanism to regulate cell surface proteins. *Bioessays* **25,** 39–46.

Schaer, C. A., Schoedon, G., Imhof, A., Kurrer, M. O., and Schaer, D. J. (2006). Constitutive endocytosis of CD163 mediates hemoglobin-heme uptake and determines the noninflammatory and protective transcriptional response of macrophages to hemoglobin. *Circ. Res.* **99,** 943–950.

Weber, M., Blair, E., Simpson, C. V., O'Hara, M., Blackburn, P. E., Rot, A., Graham, G. J., and Nibbs, R. J. (2004). The chemokine receptor D6 constitutively traffics to and from the cell surface to internalize and degrade chemokines. *Mol. Biol. Cell.* **15,** 2492–2508.

6.3. Anexo – 3

KUROWSKA-STOLARSKA, M.; KEWIN, P.; MURPHY, G.; **RUSSO, R. C.**; STOLARSKI, B.; GARCIA, C. C.; KOMAI-KOMA, M.; PITMAN, N.; LI, Y.; NIEDBALA, W.; MCKENZIE, A. N.; TEIXEIRA, M. M.; LIEW, F. Y.; XU, D. ***IL-33 induces antigen-specific IL-5+ T cells and promotes allergic-induced airway inflammation independent of IL-4.*** **J Immunol.** 2008 Oct 1;181(7):4780-90.

IL-33 Induces Antigen-Specific IL-5$^+$ T Cells and Promotes Allergic-Induced Airway Inflammation Independent of IL-4[1]

Mariola Kurowska-Stolarska,* Pete Kewin,* Grace Murphy,* Remo C. Russo,† Bartosz Stolarski,* Cristiana Couto Garcia,† Mousa Komai-Koma,* Nick Pitman,* Yubin Li,* Andrew N. J. McKenzie,‡ Mauro M. Teixeira,† Foo Y. Liew,[2]* and Damo Xu[2]*

Type 2 cytokines (IL-4, IL-5, and IL-13) play a pivotal role in helminthic infection and allergic disorders. CD4$^+$ T cells which produce type 2 cytokines can be generated via IL-4-dependent and -independent pathways. Although the IL-4-dependent pathway is well documented, factors that drive IL-4-independent Th2 cell differentiation remain obscure. We report here that the new cytokine IL-33, in the presence of Ag, polarizes murine and human naive CD4$^+$ T cells into a population of T cells which produce mainly IL-5 but not IL-4. This polarization requires IL-1R-related molecule and MyD88 but not IL-4 or STAT6. The IL-33-induced T cell differentiation is also dependent on the phosphorylation of MAPKs and NF-κB but not the induction of GATA3 or T-bet. In vivo, ST2$^{-/-}$ mice developed attenuated airway inflammation and IL-5 production in a murine model of asthma. Conversely, IL-33 administration induced the IL-5-producing T cells and exacerbated allergen-induced airway inflammation in wild-type as well as IL-4$^{-/-}$ mice. Finally, adoptive transfer of IL-33-polarized IL-5$^+$IL-4$^-$T cells triggered airway inflammation in naive IL-4$^{-/-}$ mice. Thus, we demonstrate here that, in the presence of Ag, IL-33 induces IL-5-producing T cells and promotes airway inflammation independent of IL-4. *The Journal of Immunology,* 2008, 181: 4780–4790.

It is generally accepted that CD4$^+$ T cells that express type 2 cytokines can develop from at least two pathways: the IL-4-dependent and -independent pathways (1–9). Although the IL-4-dependent classical Th2 cell development pathway has been extensively studied, the mechanism of IL-4-independent Th2 differentiation remains obscure. These cells, originally identified in IL-4 null mice, express IL-5 and/or IL-13 and play an important role in helminthic infection (2–6), vaccination (7), and asthma (8, 9).

We have previously reported that IL-1R-related molecule (ST2),[3] a member of the IL-1 receptor superfamily, is preferentially expressed on Th2 but not Th1 cells (10). Subsequent reports extended this finding and showed that soluble ST2 (sST2), a decoy receptor of ST2 ligand, could suppress type 2 responses and airway inflammation (11, 12). Interestingly, although IL-4 is capable of inducing ST2, it is not required for ST2 expression on CD4$^+$ cells (12). In line with the above, ST2$^{-/-}$ mice developed impaired type 2 functions but had normal Th2 cells, suggesting potential redundancy and heterogeneity of T cell populations involved in type 2 immunity (13–15). Recently, IL-33 has been identified as the ligand of ST2 (16). IL-33, a member of the IL-1 family, signals via a heterodimeric receptor complex consisting of ST2 and IL-1R accessory protein (16–18) and triggers the activation of NF-κB and all three MAPKs: p38, ERK1/2, and JNK1/2 in mast cells (16, 19, 20). IL-33 is expressed by a variety of cell types (16). Administration of IL-33 into naive mice induced innate type 2 immune response associated with airway hypersensitivity (16, 21). Moreover, it was found that both human and murine mast cells when stimulated in vitro with IL-33 produced a wide spectrum of cytokines and chemokines (19, 20, 22). In addition, IL-33 enhanced IL-4-driven Th2 cell responses (16, 21, 23, 24) and acted as a selective chemoattractant for Th2 cell recruitment (25). However, the potential role of IL-33 in the differentiation of uncommitted Ag-specific CD4$^+$ T cells and contribution of these cells to allergen-induced airway inflammation in an IL-4-free environment is unknown.

We report here that IL-33-polarized murine and human naive CD4$^+$ T cells into CD4$^+$ T cells that produce IL-5 and IL-13 independent of IL-4. In vivo, ST2$^{-/-}$ mice produce less IL-5 and display less inflammation in the lungs compared with wild-type (WT) mice in a model of OVA-induced allergic airway inflammation. Conversely, administration of IL-33 during Ag priming markedly increased the percentage of CD4$^+$IL-5$^+$ and exacerbated OVA-specific airway inflammation in WT and IL-4$^{-/-}$ mice. Finally, adoptive transfer of IL-33-differentiated IL-5$^+$IL-4$^-$T cells triggered airway inflammation in naive IL-4$^{-/-}$ mice. Thus, we demonstrate here that IL-33 induces IL-5-producing T cells and promotes eosinophilic airway inflammation independent of IL-4.

Materials and Methods

Mice

BALB/c, C57BL/6 mice (Harlan Olac), and STAT6$^{-/-}$ mice (The Jackson Laboratory) were used. ST2$^{-/-}$ mice on the BALB/c background (26) were backcrossed with D0.11.10 for 10 generations to generate

*Division of Immunology, Infection and Inflammation, Glasgow Biomedical Research Centre, University of Glasgow, Glasgow United Kingdom; †Departamento de Bioquimica e Imunologia, Instituto de Ciencias Biologicas, Universidade Federal de Minas Gerais, Pampulha, Brazil; and ‡Medical Research Council Laboratory of Molecular Biology, Cambridge, United Kingdom

Received for publication May 20, 2008. Accepted for publication July 27, 2008.

The costs of publication of this article were defrayed in part by the payment of page charges. This article must therefore be hereby marked *advertisement* in accordance with 18 U.S.C. Section 1734 solely to indicate this fact.

[1] This study received financial support from the Medical Research Council U.K., the Wellcome Trust, and the Conselho Nacional de Desenvolvimento Cientifico e Tecnologico, Brazil.

[2] Address correspondence and reprint requests to Dr. Foo Y. Liew and Dr. Damo Xu, Division of Immunology, Infection and Inflammation, 120 University Place, Glasgow Biomedical Research Centre, University of Glasgow, Glasgow G12 8TA, United Kingdom. E-mail addresses: f.y.liew@clinmed.gla.ac.uk and d.xu@clinmed.gla.ac.uk

[3] Abbreviations used in this paper: ST2, IL-1R-related molecule; IL-1RAcP, IL-1 receptor accessory protein; BAL, bronchoalveolar lavage; DLN, draining lymph node; EPO, eosinophil peroxidase; WT, wild type; i.n., intranasal(ly); PAS, periodic acid-Schiff; iNKT, invariant NKT; TRIF, Toll/IL-1R domain-containing adaptor inducing IFN-β.

Copyright © 2008 by The American Association of Immunologists, Inc. 0022-1767/08/$2.00

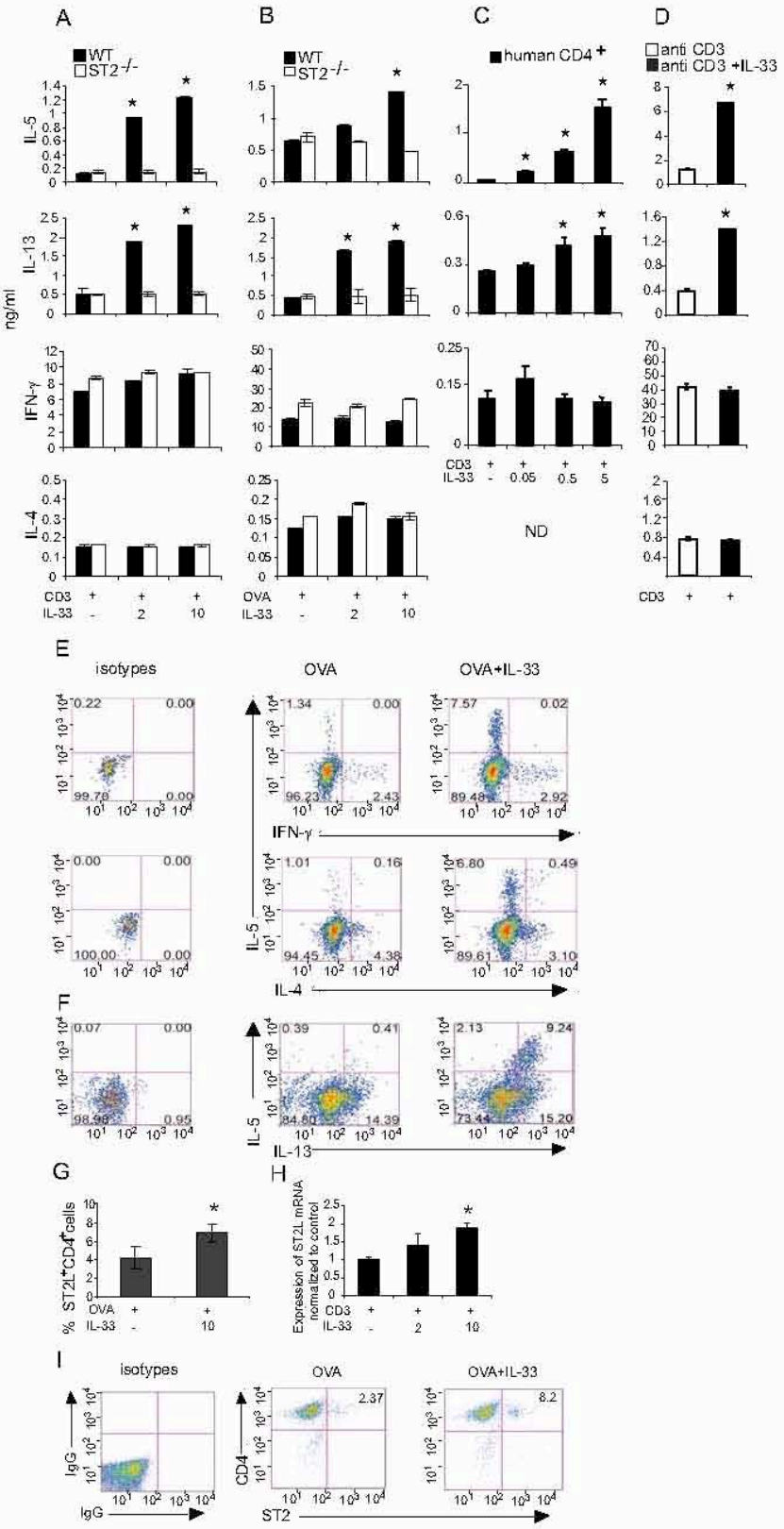


FIGURE 1. IL-33 polarizes $CD4^+$ T cells to produce IL-5 and IL-13 via ST2. *A–C*, Naive $CD4^+$ cells from BALB/c (*A*), D011.10 (*B*), $ST2^{-/-}$ (*A*), $ST2^{-/-}$ × D011.10 (*B*) mice, and human cord blood $CD4^+$ cells (*C*) were stimulated with anti-CD3 Abs (2 μg/ml) (*A* and *C*) or OVA peptide (10 nM; *B*) with or without IL-33 for 72 h. Supernatants were examined for cytokines by ELISA. *D*, BALB/c $CD4^+$ cells stimulated with anti-CD3 Abs with or without IL-33 for 6 days were washed and restimulated with anti-CD3 Abs alone for 72 h. *E* and *F*, $CD4^+$ cells from D011.10 mice were stimulated with OVA (10 nM) and myeloid dendritic cells with or without IL-33 (10 ng/ml) for 5 days followed by PMA/ionomycin restimulation and intracellular staining for cytokines. The representative dot plots of three independent experiments with similar results are shown. *G–I*, $CD4^+$ cells from D011.10 mice were stimulated with OVA peptide (10 nM) in the presence or absence of IL-33 for 72 h. Expression of ST2L was evaluated by FACS (*G*) and quantitative PCR (*H*). *I*, Representative results of ST2L expression on $CD4^+$ cells are shown. Data are presented as mean ± SEM and are representative of three independent experiments. *, $p < 0.05$ compared with control (without IL-33).

$ST2^{-/-}$/D0.11.10 mice. $IL\text{-}4R^{-/-}$ mice on the BALB/c background and $IL\text{-}4^{-/-}$ on the D0.11.10 background were provided by Dr. J. Alexander (University of Strathclyde, Glasgow, U.K.). Mice were kept at the Biological Services facilities of the University of Glasgow in accordance with the U.K. Home Office guidelines. $IL\text{-}4^{-/-}$ mice were also bred and housed at the animal facility of the Instituto de Ciências Biológicas, Universidade Federal de Minas Gerais (Belo Horizonte, Brazil).

Recombinant IL-33

IL-33 proteins were produced and purified as previously described (25). Endotoxin was removed by purification with polymyxin B columns. The purity of IL-33 was >97%. Endotoxin levels were < 0.1 endotoxin units/μg protein according to the *Limulus* amebocyte lysate QCL-1000 pyrogen test (Cambrex).

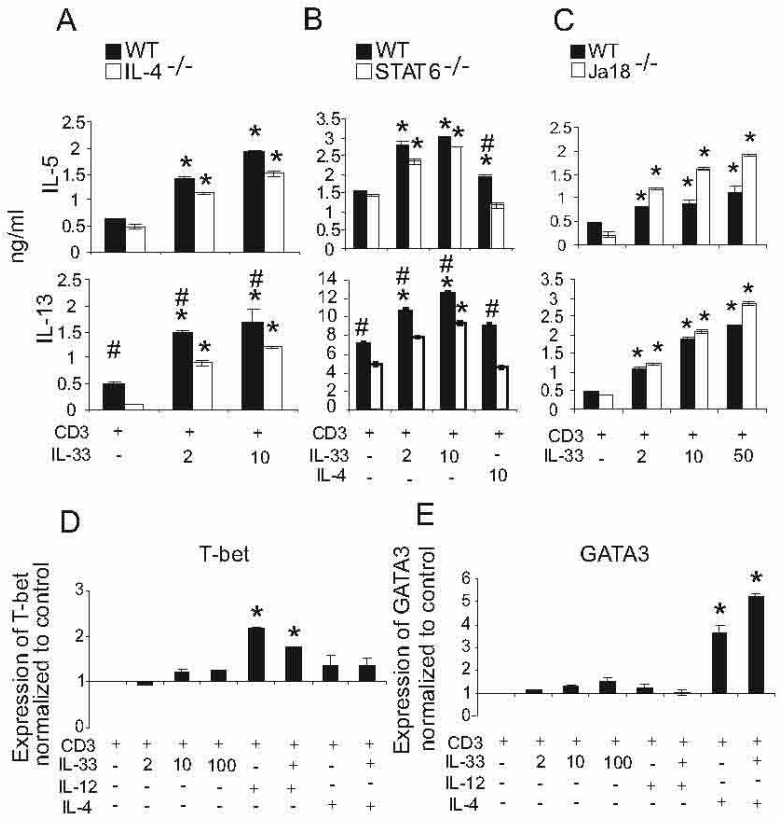


FIGURE 2. IL-33 polarizes IL-5$^+$ T cells independent of IL-4. *A–C*, CD4$^+$ cells from BALB/c (*A* and *B*), C57BL/6 (*C*), IL-4$^{-/-}$ (*A*), STAT6$^{-/-}$ (*B*), or Jα18$^{-/-}$ (*C*) mice were stimulated as described in Fig. 1, *A–C*, in the presence or absence of IL-33 or IL-4. *D* and *E*, CD4$^+$ cells from BALB/c mice were stimulated with anti-CD3 Abs (2 μg/ml) in the presence or absence of IL-33 (10 ng/ml), IL-4 (10 ng/ml), IL-12 (10 ng/ml), or a combination of these cytokines for 36 h followed by quantitative PCR. Data are presented as mean ± SEM and are representative of at least two independent experiments; *, $p < 0.05$ compared with control (without IL-33) and #, $p < 0.05$ WT vs relevant deficient mice.

CD4$^+$ T cell purification and culture

Cord blood was obtained from informed consenting mothers. Human and murine CD4$^+$ T cells were purified by negative selection (AutoMACS; Miltenyi Biotec). T cells (purity ≥98%) were cultured in RPMI 1640 supplemented with 10% FCS, 2 mM L-glutamine, 100 U/ml penicillin, 100 μg/ml streptomycin, and 0.05 M 2-ME. CD4$^+$ T cells (2×10^6 cells/ml) were activated with plate-bound anti-CD3 Abs (2–3 μg/ml; BD Biosciences), IL-4, IL-12 (all from PeproTech), and different doses of IL-33 or a combination of the cytokines. CD4$^+$ T cells from D0.11.10 mice were cultured with mitomycin C-treated APC (spleens from ST2KO mice), OVA peptide (10 nM), and cytokines as above. After 36 or 72 h, RNA and supernatants were collected for PCR and ELISA, respectively. To test the stability of IL-33-induced IL-5-producing T cells, cells stimulated with anti-CD3 Abs with or without IL-33 for 6 days were washed and restimulated with anti-CD3 Abs alone. After 72 h, supernatants were collected and ELISA was performed. To evaluate intracellular cytokine expression by IL-33-stimulated naive T cells, purified naive CD4$^+$CD62L$^+$ T cells (1.2×10^6) were cultured with bone marrow-derived myeloid dendritic cells (4×10^5) (27), OVA peptide (10 nM), and IL-33 (10 ng/ml) in 24-well plates. After 3 days, fresh medium supplemented with IL-2 (10 U/ml) was added to the culture for another 3 days. Next, cells were washed and stimulated again under the same conditions. Cells after the first and second round of stimulation were washed and activated with PMA (500 ng/ml) and ionomycin (50 ng/ml; both from Sigma-Aldrich) in the absence of IL-33 for 4 h followed by intracellular cytokine staining. To test the role of NF-κB and MAPK, CD4$^+$ cells from BALB/c mice were stimulated with anti-CD3 Abs (4 μg/ml) and IL-33 (10 ng/ml). After 5 days, cells were restimulated with immobilized anti-CD3 Abs for 24 h. Cells were then washed and rested for 2 h and incubated with IL-33 alone or in the presence of the following inhibitors or their controls: SN50M, SN50 (18 μM) SB203560 (10 μM) PD098059 (60 μM), JNK II (50 μM), or DMSO.

ELISA

Murine and human cytokines IL-4, IL-5, IL-6, IL-10, IL-13, IFN-γ, and IL-17 were analyzed by ELISA using paired Abs (BD Biosciences). Serum levels of IgE and IgG1 were measured using an OptEIA ELISA kit (BD Biosciences).

Flow cytometry

Cultured or freshly isolated cells from draining lymph nodes (DLN) or bronchoalveolar lavage (BAL) were stimulated with PMA/ionomycin for 4 h; GolgiStop was added during the final 3 h. The cells were incubated with anti-mouse CD16/32 Abs (BD Biosciences) followed by PerCP-conjugated anti-CD4 (BD Biosciences) and FITC-conjugated anti-ST2L (MD Biosciences) or F4/80 Ab and CCR3 Ab or appropriate isotype controls. Cells were then fixed with Cytofix/Cytoperm buffer (BD Biosciences), permeabilized with Perm/Wash buffer (BD Biosciences), and incubated with FITC-conjugated anti-IFN-γ, PE-conjugated anti-IL-4, allophycocyanin-conjugated anti-IL-5 (all from BD Biosciences), or rat anti-IL-33 Ab or biotinylated goat anti-IL-13 Ab (R&D Systems) or isotype controls followed by incubation with secondary Abs or streptavidin if necessary.

Western blot

CD4$^+$ T cells were stimulated with immobilized anti-CD3 Abs (4 μg/ml) in the presence of IL-33 (10 ng/ml). After 6 days, cells were restimulated with immobilized anti-CD3 Abs for 24 h and rested for 2 h. The cells were then incubated with IL-33 at different time points followed by extraction of cytoplasmic and nuclear proteins using Nuclear Extract kits (Active Motif). Cytoplasmic proteins were used in Western blotting with anti-phospho-p65, phospho-ERK1/2, phospho-p38, phospho-JNK, and p38 Abs (Cell Signaling Technology). Nuclear proteins were used to evaluate NF-κB activity with a TransAM NF-κB p62 kit (Active Motif).

Quantitative PCR

This was conducted as described previously (28, 29).

OVA-induced airway inflammation

Protocol 1. All mice were sensitized i.p. with 100 μg of OVA in 2% alum (aluminum hydroxide gel adjuvant; Brenntag) on day 0, then challenged intranasally (i.n.) on days 8–10 with 10 μg of OVA or PBS (30).

Protocol 2. To detect the effect of exogenous IL-33, the dose of OVA was reduced. Mice were immunized i.p. with 10 μg of OVA in 2% alum on day 0. On days 0–2, these mice were injected i.p. with IL-33 (2 μg/mouse) or PBS. Control mice were given PBS or IL-33 alone. Mice were challenged i.n. on days 8–10 with 2 μg of OVA, except the PBS group which received

i.n. PBS instead of OVA. All mice were sacrificed on day 11 and serum, BAL, lungs, and DLN were analyzed as described previously (31). The lung sections were stained with H&E or periodic acid-Schiff (PAS) and examined under light microscopy. Peribronchial and perivascular inflammation was scored using a semiquantitative scoring system assessing the degree of eosinophilic inflammation: 0 = no eosinophils; 1 = eosinophils make up <10% of total infiltrate or total infiltrate is <20 cells; 2 = eosinophils make up 10–50% of total infiltrate; and 3 = eosinophils make up >50% of total infiltrate. Immunohistochemical staining was performed on frozen lung sections using anti-mouse IL-33 Ab (Nessy-1; Axxora Life Science) with a biotinylated pan-specific secondary Ab followed by detection with the avidin-biotin complex/diaminobenzidine system (both Vector Laboratories). For the quantitative analysis of mucus area, images covering 81.754 μm^2 of lung sections were captured and mucus (red-stained areas) was measured with the software Image Pro-Plus (Media Cybernetics). To estimate eosinophil levels in the lungs, the eosinophil peroxidase (EPO) colorimetric assay was performed as described previously (32).

Adoptive transfer

$CD4^+$ cells were isolated from IL-$4^{-/-}$ mice sensitized with OVA or OVA plus IL-33 and challenged with OVA as described above (protocol 2). These T cells (2×10^6) or PBS were injected i.v. into naive IL-$4^{-/-}$ recipients on day 0. On days 1–3, mice were challenged with OVA (10 μg/mouse). Mice were sacrificed 24 h after the last challenge.

Statistical analysis

ANOVA followed by Tukey's test or Student's *t* test was applied to in vitro studies. Analysis between individual in vivo groups was examined by ANOVA followed by the Student-Newman-Keuls test or Student's *t* test. Experiments were performed at least twice. All data are expressed as mean ± SEM. A value of $p < 0.05$ was considered to be significant.

Results

IL-33 polarizes IL-5$^+$IL-4$^-$ T cells

Although IL-33 induces IL-5 and IL-13 production by IL-4-differentiated Th2 cells (16, 21), its role in activation of uncommitted naive T cells is unknown. To address this issue, naive $CD4^+$ T cells from WT or $ST2^{-/-}$ mice were cultured with anti-CD3 Ab with or without IL-33 for 72 h. WT but not $ST2^{-/-}$ cells produced markedly higher concentrations of IL-5 and IL-13 when stimulated with IL-33 compared with cells cultured with anti-CD3 Ab alone (Fig. 1*A*). Unexpectedly, IL-33 failed to induce any IL-4 synthesis, the signature cytokine for classical Th2 cells. IL-33 was also unable to induce IFN-γ, IL-17, or IL-10 production (Fig. 1*A* and data not shown). We further confirmed this observation by using $CD4^+CD62L^+$ naive T cells from WT or $ST2^{-/-}$ OVATcR-transgenic mice. In the presence of APC and OVA peptide, IL-33 enhanced the synthesis of IL-5 and IL-13 (but not IL-4 or IFN-γ) by WT but not $ST2^{-/-}$OVATcR-transgenic T cells (Fig. 1*B*). Furthermore, human cord blood $CD4^+$ T cells, which are mainly comprised of naive cells, also produced enhanced levels of IL-5 and IL-13 but not IFN-γ or IL-4 when cultured with anti-CD3 and IL-33 compared with anti-CD3 alone (Fig. 1*C*). Importantly, $CD4^+$T cells stimulated with anti-CD3 and IL-33 in the first round of stimulation still produced an increased amount of IL-5 and IL-13 but not IL-4 and IFN-γ after restimulation with anti-CD3 alone (Fig. 1*D*). Consistent with the cytokine ELISA data, intracellular staining shows that IL-33-polarized $CD4^+$ T cell population selectively expressed IL-5 and IL-13 but not IL-4 and IFN-γ after the first and second round of stimulation (Fig. 1, *E* and *F*, and data not shown). IL-33 also enhanced ST2 protein and mRNA expression in $CD4^+$ T cells (Fig. 1, *G–I*), suggesting a self-amplification circuit in the induction of IL-5-producing cells. Thus, IL-33, in the presence of Ag, preferentially polarizes a population of IL-5^+IL-13^+IL-4^- T cells.

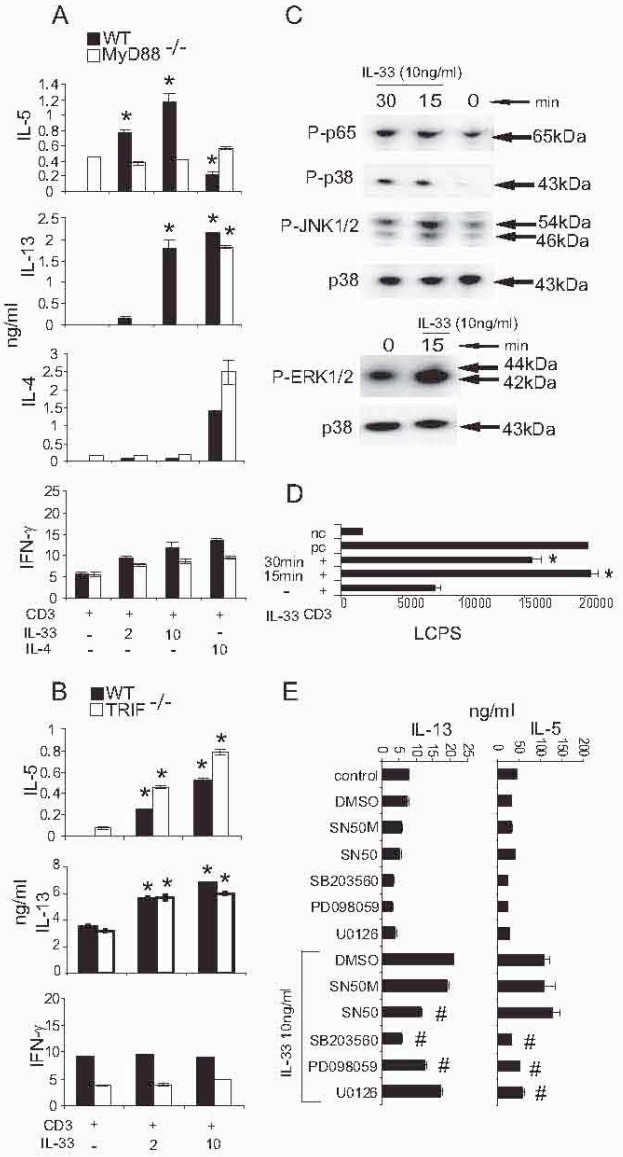


FIGURE 3. IL-33 induces cytokine production via MyD88 and p38. *A* and *B*, Naive $CD4^+$ cells from C57BL/6 (*A* and *B*), MyD88$^{-/-}$ (*A*), or TRIF$^{-/-}$ (*B*) mice were stimulated as described in Fig. 1, *A–C*. *C–E*, $CD4^+$ T cells stimulated with immobilized anti-CD3 Abs were rested for 2 h followed by incubation with IL-33 and/or various inhibitors: NF-κB (SN50 or control SN50M), p38 (SB203560), or ERK1/2 (PD098059 and U0126) for different time points. *C*, Cytosolic proteins were Western blotted with Abs specific for phosphorylated (P) p65, p38, JNK1/2, ERK1/2, and non-phosphorylated p38 (loading control). *D*, Nuclear proteins were evaluated in a TransAM NF-κB p65 assay (nc, negative control; pc, positive control provided by the assay kit; LCPS, luminescence count per second). *E*, The amount of IL-5 and IL-13 was determined by ELISA. Data are presented as mean ± SEM and are representative of at least two independent experiments. *, $p < 0.05$ compared with control (without IL-33) and #, $p < 0.05$, IL-33 plus inhibitors vs IL-33 alone.

IL-33 induces IL-5-producing T cells independent of IL-4, IL-4R, and STAT6

IL-4, IL-4R, and STAT6 are essential for classical Th2 cell development (33–35). To further characterize the IL-33-polarized IL-5^+T cells, we tested whether IL-33 is able to activate $CD4^+$ T cells in the absence of IL-4, IL-4Rα, or STAT6. As shown in Fig. 2*A*,

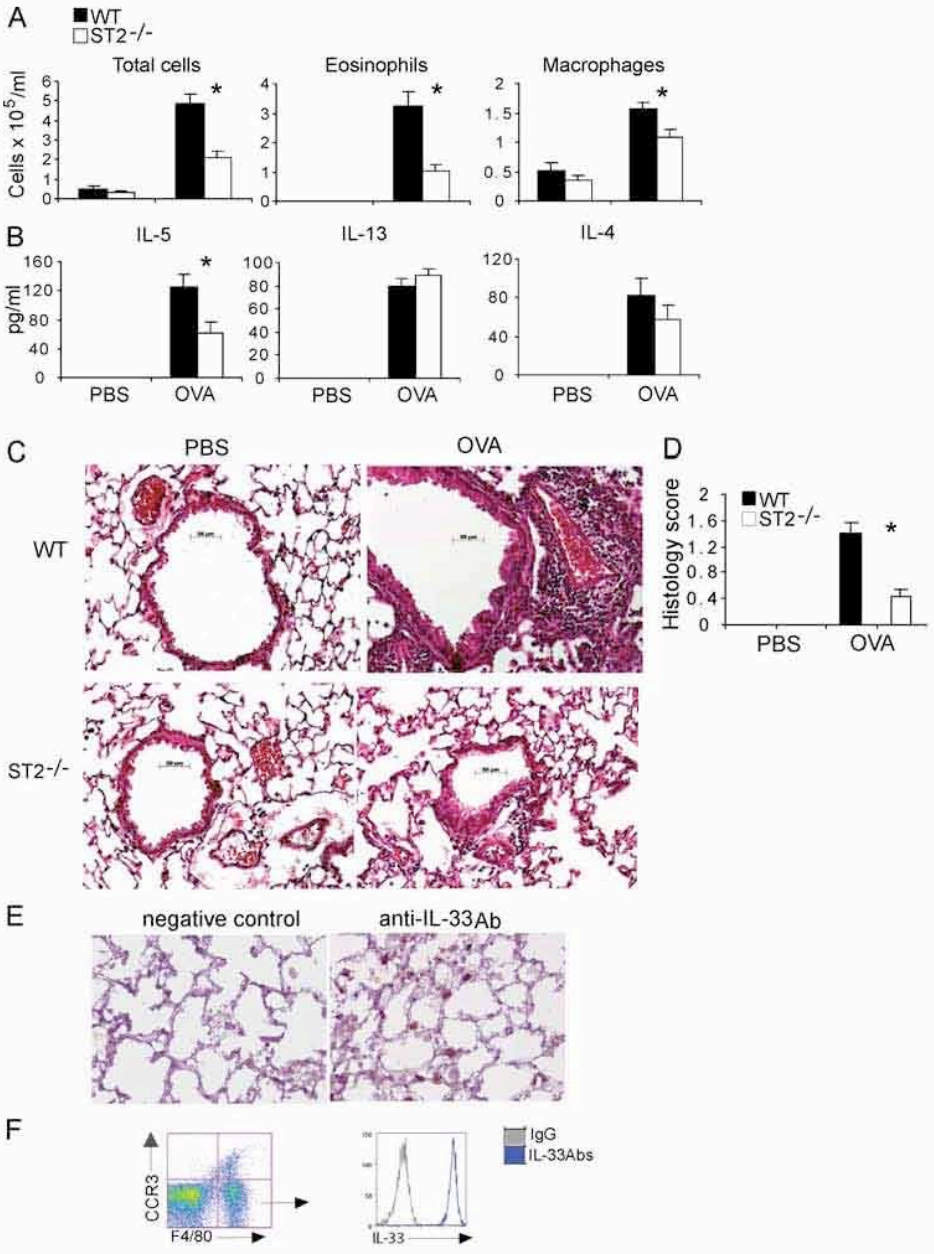


FIGURE 4. ST2$^{-/-}$ mice develop attenuated OVA-induced airway inflammation. BALB/c and ST2$^{-/-}$ mice were sensitized by i.p. injection of 100 μg of OVA in 2% alum. Allergic airway inflammation was induced by i.n. instillation of 10 μg of OVA on days 8–10. Negative controls were mice challenged with PBS alone. Mice were culled 24 h after the third challenge. *A*, Total cells, eosinophil, and macrophage cell counts in the BAL. *B*, Cytokine concentrations in the BAL were measured by ELISA. *C* and *D*, H&E-stained lung sections were examined by light microscopy and eosinophils identified by morphology. *C*, Photomicrographs show representative sections from BALB/c and ST2$^{-/-}$ mice challenged with PBS or OVA. Original magnification, ×20. *D*, The extent of peribronchial and perivascular inflammation was scored. Data are means ± SEM, n = 8, and are representative of three independent experiments. *, $p < 0.05$, WT vs ST2$^{-/-}$ mice. *E* and *F*, IL-33 is present in the lungs. *E*, Immunohistochemical staining of lung sections with anti-IL-33 Ab shows the presence of IL-33 (brown) in lungs of mice primed and challenged with OVA, original magnification, ×40; negative control, tissue stained without primary Ab. *F*, F4/80$^+$ CCR3$^-$ alveolar macrophages were stained with anti-IL-33 Abs or appropriate isotype control. Data are representative histogram of two independent experiments.

IL-33 increased IL-5 and IL-13 production in both WT and IL-4$^{-/-}$ cells, although the level of IL-13 remained slightly lower in IL-4$^{-/-}$ compared with WT. Similar results were observed with CD4$^+$ T cells from IL-4R$\alpha^{-/-}$ mice (data not shown) and STAT6$^{-/-}$ mice (Fig. 2*B*). Invariant NKT (iNKT) cells can also express CD4 and have been shown to be involved in type 2 immunity (36). To exclude a role for iNKT cells in this context, we polarized CD4$^+$ T cells from iNKT-deficient Jα18$^{-/-}$ mice (37). CD4$^+$ T cells from WT and Jα18$^{-/-}$ mice produced comparable levels of IL-5 and IL-13 when activated with IL-33 and anti-CD3 (Fig. 2*C*), indicating that NKT cells did not contribute to the IL-33-induced IL-5-producing T cells. IL-33 did not significantly affect the production of IFN-γ or IL-4 in IL-4$^{-/-}$, IL-4R$^{-/-}$, STAT6$^{-/-}$, or Jα18$^{-/-}$ mice (data not shown). Taken together, these results demonstrate that IL-33 triggers IL-5 and IL-13 production from naive CD4$^+$ T cells independent of IL-4, IL-4Rα, and STAT6 signaling.

We also investigated the involvement of GATA3 and T-bet in IL-33-induced T cell polarization. IL-4 and IL-12 induced the transcription of GATA3 and T-bet, respectively (38, 39). In contrast, IL-33 failed to induce GATA3 or T-bet even at high concentrations (Fig. 2, *D* and *E*). These results indicate that IL-33 polarizes the IL-5-producing T cell via a distinct signaling pathway from Th1 or classical Th2 cells.

IL-33 polarizes IL-5-producing T cells via MyD88

As a member of the IL-1 family, IL-33 may signal via the MyD88-dependent and -independent pathways (21, 40, 41). We therefore investigated the role of MyD88 and Toll/IL-1R domain-containing adaptor-inducing IFN-β (TRIF) in IL-33-mediated T cell polarization. As shown in Fig. 3*A*, IL-33 failed to induce IL-5 and IL-13 secretion by MyD88$^{-/-}$ T cells. In contrast, IL-33 stimulated normal levels of IL-5 and IL-13 production by CD4$^+$ cells from

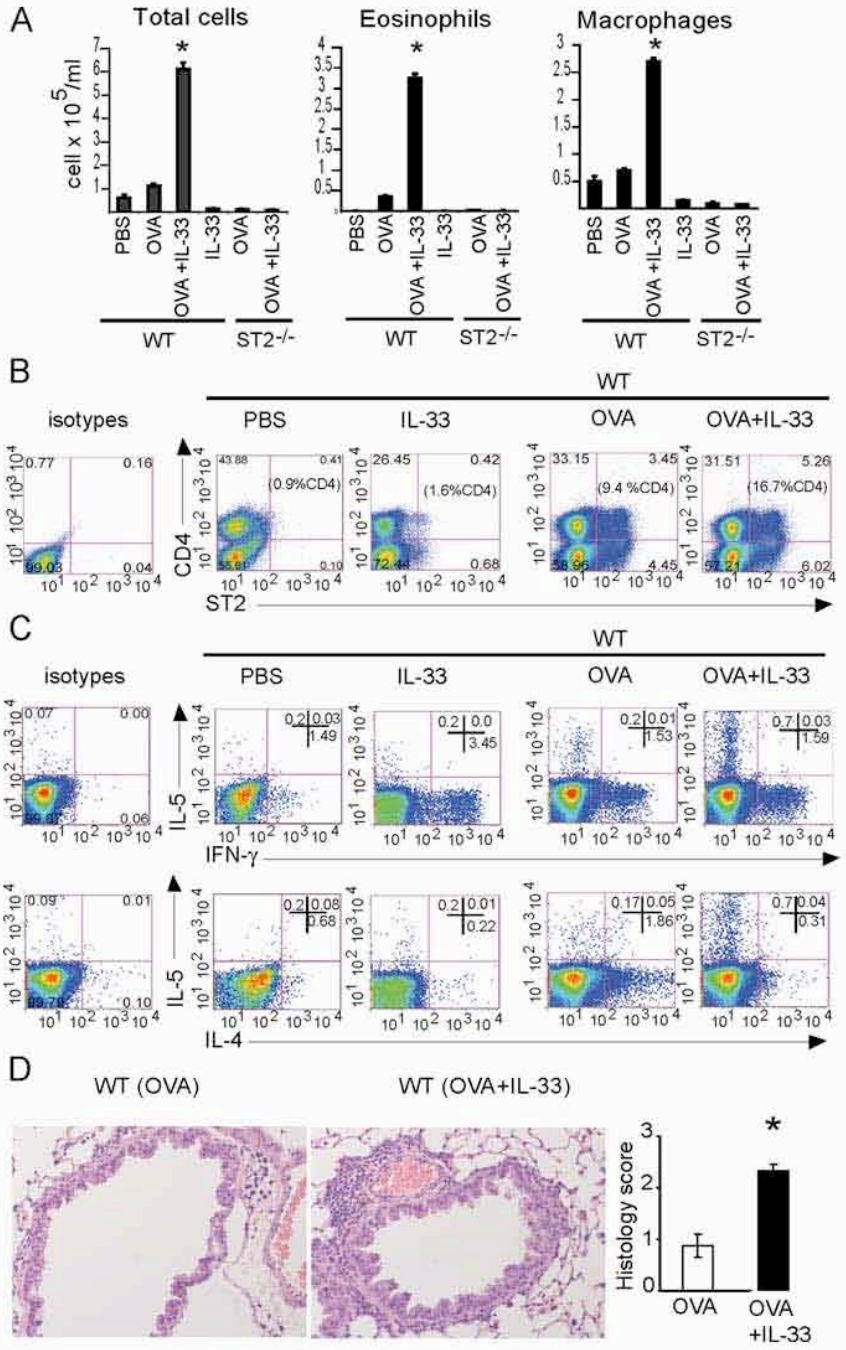


FIGURE 5. IL-33 polarizes IL-5-producing cells in vivo and exacerbates OVA-induced airway inflammation. WT and ST2$^{-/-}$ BALB/c mice were sensitized by i.p. injection of 10 μg of OVA on day 0 and IL-33 (2 μg/mouse) or PBS were given i.p. on days 0–2. Some mice were treated with IL-33 or PBS alone. Mice were challenged i.n. on days 8–10 with 2 μg of OVA. Mice were sacrificed on day 11. *A*, Total cells, eosinophil, and macrophage cell counts in the BAL. *B*, ST2L expression on DLN cells is shown. *C*, Intracellular staining for IFN-γ, IL-5, and IL-4 in CD4$^+$ cells from the DLN is shown. *D*, H&E staining of lung sections were examined by light microscopy and eosinophils identified by morphology. Photomicrographs of representative lung sections from WT mice sensitized and challenged with OVA and treated with PBS (OVA) or IL-33 (OVA + IL-33) are shown. Original magnification, ×20. The extent of peribronchial and perivascular inflammation was scored. Data are means ± SEM, $n = 10$, and are representative of two independent experiments. *, $p < 0.05$, IL-33 treated vs control mice.

TRIF$^{-/-}$ mice (Fig. 3*B*). Thus, IL-33 polarization of IL-5- producing T cells was MyD88 dependent but TRIF independent. We further explored the involvement of the key signaling components in IL-33 signaling. It has been reported that IL-33 triggers all three MAPK pathways and the NF-κB pathway in mast cells (16, 20). Little, however, is known about the signaling pathways triggered by IL-33 in T cells and their contribution to cytokine production. We found that IL-33 induced the phosphorylation of NF-κBp65 and the MAPK p38, JNK1/2, and ERK1/2 (Fig. 3*C*). The NF-κB activity induced by IL-33 was further confirmed by nuclear translocation of NF-κBp65 (Fig. 3*D*). IL-33-induced IL-5 synthesis was suppressed by the inhibitors of p38 (SB203560), ERK1/2 (PD098059 and U0126), and JNK1/2 (JNK II) but not by the inhibitor of NF-κB (SN50) (Fig. 3*E* and data not shown). In contrast, the production of IL-13 was suppressed by p38, NF-κB, and, to a lesser extent, by ERK1/2 and JNK1/2 inhibitors (Fig. 3*E* and data not shown). Thus, IL-33 polarizes IL-5- producing T cells via the ST2, MyD88, MAPK, and NF-κB pathways. Interestingly, IL-33 appears to induce IL-5 and IL-13 production by different signaling mechanisms.

ST2$^{-/-}$ mice develop attenuated allergic airway inflammation

The role of ST2 in the asthma model is controversial (10, 11, 13–15, 42). We sought to further determine the role of ST2/IL-33 in type 2 responses by using WT and ST2$^{-/-}$ BALB/c mice in the OVA-specific model of airway inflammation (30). WT and ST2$^{-/-}$ mice were sensitized once with OVA (100 μg), then challenged i.n. with 10 μg of OVA for 3 subsequent days. ST2$^{-/-}$ mice showed significantly less severe airway inflammation compared with WT mice. This was evident in a reduced number of

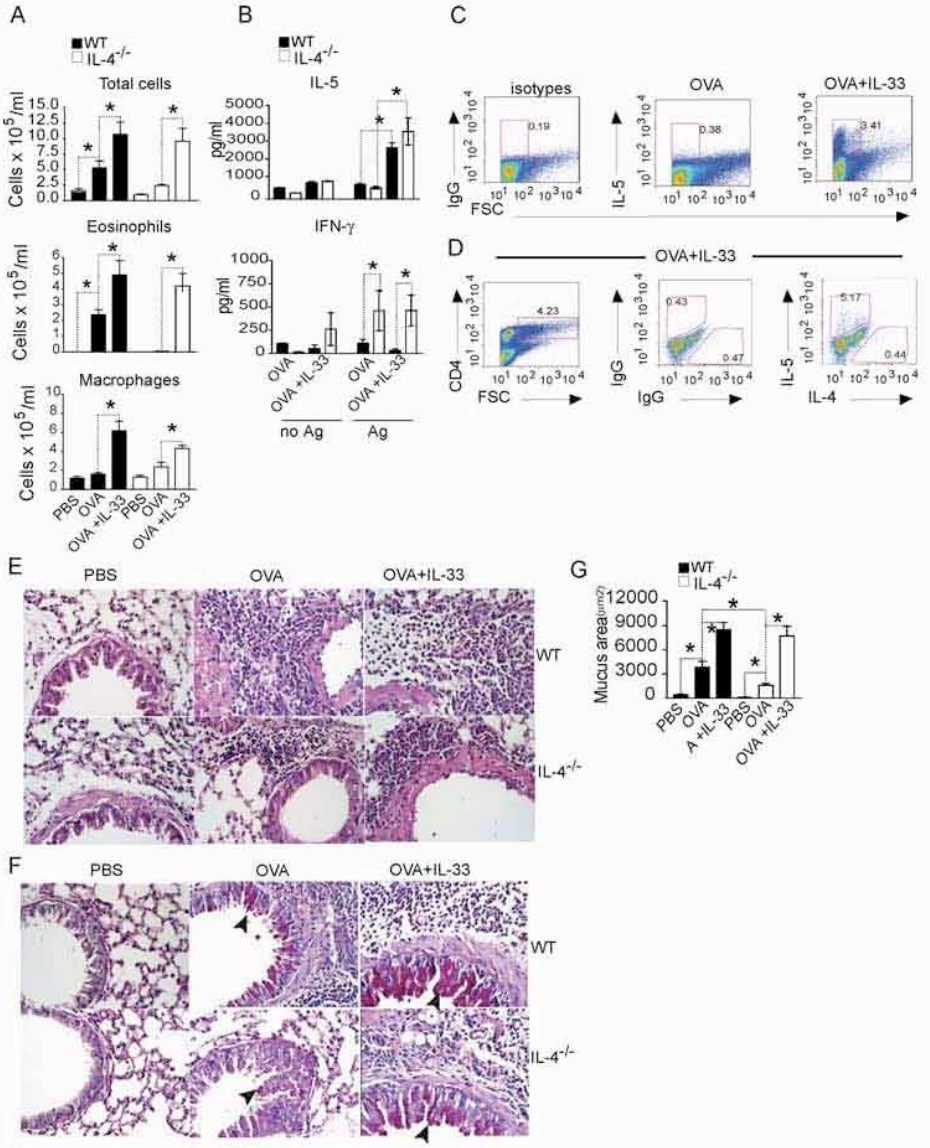


FIGURE 6. IL-33 polarizes IL-5-producing T cells and exacerbates airway inflammation independent of IL-4. WT and IL-4$^{-/-}$ BALB/c mice were sensitized and challenged as in Fig. 5. *A*, Total, eosinophil, and macrophage cell counts in the BAL. *B*, Cytokine concentrations in the culture supernatant of DLN cells cultured with OVA were assayed by ELISA. *C*, Intracellular staining for IL-5 in total DLN cells of IL-4$^{-/-}$ mice sensitized with OVA or OVA + IL-33 is shown. *D*, Intracellular staining for IL-5 and IL-4 in CD4$^+$ T cells from DLN of IL-4$^{-/-}$ mice sensitized and challenged with OVA + IL-33 is shown. *E* and *F*, Representative lung sections from WT and IL-4$^{-/-}$ mice sensitized with OVA or OVA + IL-33 or PBS alone were stained with H&E (*E*) or PAS (*F*). Original magnification, ×20. PAS$^+$ mucus cells are red and identified with arrows. *G*, Quantitative analysis of mucus area is shown. Results were expressed as the mean of mucus area per μm^2 of tissue. Data are means ± SEM, $n = 8$, and are representative of two independent experiments. *, $p < 0.05$ as indicated. No Ag, no Ag in the culture; Ag, Ag added to the culture.

total cells, eosinophils, and macrophages in the BAL of the ST2$^{-/-}$ mice compared with WT mice (Fig. 4*A*). The BAL from ST2$^{-/-}$ mice also contained significantly less IL-5 than that of the WT mice, but IL-13 and IL-4 levels were not significantly different (Fig. 4*B*). The serum IgE and IgG levels were similar in the ST2$^{-/-}$ and WT mice (data not shown). ST2$^{-/-}$ mice also exhibited reduced lung pathology after Ag challenge, showing significantly less inflammatory cell infiltration in the peribronchial and perivascular areas of the lungs than that of the WT mice (Fig. 4, *C* and *D*). The contribution of endogenous IL-33 in OVA-induced airway inflammation was further supported by our immunohistochemical analysis which clearly demonstrated the presence of endogenous IL-33 in the lungs of mice sensitized and challenged with OVA (Fig. 4*E*). Since the morphological appearance of IL-33-positive cells suggested that these might be macrophages, we isolated alveolar macrophages and stained them with anti-IL-33-specific Ab. Indeed, as shown in Fig. 4*F*, F4/80$^+$CCR3$^-$ alveolar macrophages abundantly expressed IL-33. Altogether these results therefore demonstrate that IL-33/ST2 signals are required for an optimal allergen induced-airway inflammation and IL-5 but not IL-4 production.

IL-33 induces IL-5$^+$IL-4$^-$ T cells in vivo and exacerbates Ag-induced airway inflammation

Our result from ST2$^{-/-}$ mice, as well as previous data showing the beneficial effect of soluble ST2 in airway inflammation (11), suggested that IL-33 participates in Ag-specific airway inflammation. We therefore further investigated whether IL-33 could induce IL-5-producing T cells in vivo and exacerbate OVA-triggered airway inflammation. To be able to define the effect of exogenous IL-33, we reduced the dose of OVA in our model. As shown in Fig. 5*A*, mice sensitized (10 μg) and challenged (2 μg) with OVA alone exhibited a low inflammatory response in the BAL. In contrast, mice sensitized with OVA plus IL-33 displayed markedly elevated total cell numbers, eosinophils, and macrophages in the BAL (Fig. 5*A*). The IL-33-enhanced inflammation was not evident in ST2$^{-/-}$ mice. Importantly, OVA-nonsensitized WT mice injected with IL-33 and challenged with OVA showed no increase in the total cell count and eosinophilia compared with the PBS group. We then analyzed the ST2 expression and cytokine profile on DLN T cells. IL-33 administration without Ag sensitization slightly increased the percentage of CD4$^+$ ST2$^+$ cells compared with the PBS group

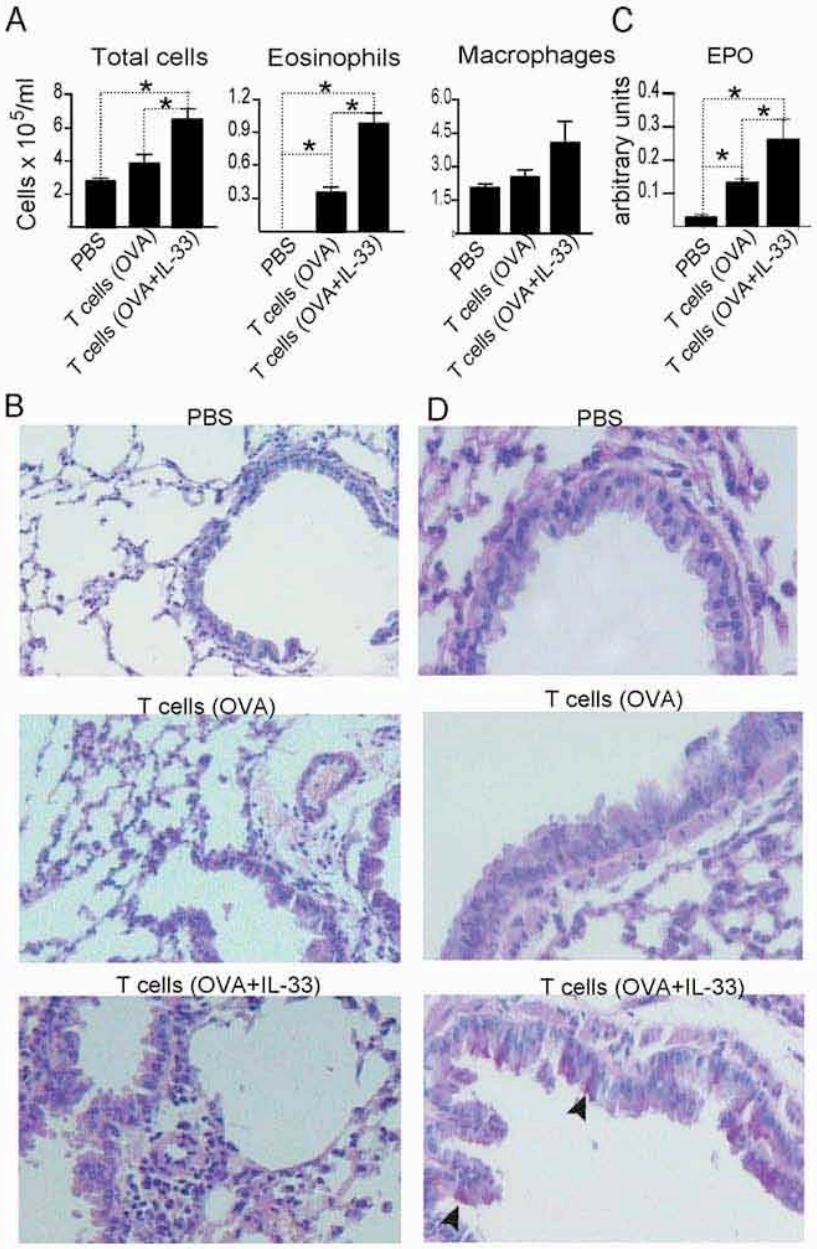


FIGURE 7. Adoptive transfer of IL-33-polarized OVA-specific IL-5$^+$IL-4$^-$ T cells induces airway inflammation independent of IL-4. CD4$^+$ cells were isolated from IL-4$^{-/-}$ mice sensitized with OVA or OVA + IL-33 as in Fig. 5. These T cells (2×10^6) or PBS were injected i.v. into naive IL-4$^{-/-}$ recipients on day 0. All recipients were challenged with OVA (10 μg/mouse) on days 1–3 and sacrificed on day 4. *A*, Total cell, eosinophil, and macrophage counts in the BAL. *B*, Representative H&E-stained lung sections from recipients receiving T cells from OVA or OVA + IL-33-treated IL-4$^{-/-}$ mice are shown. Original magnification, ×20. *C*, The level of EPO in lung homogenates. *D*, Representative lung sections stained with PAS for mucus-producing cells are shown. Original magnification, ×40. PAS$^+$ mucus cells are red and identified with arrows. Data are means ± SEM, $n = 5$, and are representative of two independent experiments. *, $p < 0.05$ as indicated.

(1.6 and 0.9%, respectively; Fig. 5*B*). Cells from WT mice sensitized and challenged with OVA showed a substantial increase in the percentage of ST2$^+$CD4$^+$ cells (9.4%). This was further increased by the IL-33 treatment at sensitization (16.7%). Intracellular staining of DLN CD4$^+$ T cells revealed that IL-33 alone had no effect on the type 2 cytokine profile, but increases the percentage of IFN-γ^+ cell population compared with the PBS group. In contrast, CD4$^+$ cells from OVA-sensitized and challenged mice showed an increase in percentage of IL-4$^+$ cells but not IL-5$^+$ cells compared with either IL-33 alone or the PBS-treated groups. Importantly, the administration of IL-33 during the OVA sensitization markedly enhanced the percentage of IL-5$^+$ T cells but decreased the percentage of IL-4$^+$ T cells and did not change the percentage of IFN-γ^+ cells compared with the OVA group (Fig. 5*C*). The injection of IL-33 in the OVA- sensitizing phase also triggered IL-13 production in WT mice (66.6 ± 4.4 pg/ml), which was undetectable in other groups. IL-33 did not affect the cytokine production by CD4$^+$ T cells in ST2$^{-/-}$ mice (data not shown). Thus, IL-33 markedly and specifically increased the number of CD4$^+$IL-5$^+$ T cells in vivo during Ag priming via ST2. Lung histology analysis showed that IL-33 given during OVA sensitization significantly increased inflammatory cell infiltration in the peribronchial and perivascular areas of the lungs compared with that from mice injected with OVA alone (Fig. 5*D*). Mice given PBS or IL-33 without Ag did not have any detectable histological changes (data not shown). Together, these results suggest that IL-33 is a pathogenic factor for Ag-specific airway inflammation accompanied by the polarization of CD4$^+$IL-5$^+$ T cells in vivo.

IL-33 exacerbates allergic airway inflammation independent of IL-4

To further investigate the relationship between IL-33 and IL-4 in the polarization of IL-5-producing T cells and allergic response, we determined whether IL-33 can induce allergic airway inflammation in IL-4$^{-/-}$ mice. IL-4$^{-/-}$ and WT mice were sensitized with OVA or OVA plus IL-33 and challenged with OVA as before.

IL-4$^{-/-}$ mice developed less severe allergic inflammation as demonstrated by the number of total cells, eosinophils, and macrophages in the BAL compared with those in WT mice when sensitized and challenged with OVA alone. This cellular deficit was completely reversed by the presence of IL-33 at sensitization (Fig. 6*A*). The airway inflammation in OVA plus IL-33-treated WT and IL-4$^{-/-}$ mice was accompanied by elevated IL-5 and IL-13 synthesis in DLN cells when restimulated with OVA peptide in vitro (Fig. 6*B* and data not shown). Intracellular cytokine staining confirmed that DLN cells from IL-4$^{-/-}$ mice sensitized and challenged with OVA alone produced limited amounts of IL-5. Treatment with IL-33 during OVA sensitization significantly increased the percentage of IL-5$^+$ cells (Fig. 6*C*). Gating on the CD4$^+$ cell population revealed the presence of an increased percentage of CD4$^+$IL-5$^+$ T cells in IL-4$^{-/-}$ mice treated with OVA and IL-33 compared with mice treated with OVA alone (Fig. 6*D*). Furthermore, IL-33 treatment increased cellular infiltration in the peribronchial and perivascular areas of the lungs of the IL-4$^{-/-}$ mice to a level comparable to that in the WT mice (Fig. 6*E*). The administration of IL-33 during sensitization also enhanced goblet cell hyperplasia and mucus production in the airways of WT and IL-4$^{-/-}$ mice (Fig. 6, *F* and *G*). Taken together, these results demonstrate that in the presence of allergen, IL-33 can induce a population of IL-5-producing T cells and airway pathology in vivo in the absence of IL-4.

Adoptive transfer of IL-33-polarized IL-5$^+$IL-4$^-$ T cells triggers airway inflammation in an IL-4-free environment

To confirm that IL-5-producing T cells can mediate the allergic airway inflammation in IL-4$^{-/-}$ mice, CD4$^+$ cells from IL-4$^{-/-}$ mice sensitized and challenged with OVA, with or without IL-33 at sensitization, were purified and adoptively transferred into naive IL-4$^{-/-}$ recipients. Control mice were injected with PBS. All recipients were challenged with OVA peptide i.n. the day after cell transfer for 3 subsequent days. Adoptive transfer of T cells from OVA or OVA plus IL-33-treated mice increased the total number of inflammatory cells in the BAL of the recipients (Fig. 7*A*). However, the number of cells in the BAL was significantly higher in mice receiving CD4$^+$ cells from OVA plus IL-33-treated mice compared with those with T cells from mice given OVA alone. Differential cell counts revealed that whereas transfer of T cells from OVA-treated donors induced a modest increase in eosinophil and macrophage influx into the BAL, a significantly higher number of eosinophils and, to a lesser extent, macrophages were found in recipients receiving T cells from OVA plus IL-33-treated donors. Histological examination showed that injection of T cells from OVA plus IL-33-treated mice induced significantly increased cellular infiltration in the peribronchial and perivascular areas of the lungs of the recipients compared with mice that received PBS or T cells from OVA-treated mice (Fig. 7*B*). Assay for EPO confirmed the presence of eosinophils in the lung tissue (Fig. 7*C*). In addition, mice receiving CD4$^+$ T cells from OVA plus IL-33-treated mice developed an increased mucus production compared with other groups (Fig. 7*D*). Thus, IL-33-polarized IL-5$^+$IL-4$^-$ CD4$^+$ T cells are able to induce allergic airway inflammation in the complete absence of IL-4.

Discussion

Data presented here demonstrate that the newly discovered cytokine IL-33 is a potent driver of a population of CD4$^+$ T cells producing mainly IL-5 and IL-13 but not IL-4. The IL-33-induced IL-5-producing T cells differ from the classical Th2 cells in several aspects. Th2 cells are driven by IL-4 via IL-4R and produce principally IL-4 (43). In contrast, the IL-5-producing T cells reported here are polarized by IL-33 via ST2 and secrete mainly IL-5 and IL-13 but not IL-4. Moreover, differentiation of Th2 cells requires signaling via STAT6 (34) and GATA3 (38, 39), whereas IL-33 failed to induce GATA3 or T-bet and induced IL-5$^+$ T cell differentiation through the classical Toll/IL-1R pathway via MyD88, MAPKs, and NF-κB, independent of IL-4 and STAT6. It should be noted that naive CD4$^+$ cells can be polarized into IL-5-producing T cells only in the presence of TCR activation. This is consistent with a recent report that, in contrast to IL-18, IL-33 does not stimulate CD4$^+$ cells in the absence of TCR engagement (21).

The role of ST2 in the asthma model has been controversial (10, 11, 13–15, 42). Data presented here clearly demonstrate that IL-33 is important for Ag-specific asthma. Consistent with the mRNA data reported previously (44), we show here that IL-33 protein is abundantly expressed in the lungs of mice with OVA-induced airway inflammation and alveolar macrophages are one of the cell types that express IL-33. Importantly, we also found that ST2 deficiency resulted in a significantly attenuated OVA-induced IL-5 but not IL-4 and IL-13 production, eosinophilia in the BAL and lung inflammation. Our results are in agreement with a previous report which demonstrated that treatment with soluble ST2 ameliorated OVA-induced airway inflammation (11) and with the finding that ST2 is not required for IL-4 production (14). However, our results are in contrast to the reports that ST2$^{-/-}$ mice developed unchanged or enhanced eosinophilia in the airway inflammation (14, 42). This discrepancy can be explained by the difference in the mouse strain used and experimental protocols. Our data presented here are based on ST2$^{-/-}$ of the BALB/c background and a short model of asthma, using only one sensitization and three challenges over a period of 12 days (30) In agreement with the report of Hoshino et al. (14), we failed to detect any significant difference between WT and ST2$^{-/-}$ mice by using the long protocol with two sensitizations and four challenges over a period of 28 days. All together, it appears that the preferential contribution of IL-33/ST2 signaling to allergic airway inflammation may depend on the time and dose of Ag, with IL-33/ST2 more involved in acute response than chronic immune response. Consistent with this notion, we demonstrate here that administration of IL-33 along with a low dose of Ag (OVA, 10 μg) selectively promoted allergen-specific IL-5-producing T cells but not the classical IL-4-producing Th2 cells and exacerbated airway inflammation. However, in the presence of the standard dose of OVA (100 μg), IL-33 enhanced the induction of both classical Th2 and IL-5$^+$IL-4$^-$ T cells (data not shown). This finding suggests that the preferential induction of the IL-5-producing T cells over the classical Th2 cells might be largely determined by the dose of allergen and the availability of IL-33 during sensitization. Importantly, we demonstrated that IL-33 could drive the development of Ag-specific IL-5-producing T cells in vivo and exacerbate OVA-induced airway inflammation in IL-4$^{-/-}$ mice to a similar extent as in WT mice. Furthermore, adoptive transfer of OVA plus IL-33-polarized T cells from IL-4$^{-/-}$ asthmatic mice into naive IL-4$^{-/-}$ mice induced airway inflammation. These data clearly demonstrate that IL-33 is capable of driving a population of IL-5-producing T cells independent of IL-4 and may play an important role in allergic airway inflammation.

Several cytokines, including IL-25, IL-1, and IL-18, can induce IL-5 and IL-13 in conjunction with IL-4 (45–50). To our knowledge, IL-33 is the only cytokine described to date which polarizes IL-4-independent IL-5$^+$ T cells. These results also suggest that type 2 responses may result from at least two pathways: the IL-4-dependent and the IL-33-dependent pathways. Both routes might be required for an optimal type 2 response, since these responses are reduced in IL-4$^{-/-}$ and ST2$^{-/-}$ mice (2, 13). Our finding may

also explain the long-held conundrum that ST2 played an important role in type 2 responses, but was not required for the Th2 cell development in $ST2^{-/-}$ mice (10, 11, 13–15).

Interestingly, an increase in the percentage of IFN-γ^+CD4^+ cells in mice given IL-33 without Ag indicates that IL-33 may amplify existing type 1 responses in these mice. This is in agreement with recent findings that IL-33 can affect both type 2 and type 1 immune responses depending on local environment (51).

Schmitz et al. (16) observed a systemic innate type 2 response in conjunction with lung eosinophilia in naive mice when 2 μg of IL-33 was administrated i.p. daily for 7 days (16). We evaluated a contribution of IL-33-induced innate immunity to our experimental model by administration of IL-33 but not Ag at the sensitization phase followed by Ag challenge. We found that without Ag at sensitization, a low dose of IL-33 (2 μg) and a short time of administration (3 days) failed to induce inflammation in the lungs. It thus appears that in our experimental model, IL-33- driven exacerbation of OVA-induced airway inflammation is mainly attributed to the direct effect of IL-33 on adaptive rather than innate immunity such as mast cells, NK cells, or basophils. Along this line, we have found that IL-33 did not affect the total cell number or eosinophilia in the BAL of mast cell-deficient (Kit^{Wsh}/Kit^{Wsh}) mice treated with IL-33 (N. Pitman, G. Murphy, D. Xu, and F. Y. Liew, unpublished data), which was recently confirmed by Kondo et al. (21).

Our earlier report (26) shows that ST2 down-regulated the LPS-induced inflammatory response. Thus, $ST2^{-/-}$ mice produced more IL-1, TNF-α, and IL-12 in response to LPS stimulation and were more susceptible to LPS-induced shock compared with WT mice. In the present study, the levels of IL-1, TNF-α, and IL-12 production could not be detected in WT and $ST2^{-/-}$ mice in the experimental asthma setting. This result suggests that even if the OVA used was contaminated with trace amounts of LPS (<0.18 endotoxin units/μg by *Limulus* test), the effect observed was unlikely to be due to LPS-induced shock. Therefore, ST2 may play different roles in allergic response and LPS tolerance.

Although the molecular mechanism by which IL-33 preferentially induces IL-5/IL-13 is currently unknown, IL-5 and IL-13 are likely to be responsible for IL-33-induced exacerbation of OVA-specific airway inflammation in WT and $IL\text{-}4^{-/-}$ mice. IL-5 is critical for eosinophil differentiation, recruitment from bone marrow, and migration to the lungs (52). IL-13 stimulates mononuclear cell influx to the lungs by triggering a variety of chemokines from resident lung cells (53, 54). It is also well documented that IL-13 is indispensable for epithelial cell hyperplasia, mucus production, and IgE synthesis (16, 21, 53, 54). Although IL-33/ST2 may not be able to drive the classical Th2 cell differentiation directly, it may still be able to increase IL-4 synthesis by Th2 cells indirectly (16, 23, 24, 55), possibly via the production of IL-13, vascular endothelial growth factor, and GM-CSF which have been reported to enhance Th2 cell polarization (55–57). We have detected an increase in vascular endothelial growth factor and GM-CSF production by IL-33-stimulated $CD4^+$ T cells (data not shown). In addition, IL-33 enhanced the expression of ST2 on both $IL\text{-}5^+CD4^+$ and classical Th2 cells and stimulated IL-5 and IL-13 production by mature Th2 cells (16, 21). Therefore, it is likely that IL-33 is capable of activating both IL-4-dependent (indirectly) and IL-4-independent (directly) pathways.

IL-33 is clearly detected in clinical disease (58). Moreover IL-33 mRNA (44) and protein are present in the lungs of mice with OVA-induced airway inflammation. We propose here that under pathological conditions such as the presence of allergens, locally expressed IL-33 may polarize IL-5-producing T cells even in the absence of IL-4. In addition, our study provides a possible mechanism explaining the existence and activation of IL-5-producing T cells in IL-4-deficient mice in different disease models (3, 6–9). Importantly, there is an increasing interest in different pathological phenotypes of asthma and how they relate to clinical syndromes and respond to treatment (59). Therefore, further clinical studies into the relative contribution of classical Th2 cells and IL-33-triggered IL-5-producing T cells to airway inflammation and changes in airway physiology may provide important insights into the etiology of different phenotypes of asthma, which may provide a novel therapeutic target.

Acknowledgments

We thank Roderick Ferrier and Dr. Ashley Miller for experimental assistance. The cells from $J\alpha18^{-/-}$ mice were provided by Prof. Vincenzo Cerundolo (Weatherall Institute of Molecular Medicine, University of Oxford, U.K.). Cells from $MyD88^{-/-}$ mice were provided by Prof. Richard K. Grencis (University of Manchester, Manchester, U.K.). Cells from $TRIF^{-/-}$ mice were provided by Dr Clare Bryant (University of Cambridge, Cambridge, U.K.). $IL\text{-}4^{-/-}$ and $IL\text{-}4R^{-/-}$ mice were generously provided by Prof. James Alexander (University of Strathclyde).

Disclosures

The authors have no financial conflict of interest.

References

1. McKenzie, G. J., P. G. Fallon, C. L. Emson, R. K. Grencis, and A. N. McKenzie. 1999. Simultaneous disruption of interleukin (IL)-4 and IL-13 defines individual roles in T helper cell type 2-mediated responses. *J. Exp. Med.* 189: 1565–1572.
2. Kopf, M., G. Le Gros, M. Bachmann, M. C. Lamers, H. Bluethmann, and G. Kohler. 1993. Disruption of the murine IL-4 gene blocks Th2 cytokine responses. *Nature* 362: 245–248.
3. Pearce, E. J., A. Cheever, S. Leonard, M. Covalesky, R. Fernandez-Botran, G. Kohler, and M. Kopf. 1996. *Schistosoma mansoni* in IL-4-deficient mice. *Int. Immunol.* 8: 435–444.
4. Noben-Trauth, N., P. Kropf, and I. Muller. 1996. Susceptibility to *Leishmania major* infection in interleukin-4-deficient mice. *Science* 271: 987–990.
5. von der Weid, T., M. Kopf, G. Kohler, and J. Langhorne. 1994. The immune response to *Plasmodium chabaudi* malaria in interleukin-4-deficient mice. *Eur. J. Immunol.* 24: 2285–2293.
6. Hogarth, P. J., M. J. Taylor, and A. E. Bianco. 1998. IL-5-dependent immunity to microfilariae is independent of IL-4 in a mouse model of onchocerciasis. *J. Immunol.* 160: 5436–5440.
7. Brewer, J. M., M. Conacher, C. A. Hunter, M. Mohrs, F. Brombacher, and J. Alexander. 1999. Aluminum hydroxide adjuvant initiates strong antigen-specific Th2 responses in the absence of IL-4- or IL-13-mediated signaling. *J. Immunol.* 163: 6448–6454.
8. Hogan, S. P., A. Mould, H. Kikutani, A. J. Ramsay, and P. S. Foster. 1997. Aeroallergen-induced eosinophilic inflammation, lung damage, and airways hyperreactivity in mice can occur independently of IL-4 and allergen-specific immunoglobulins. *J. Clin. Invest.* 99: 1329–1339.
9. Herrick, C. A., H. MacLeod, E. Glusac, R. E. Tigelaar, and K. Bottomly. 2000. Th2 responses induced by epicutaneous or inhalational protein exposure are differentially dependent on IL-4. *J. Clin. Invest.* 105: 765–775.
10. Xu, D., W. L. Chan, B. P. Leung, F. Huang, R. Wheeler, D. Piedrafita, J. H. Robinson, and F. Y. Liew. 1998. Selective expression of a stable cell surface molecule on type 2 but not type 1 helper T cells. *J. Exp. Med.* 187: 787–794.
11. Coyle, A. J., C. Lloyd, J. Tian, T. Nguyen, C. Erikkson, L. Wang, P. Ottoson, P. Persson, T. Delaney, S. Lehar, et al. 1999. Crucial role of the interleukin 1 receptor family member T1/ST2 in T helper cell type 2-mediated lung mucosal immune responses. *J. Exp. Med.* 190: 895–902.
12. Lohning, M., A. Stroehmann, A. J. Coyle, J. L. Grogan, S. Lin, J. C. Gutierrez-Ramos, D. Levinson, A. Radbruch, and T. Kamradt. 1998. T1/ST2 is preferentially expressed on murine Th2 cells, independent of interleukin 4, interleukin 5, and interleukin 10, and important for Th2 effector function. *Proc. Natl. Acad. Sci. USA* 95: 6930–6935.
13. Townsend, M. J., P. G. Fallon, D. J. Matthews, H. E. Jolin, and A. N. McKenzie. 2000. T1/ST2-deficient mice demonstrate the importance of T1/ST2 in developing primary T helper cell type 2 responses. *J. Exp. Med.* 191: 1069–1076.
14. Hoshino, K., S. Kashiwamura, K. Kuribayashi, T. Kodama, T. Tsujimura, K. Nakanishi, T. Matsuyama, K. Takeda, and S. Akira. 1999. The absence of interleukin 1 receptor-related T1/ST2 does not affect T helper cell type 2 development and its effector function. *J. Exp. Med.* 190: 1541–1548.
15. Senn, K. A., K. D. McCoy, K. J. Maloy, G. Stark, E. Frohli, T. Rulicke, and R. Klemenz. 2000. T1-deficient and T1-Fc-transgenic mice develop a normal protective Th2-type immune response following infection with *Nippostrongylus brasiliensis*. *Eur. J. Immunol.* 30: 1929–1938.
16. Schmitz, J., A. Owyang, E. Oldham, Y. Song, E. Murphy, T. K. McClanahan, G. Zurawski, M. Moshrefi, J. Qin, X. Li, et al. 2005. IL-33, an interleukin-1-like cytokine that signals via the IL-1 receptor-related protein ST2 and induces T helper type 2-associated cytokines. *Immunity* 23: 479–490.

17. Chackerian, A. A., E. R. Oldham, E. E. Murphy, J. Schmitz, S. Pflanz, and R. A. Kastelein. 2007. IL-1 receptor accessory protein and ST2 comprise the IL-33 receptor complex. *J. Immunol.* 179: 2551–2555.
18. Ali, S., M. Huber, C. Kollewe, S. C. Bischoff, W. Falk, and M. U. Martin. 2007. IL-1 receptor accessory protein is essential for IL-33-induced activation of T lymphocytes and mast cells. *Proc. Natl. Acad. Sci. USA* 104: 18660–18665.
19. Ho, L. H., T. Ohno, K. Oboki, N. Kajiwara, H. Suto, M. Iikura, Y. Okayama, S. Akira, H. Saito, S. J. Galli, and S. Nakae. 2007. IL-33 induces IL-13 production by mouse mast cells independently of IgE-FcvarεRI signals. *J. Leukocyte Biol.* 82: 1481–1490.
20. Iikura, M., H. Suto, N. Kajiwara, K. Oboki, T. Ohno, Y. Okayama, H. Saito, S. J. Galli, and S. Nakae. 2007. IL-33 can promote survival, adhesion and cytokine production in human mast cells. *Lab. Invest.* 87: 971–978.
21. Kondo, Y., T. Yoshimoto, K. Yasuda, S. Futatsugi-Yumikura, M. Morimoto, N. Hayashi, T. Hoshino, J. Fujimoto, and K. Nakanishi. 2008. Administration of IL-33 induces airway hyperresponsiveness and goblet cell hyperplasia in the lungs in the absence of adaptive immune system. *Int. Immunol.* 20: 791–800.
22. Allakhverdi, Z., D. E. Smith, M. R. Comeau, and G. Delespesse. 2007. Cutting edge: the ST2 ligand IL-33 potently activates and drives maturation of human mast cells. *J. Immunol.* 179: 2051–2054.
23. Humphreys, N. E., D. Xu, M. R. Hepworth, F. Y. Liew, and R. K. Grencis. 2008. IL-33, a potent inducer of adaptive immunity to intestinal nematodes. *J. Immunol.* 180: 2443–2449.
24. Miller, A. M., D. Xu, D. L. Asquith, L. Denby, Y. Li, N. Sattar, A. H. Baker, I. B. McInnes, and F. Y. Liew. 2008. IL-33 reduces the development of atherosclerosis. *J. Exp. Med.* 205: 339–346.
25. Komai-Koma, M., D. Xu, Y. Li, A. N. McKenzie, I. B. McInnes, and F. Y. Liew. 2007. IL-33 is a chemoattractant for human Th2 cells. *Eur. J. Immunol.* 37: 2779–2786.
26. Brint, E. K., D. Xu, H. Liu, A. Dunne, A. N. McKenzie, L. A. O'Neill, and F. Y. Liew. 2004. ST2 is an inhibitor of interleukin 1 receptor and Toll-like receptor 4 signaling and maintains endotoxin tolerance. *Nat. Immunol.* 5: 373–379.
27. Inaba, K., M. Inaba, N. Romani, H. Aya, M. Deguchi, S. Ikehara, S. Muramatsu, and R. M. Steinman. 1992. Generation of large numbers of dendritic cells from mouse bone marrow cultures supplemented with granulocyte/macrophage colony-stimulating factor. *J. Exp. Med.* 176: 1693–1702.
28. Patel, M., D. Xu, P. Kewin, B. Choo-Kang, C. McSharry, N. C. Thomson, and F. Y. Liew. 2005. Glucocorticoid-induced TNFR family-related protein (GITR) activation exacerbates murine asthma and collagen-induced arthritis. *Eur. J. Immunol.* 35: 3581–3590.
29. Ospelt, C., M. Kurowska-Stolarska, M. Neidhart, B. A. Michel, R. E. Gay, S. Laufer, and S. Gay. 2008. The dual inhibitor of lipoxygenase and cyclooxygenase ML3000 decreases the expression of CXCR3 ligands. *Ann. Rheum. Dis.* 67: 524–529.
30. Stock, P., O. Akbari, G. Berry, G. J. Freeman, R. H. Dekruyff, and D. T. Umetsu. 2004. Induction of T helper type 1-like regulatory cells that express Foxp3 and protect against airway hyper-reactivity. *Nat. Immunol.* 5: 1149–1156.
31. Patel, M., D. Xu, P. Kewin, B. Choo-Kang, C. McSharry, N. C. Thomson, and F. Y. Liew. 2005. TLR2 agonist ameliorates established allergic airway inflammation by promoting Th1 response and not via regulatory T cells. *J. Immunol.* 174: 7558–7563.
32. Negrao-Correa, D., V. Pinho, D. G. Souza, A. T. Pereira, A. Fernandes, K. Scheuermann, A. L. Souza, and M. M. Teixeira. 2006. Expression of IL-4 receptor on non-bone marrow-derived cells is necessary for the timely elimination of *Strongyloides venezuelensis* in mice, but not for intestinal IL-4 production. *Int. J. Parasitol.* 36: 1185–1195.
33. Mohrs, M., B. Ledermann, G. Kohler, A. Dorfmuller, A. Gessner, and F. Brombacher. 1999. Differences between IL-4- and IL-4 receptor α-deficient mice in chronic leishmaniasis reveal a protective role for IL-13 receptor signaling. *J. Immunol.* 162: 7302–7308.
34. Shimoda, K., J. van Deursen, M. Y. Sangster, S. R. Sarawar, R. T. Carson, R. A. Tripp, C. Chu, F. W. Quelle, T. Nosaka, D. A. Vignali, et al. 1996. Lack of IL-4-induced Th2 response and IgE class switching in mice with disrupted Stat6 gene. *Nature* 380: 630–633.
35. Takeda, K., T. Tanaka, W. Shi, M. Matsumoto, M. Minami, S. Kashiwamura, K. Nakanishi, N. Yoshida, T. Kishimoto, and S. Akira. 1996. Essential role of Stat6 in IL-4 signalling. *Nature* 380: 627–630.
36. Sakuishi, K., S. Oki, M. Araki, S. A. Porcelli, S. Miyake, and T. Yamamura. 2007. Invariant NKT cells biased for IL-5 production act as crucial regulators of inflammation. *J. Immunol.* 179: 3452–3462.
37. Cui, J., T. Shin, T. Kawano, H. Sato, E. Kondo, I. Toura, Y. Kaneko, H. Koseki, M. Kanno, and M. Taniguchi. 1997. Requirement for Vα14 NKT cells in IL-12-mediated rejection of tumors. *Science* 278: 1623–1626.
38. Szabo, S. J., S. T. Kim, G. L. Costa, X. Zhang, C. G. Fathman, and L. H. Glimcher. 2000. A novel transcription factor, T-bet, directs Th1 lineage commitment. *Cell* 100: 655–669.
39. Zheng, W., and R. A. Flavell. 1997. The transcription factor GATA-3 is necessary and sufficient for Th2 cytokine gene expression in CD4 T cells. *Cell* 89: 587–596.
40. Adachi, O., T. Kawai, K. Takeda, M. Matsumoto, H. Tsutsui, M. Sakagami, K. Nakanishi, and S. Akira. 1998. Targeted disruption of the MyD88 gene results in loss of IL-1- and IL-18-mediated function. *Immunity* 9: 143–150.
41. Yamamoto, M., S. Sato, H. Hemmi, K. Hoshino, T. Kaisho, H. Sanjo, O. Takeuchi, M. Sugiyama, M. Okabe, K. Takeda, and S. Akira. 2003. Role of adaptor TRIF in the MyD88-independent Toll-like receptor signaling pathway. *Science* 301: 640–643.
42. Mangan, N. E., A. Dasvarma, A. N. McKenzie, and P. G. Fallon. 2007. T1/ST2 expression on Th2 cells negatively regulates allergic pulmonary inflammation. *Eur. J. Immunol.* 37: 1302–1312.
43. Mosmann, T. R., and R. L. Coffman. 1989. TH1 and TH2 cells: different patterns of lymphokine secretion lead to different functional properties. *Annu. Rev. Immunol.* 7: 145–173.
44. Hayakawa, H., M. Hayakawa, A. Kume, and S. Tominaga. 2007. Soluble ST2 blocks interleukin-33 signaling in allergic airway inflammation. *J. Biol. Chem.* 282: 26369–26380.
45. Xu, D., V. Trajkovic, D. Hunter, B. P. Leung, K. Schulz, J. A. Gracie, I. B. McInnes, and F. Y. Liew. 2000. IL-18 induces the differentiation of Th1 or Th2 cells depending upon cytokine milieu and genetic background. *Eur. J. Immunol.* 30: 3147–3156.
46. Helmby, H., and R. K. Grencis. 2004. Interleukin 1 plays a major role in the development of Th2-mediated immunity. *Eur. J. Immunol.* 34: 3674–3681.
47. Yamane, H., J. Zhu, and W. E. Paul. 2005. Independent roles for IL-2 and GATA-3 in stimulating naive CD4$^+$ T cells to generate a Th2-inducing cytokine environment. *J. Exp. Med.* 202: 793–804.
48. Rincon, M., J. Anguita, T. Nakamura, E. Fikrig, and R. A. Flavell. 1997. Interleukin (IL)-6 directs the differentiation of IL-4-producing CD4$^+$ T cells. *J. Exp. Med.* 185: 461–469.
49. Fort, M. M., J. Cheung, D. Yen, J. Li, S. M. Zurawski, S. Lo, S. Menon, T. Clifford, B. Hunte, R. Lesley, et al. 2001. IL-25 induces IL-4, IL-5, and IL-13 and Th2-associated pathologies in vivo. *Immunity* 15: 985–995.
50. Dillon, S. R., C. Sprecher, A. Hammond, J. Bilsborough, M. Rosenfeld-Franklin, S. R. Presnell, H. S. Haugen, M. Maurer, B. Harder, J. Johnston, et al. 2004. Interleukin 31, a cytokine produced by activated T cells, induces dermatitis in mice. *Nat. Immunol.* 5: 752–760.
51. Smithgall, M. D., M. R. Comeau, B. R. Park Yoon, D. Kaufman, R. Armitage, and D. E. Smith. 2008. IL-33 amplifies both Th1- and Th2-type responses through its activity on human basophils, allergen-reactive Th2 cells, iNKT and NK Cells. *Int. Immunol.* 20: 1019–1030.
52. Foster, P. S., S. P. Hogan, A. J. Ramsay, K. I. Matthaei, and I. G. Young. 1996. Interleukin 5 deficiency abolishes eosinophilia, airways hyperreactivity, and lung damage in a mouse asthma model. *J. Exp. Med.* 183: 195–201.
53. Wills-Karp, M., J. Luyimbazi, X. Xu, B. Schofield, T. Y. Neben, C. L. Karp, and D. D. Donaldson. 1998. Interleukin-13: central mediator of allergic asthma. *Science* 282: 2258–2261.
54. Corry, D. B. 1999. IL-13 in allergy: home at last. *Curr. Opin. Immunol.* 11: 610–614.
55. Grunig, G., M. Warnock, A. E. Wakil, R. Venkayya, F. Brombacher, D. M. Rennick, D. Sheppard, M. Mohrs, D. D. Donaldson, R. M. Locksley, and D. B. Corry. 1998. Requirement for IL-13 independently of IL-4 in experimental asthma. *Science* 282: 2261–2263.
56. Lee, C. G., H. Link, P. Baluk, R. J. Homer, S. Chapoval, V. Bhandari, M. J. Kang, L. Cohn, Y. K. Kim, D. M. McDonald, and J. A. Elias. 2004. Vascular endothelial growth factor (VEGF) induces remodeling and enhances TH2-mediated sensitization and inflammation in the lung. *Nat. Med.* 10: 1095–1103.
57. Faith, A., J. McDonald, E. Peek, D. Richards, J. Caulfield, E. Chevretton, D. Roberts, T. Lee, C. Corrigan, and C. Hawrylowicz. 2005. Functional plasticity of human respiratory tract dendritic cells: GM-CSF enhances T_H2 development. *J. Allergy Clin. Immunol.* 116: 1136–1143.
58. Carriere, V., L. Roussel, N. Ortega, D. A. Lacorre, L. Americh, L. Aguilar, G. Bouche, and J. P. Girard. 2007. IL-33, the IL-1-like cytokine ligand for ST2 receptor, is a chromatin-associated nuclear factor in vivo. *Proc. Natl. Acad. Sci. USA* 104: 282–287.
59. Wenzel, S. E. 2006. Asthma: defining of the persistent adult phenotypes. *Lancet* 368: 804–813.